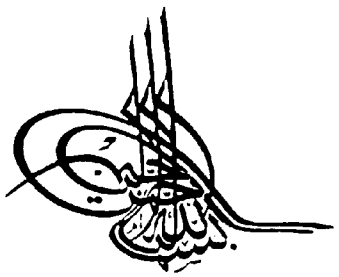

SWELLING SHRINKAGE AND SHEAR STRENGTH OF UNSATURATED EXPANSIVE CLAYS

SWELLING, SHRINKAGE AND SHEAR STRENGTH OF UNSATURATED EXPANSIVE CLAYS

ALI KHAKBAZAN B.Sc., M.Sc.

A thesis submitted in partial fulfilment
of the requirements for the award of the
Degree of Doctor of Philosophy
of the
University of Glamorgan.

Department of Civil Engineering and Building,
University of Glamorgan,
Wales, U.K.

May 1995

CERTIFICATION OF RESEARCH

This is to certify that, except when specific reference to other investigation is made, the work described in this thesis is the result of the investigation by the candidate.

A. KHAKBAZAN

A. Khakbazan

(Candidate)

2 May 1995

(Date)

R. B. Robinson

Dr. R. B. Robinson

(Director of Studies)

2 May 1995

(Date)

G. I. Jones

Mr. G. I. Jones

(Supervisor)

2 May 1995

(Date)

P. S. Coupe

Prof. P. S. Coupe

(Supervisor)

2 May 1995

(Date)

ACKNOWLEDGEMENT

The one who deserves to be most sincerely thanked, always and everywhere is God, the merciful and compassionate. He is the Creator who gave us the wisdom and ability to discover the secrets and mysteries surrounding us.

The author wishes to express his profound gratitude to Dr. R. B. Robinson, his Director of Studies, and Mr. G. I. Jones, his Supervisor, at the University of Glamorgan for their continuous help and encouragement.

The author is indebted to his Supervisor Professor P. S. Coupe, Head of Department, who has read the thesis thoroughly and made constructive comments on the manuscript.

I would like to thank the many colleagues, especially Dr. M. R. Abdi, Dr. A. Siraty and Dr. F. Wu with whom I shared a research room. They helped me survive the vicissitudes of research work.

The help provided by some members of the technical staff at the University especially that of Mr. B. Lloyd and Mr. D. Crocker, of the Geotechnics Laboratory, is appreciated.

The author wishes to express his most sincere gratitude to his wife, for her support, and his parents for the provision and organisation of the funding and the sacrifices they endured to make this thesis possible.

The role of The Ministry of Culture and Higher Education of the Islamic Republic of Iran, in facilitating the transfer of funds, is also acknowledged.

SUMMARY

The swelling, shrinkage and shear strength properties of unsaturated expansive clays are examined in this thesis. This research was instigated to provide the engineer with improved techniques for predicting the swelling behaviour encountered in unsaturated expansive clays. To achieve this objective, a double-walled triaxial cell was developed. This was necessary to eliminate the effects of creep on the perspex walling of the inner chamber as pressures within the cell varied. Swell and consolidated drained tests were conducted on the soil samples. They were sheared after expansion had taken place, without expansion and without prior expansion or the use of back pressures.

The clay samples used for this study were a mixture of kaolinite and sodium montmorillonite. They were artificially constituted to produce identical test specimens prior to testing.

Three series of swell and swell pressure tests were conducted under controlled environmental conditions. The test series consisted of samples containing 10%, 20% and 30% sodium montmorillonite.

The data from the experimental programme were analysed and the results showed:

a) The water intake and total sample volumes generally exhibited an initial large and rapid increase and then tended to equilibrium.

b) The samples were fully restrained axially during testing. However when the loads were removed, free axial expansion, due to the stress release, took place.

c) The affinity of clay particles for water was demonstrated when the water intake by the soil samples showed a greater gradient as montmorillonite content increased.

d) A time delay was found between the water intake by the soil samples and the reaction time with montmorillonite.

e) The axial swell pressures increased rapidly in the first hour from zero to approximately 220 kN/m^2. Further increases were recorded in the following twenty hours and then tended to a near constant value.

f) The volume increase between samples within the ranges of 10% to 30% montmorillonite was non-linear. Where free expansion was taken into consideration, the volume increased curvi-linearly. However, under test conditions, a reduced rate of expansion was experienced.

g) The values of the angles of internal friction, whether total or effective, decreased as the amount of montmorillonite in the soil samples increased.

h) The values of ϕ^b were found to be consistently less than ϕ'' with respect to pore air back pressure. This further emphasised the role that matrix suction plays in the behaviour of unsaturated soils. Therefore, it is not sufficient to determine values of ϕ'' alone in the case of unsaturated soils.

CONTENTS

CHAPTER SIX

TESTING EQUIPMENT AND SAMPLE PREPARATION

CHAPTER SEVEN

PRESENTATION OF DATA AND ANALYSIS

TABLES

Page

CHAPTER SIX

TESTING EQUIPMENT AND SAMPLE PREPARATION

CHAPTER SEVEN

PRESENTATION OF DATA AND ANALYSIS

FIGURES

Page

CHAPTER ONE

CLAYS AND CLAY MINERALS

CHAPTER TWO

EXPANSIVE CLAYS

CHAPTER THREE

LABORATORY REVIEW OF EXPANSIVE CLAYS

CHAPTER FOUR

UNSATURATED SOILS

CHAPTER FIVE

REVIEW OF SUCTION MEASUREMENT TECHNIQUES

CHAPTER SIX

TESTING EQUIPMENT AND SAMPLE PREPARATION

CHAPTER SEVEN

PRESENTATION OF DATA AND ANALYSIS

PLATES

PAGE

CHAPTER SIX

TESTING EQUIPMENT AND SAMPLE PREPARATION

CHAPTER SEVEN

PRESENTATION OF DATA AND ANALYSIS

CHEMICAL SYMBOLS

Al	Aluminium
Ba	Barium
Be	Beryllium
Ca	Calcium
Cl	Chlorine
Cs	Caesium
Fe	Iron
H	Hydrogen
K	Potassium
Li	Lithium
Mg	Magnesium
Na	Sodium
NH_4	Ammonium
O	Oxygen
Rb	Rubidium
Si	Silicon
Th	Thorium

NOTATION

1 Angstrom Unit (Å) = 1 x 10^{-10}m

ABBREVIATIONS

AASHO
American Association of State Highway Officials.

AASHTO
American Association of State Highway and Transportation Officials.

ASCE
American Society of Civil Engineers.

BGS
British Geotechnical Society.

ECSMFE
European Conference on Soil Mechanics and Foundation Engineering.

HMSO
Her Majesty's Stationery Office.

ICSMFE
International Conference on Soil Mechanics and Foundation Engineering.

SAICE
South African Institution of Civil Engineers.

SM & FD
Soil Mechanics and Foundation Division.

SM & FE
Soil Mechanics and Foundation Engineering.

USBR
United States Bureau of Reclamation.

DEFINITIONS

A number of phrases have been used throughout this thesis. The following brief definitions will help towards easier understanding of the terms.

Absorbed Water
Water held mechanically in a soil mass and having physical properties not much different from ordinary free water at the same temperature and pressure.

Absorption
The process of assimilating fluids or gasses into the structure of the soil.

Adsorbed Water
Water in a soil held by physico-chemical forces. Its physical properties are substantially different from absorbed water at the same temperature and pressure.

Adsorption
To undergo or cause to undergo a process in which a substance, usually a gas, accumulates on the surface of a solid forming a thin film, often only one molecule thick.

Aliphatic (of an organic compound)
Not aromatic; having an open chain structure, such as alkanes, alkenes and alkynes.

Amine
An organic base formed by replacing one or more of the hydrogen atoms of ammonia by organic groups.

Axis Translation
Axis translation is a technique used to establish suctions in the laboratory greater than the cavitation suction. The suction gradient is generated by applying a high pore air pressure within the sample and using a high air entry porous plate below the sample. It is the basis on which all pressure plate and pressure membrane apparatus work.

Carbowax
Poly Ethylene Glycol, (polymer of a particular molecular weight).

Free Swell
A free swell test is performed by pouring 10 cc of dry soil into a 100 cc graduated cylinder filled with water and noting the volume of soil after it comes to rest at the bottom of the cylinder (Holtz and Gibbs (1956)). It is in fact a sedimentation test not a swell test and is sensitive to many factors such as salt concentration, temperature and salt type (Lambe and Whitman (1969)).

Heave
Movement of soil caused by expansion or displacement resulting from phenomena such as moisture absorption, removal of pressure, driving of piles, frost action, and/or loading of an adjacent area.

Intrinsic Expansiveness
Intrinsic expansiveness of a soil is a property of that soil resulting from its mineral composition and grading and its interaction with water. It is a measure of the change in water content caused by or giving cause to a change in suction.

Matrix Suction
Matrix suction is defined as the negative gauge pressure to which a solution identical to the soil water must be subjected in order to be in equilibrium with the soil water through a porous wall.

The International Society of Soil Science defined it as the negative gauge pressure, relative to the external gas pressure on the soil water, to which a solution identical in composition with the soil water must be subjected, in order to be in equilibrium through a porous permeable wall with the soil water.

McKeen (1981) defined matrix suction as the negative pressure which will hold soil water in equilibrium through a porous membrane with the same soil water within a sample of the soil. Matrix suction results from surface adsorption and capillary forces.

Osmotic Suction
Osmotic suction and solute suction mean the negative gauge pressure to which a pool of pure water must be subjected in order to be in equilibrium with a pool of soil water (i.e. pore fluid) through a semi-permeable membrane.

The International Society of Soil Science defined it as the negative gauge pressure to which a pool of pure water must be subjected in order to be in equilibrium through a semi-permeable (i.e. permeable to water molecules only) membrane with a pool containing a solution identical in composition with the soil water.

McKeen (1981) defined osmotic (solute) suction as a negative pressure which will hold pure water in equilibrium with soil water through a membrane which allows only water molecules to pass. Osmotic suction results from variation in ion concentration in the fluid. Matrix suction is directly influenced by mechanical loads and water content whereas osmotic suction is not.

Percent Swell
Percent swell is commonly used to describe the result of a test to measure the vertical strain on wetting up of a sample. It is often taken to be an intrinsic soil property, although both initial and final moisture conditions are inadequately controlled or defined and various surcharges are applied in the various test procedures.

Potential Swell
Potential swell describes the vertical strain expressed as a percent that is determined to be possible in wetting up from the initial moisture content to a state of zero pore pressure or suction.

Semi-permeable membrane
A membrane through which the solvent but not certain dissolved or colloidal substances may pass. Thus a membrane that is semi-permeable with regard to carbowax and water may be fully permeable with regard to salts and water.

Sorption
The process in which one substance takes up or holds another.

Swell
Swell is a change in volume of a soil in the field or in the laboratory due to a decrease in suction or applied stress. It can occur in saturated or partially saturated (unsaturated) soils.

Swell of an intrinsically expansive soil may be described as the volume change that results from a change in moisture content or suction. It can also occur in all soils due to a reduction in effective stress, or in some solids due to chemical changes.

Swell Pressure
Swell pressure describes the results of two very different test procedures. In one the swell pressure is defined as the pressure required to maintain constant volume on wetting up from an unspecified initial moisture content to a state of zero pore pressure or suction. In the other, the sample is allowed to swell to a state of zero pore pressure or suction under a small surcharge and then the swell pressure is defined as the pressure required to consolidate the sample to its original height.

Swelling Index
The void ratio increases during 1 log cycle pressure decrease in an oedometer (Schmertman (1969)).

Total Suction
Total suction is the negative gauge pressure relative to the external gas pressure on the soil water to which a pool of pure water must be subjected in order to be in equilibrium through a semi-permeable membrane with the soil water. Total suction is thus equal to the sum of matrix or soil water suction and osmotic suction.

van der Waals Force
The attractive force between dispersed particles is attributed to the general van der Waals attraction force between all the atoms of one particle and all the atoms of another.

CHAPTER ONE

CLAYS AND CLAY MINERALS

1.0 Introduction

Soil may be defined as an accumulation of solid particles produced by mechanical or chemical disintegration of rocks and decomposition of organic matter. The minerals derived from parent rock material constitute the primary minerals of soils.

Clay minerals form at or near the earth's surface as a consequence of weathering processes. The particular clay minerals that form vary, depending on the climate, topography, vegetation cover, parent rock and time during which the weathering has continued.

The constituent particles of soils are grouped on the basis of size into clay, silt, sand and gravel. Each size fraction contributes different properties to the soil. The term clay refers to that size fraction of soils with particles of less than 0.002 mm (2 micron) diameter.

Clays are important to the designer and the construction engineer because structures frequently rest upon clayey formations, excavations are commonly made into clayey materials, vast quantities of earth materials containing clays are used in embankments and linings and clays occur commonly as constituents of engineering materials such as aggregate, pozzolan and grout. Moreover, clays present many unique problems to the engineer primarily because their physical and chemical instability can render soil masses

susceptible to repeated changes of form and volume in response to loading, unloading, vibration and changing moisture content.

Clay is highly plastic and has a strong tendency for physico-chemical interaction when water is present. To the geologist, the term clay implies:

i) a natural material with plastic properties,

ii) a material of very fine particle size, and

iii) crystalline fragments of minerals consisting mainly of hydrous aluminium silicates and occasionally hydrous magnesium silicates.

A typical engineering definition of clay was forwarded by Gillot (1987) as:

> "A fine-textured soil, with grains colloidal in size, composed mainly of hydrated aluminium silicates containing various impurities. It is plastic and cohesive, shrinks when dry, expands when wet and gives up its water when compressed."

1.1 Formation of Clay Minerals

The formation of clay minerals is discussed in detail by Hoskings (1940), Grim (1942) and Ross and Hendricks (1945). All clay minerals are formed by the alteration of pre-existing source minerals, the clay mineral formed being a result of complex relations between the source mineral and the kind of alteration process involved.

Alteration that takes place on the surface of the land is weathering. Alteration that takes place on the sea floor or generally in any body of water is called halmyrolysis. No matter where alteration takes place, the processes of disintegration, oxidation, hydration and leaching are

involved. Conditions, important for alteration, are oxidation reduction, acidity-alkalinity and temperature.
Oxidation reduction refers to the tendency of the elements in the system to be in either high or low valence states depending on the availability of oxygen. Elements exposed to a stream will tend to be in a high valence state. In a stagnant pool, however, where abundant organic matter consumes free oxygen, most elements tend to be in a low valence state. The valence states provide limits within which the compounds conform.
Acidity-alkalinity refers to the concentration of hydrogen ions in solution. Where this concentration is high, the solution is acid and where it is low, the solution is alkaline. The solubility of many compounds is directly controlled by acidity-alkalinity conditions.
Temperature strongly controls most rates of reaction. Most reactions occur within the range of climatic temperatures.
Disintegration involves an increase in the surface area of the source minerals. This can take place by diverse mechanisms, for example, cycles of freezing and thawing, drying and wetting, and abrasion such as found at the base of a glacier or caused by the transport of grains in streams. Disintegration is fundamental in controlling the rates of other alteration processes simply because it facilitates the attack of water which is the agent by which all chemical changes are caused.

Hydration involves reactions between elements or compounds and water that make it possible for the elements to form new combinations and, eventually, new minerals.

Leaching is the process by which the hydrated and dissolved elements leave the alteration system and hence become unavailable for further reactions within the system.

1.1.1 Weathering

Weathering or disintegration of rock may be by physical or chemical processes or a combination of both. In physical weathering there is generally no alteration of the chemical or mineralogical composition of the rock material. This process involves the break down of a rock mass into smaller sizes such as gravels, sands and silts. The main causes of this phenomena are changes in temperature, glacial activity, human activity and water.

In chemical weathering, the less stable minerals in rocks are chemically altered over long periods of time. Chemical weathering produces very small particles that are often in crystalline form. Typically, these particles are two dimensional or flake shaped, and result in the formation of clay soils. The characteristics of the clay depend on the nature of the parent rock, the environment in which the weathering takes place and the length of time available for chemical alteration to develop.

1.1.2 Sedimentation

Weathered material may be washed into rivers and then carried into lakes or to the sea. Essentially this means that weathered debries may be transported from one environment to another, for example, from fresh water to marine conditions. Grim (1959) indicated that there may be a

change in the clay mineral composition of argillaceous debries as they are carried from one environment to another.

1.1.3 Metamorphism

Deep burial and the application of tectonic forces tend to squeeze out water from between the silicate sheets and to increase the size and perfection of crystallinity of the micas. They tend, therefore, to change the expandable clay minerals (montmorillonite) and mixed-layers in the direction first of illite and clay mineral mica and then to muscovite, biotite, chlorite, etc. With very intense metamorphism the minerals may be completely dehydrated and changed over to non-hydrous crystalline compounds. It appears that kaolinite is not changed until the very intense phases of metamorphic alteration (Grim (1959)).

1.1.4 Hydrothermal

Hot gasses and vapours, derived from cooling igneous material or extremely deep meteoric circulations, frequently cause substantial alteration of the rocks through which they pass. Thus many veins of ore minerals, which have been formed by hydrothermal waters, are surrounded by an aureole in which the wall rock has been changed to clay material by the same water that deposited the vein material. Frequently there is a zonal arrangement of clay mineral alteration, with an inner zone of white mica followed in turn by kaolinite, montmorillonite and chlorite.

1.2 Clay Mineral Petrology

In a paper presented to the Royal Society of London in 1984, Eberl proposed three questions when considering clay mineral formation. These were:

1) what is clay?
2) how did it form?
3) under what conditions did it form?

An answer to the first question requires an analysis of the clay's chemical composition and crystal structure. The second question concerns mechanisms of the clay formation. Eberl (1984) considered three mechanisms, generally based on ideas of Esquevin (1958) and Millot (1970). These mechanisms are:

i) inheritance,
ii) neoformation, and
iii) transformation.

Origin by inheritance simply means that a clay mineral found in a natural deposit originated from reactions that occurred in another area during a previous stage in the rock cycle, and that the clay is stable enough to remain inert in its present environment. Its stability may result either from slow reaction rates or from being in chemical equilibrium. Origin by neoformation means that the clay has precipitated from solution or has formed from reaction of amorphous material. Origin by transformation requires that the clay has kept some of its inherited structure intact while undergoing chemical reaction. This reaction may take two forms:

i) ion exchange, in which loosely bound ions are exchanged with those of the environment, and
ii) layer transformation, in which the arrangements of tightly bound octahedral, tetrahedral or fixed

interlayer cations are modified.

The third question of interest to the clay petrologist concerns the clay's environment of formation. This is discussed in Section 1.1.

1.2.1 Clay Minerals

1.2.1.1 Introduction

Some clays swell when wetted (swelling clays) and shrink when dried. Such clays can cause problems in foundations of buildings. Other clay minerals can exchange cations in their structure by the base exchange process. The types of clay minerals in a mass of clay control its mechanical properties and these can be very variable. Important types of clay minerals are: chlorite, glauconite, halloysite, illite, kaolinite, montmorillonite and vermiculite. Kaolinite and montmorillonite are studied in detail in Sections 1.2.2.1 and 1.2.2.2.

1.2.2 Structure of Clay Minerals

Bailey (1980) described clay minerals as:

> "belonging to the family of phyllosilicates and containing continuous two-dimensional tetrahedral sheets of composition T_2O_5 (T=Si, Al, Be .....) with tetrahedra linked by sharing three corners of each with a further corner pointing in any direction. The tetrahedral sheets are linked in the unit structure to octahedral sheets and to groups of coordinated cations or individual cations."

Clay minerals are complex silicates of aluminium, magnesium and iron. Two basic crystalline units form the clay minerals:

1) a silicon-oxygen tetrahedron, and

2) an aluminium or magnesium octahedron.

A silicon-oxygen tetrahedral unit, shown in Figure 1.1, consists of four oxygen atoms surrounding a silicon atom. The tetrahedral units combine to form a silica sheet as shown in Figure 1.2. Das (1985) drew attention to the fact that the three oxygen atoms located at the base of each tetrahedron are shared by neighbouring tetrahedra. Each silicon atom, with a positive valence of four, is linked to four oxygen atoms with a total negative valence of eight. However, each oxygen atom at the base of the tetrahedron is linked to two silicon atoms. This leaves one negative valence charge of the top oxygen atom of each tetrahedron to be counter balanced.

Figure 1.3 shows an octahedral unit consisting of six hydroxyl units surrounding an aluminium or magnesium atom. The combination of the aluminium octahedral units forms a gibbsite sheet shown in Figure 1.4. If the main metallic atoms in the octahedral units are magnesium, these sheets are referred to as brucite sheets. In Figure 1.5 the silica sheets are stacked over the octahedral sheets, the oxygen atoms replacing the hydroxyls to satisfy their valence bonds. In kaolinite and montmorillonite, the fundamental units are arranged in the respective atomic lattices shown in Figures 1.5 and 1.6 after Harvey (1982) and Bell (1983). The units formed by linking one octahedral sheet to one tetrahedral sheet, for example kaolinite, is named a 1:1 layer and the exposed surface of the octahedral sheet consists of OH groups. A similar linkage can occur on the other side of an octahedral sheet to form a 2:1 layer, like montmorillonite, both surfaces of which consist of the

hexagonal mesh of basal oxygen. Structures exist in which the 1:1 or 2:1 layers are not electrically neutral. Charge balance is maintained in such structures by interlayer material which may be individual cations as in the mica group, hydrated cations as in vermiculites and smectites, or octahedrally coordinated hydroxide groups or linked sheets of the latter, as in the chlorite minerals (Brown (1984)).
The shape, size and specific surface area all influence the engineering behaviour of clay minerals. Clay minerals have a plate-like shape. They are very small in size, being measured in Angstrom (Å) units. For example, an individual particle of montmorillonite is typically 1000 Å by 10 Å thick, whilst kaolinite is 10000 Å by 1000 Å thick (Bell (1983)). Das (1985) however, gave dimensions ranging from 1000 Å to 5000 Å with thicknesses of 10 Å to 50 Å for montmorillonite and 1000 Å to 20000 Å with thicknesses of 100 Å to 1000 Å for kaolinite.

1.2.2.1 Clay Minerals With Two-layer Sheets

Some clay minerals consist of repeating layers of two-layer sheets. A two-layer sheet is a combination of a silica sheet with a gibbsite sheet, or a combination of a silica sheet with a brucite sheet. The sheets are about 7.2 Å thick. The repeating layers are held together by hydrogen bonding and secondary valence forces. Kaolinite (Figure 1.7) is the most important clay mineral belonging to this type.
The minerals of the kaolin group consist of unit layers formed by the linkage of one Si (Al, Fe) - O tetrahedral sheet with one Al (Mg, Fe) - OH octahedral sheet in regular succession.

Kaolinite is represented by $Al_2 (OH)_4 Si_2 O_5$. It may be formed by the weathering of K and Na feldspars from magmatic and metamorphic rocks or by a hydrothermal attack of carbonic and sulphuric acid solutions on feldspars and micas. All these minerals occur in many kinds of rocks (granite, gneiss, porphyr and others), so that the resulting kaolinite is widespread. On the other hand kaolinite may be formed by silicification of hydrar-gillite by silicic acid solutions. Well crystallised kaolinite may be found in varying sizes from 0.2 micron to several microns. Particle size and thickness vary with the type of deposit or method of particle fractions.
The name kaolinite is derived from the Kauling hills near Jauchau-Fu in China.

1.2.2.2 Clay Minerals With Three-layer Sheets

One of the most common clay minerals with three-layer sheets is montmorillonite (Figure 1.8). The minerals belonging to the montmorin group consist of a series of successive layers, each formed by one Al (Mg, Fe) - OH octahedral sheet enclosed between two (Si, Al) - O tetrahedral sheets. These kinds of minerals are indicated as 2:1 minerals. Because of the weak interlayer charge, the large surface area (400-800 m^2/g), the large amount of exchangeable cations (60-120 meq/100g) and the poor ordering of the several layers, the montmorin minerals will swell when treated with H_2O or other liquids of high polarisability. Swelling occurs most strongly in samples with smallest particle size and the most hydrated cations.

Montmorillonite is represented by:

$$\left[\begin{matrix} (Al, Mg, Fe)_2 (OH)_2 Si_4 O_{10} \\ (Ca^{2+}, Mg^{2+}, Na^{+}) \end{matrix} \right]^{n} H_2O$$

It results from hydrothermal alteration of volcanic ashes with an acidic to basic character. Therefore it is found only in some localities in the world called bentonite beds. The soil montmorillonite is the commonest clay mineral in large areas of the world with heavy easily swelling soils. This typical behaviour has been indicated by certain names, for example, black regur/cotton (India), tirnoir (Morrocco), margalite (Indonesia), black turf (South Africa) and adobe (Sudan).

1.3 Clay Surfaces

Clays are hydrous silicates with a layered structure and they belong to the larger group of phyllosilicates (Brown (1984)). Layer silicates are so named because the ions (or atoms) in their structures are arranged in sets of parallel planes which are strongly bonded together to form layers. Their morphology, usually thin platy crystals, reflect the underlying atomic arrangement.

The atomic structure at the external surfaces of layer silicates is of three basic types, all of which are demonstrated by a 1:1 type mineral like kaolinite. The basal surface consists of the close-packed hydroxyl ions on the exposed side of the octahedral sheet, whilst the opposite basal surface is composed of the oxygen atoms coordinated to silicon in six-membered siloxane rings of the tetrahedral sheet. The third type of surface is at the lateral boundary

of the sheet structure. Here the chemical composition and bonding of the bulk structure cannot be maintained without additional ions or atoms. These are required to complete the coordination spheres of the cations (Newman (1987)).
Newman (1987) stated that the broken bonds at the edge surfaces are usually completed by H^+ or OH^-, which are the potential determining ions, the net charge balance being dependent on the pH of the medium in which the clay is immersed. Changes in the net charge balance have a fundamental effect on dispersion and flocculation behaviour. The surface of a clay particle has a negative charge. This means that a clay particle is surrounded by a strongly attracted layer of water, but as the dipolar water molecules do not satisfy the electrostatic balance at the surface of the clay particle, some metal cations are also adsorbed. The ions are usually weakly held and can be readily replaced by others. Consequently, they are referred to as exchangeable ions.

1.4 Exchangeable Ions and Ion Exchange

Ion exchange is defined by the fact that a given cation has taken the place of a different one in the surface phase of the clay.
In theory, neither kaolinite nor illite should be capable of cation exchange reactions, but in practice they both are, though to a limited extent. One reason is that generally clay minerals form at low temperatures as very small crystals which are likely to contain imperfections. Another is that the layered arrangement of the structures is liable to distortions, for instance by collisions between particles

during transport to the site of deposition. So there is generally a negative charge imbalance on all clay mineral particles, and they can attract cations, which are loosely held between or on the edges of the layers. This process is called adsorption and it is mainly these adsorbed ions that are exchangeable. Illite has a greater exchange capacity than kaolinite but it is negligible compared with that of montmorillonite.

The most unique property of the smectite clay group, which contains montmorillonite, is the presence of exchangeable cations that are primarily adsorbed on interlamellar surfaces. The most common of these exchangeable ions in order of dominance in nature are: Ca, Mg, Na and H, but small amounts of exchangeable K and Li also occur in some smectites. It is now generally realised that exchangeable Mg may be very abundant in some smectite clays. As a rule Ca and Mg occur together and, in rare instances the amount of exchangeable Mg exceeds the amount of exchangeable Ca. As exchangeable ions, the chemical properties of Ca and Mg are similar, apparently because these ions have similar hydration characteristics. Among the major commercial smectite clay deposits, a far greater number contain Ca and Mg than contain Na or H as exchangeable ions.

1.4.1 Cation Exchange Capacity

Isomorphous substitution and broken continuity of structures result in a net negative charge at the faces of the clay particles. There are also some positive charges at the edges of these particles. To balance the negative charge, clay particles attract positively charged ions from salts in

their pore water. These are referred to as exchangeable ions. Some are more strongly attracted than others. The cations can be arranged in terms of their affinity for attraction as follows:

$$Al^{3+} > Ca^{2+} > Mg^{2+} > NH_4^{+} > K^{+} > H^{+} > Na^{+} > Li^{+}$$

This series indicates that, for example, Al^{3+} ions can replace Ca^{2+}, and Ca^{2+} ions can replace Na^{+}. The process is called cation exchange, for example;

$$2Na\ clay + CaCl_2 \longrightarrow Ca\ clay + 2Na\ Cl$$

Cation exchange capacity of a clay is defined as the amount of exchangeable ions, expressed in milliequivalents (meq) per 100 gram of dry clay.

Sposito (1989) defined the ion exchange capacity of a soil as:

> "the number of moles of adsorbed ion charge that can be desorbed from a unit mass of soil, under given conditions of temperature, pressure, soil solution composition and soil ion mass ratio."

The ion exchange capacity of soils normally ranges up to 40 meq/100g. Bell (1983) related 3 to 15 and 60 to 100 meq/100g to kaolinite and montmorillonite respectively whereas Odom (1984) gave 70 to 130 meq/100g as the cation exchange capacity of relatively pure smectite clays. According to Weaver and Pollard (1973), about 80% of the cation exchange capacity of smectite clays is due to charges resulting from structural substitution, and about 20% is due to charges from broken bonds at the edges of crystals. Due to natural chemical and physical factors, the abundance of natural exchangeable ions in even relatively pure smectite is usually less than the cation exchange capacity of the same smectite. If the abundance of exchangeable ions should

exceed the cation exchange capacity, the presence of soluble salts should then be suspected (Odom (1984)).

The exchangeable ions associated with smectite clays are easily and reversibly replaceable. Because of its valency, Na is readily replaced by Ca and Mg, so that smectite clays tend to be depleted of Na when subjected to leaching conditions. Exchangeable ions play a dominant role in the commercial use of smectite clays. Where Na is the predominant exchangeable ion, smectite clays may have a high swelling capacity. Na tends to promote the development of many oriented water layers on interlamellar surfaces. The hydration associated with Na may produce swelling to the extent of complete dissociation of the individual smectite crystals, the result being a high degree of dispersion and maximum development of colloidal-like properties, that is, high natural viscosity. However, some smectite clays, having similar internal chemistry, but containing exchangeable Ca plus Mg, show only a small degree of swelling even when fully hydrated.

The type of adsorbed cations influence the behaviour of the soil in that the greater their valency, the better the mechanical properties. For instance, clay soils containing montmorillonite with Na cations are characterised by high water adsorption and considerable swelling. If these are replaced by Ca, a cation with a higher valency, both these properties are appreciably reduced. The thickness of the adsorbed layer influences the soil permeability; the thicker the layer, the lower the permeability since a greater proportion of the pore space is occupied by strongly held

adsorbed water. As the ion exchange capacity of a cohesive soil increases so does its plasticity index, the relationship between the two being almost linear (Bell (1983)).

1.5 Specific Surface of Clay

The specific surface refers to the magnitude of the surface in relation to the mass; the smaller the particle, the larger the specific surface. The specific surface provides a good indication of the relative influence of electrical forces on the behaviour of a particle. If one considers several clay samples all having the same mass, the highest surface area will be in the sample in which the particle sizes are the smallest. So, it is easy to realise that the specific surface of kaolinite will be small compared to that of montmorillonite. The specific surfaces of kaolinite and montmorillonite are about 15 and 800 m^2/g respectively (Yong and Warkentin (1975) and Das (1985)).

1.6 Mechanisms of Interlamellar Sorption

The term interlamellar sorption was first proposed by MacEwan in 1948 to designate the penetration of ions and neutral molecules between the layers of a lamellar structure, resulting in a reversible, one-dimensional swelling.

The sorption of large complex ions may be attributed to an ordinary cation exchange process, the ions being held to the negatively charged sheets by electrostatic forces. Hendricks (1941) suggested that van der Waals forces play an important part in determining the extra stability of such complexes,

and the flat orientation of the molecule. Van der Waals forces are of importance in the case of adsorption of neutral molecules. Bradley (1945) however, suggested another mechanism, namely hydrogen bonds between the carbon atoms and the surface oxygen atoms of the mineral. These forces provide an explanation of the attachment of neutral molecules to the sheets, and therefore of the repulsion between them. The balancing attractive force may be partly electrostatic in character, and partly van der Waals attraction between neighbouring layers, but the electrostatic force appears to be the only effective one at short distances.

MacEwan (1955) made calculations on the probable variation of the electrostatic attractive potential with distance, and found that it dies off very rapidly for a surface with high charge density but less rapidly for one with low charge density. At separations of the order of 100 Å, the Gouy layer repulsion and van der Waals attraction may be the only forces of importance. MacEwan (1955) therefore suggested that a suitable value of the surface charge density is essential for these interlamellar adsorption complexes to be formed.

A complicating factor which must be taken into account is that the interlamellar molecules interact with the exchange cations as well as with the clay mineral surface. This is clearly shown by the fact that the number of sheets of organic liquid which penetrate between the montmorillonite layers is dependent on the exchangeable cations, and may differ even for two cations of the same size. It seems

likely that this type of short range equilibrium is of general occurrence when charged surfaces are brought together in a liquid medium, and therefore that it ought to be taken into account in explaining colloidal phenomena (MacEwan (1955)).

1.6.1 Molecular Adsorption

The exchangeable cation in a clay mineral of the expanding lattice type determines the amount of water vapour taken up under equilibrium conditions. Hendricks et al (1940) demonstrated that the water adsorbed at low relative humidity by Ca, Mg and Li montmorillonites hydrates the exchangeable cation which lies in the interpacket space. According to Mielenz and King (1955) Ca^{2+} and Mg^{2+} cations are hydrated by 6 molecules of water, whereas Li^{+} is hydrated by 3. Other cations such as Na^{+}, K^{+} and H^{+} apparently are not hydrated. Development of the hexagonal water net is completed only after hydration of available Ca^{2+}, Mg^{2+} and Li^{2+} in exchange positions. At relative humidity in the range of 5 to 90 percent, Na and K montmorillonites adsorb less water from the vapour phase than Ca and Mg montmorillonites. However, Na montmorillonite adsorbs more water from the liquid state than Ca or Mg montmorillonites.

1.6.2 Cationic Adsorption

Either organic or inorganic cations may be adsorbed by clay minerals. If the adsorptive process is reversible, that is, if an equivalent number of previously adsorbed cations are released into solution while the introduced cations are

being adsorbed, the term cationic exchange is used. All clay minerals possess a cation exchange capacity, but the capacity varies greatly. This is due to the differences in crystallographic structure, particle size distribution, location in the crystal lattice at which atomic substitution occurs, that is, in the octahedral in contrast to the tetrahedral portions of the lattice. As only limited substitution occurs in the crystal lattice of kaolinite and because kaolinite clay minerals are comparatively coarse, cation exchange capacity is low. Spiel (1940) showed that the cationic exchange capacity of kaolinite increases with fine grinding. This increase is probably due to the greater number of broken bonds and the partial destruction of the clay lattice. The exchange positions for kaolinite are located mainly on the external surfaces.

Atomic substitution in the lattice is much greater in montmorillonite than in kaolinite minerals. This, together with characteristically very small particle sizes, produces high exchange capacity in montmorillonite. In contrast to kaolinite, Spiel (1940) found that fine grinding does not increase the cation exchange capacity in montmorillonite. This is because, as mentioned earlier, montmorillonite particles are so small and their specific surface per gram is large compared to kaolinite that further grinding will not produce any more particles or surfaces.

1.7 Soil / Water Behaviour

Three broad approaches are identified in the description of soil / water behaviour. These are: the model, energy / thermodynamic and electrical charge.

The model approach attempts to describe the geometry of the soil structure and can be employed to either determine the shape of the pore water films and amount of air voids or relate the mechanical behaviour of the soil to the applied stresses.

The energy / thermodynamic approach considers the total energy of the system rather than the soil geometry and in particular the energy with which water is held within a soil.

The electrical charge approach considers soil behaviour (for example, expansion) in terms of the attractive and repulsive electrical charges at interparticle level.

1.8 Clay / Water Systems

Clay and water are two of the most common substances in the earth's crust. Frequently the mutual interaction between clay and water controls the formation of clouds and the infiltration of rain water into the soil. It is often responsible for the failure of buildings and highways and the decreased production of oil wells.

All clay minerals are built up of three basic parts: a silica sheet, an octahedral layer and a water layer. The first two parts have been explained in Section 1.2.2.

The third component of all clay minerals is a structural water layer sometimes contaminated with foreign ions. There is still some ambiguity on the physical arrangement of this layer. However, some form of rigidly held non liquid layer of H_2O attached to the exposed surfaces of the sheet must be present to explain many of the properties exhibited by clays (Dennen and Moore (1986)). This layer is not of fixed

thickness but may be several, perhaps 5 to 10, molecules thick before its rigidity is lost. The attachment of a water layer to the basal surfaces of clay mineral particles provides both an interparticle bond and an interparticle lubricant depending on the number of water molecules involved. Changes in its thickness due to wetting or drying can cause significant swelling or shrinkage in a clay mass. Over thickening leads to dispersal of the particles and over thinning to increased rigidity.

The interparticle water serves to bind the individual particles together and provides some resistance to deformation of the mass. The clay / water mass will, however, yield to relatively small differential forces without rupture, that is, be plastic. The degree of plasticity is thus a function of the water content. As the amount of water decreases, its ability to lubricate the system lessens and eventually failure will be brittle. Increasing the amount of interparticle water eventually separates the particles until there is no cohesion between them and the system is liquid. The Atterberg limits, which describe these mechanical differences, are dependent upon many factors e.g. clay mineral type, kind, amount and ionisability of ions adsorbed or included in the water layers, particle size, ionic substitution within the clay mineral structure and desiccation history. Dennen and Moore's (1986) variation of plasticity index with liquid limit is shown in Figure 1.9. This includes the effects of two minerals, kaolinite and montmorillonite, and three different adsorbed cations, Ca, Na and Li. Plastic limit,

liquid limit and plasticity index, all increase with decreasing particle size.

1.8.1 Clay Mineral Surface / Water Interaction

Clay hardens as it dries from a liquid slurry to a plastic material and eventually to a brittle solid. Reversing this process is more difficult and, although on rewetting from the solid state a few types of clay will imbibe water spontaneously to form a slurry, mechanical work is generally needed. This irreversibility results from the nature of forces between the clay particles and how these are influenced by diffuse electrical double layers that form on their surfaces. Further differences are attributable to the types of cation balancing negative charge on the clay surface, and also to specific effects such as the chemical composition of the mineral and the density of electric charge that forms as a result on the particle surfaces.

The application of modern physical techniques to the study of clay / water systems has greatly increased the knowledge about the state and properties of water on clay surfaces. Nuclear magnetic resonance (NMR) (Newman (1987)), electron spin resonance (ESR) (Newman (1987)) and infrared spectroscopy (Farmer and Palmieri (1975) and Newman (1987)), details of which are beyond the scope of this thesis, have all combined to define the diffusion, rotation and bonding of water near clay surfaces much more precisely. These studies suggest that the influence of the clay surface on the ordering of H_2O molecules does not extend much beyond the second or third layer of molecules. Beyond this distance

water appears to behave very much like liquid water (Newman (1987)).

1.9 Properties and Performance of Clays

1.9.1 Particle Size Distribution

Clays are predominantly composed of particles less than 2 microns in diameter, but sand, silt, gravel and fragments of organic remains in varied proportions are always present.

Clay minerals of montmorillonite, especially with sodium as the exchangeable cation, are particularly prone to cleave and disintegrate along cleavage surfaces during agitation in water. Consequently, particle size analysis made by differential settling almost always indicates smaller sizes than are actually present in the natural clay. Montmorillonite minerals segregate into fractions less than 0.08 micron during fractionation of clays and shales (Pennington and Jackson (1947)). Ca, Mg, K and H montmorillonites are not as dispersable, especially after drying, as Na montmorillonites so that apparent particle size will be greater if cations other than Na predominate (Winterkorn and Moorman (1941)). Adsorption of organic molecules may also inhibit dispersion of clay particles.

Kaolinite tends to concentrate in the size range 0.2 to 2.0 microns. Many kaolins are difficult to disperse to particles as small as 1 micron. Yet individual kaolins release kaolinite into fractions as small as 0.08 micron.

The primary cause of the differing contribution of the several clay minerals to soil mechanics properties lies in the facility with which they are dispersed to particles less than 0.05 micron. The proportion of the fraction less than

0.05 micron decreases from montmorillonite to illite to halloysite to kaolinite (Marshall (1949)). Of all these minerals, the particle size distribution of montmorillonite clay is controlled most strongly by the exchangeable cation.

1.9.2 Liquid and Plastic Limits

Mielenz and King (1955) compiled data from the works of Winterkorn and Moorman (1941) and Samuels (1950). It demonstrates the marked reduction in liquid limit and plasticity index of montmorillonite (Wyoming bentonite) by replacement of naturally occurring sodium. The liquid limit and plasticity index decrease in the order:

$$Na^{+} > H^{+} > K^{+} > Mg^{2+} > Al^{3+} > Fe^{3+} = Th^{3+}$$

Changes in liquid limit and plasticity index are far less marked for kaolinite, illite and beidellite.

Sodium influences properties of clays far beyond relative abundance in the exchange positions. According to Winterkorn (1953), if as little as 15 percent of the exchange capacity is occupied by sodium, montmorillonite exhibits the properties of homo-ionic Na montmorillonite. Introduction of any of several cationic aliphatic amines to montmorillonite clay causes hydrophobic qualities. This radically decreases the liquid limit and plasticity index, and significantly changes other physical and physical-chemical properties (Davidson (1949) and Davidson and Glab (1949)).

1.9.3 Permeability

In their usual occurrence, clay minerals in earth materials are extremely fine and tend to fill void spaces lying between grains of silt, sand and gravel. Consequently, clay

minerals characteristically decrease permeability of earth materials, especially of remoulded clays in which structural features such as shrinkage cracks, joints, stratification or shear zones have been destroyed. Permeability decreases with the regularity of particle size distribution of the material, especially with the extension of the size range into fractions below 1 micron. According to Lambe (1954), the major factors influencing the permeability of fine grained soils are:

1) soil composition,
2) characteristics of the fluid,
3) void ratio,
4) fabric, and
5) degree of saturation.

For remoulded clays, under ordinary circumstances of saturation by relatively pure water, permeability of earth materials is least if montmorillonite type clays are present and greatest if kaolinite is the clay mineral component. In comparable tests of modifications of Wyoming bentonite, Samuels (1950) determined the permeability relation to be Th > Al > Ca > Na at pressures less than 107.3 kN/m^2. At greater pressures, the permeability of the Ca and Na modifications were found to be virtually zero. The permeability of the Al modification became negligible at pressures of about 536.5 kN/m^2. Permeability of treated kaolin was similarly affected by exchange of ions but the permeability was 4 to 20 times greater than that for the bentonite modifications. For the kaolin the permeability decreased in the order Al > Ca > H > Na, for a given pressure. The permeability of kaolin can be decreased greatly by a decrease in particle size and an increase in surface area (Harman and Fraulini (1940)). With an increase

of apparent surface area from about 30 to 240 m^2/g, Mielenz and King (1955) found that the permeability of kaolin decreased by a factor of 3.5.

1.9.4 Thixotropy

As originally defined (Freundlich (1935) and Green and Weltmann (1946)) thixotropy is an isothermal, reversible, solution-gel transformation. The phenomenon is well exemplified by a marked increase in viscosity of Na bentonite solutions with rest, and the subsequent decrease in viscosity with agitation.

Thixotropy develops to a degree in almost all solutions. However, the rate of formation and break down and its strength vary greatly with factors such as particle size, particle shape, surface activity, exchangeable cations, concentration, nature of the fluid phase and electrolyte content. Among clay minerals, the property is most easily demonstrated in bentonite water slurries. For Na montmorillonite, 80 millilitres of water can be added to 1 gram of clay and the mixture forms a gel which will not flow from a test tube 8 mm in diameter 1 minute after agitation has stopped. In a similar test, 30 millilitres of water can be added to 1 gram of kaolinite (Winkler (1949)) to have the same effect. Thixotropy of bentonite is reduced if alkali ions are replaced by Ca^{2+} or Ba^{2+} and is eliminated by complete removal of alkali ions and their replacement by H^+ or polyvalent ions (Freundlich (1935) and Houwink and Burgers (1939)).

1.9.5 Shear Resistance

Resistance to shearing stress is developed in soils by particle interlocking, meshing of irregularities on particle surfaces, adhesion, cohesion and cementation. This is supplemented by secondary minerals, such as iron oxides, carbonates and quartz which are deposited interstitially. Clay minerals are of fundamental importance in establishing shear resistance of earth materials. At low water content, restricted water films subject the mass to compressive stresses of considerable magnitude and thus increase shear resistance. However, an increasing degree of saturation decreases the effective compressive stress due to the development of water films around the clay minerals. In the same way, if the degree of saturation is increased by rapid consolidation of the earth material with loading, shear resistance of the material is reduced by pore water pressure. Consequently, shear resistance of earth materials depends not only upon the structural integrity of the solid constituents, but also upon the ability of the material to drain contained water and air as readjustment of the structure takes place in response to load.

Clay minerals and the fabric of granular earth materials play critical roles in both phenomena. Winterkorn and Moorman (1941) found the shear resistance of cohesive soils to be approximately a logarithmic function of the moisture content in the lower part of the plastic range. For remoulded soils, the moisture content yielding maximum cohesion is so low that the workability of the material is poor and low void ratio and high density in the remoulded

specimen are attained only with great difficulty. To obtain both high density and high shear resistance Johnson and Davidson (1947) recommended compaction at optimum moisture content, followed by drying to the moisture range producing maximum shear resistance.

In studies of Wyoming bentonite, Samuels (1950) demonstrated increasing shear resistance with the exchange of cations in the series Na < Ca < Al. Samuels (1950) also found that the shear resistance of Na, Ca and Al modifications of kaolin is essentially identical and similar to the shear resistance of Wyoming bentonite containing Al as the exchangeable cation. Shear resistance is increased in clayey materials by development of thixotropic strength, but Hvorslev (1939) stated that this element of shear resistance is lost with disturbance of the fabric by vibration or rapid strain (Mielenz and King (1955)).

1.9.6 Unconfined Compressive Strength

Unconfined compressive strength depends upon many aspects of fabric and composition, including size, shape and the distribution of voids and the content of water and air. These factors control the response of earth materials to loading, including elastic and plastic adjustments, as well as shear failure.

Clay minerals make a significant contribution to the response of earth materials to loading. It is because, when dry, they develop relatively high strength through formation of adhesive and cohesive bonds throughout the mass. Introduction of small proportions of clay minerals to a sand or silt greatly increases compressive strength, the maximum

strength of the mixture exceeding that of either the sand or silt or the clay alone. The strength of such mixtures increases more rapidly with small additions of montmorillonite minerals in contrast to kaolinite, halloysite or illite types. This is due to the finer particle size distribution and greater dispersion of the montmorillonite minerals.

1.9.7 Consolidation

Consolidation of earth materials with loading represents adjustment of the internal structure of the solid framework by rotation and sliding of the constituents (Mielenz and King (1955)) and expulsion of water from the consolidating mass. For natural earth materials, consolidation as a result of structural adjustment is greatest in materials of very low unit weight, such as loess, volcanic ash or organic soils. The rate and magnitude of consolidation are greatly increased by wetting. There is consequent decrease in shear resistance of the soil constituents, especially if expansive clay minerals are an essential binding agent.

As the content of clay minerals increases in the soil, the size of voids and their continuity decrease so that pore pressures develop unless application of load is very slow. Consolidation is dependent mainly upon drainage of air and water from voids. Consequently, permeability is the critical control of consolidation rate. Samuels (1950) found the consolidation rate of Wyoming bentonite increases in the order Na < Ca < Al < Th, and that of kaolinite to be Na < Ca. This sequence is the order of increasing permeability in these clays. As reported by Preece (1947),

Cooling demonstrated the dependence of consolidation of bentonite upon exchangeable cations. At a given pressure up to 536.5 kN/m^2, void ratio decreases in the order Na > Ca > Th > Al. At slightly greater pressures, the void ratio of all modifications is in the range 1.3 to 1.5. The compressibility is greatest for sodium and decreases in the order Na > Ca > Al > Th, the latter two exhibiting similar rates.

With normal fabrics, earth materials containing kaolinite as the predominant clay mineral consolidate less than those containing members of the montmorillonite group. Samuels (1950) demonstrated the lesser degree of consolidation of kaolinite in contrast to bentonite, the change in void ratio for the sodium kaolinite, with pressure from zero to 858.4 kN/m^2, being only 1/14 that of sodium bentonite. The compressibility decreased in the order Al > H > Ca > Na. This sequence is essentially the reverse of that exhibited by bentonite, the difference arising from the distinctly different proportions of particles less than 1 micron in the cationic modifications of the two soil types (Mielenz and King (1955)). For the bentonite, the fraction smaller than 1 micron is about 90% for the Na modification, 81% for the Ca type and 60% for the Al type. For kaolinite, the less than 1 micron fraction ranges only from 82% for the H and Al types to 88% for the Na types.

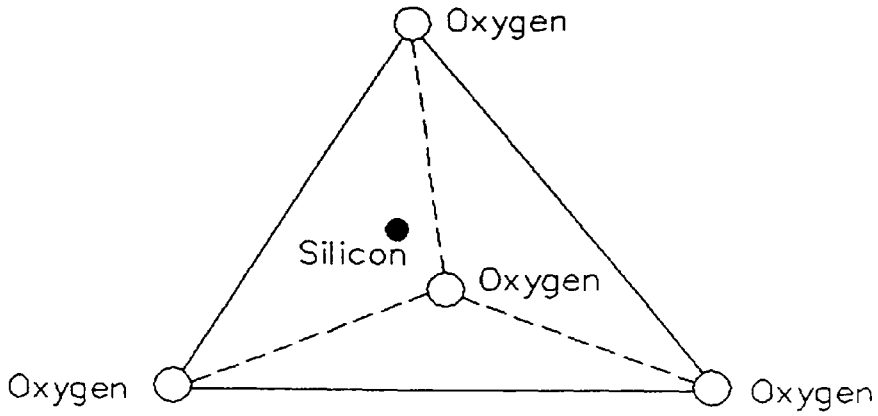

Figure 1.1 Silicon-Oxygen tetrahedral unit.

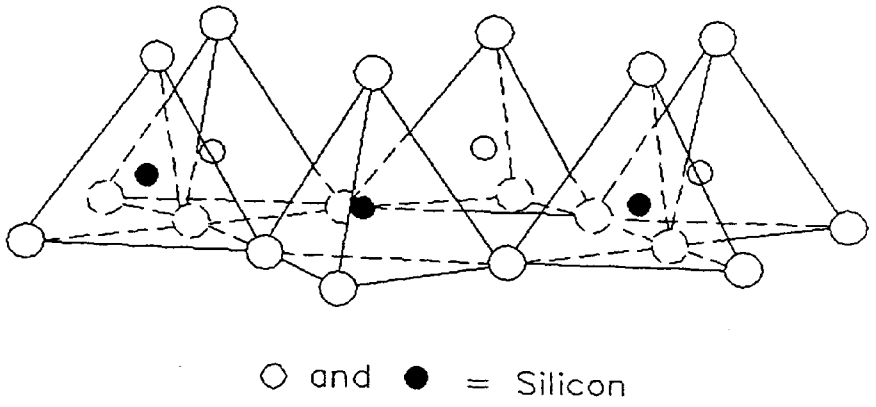

Figure 1.2 Tetrahedral units forming silica sheet.

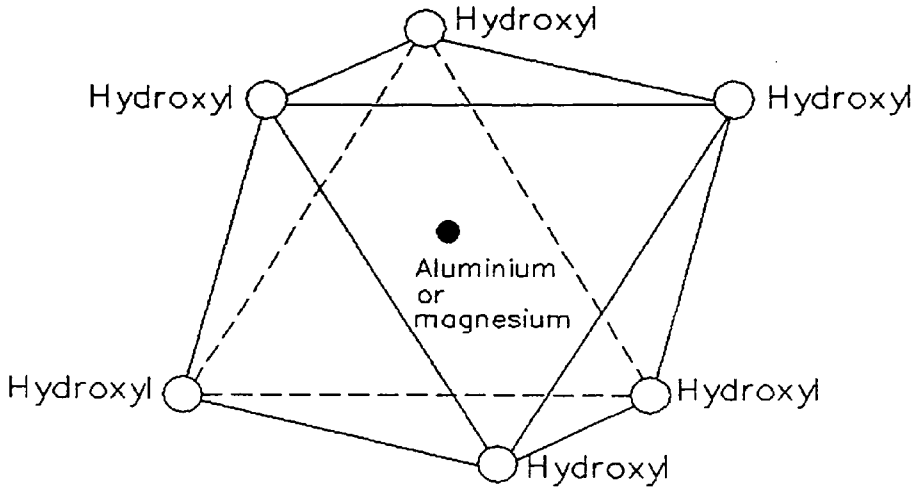

Figure 1.3 Aluminium or magnesium octahedral unit.

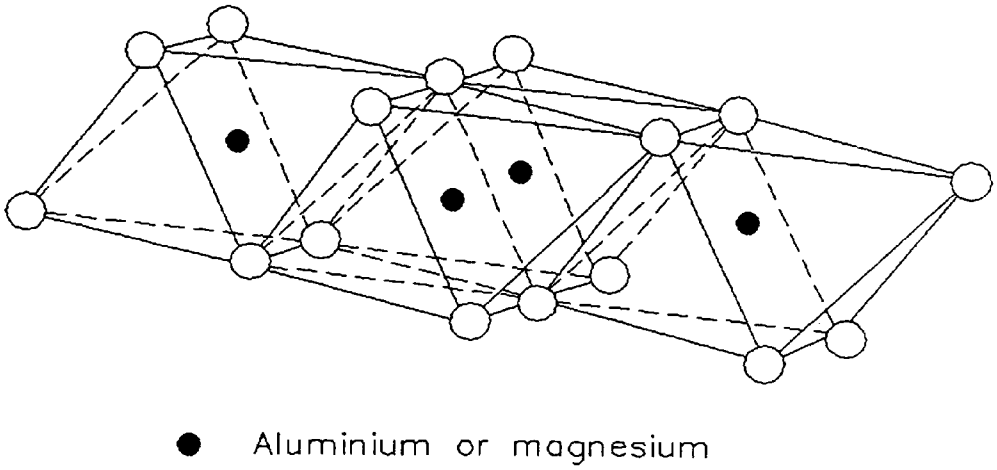

Figure 1.4 Octahedral units forming gibbsite sheet.

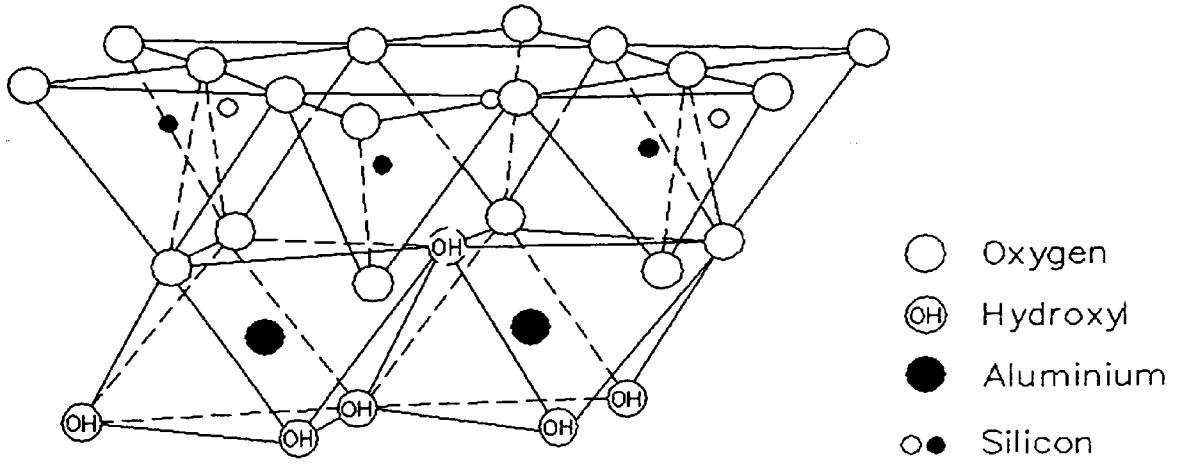

Figure 1.5 Diagrammatic sketch of kaolinite structure.

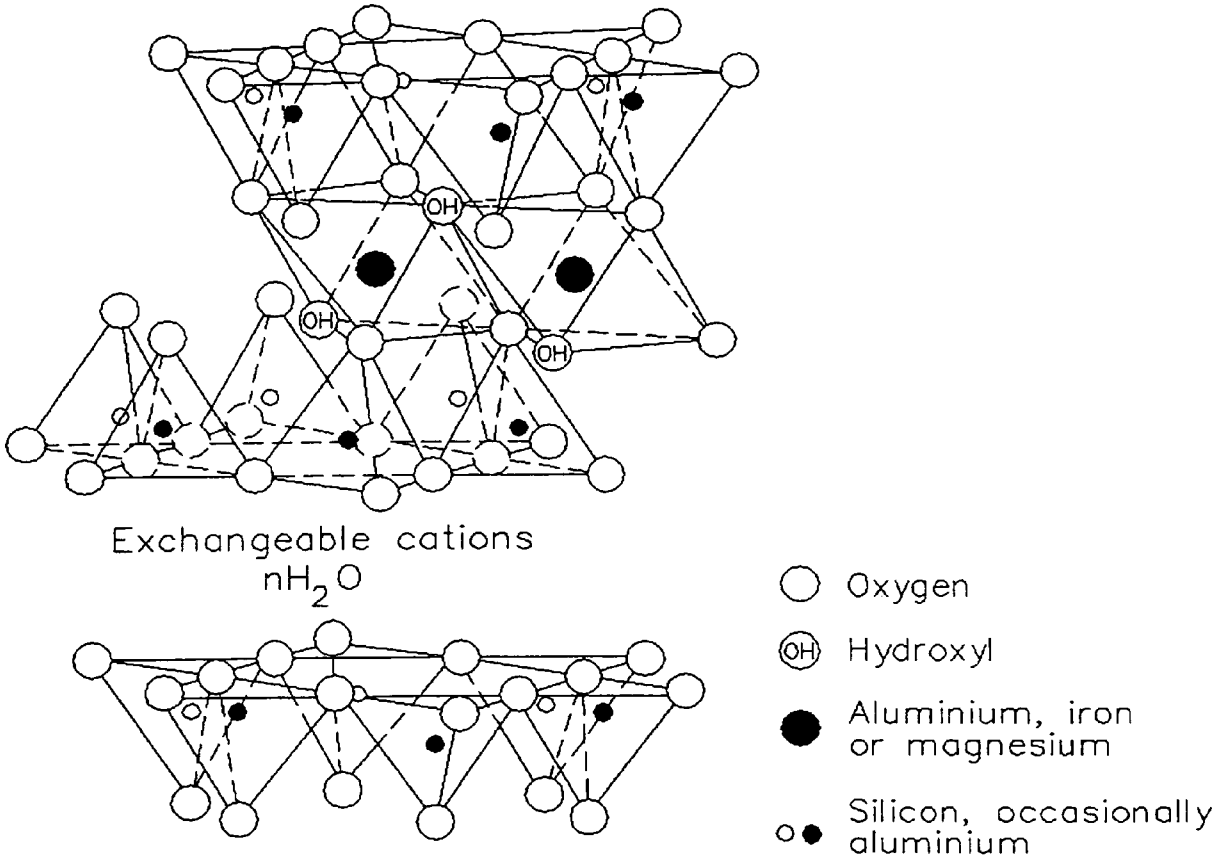

Figure 1.6 Diagrammatic sketch of montmorillonite structure.

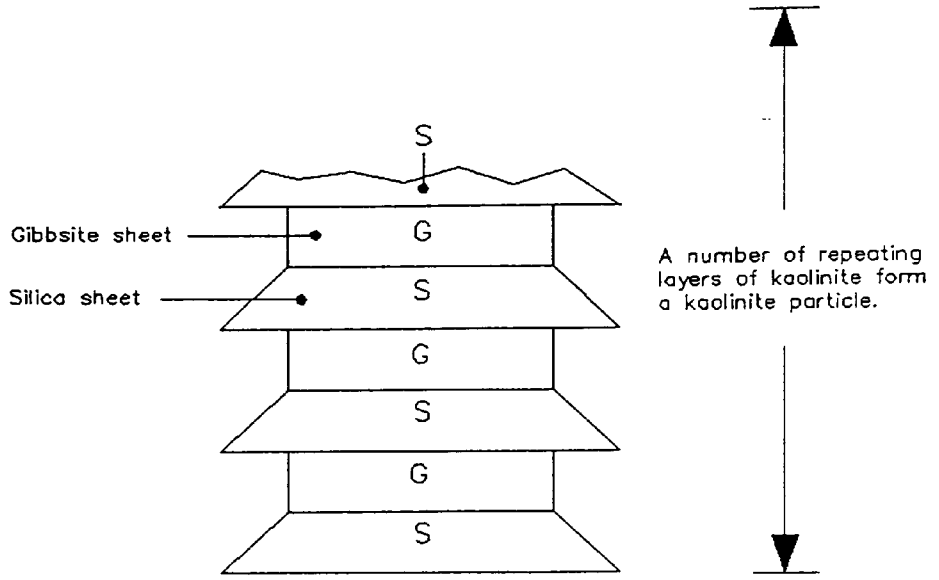

Figure 1.7 Symbolic structure of kaolinite.

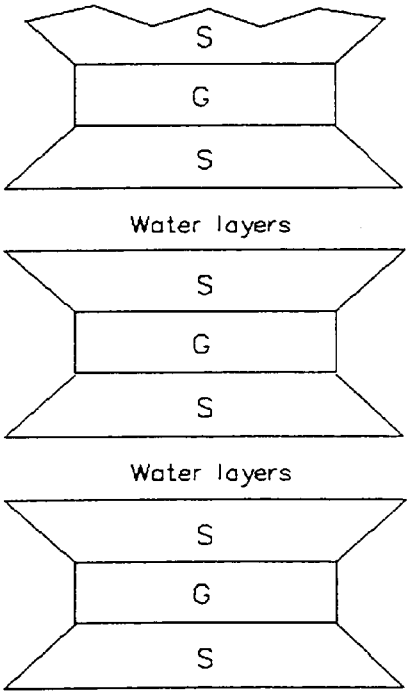

Figure 1.8 Symbolic structure of montmorillonite.

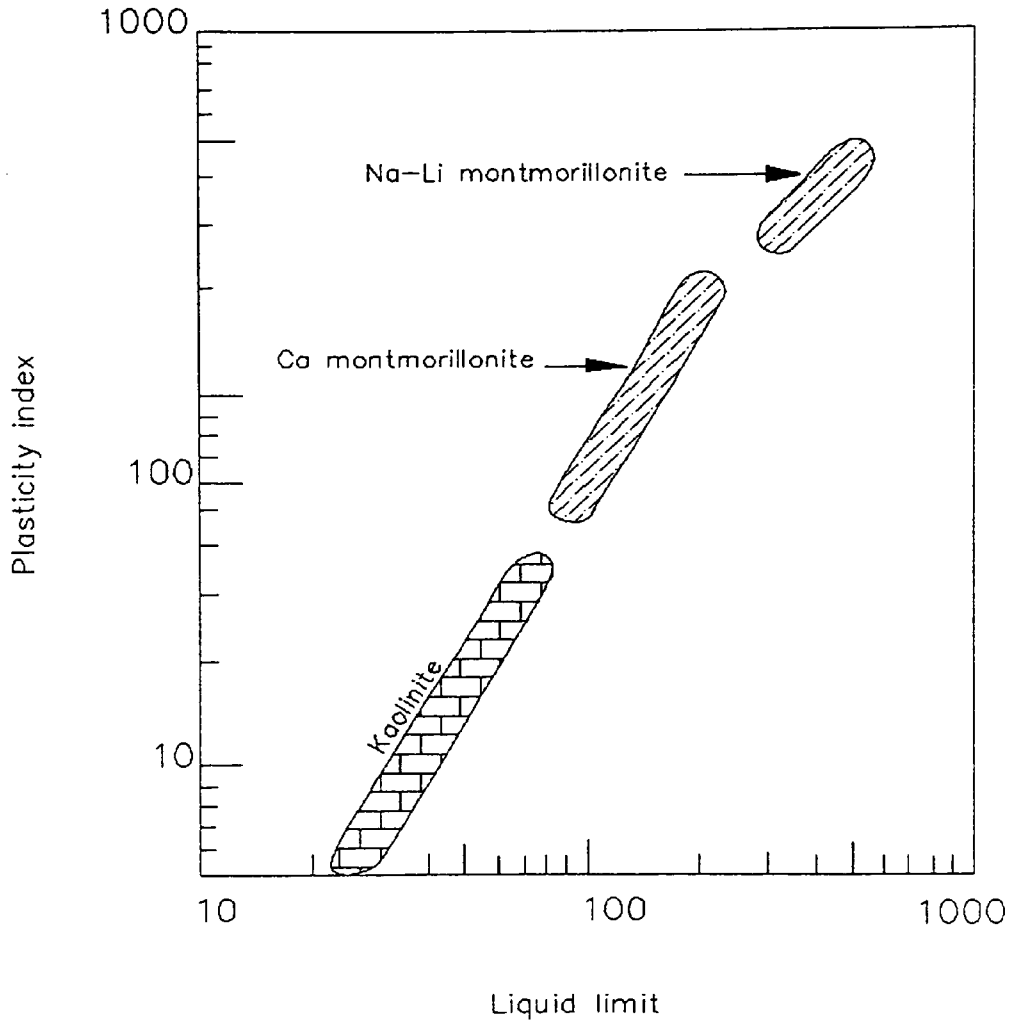

Figure 1.9 Liquid limit and plasticity index (After Dennen and Moore (1986)).

CHAPTER TWO

EXPANSIVE CLAYS

2.0 Introduction

One class of clay minerals, the smectites, formed by rock weathering, especially by the breakdown of volcanic ash, has the ability to readily adsorb or lose water molecules between the sheets of atoms that comprise its structure. Smectites have montmorillonite as the most common mineral. If these clay minerals accumulate in a soil or are concentrated into beds by transport and deposition, the resulting mass will swell or shrink, depending upon the availability of water, with disasterous results to structures on or within it. It is termed a vertisol by pedologists and expansive or swelling soil or clay by engineers.

The term expansive soil has generally been applied to soil volume, which may increase or decrease as the soil's moisture content varies. When the ASCE organised the Expansive Soil Research Council (1960s) on the Expansive Behaviour of Earth Materials, it recognised that such diverse natural materials as pyrites and white alkali (sodium sulphate), as well as many clays, can cause abrupt volume changes due to swelling and shrinking. It also recognised that expansive materials occur both as soil and as rock, so that use of the term soil may be misleading. For convenience, however, all expansive earth materials subject

to shrink-swell volume changes are commonly termed expansive soils.

The detrimental effect of expansive clays on structures has been noted frequently in the past. It has stimulated numerous studies of the factors causing swelling and swelling pressure. These include the mineralogical composition of the soil, its initial water content and physical structures, the effect of confining pressure, the availability of free water or electrolytes, the presence of exchangeable cations and anions, the stress history, time and temperature.

One problem with expansive soils is that they move. Expansive soils change their horizontal and vertical positions beneath construction works, resulting in damage. Horizontal movements of expansive soils significantly affect construction on slopes and are a factor in many landslides. Measured free swelling of montmorillonite ranges between 50% and 2000% and the expansive pressures generated are in the range 150 kN/m^2 to 500 kN/m^2 (Dennen and Moore (1986)). These pressures are well in excess of those imposed by small buildings which will, in consequence, be uplifted and rotated by the expanding soil. A less obvious but potentially more dangerous failure is that of buried utility lines.

In the United States each year, shrinking and swelling soils inflict about $8b in damages to houses, buildings, roads and pipelines. Within the average American's lifetime, 14% of the land will be lashed by earthquakes, tornadoes and floods but over 20% will be affected by expansive soil movements.

Expansive soils, found in every state, cover 1/4 of the U.S. Over 250,000 new houses are built on expansive soils each year (1973 figures); of these 60% will experience only minor damage during their useful lives but 10% will undergo significant damage. In America, one person in ten is affected by floods but one in five by expansive soils (Jones and Holtz (1973)).

In the United Kingdom, figures published by the Building Research Establishment show the value of claims as a result of shrinking soils running at £200m, three times the 1988 level. This well exceeds the last record in 1984 and some experts predict claims could reach as much as £500m. If the dry seasons are followed by wet ones again, the claims will increase greatly as heave damage is twice as costly as subsidence damage.

The presence of expansive soil at an engineering site will probably be known to local builders or engineers. A characteristic microtopography of irregular ridges termed gilgai develops on undisturbed ground and soil and mechanical testing should be used when assessing soil conditions at any project site of significant size. The more reliable tests use the consolidometer, whereby the expansive pressure caused by introduction of water to a confined sample is directly measured. In Figure 2.1 it can be seen that percentage swell is influenced by both dry density and liquid limit values. A percentage swell greater than 3 indicates significant swelling potential.

2.1 Mechanics of Heave or Shrinkage

Ordinarily, the pressures applied to an expansive clay by a highway pavement or a light building are very small, rarely getting above 20 kN/m^2. These pressures are insignificant compared with the kinds of swelling and shrinking stresses these soils can develop. Consequently, it is the usual practice to predict heaving or shrinking based on the expected change of water volume (McDowell (1956) and Livneh et al (1973)) or void ratio (Jennings and Knight (1957)) or expected strain due to a change of suction (Lytton and Woodburn (1973)). Some prediction methods use a combination of suction and water content change (Richards (1967) and Johnson and Desai (1975)) to predict the vertical movement. In every case, the prediction is more accurate if the weight of the overburden, the stresses applied by the overlying structure, the cracking fabric of the soil and the actual change of moisture or suction are used.

2.2 Expansive Soil Occurrence

Donaldson (1969) and Chen (1975) have reviewed the occurrence of expansive soils on a worldwide basis. The latter author's review is based largely on the former's work. Donaldson (1969) showed his findings of heave on a map in Figure 2.2. However, much more data on the location of expansive soils are now available which render Donaldson's map inadequate.

2.3 Identification of Expansive Soils

In identifying expansive soils, it is useful to specify some of the geological characteristics that indicate the presence

of expansive soils. Jones (1979) listed guidance notes for visual observation under the following sub-headings:

- under dry soil conditions,
- under wet soil conditions,
- under any conditions,
- alkali in soils,
- pyrites in soils.

Typical laboratory tests for examining suspect soils are:

1) Atterberg limit tests will often identify expansive soils, as most expansive soils will have a plasticity index greater than 15. The expansive potential of soils generally increases with increasing plasticity index.
2) Shrinkage limit tests are simple and generally provide significant guidance regarding a soil's possible expansive behaviour.
3) Consolidometer tests, in which compacted soils are loaded and then wetted, with measurements of displacements, generally provide reliable quantifications of a soil's expansive potential.

Ranganatham and Satyanarayana (1965) proposed a method of identifying expansive soil from the shrinkage index SI = LL - SL. They did not take plasticity characteristics of the soil into consideration. Komornik and David (1969) reported that there is a good correlation between plasticity index (the parameter related to the specific surface area of clay minerals) and free swell. They also reported that there was almost no correlation between shrinkage limit and free swell. Dakshanamurthy and Raman (1973) were also of the opinion that the plasticity characteristics of the soil should be considered to identify an expansive soil rather

than mere shrinkage index value. They proposed a chart (Figure 2.3) in which (PI, LL) data provide plasticity rating of the expansive soil and (SI, LL) provide swelling rating. It may be noted that as the plasticity of the soil increases, the swelling also increases. They concluded that the chart involving index properties (liquid limit, plasticity index and shrinkage index) is a reliable method for identifying expansive soils from non-expansive ones.

The plasticity index and shrinkage limit tests are much less definitive for measuring expansion than the consolidometer tests. This is because there are some soils that have a high plasticity index but a low swell potential and vice versa.

Holtz and Gibbs (1956) were the first to study the identification of expansive soils based on classification tests. In addition to this they gave a new method called free swell which is the amount of swelling that a soil experiences when allowed to swell under no load; a free swell value of less than 50 percent indicates a non-expansive soil whereas a value more than 100 percent indicates a highly expansive soil. They also found that high liquid limit and plasticity index values usually indicate the characteristic property of expansive soil. Altmeyer (1956) criticised Holtz and Gibbs and postulated that the shrinkage limit was a better indication than liquid limit. The basis of the application of shrinkage limit for the identification of expansive soils according to Altmeyer (1956) was as:

Shrinkage Limit	Volume Change
< 10	critical
10 - 12	marginal
> 12	non critical

Raman (1967) quoting Sowers gave volume change potential of soils based on plasticity index and shrinkage limit values as below:

PI	SL	Volume Change
0 - 15	> 12	low
15 - 30	10 - 12	moderate
> 30	0 - 10	high

Ladd and Lambe (1961) gave an empirical approach to identify expansive soils from the tests carried out on a potential volume change PVC meter. Soils were classified according to four categories:

PVC Rating	Category
< 2	non critical
2 - 4	marginal
4 - 6	critical
> 6	very critical

Seed et al (1963) studied the prediction of swelling potential of artificial soils with reference to activity, clay fraction of whole sample and percentage swelling.
Williams (1958) gave a simple classification based on the relationship between the plasticity index of the whole sample and the percentage clay fraction for potential expansiveness of soils.

2.4 Factors Affecting the Soil's Expansive Behaviour

The behaviour of an expansive soil is affected by a wide variety of factors. Any environmental factor that can affect

the amount or character of water reaching an expansive soil may be expected to affect its behaviour. The way in which an expansive soil occurs, such as whether or not there is a shallow ground water table beneath it, has a significant bearing upon its probable behaviour. Its natural behaviour can be materially altered (usually aggravated) by remoulding. The type of structure and how it is constructed can have a major effect upon its subsequent performance on an expansive soil. Preparation and drainage of construction sites, as well as any landscaping of the completed construction, can either aggravate or minimise heave. The soil can be chemically stabilised as well.

The behaviour of expansive soil can be predicted and included in design considerations only if the problem is recognised at the site investigation stage.

2.5 Causes of Soil Swelling

The current concepts of the causes and effects of swelling in clay soils postulate the existence of forces of attraction and repulsion between the elemental soil particles. The forces of attraction are constituted primarily by so-called van der Waal forces plus electrical forces between positively charged particle corners or edges which may be cross linked to negatively charged particle forces. Both of these sets of forces act at very short distances. The van der Waal forces are largely independent of the medium in the voids of the soil, but the electrical forces of attraction are affected to a degree by the existence and nature of water which may be in the voids. The forces of repulsion are predominantly constituted by, first,

the forces of hydration at the surface of particles, and second, osmotic forces produced in the diffuse electrical double layers in the aqueous phase occupying the voids in the soil. The forces of hydration are operative over distances of only molecular order of magnitude, but the osmotic forces are effective over much greater distances of a maximum order of 0.1 micron.

2.6 Swelling Potential of Clay Soils

A solid is said to swell when it takes up a liquid (Katz (1933)), and satisfies the three conditions:

a) it does not lose its apparent (microscopic) homogeneity,
b) its dimensions are enlarged, and
c) its cohesion is diminished: instead of hard and brittle, it becomes soft and flexible.

The swelling of clays results from the increase in the thickness of the diffusion ion layer as water is supplied. A number of attempts have been made by various investigators to develop a reliable method for identifying the swelling e.g. Holtz and Gibbs (1956), Jennings and Knight (1957), De Bruijn (1961), Seed et al (1962) and Nayak and Christensen (1971). Holtz and Gibbs (1956) proposed a criterion for determining qualitative expansibility of clays based on colloid content, plasticity index and shrinkage limit. Methods of identification of swelling clays on the basis of the plasticity index primarily, have been described by Seed et al (1962). Another method utilising the dry density and liquid limit was suggested by Vijayvergiya and Sullivan (1972). Vijayvergiya and Ghazzaly (1973) proposed a simple

way of identifying the swell potential of clays based on the swell index (Is) where

$$Is = \frac{W}{LL} \qquad (2.1)$$

where: W = natural water content (%), and
LL = liquid limit (%)

The relationship between Is and swell potential for a wide range of liquid limits is shown in Figure 2.4.

Swell potential is defined as the percentage of axial swell under 1 psi (6.9 kN/m^2) surcharge of a laterally confined specimen compacted at optimum moisture content to maximum dry density in the standard AASHTO compaction test.

Based on these criteria, a well defined relationship was established by Das (1985) between the swell potential (S), the activity (A) and percentage of clay fraction (C) (<2 μm) in the soil.

$$S = (3.6 \times 10^{-5})\, A^{2.44}\, C^{3.44} \qquad (2.2)$$

where:

S = swell potential (percentage of axial swell under 1 psi)

C = percentage of clay fraction, by weight

A = activity = $\Delta(PI)\ /\Delta C$

The above equation was further extended for an empirical relationship between swell potential and plasticity index of soil to

$$S = K(60)(PI)^{2.44} \qquad (2.3)$$

where C is assumed equal to 60.

For $K = 3.6 \times 10^{-5}$ $\quad S = (2.16 \times 10^{-3})(PI)^{2.44}$

Seed et al (1962) made the following classification of degrees of expansion:

Degree of Expansion	S
low	0 - 1.5
medium	1.5 - 5
high	5 - 25
very high	> 25

Ranganatham and Satyanarayana (1965) suggested a correlation for the swell potential S similar to that given by Seed et al (1962). This is based on shrinkage index SI, swell activity SA and percentage of clay fraction C in the soil. Swell activity (SA) is defined as:

$$SA = \frac{\Delta (SI)}{\Delta C} \qquad (2.4)$$

The correlations for swell potential S given by Ranganatham and Satyanarayana (1965) are:

$$S = (4.57 \times 10^{-5}) (SA)^{2.67} C^{3.44} \qquad (2.5)$$

$$S = (41.13 \times 10^{-5}) (SI)^{2.67} \qquad (2.6)$$

where C = 17.35.

The classification for degree of soil expansion based on the shrinkage index (SI) are:

Degree of Expansion	SI
low	0 - 20
medium	20 - 30
high	30 - 60
very high	> 60

2.7 Volume Change Behaviour of Clays

Numerous investigators have attempted to explain the volume change behaviour of clays. On the basis of published findings by Bolt (1956), Leonards and Altschaeffl (1964), Olson and Mesri (1970) and Sridharan and Venkatappa Rao (1971, 1972 and 1973), Sridharan and Allam (1982) proposed

two mechanisms for controlling the volume change behaviour of clays and related these to the modified effective stress concept.

In mechanism I, the compressibility of a clay is primarily controlled by the shearing resistance at the near contact points (the shearing resistances of which are not equal at all contacts), and volume changes occur by shearing displacements or sliding between particles. In mechanism II, the compressibility is primarily governed by the long range osmotic repulsive forces (also called double layer repulsive forces). Tests by Sridharan and Allam indicated that mechanism I primarily controls the volume change behaviour of non-expanding lattice structured clay minerals, whereas mechanism II operates in the case of expanding lattice structured clay minerals.

Few published data exist regarding the geotechnical behaviour of desiccated soils. These soils are subjected to periodic wetting and drying as a result of climatic changes. Review of literature on the action of climatic changes and also of water on soils (Sridharan and Allam (1982)) indicated that repeated wetting and drying can result in the aggregation of soil particles and cementation by compounds of Ca, Mg, Al and Fe. Presence of such cementing agents can reduce the compressibility of cemented soils. Such agents can also be removed by chemical treatment (Kenney et al (1967) and Loiselle et al (1971)). It has also been reported that the effect of desiccation is similar to that of heavy overconsolidation.

2.8 Volume Change Due to Hydration

Hydration volume changes are often measured by determining the free swell capacity. Data from Mielenz and King (1955) on selected clay minerals are presented in Figure 2.5. Kaolinite has the smallest swelling capacity of any of the clay minerals and nearly all of the swelling is of the interparticle kind. Illite swells between 15% and 120% depending on its mix with kaolinite or Ca montmorillonite. Ca depresses the swelling capacity of montmorillonite significantly; Na however can increase the swelling capacity to 2000%. Natural montmorillonites generally contain a mixture of Mg, K, Fe, and these exchangeable cations lead to swelling in amounts intermediate between those of the Ca and Na montmorillonites. Clearly, montmorillonites, which are widespread throughout the world, need investigating carefully before being constructed on.

According to MacEwan and Wilson (1980), the hydration of smectite is controlled by three interrelated factors:

i) the magnitude of the negative charge on the clay mineral interlamellar surface,

ii) the exchangeable cations which occur between the interlamellar surfaces and balance the overall negative charge on the layer surface, and

iii) the interaction of the water molecules (or other natural molecules) with the cations and with the clay mineral interlamellar surface.

2.9 Adsorption and Swelling Properties of Clay/Water Systems

Adsorption and swelling properties of clay/water systems may be divided into three parts:

1) clay-water vapour system,
2) clay-water liquid system in the gel state, and
3) clay-water liquid system in the fluid state.

In studying the swelling of clays in relation to hydration, it is necessary to distinguish between the two kinds of swelling:

1) intramicellar swelling which involves the expansion of the crystal lattice itself, commonly known as interlayer or interlamellar expansion, as found in montmorillonite,
2) intermicellar swelling which involves an increase in volume due to adsorption of water molecules between individual clay particles.

Intramicellar swelling can be identified and measured only by x-ray analysis, whereas intermicellar swelling can be determined from a measurement of the total increase in volume of the clay body or of the clay-bearing material with especially designed apparatus (Keen and Raczkowski (1921) and Winterkorn and Baver (1934)).

Initial swelling of dehydrated clay is characterised by sorption of the first few monolayers and by exchangeable cations adsorbing water molecules. The exchangeable cations attracted to internal and external mineral surfaces originate in the pore solutions (electrolytes). The fact that they are exchangeable can in turn influence the degree of interparticle and intraparticle swelling.

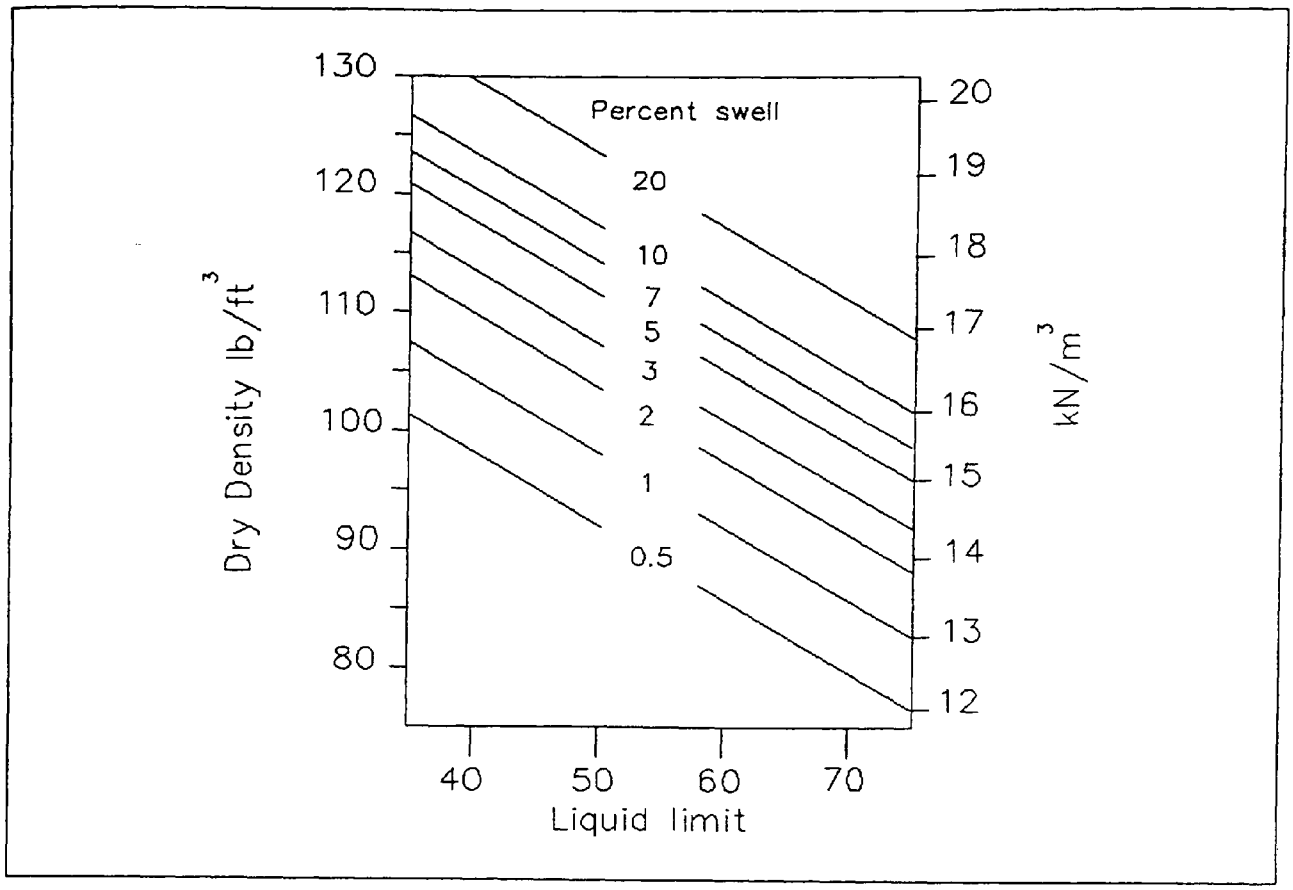

Figure 2.1 Percent swell as a function of dry density and liquid limit (After Dennen and Moore (1986)).

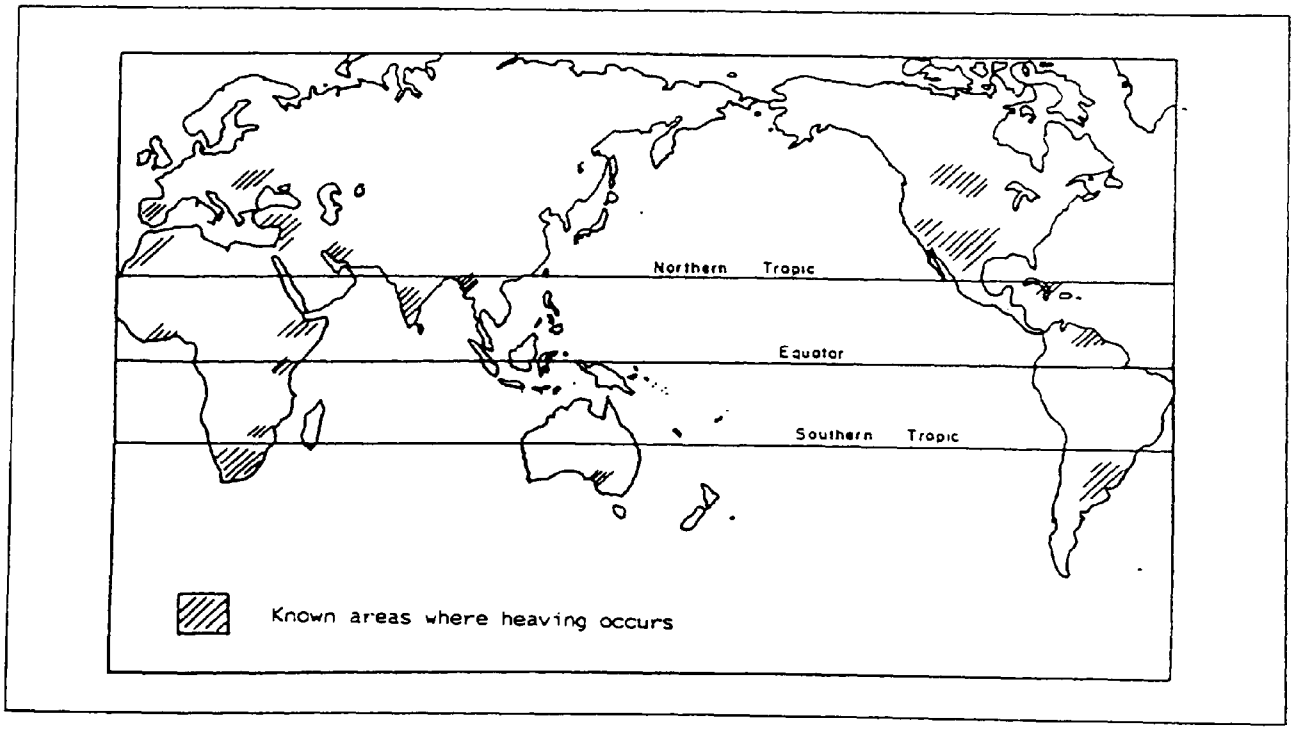

Figure 2.2 Distribution of reported instances of heaving (After Donaldson (1969)).

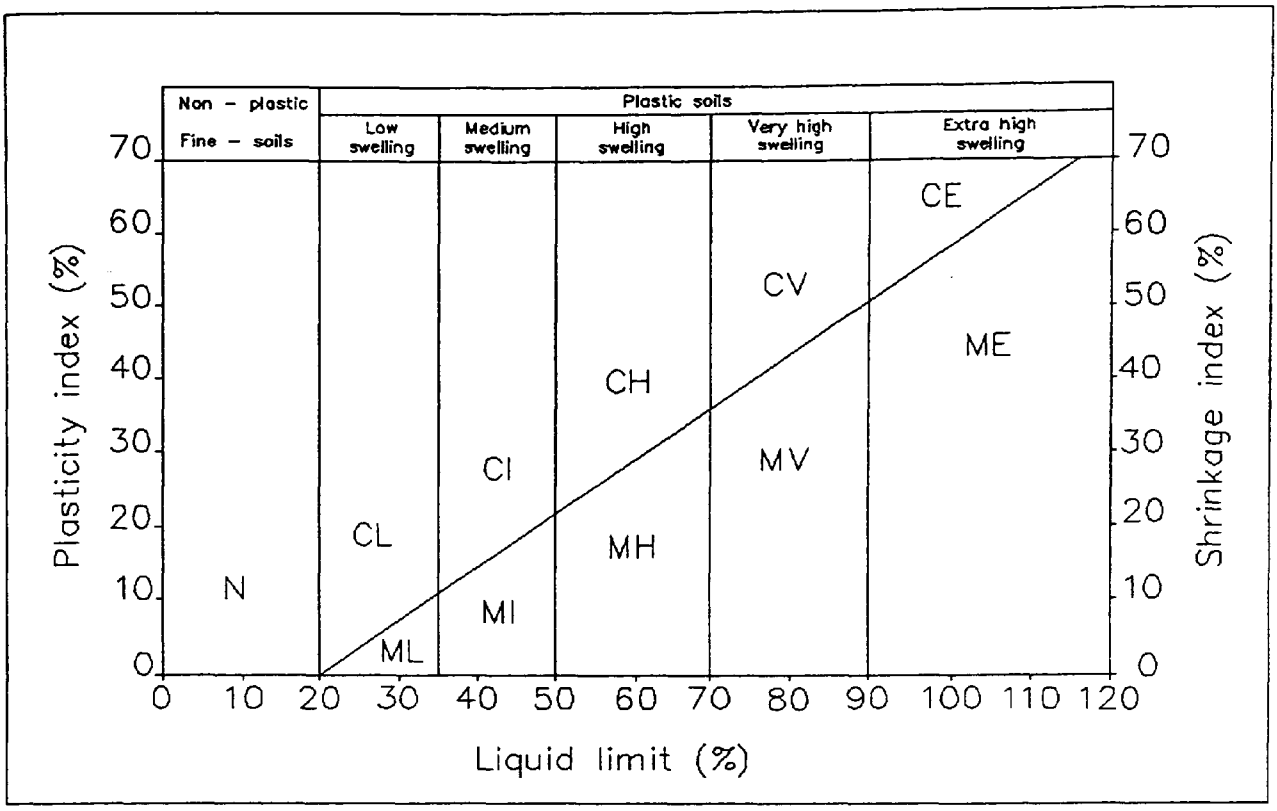

Figure 2.3 Proposed chart for potential expansiveness of soils (After Dakshanamurthy and Raman (1973)).

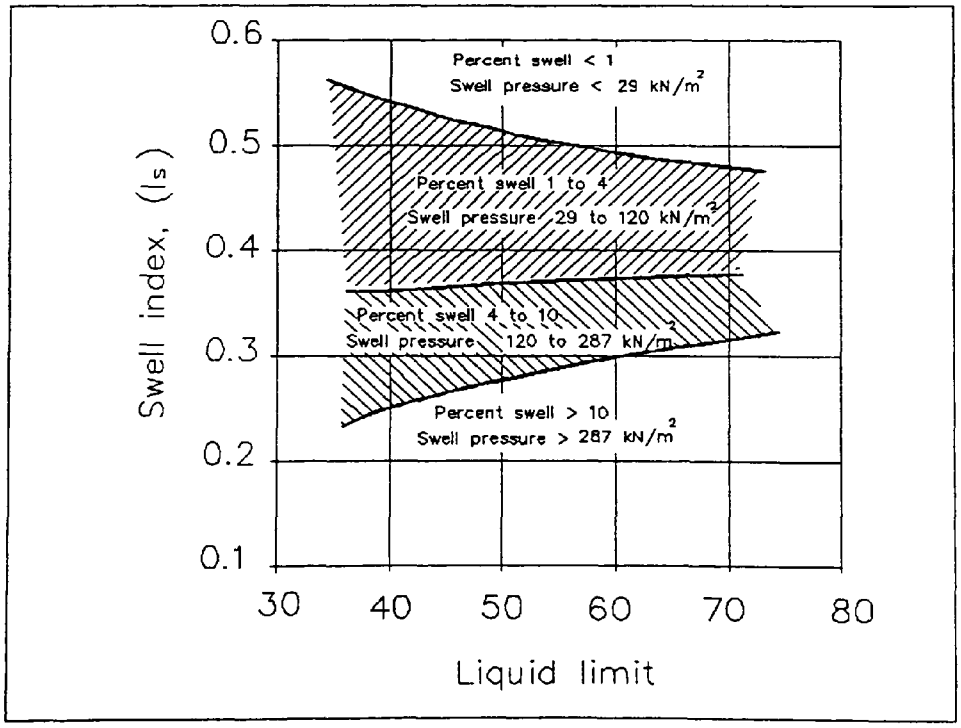

Figure 2.4 Relationship between water content and liquid limit for expansive clays (After Vijayvergiya and Ghazzaly (1973)).

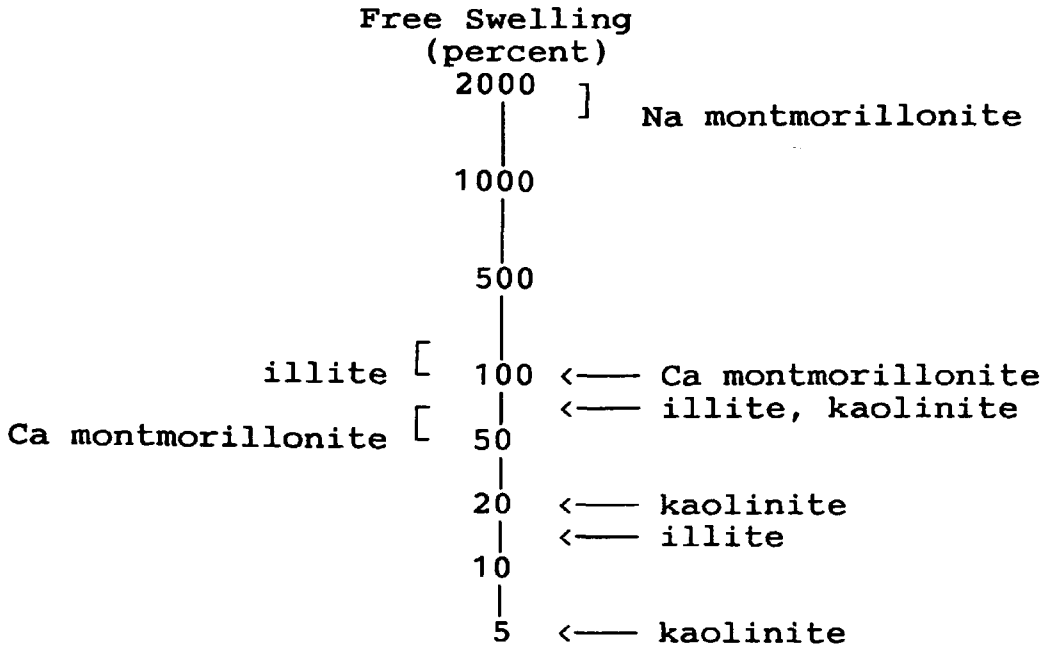

Figure 2.5 Free swell data on clay minerals (Modified from Mielenz and King (1955)).

CHAPTER THREE

LABORATORY REVIEW OF EXPANSIVE CLAYS

3.0 Introduction

Several general reviews of unsaturated expansive clays have been published, the most recent of which are by Johnson (1979) and Justo and Saetersdal (1981). Reviews of parts of the field have been published by several authors, for example, Mitchell and MacKechnie (1972), Chen (1975), Hamilton (1980), Krohn and Slosson (1980), Williams and Donaldson (1980), Driscoll (1984), Osman and Charlie (1984), and Williams et al (1985).

Damage caused by expansive soils is almost entirely restricted to light structures, such as houses and surface coverings, such as for roads and factory floors. The greater imposed stresses and the greater depth of foundations of larger structures help minimise swell.

Good reviews of the basic mechanisms of heave due to expansive soils are given by Jennings (1969, 1973). The types of foundation or construction used to minimise damage to light structures have been largely unchanged since the early 1960s, when Jennings and Evans (1962) and Jennings and Kerrich (1962) described five types of construction in terms of the estimated total heave. A sixth type of construction, the stiffened raft foundation, has been developed since then. This technique relies to a far greater extent on the correct prediction of the ground movements and the soil-raft interaction. In some cases it has been found to be

unsuitable in geographical areas that differ from South Africa where the development took place (Pidgeon (1980)). The Building Research Establishment (BRE) in the U.K. commissioned a study to standardise procedures for the design of foundations for low-rise buildings. Tomlinson et al (1978) outlined procedures for raft, pile, and pad and stem types of foundation.

Monotonic heave is reported to occur where relatively stable moisture conditions exist under a covered surface; a domed ground profile generally results. Since a stable condition is achieved after a number of years, design and remedial works can take account of these movements.

Alternate seasons of wet and dry climatic cycles make heave predictions difficult. The effect of this was demonstrated in the UK in 1976. This form of alternating heave and subsidence is generally accepted as the primary cause of longitudinal cracking in sealed roads (Dagg and Russam (1966)).

3.1 Test Data on Expansive Behaviour

Clay minerals determine expansiveness while the moisture content or suction change controls the actual amount of swell that a particular soil type will undergo.

Ladd and Lambe (1961) performed swell tests under a surcharge of 10 kN/m^2. Figure 3.1 shows a plot of heave versus plasticity index (PI). The remoulded clays ranged initially from dry to wet and were finally fully saturated. The results are limited by the different compactive efforts resulting in different densities at the different moisture contents.

Seed et al (1962) showed that two samples of the same soil having the same initial density and water content, but prepared by different methods of compaction, exhibit different swelling - time characteristics on soaking as shown in Figure 3.2. This is due to their different initial structures (Seed and Chan (1961)). The amount of expansion of a soil due to swell is influenced by two groups of factors listed below. Those in group 1 depend on the nature of the soil particles whereas those in group 2 are not related to the nature of the soil particles.

Group 1	Group 2
Type of clay in soil Amount of clay in soil	Structure of soil Dry density of soil Water content at compaction Method of compaction Availability of water Electrolyte concentration in water Surcharge pressure

Swell tests under 1 psi (6.9 kN/m^2) surcharge were performed by Seed et al (1962) using compacted samples. The initial air dried soils were compacted to standard proctor density at optimum moisture content and then fully saturated. The dependence of volume change on colloid content, plasticity index, and shrinkage limit is shown in Figure 3.3. Accurate relationships could not however be deducted because of data scatter.

It is important to clarify the difference between prediction of swell and swelling potential. Since mineral grains, with the exception of clay minerals, have no capacity to promote swell, the factors in group 1, above, determine the swelling of a soil. The factors in group 2 are determined by the

placement and environmental conditions and determine the magnitude of swell.

It is therefore more meaningful to consider the expansion characteristics of soils in two stages. First, determine the relative capacities of the particles comprising different soils to promote expansion by evaluating the swelling potential. Second, determine from a consideration of the initial composition, the method of placement and the environmental conditions, the extent to which the swelling potential may be realised in the given field conditions.

On this basis, two soils may have the same swelling potential but exhibit quite different amounts of swell because they are:

a) placed at different compositions,

b) compacted differently, or

c) subjected to different climatic conditions.

Alternatively, a soil exhibiting higher swelling potential than another may swell much less because of differences in placement conditions. This is illustrated by the data in Figure 3.4 that show the measured expansions of samples of a clay soil compacted at different water contents and densities. The specimens were placed at initial moisture contents of approximately 15%, 20% and 25%, indicated by circular dot points. The percentage expansion of initial volume is shown beside each point. The trend of expansion is shown by thin dotted lines drawn from these points to the triangular points that represent the final conditions of density and moisture content after swell. The 0% swell potential is indicated by a heavy dashed line through the

triangular points. A series of heavy dashed lines are shown for 1%, 2%, 4%, 6%, 8% and 10% swell potential.

It can be seen from Figure 3.4 that a combination of placement densities beneath the standard compaction curve coupled with high moisture contents are needed to ensure low swell potential. Reduction of density alone will not always provide the desired reduction in expansion. Increased moisture content provides increased expansion control, especially for the higher swell potentials. It can be seen that, if a soil is compacted at a water content of 20% to a dry density of 94 lb/ft^3, it would expand about 5.7% on soaking. However, if the same soil is compacted at a water content of 27% to a dry density of 94 lb/ft^3, it would expand by only 1% on soaking.

Van der Merwe (1964) classified soils into four categories of potential expansiveness by their plasticity index and clay fraction, as shown in Figure 3.5, ranging from 0.083 m expansion per meter thickness for very high potential expansiveness down to zero expansion for low potential expansiveness.

At the 6th Regional Conference for Africa on Soil Mechanics and Foundation Engineering in 1975, several suggestions were made for modifying the classification chart as shown in Figure 3.6.

Komornik and David (1969) produced linear relationships between plasticity index and free swell for two different clays as shown in Figure 3.7.

Vijayvergiya and Ghazzaly (1973), using data from Sullivan and McClelland (1969), presented the following equations in

which they related percent swell to either liquid limit and water content or liquid limit and dry density:

$$\text{Log } S = 1/12\ (0.4\ LL - W + 5.5) \qquad (3.1)$$

where: S = percent swell
LL = liquid limit (%)
W = water content (%)

Since the water content and the dry density of a natural undisturbed sample are interdependent, Vijayvergiya and Ghazzaly (1973) concluded that swell should also be related to the dry density. The relationship between percent swell, dry density and liquid limit was hence expressed in the following form:

$$\text{Log } S = 1/19.5\ (\gamma_d + 0.65\ LL - 130.5) \qquad (3.2)$$

where: S = percent swell
LL = liquid limit (%)
γ_d = dry density (lb/ft^3)

Figures 3.8 and 3.9 show a family of fitted lines for correlation of percent swell with various values of liquid limit and water content or dry density respectively. The relationship between percent swell and water content for any liquid limit shown in Figure 3.8 represents natural clay samples with different initial dry densities. Similarly, the relationship between percent swell and dry density for any liquid limit in Figure 3.9 is for samples with different initial water contents.

The swell pressure of a clay specimen under no volume change and the potential swell after the load is released are interdependent. Since good relationships were formed in Figures 3.8 and 3.9 between percent swell and the water

content or the dry density, similar correlations were attempted for swell pressure.

Figure 3.10 shows the data plotted for swell pressure versus initial water content for different values of liquid limit for natural clay samples. Figure 3.11 similarly shows the correlation of swell pressure with different values of liquid limit and dry density.

As these lines are equally spaced, Vijayvergiya and Ghazzaly (1973) derived generalised expressions for percent swell. They plotted percent swell predicted by Equation 3.1 against the observed percent swell as shown in Figure 3.12. There appears to be an excellent agreement between the predicted and observed percent swell. Thus, they concluded, "it would seem that Equation 3.1 can also be used for predicting swell of highly expansive clays."

The magnitude of swell pressure as predicted by the correlations presented in Figures 3.10 and 3.11 were expressed respectively in the following formulations:

$$\text{Log } P = 1/12\ (0.4\ LL - W - 0.4) \qquad (3.3)$$

$$\text{Log } P = 1/19.5\ (\gamma_d + 0.65\ LL - 139.5) \qquad (3.4)$$

where: P = the swell pressure (t/ft^2)
γ_d = dry density (lb/ft^3)

Abeyesekera and Lovell (1981) conducted triaxial and oedometer volume change tests on two troublesome fill materials: a highly plastic clay and a medium hard, non-durable shale. The moisture contents of the samples were increased from the optimum at compaction to saturation. They used equations derived by others and developed rather long equations themselves. A range of surcharges was used in the

testing. One of the equations presented gives the volume change as a function of the initial void ratio and the log of the isotropic consolidation pressure.

Bandyopadhyay (1981) compacted samples to 92% standard AASHO dry density at optimum water content. Soaking was allowed for 96 hours, regardless of the time required to reach equilibrium. The correlation between index properties and swelling characteristics was essentially the same as that derived by Seed et al (1962), even though the compaction densities and moisture changes differed. Brackley (1983), on the other hand, performed tests on samples of various soils compacted to a range of initial void ratios and moisture contents. The moisture content of all the samples was increased from the optimum condition to saturation. Brackley (1983) presented Equation 3.5 to determine potential percent swell S as

$$S = (5.3 - \frac{147e}{PI} - \log_{10}P)(0.525\ PI + 4.1 - 0.85\ W) \quad (3.5)$$

where: e = original void ratio
PI = plasticity index
P = external pressure (kN/m^2)
W = original moisture content (%)

He pointed out that comparison between predicted and measured heaves are not good, with the predictions ranging from 1/2 to 1/6 the measured values. The use of compacted samples for predicting the heave in undisturbed soils may contribute to the inaccuracy of the method.

Nagaraj and Srinavasa Murthy (1983) presented two equations for predicting the swollen void ratio. The first equation requires knowledge of the preconsolidation pressure.

$$(e/e_1) = 0.6525 - 0.1765 \log_{10} P_c - 0.0472 \log_{10} P \quad (3.6)$$

where: e = the in situ void ratio,
e_1 = void ratio at liquid limit water content,
P_c = preconsolidation pressure (kg/cm^2) and
P = present over burden effective pressure (kg/cm^2).

The second equation requires measurement of the swell pressure.

$$P_s = 17.86 - \frac{100\ (e_o/e_1)}{4 - \log_{10} P_c} \qquad (3.7)$$

where: P_s = the swelling pressure (kg/cm^2),
e_o = initial void ratio,
e_1 = void ratio at liquid limit water content, and
P_c = preconsolidation pressure (kg/cm^2).

All samples tested were compacted to at least 96% saturation. They indicated the swelling pressure development for the same void ratio under different over burden pressures or corresponding different preconsolidation pressures.

The Instability index (I Pt), was defined as the ratio of vertical strain ε_{vert} to suction change (Mitchell and Avalle (1984)). It was originally introduced by Aitchison and Woodburn (1969) and Lytton and Woodburn (1973). This index is equivalent to the suction index used by Johnson (1979) and Snethen (1980) or the term suction compression index used by McKeen and Hamberg (1981). The I Pt can hence be determined from:

$$I\ Pt = \varepsilon_{vert} / \Delta U = \frac{\varepsilon_{vert}}{\Delta W} \times \frac{\Delta W}{\Delta U} \qquad (3.8)$$

The ratio C between the amount of moisture a soil gains or loses ΔW per unit change of soil suction ΔU is defined as

$$C = \frac{\Delta W}{\Delta U}$$

Considerable scatter existed in the relationships between I pt and plasticity index for soils tested by Mitchell and Avalle (1984). However, in general, the higher the Plasticity index, the higher the I pt.

Snethen (1984) saturated undisturbed samples from the in situ moisture content under the field over burden pressure. They considered limited suction ranges for each plasticity range.

Tadanier and Nguyen (1984) also used a similar test method to that by Sullivan and McClelland (1969). A constant volume swell pressure test is followed by unloading of the same sample to 10 kN/m^2. Samples were compacted to standard maximum compaction density at optimum moisture content, and full saturation was permitted. Using linear and quadratic regression, they plotted Figures 3.13 to 3.16 to show liquid limit, plasticity index, shrinkage index and shrinkage limit versus linear shrinkage.

3.2 Volume Change Due to Suction and Applied Stress

The properties most often studied in expansive soil engineering are volume change due to suction and applied stress. Considerable amounts of data have been produced during the past 30 years. Unfortunately, due to considerable variations in the test methods and in the parameters measured or controlled, it is often not possible to compare or combine the data published on similar topics by different authors. Volume change due to suction is usually far more significant in expansive soils than volume change due to applied stress. Considerable progress has been made in the measurement of suction, but the interpretation of the

measured values is still open to significant questions, both in terms of suction itself and in terms of the effect on the soil. The effects of applied stress have also been extensively studied, and are better understood.

3.2.1 Swell Under Load

The earliest report of measurement of swell under varying surcharge conditions is that by Rengmark and Eriksson (1953). They found that increasing the surcharge reduced the swell of compacted samples. The relationship was not linear but exhibited a concave upward curve on natural scales. Salas and Serratosa (1957) also found an inverse relation, concave upward in a plot of swell versus log surcharge for undisturbed samples. Similar results have been presented by several authors. Noble (1966), for example, obtained concave upward curves on natural scales for remoulded and undisturbed samples, as did Kassiff et al (1973) and Chen (1973) for compacted samples. Kassiff et al (1973) also found that changes in the final suction using an osmotic oedometer led to a series of similar swell versus surcharge curves showing less swelling for higher final suctions. Brackley (1975a) demonstrated that the swell under load relationship for compacted samples was an inverse logarithmic function. Didier et al (1980) and Morgenstern and Balasubramonian (1980) reported inverse linear relationships in swell versus log surcharge plots for remoulded and undisturbed samples respectively.

Cox (1979) found that at some particular compacted dry densities and moisture contents, little volume change, either swell or collapse, would occur on wetting up. Since

his work was related to a dam project in a wet climate, he did not investigate subsequent drying of the soil. El-Sohby and Rabbaa (1984) found separate curves in the clay fraction versus vertical effective stress plots defining the zero volume state for two compacted dry densities.

It is clearly evident from these studies that swelling due to suction change and surcharge are interdependent but the precise form of the relationship has not been determined. It is worth noting that none of these studies considered the effect of initial suction.

The significance of stress paths on swelling have been demonstrated by Aitchison and Woodburn (1969), Ali and Elturabi (1984) and Justo et al (1984). The stress paths are in fact undefined, as the lateral stress is unknown. It would therefore be better to refer to them as test sequences rather than stress paths (Schreiner (1988)).

Ali and ElTurabi (1984) compared constant volume and swell and reload swell pressure for undisturbed and compacted samples. There was no consistent correlation between the results of the two techniques.

Justo et al (1984) allowed soaking of undisturbed and compacted samples under various surcharges and then performed consolidation tests on the soaked samples. The most significant finding was that for samples soaked under a low surcharge, the consolidation curve remained above the curves for samples soaked under a moderate to high surcharge. Similar data had been found by Wiseman and Zeitlen (1960). This was explained by Brackley (1975b) for compacted samples as due to distortion of soil particles

during swelling under load, but could also be due to a change in the osmotic suction in the soil due to uptake of pure water during swelling and expulsion of water and solutes during compression. It should also be noted that the vertical to lateral stress ratios will be very different for these test procedures. Komornik and Zeitlen (1965) noted that the horizontal stress was greater than the vertical stress after swelling tests. This is not the case in compression or during reloading after swell at low vertical stresses.

3.2.2 Swell Under Controlled Suction

Blight (1965a) measured volumetric swell under constant isotropic total stress conditions in multi stage tests. He showed it is possible to swell from the partly saturated compression curve to the saturated compression curve if both suction and isotropic total stresses are decreased. In multi stage constant volume tests he found non-linear relationships between decreasing suction and increasing isotropic total stress. Variations between radial and axial strains were not given. His work indicated the non-linear relationship between total stress and suction and volume change, and the influence of test conditions on these relationships. This is perhaps the most significant aspect of Blight's (1965a) work, and is thought to be influenced by the anisotropic nature of the soil interacting with the isotropic total stresses and suction.

Escario and Sáez (1973) measured swell due to decreasing suction in a pressure membrane oedometer. They used 5 decrements of suction on each sample, but presented no

comparison with the single stage saturation in conventional swell testing. They found a non-linear relationship between swell and suction for a range of vertical stresses, with a greater rate of swell at low suctions.

Kassiff et al (1973) measured swell due to single suction changes on samples in an osmotic consolidometer. The final suctions were non-zero and they demonstrated that the swell decreased with increasing final suction for the same change in suction.

Komornik et al (1980) used single stage tests to investigate swell and swell pressure under isotropic total stresses. They obtained a family of curves in percent swell / suction for various isotropic total stresses, demonstrating less swell for high confining stress and high suction. A similar set of curves was presented in a percent swell / total stress diagram for various suctions. Their relationship between final suction and swell pressure is an inverse linear function with a slope of about 1 to 4, except at very low suctions where the slope becomes 1 to 1. In constant water content triaxial shear tests they found that the shear strength was a function of the total isotropic consolidation stress plus the suction multiplied by the saturation ratio.

Justo et al (1984) measured swell in suction controlled oedometers and plotted contours of swell for various suction values from swell under load tests. The swell from incremental suction changes was similar in most cases to that for saturation swell under load tests but not for saturation swell followed by reloading. Zein (1985) used a Rowe type oedometer with suction control to demonstrate that

the stress path (for vertical stress and suction) influenced the volumetric strain. Simple single stage changes in suction and external stress were used.

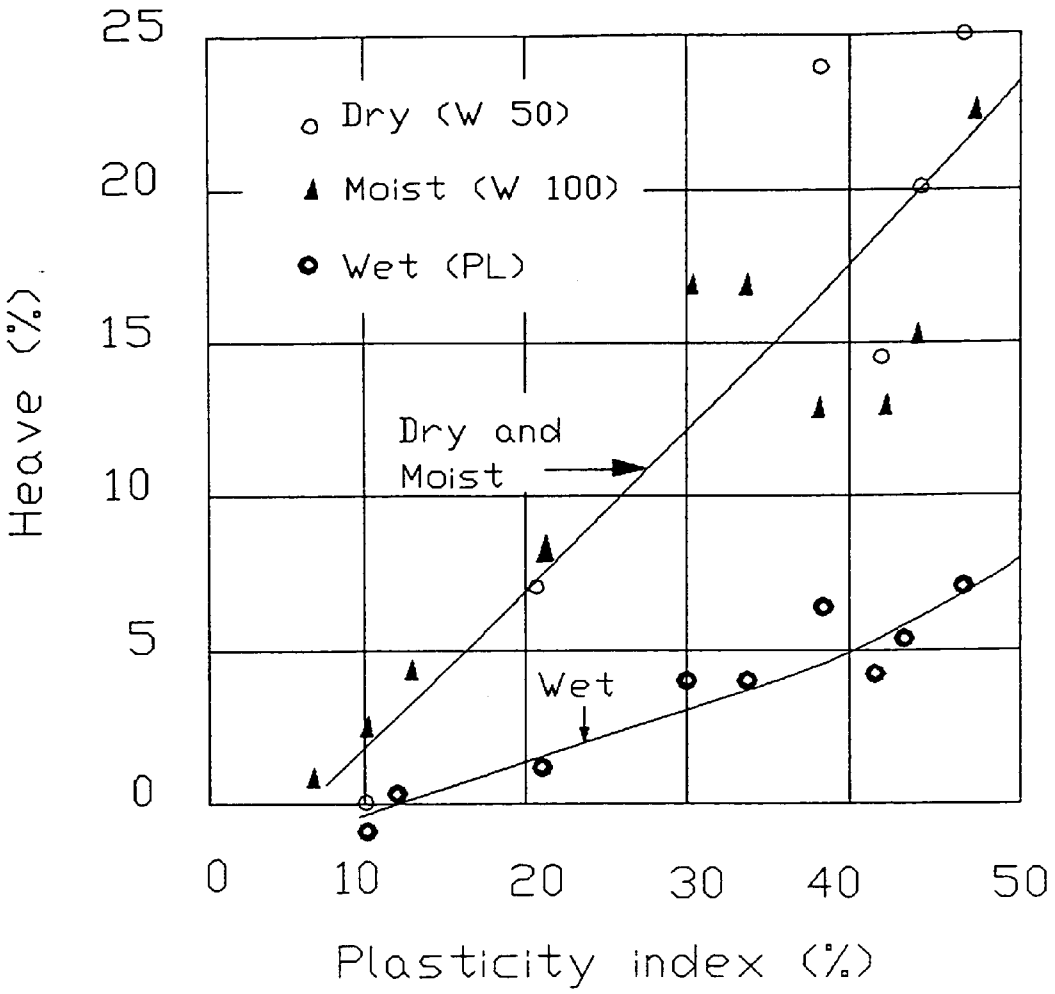

Figure 3.1 Heave versus plasticity index for a surcharge of 10 kN/m^2 (After Ladd and Lambe (1961)).

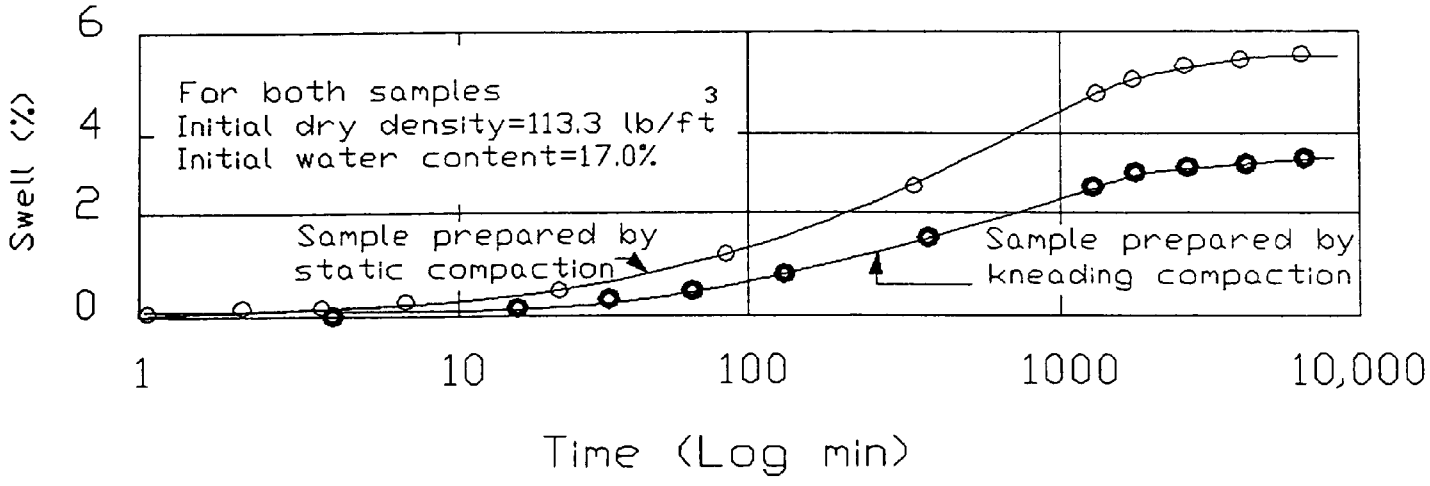

Figure 3.2 Effect of method of compaction on swelling characteristics of sandy clay (After Seed et al (1962)).

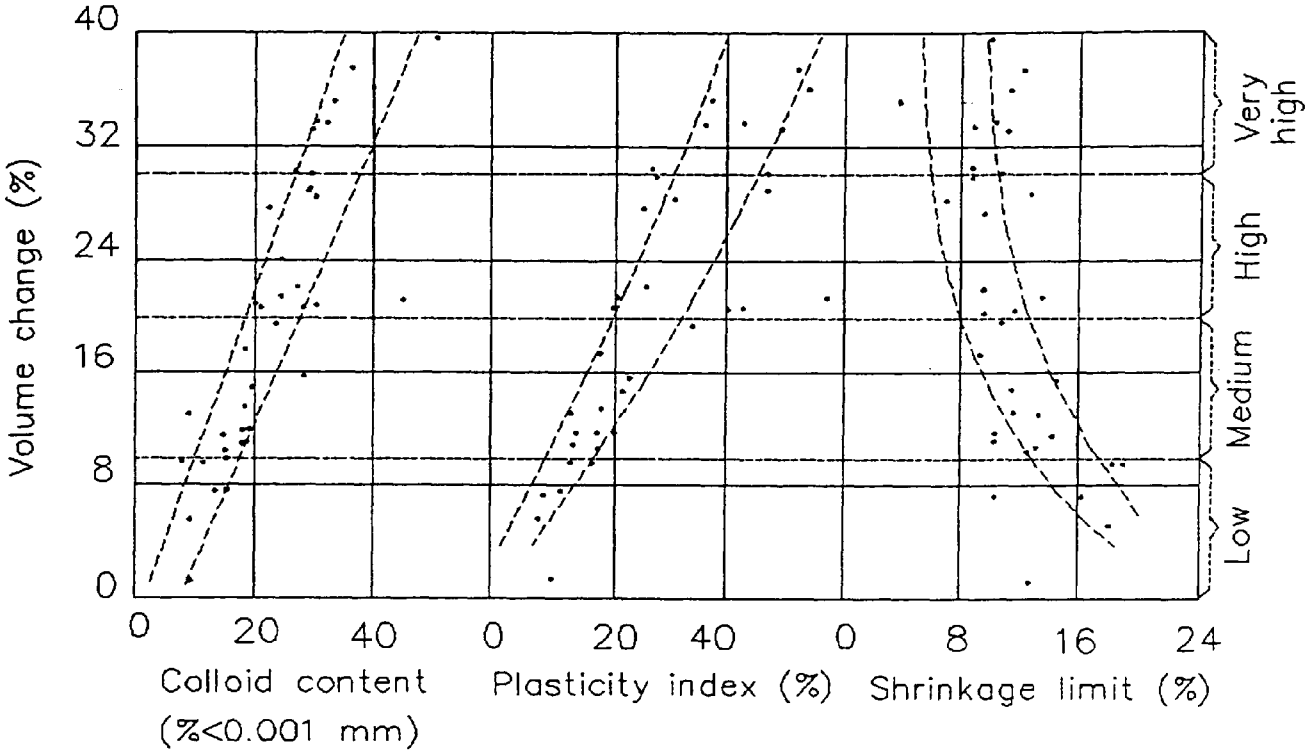

Figure 3.3 Relation of volume change to colloid content, plasticity index and shrinkage limit (After Seed et al (1962)).

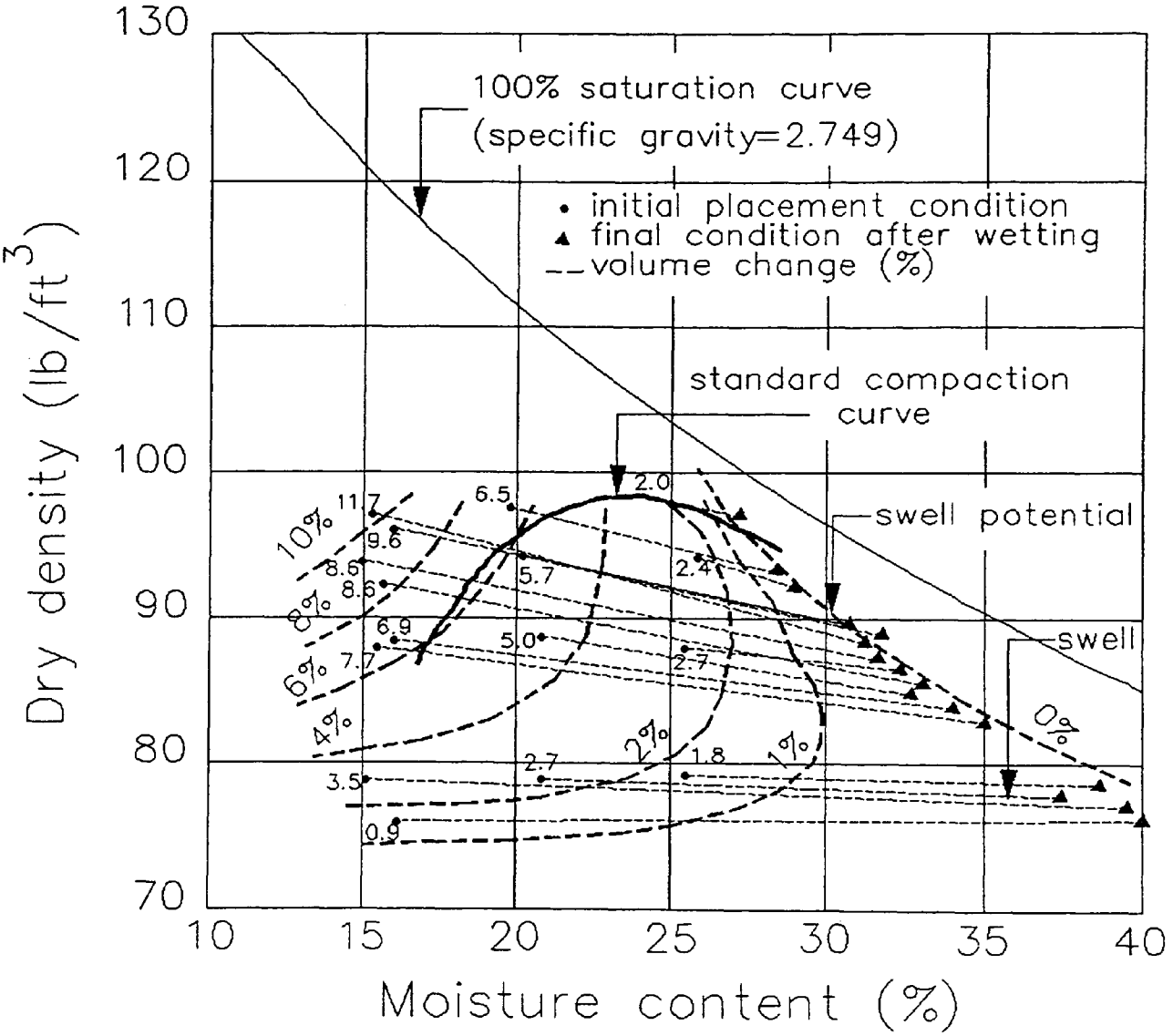

Figure 3.4 Swell potentials of 0%, 1%, 2%, 4%, 6%, 8% and 10% under 6.9 kN/m^2 surcharge (After Seed et al (1962)).

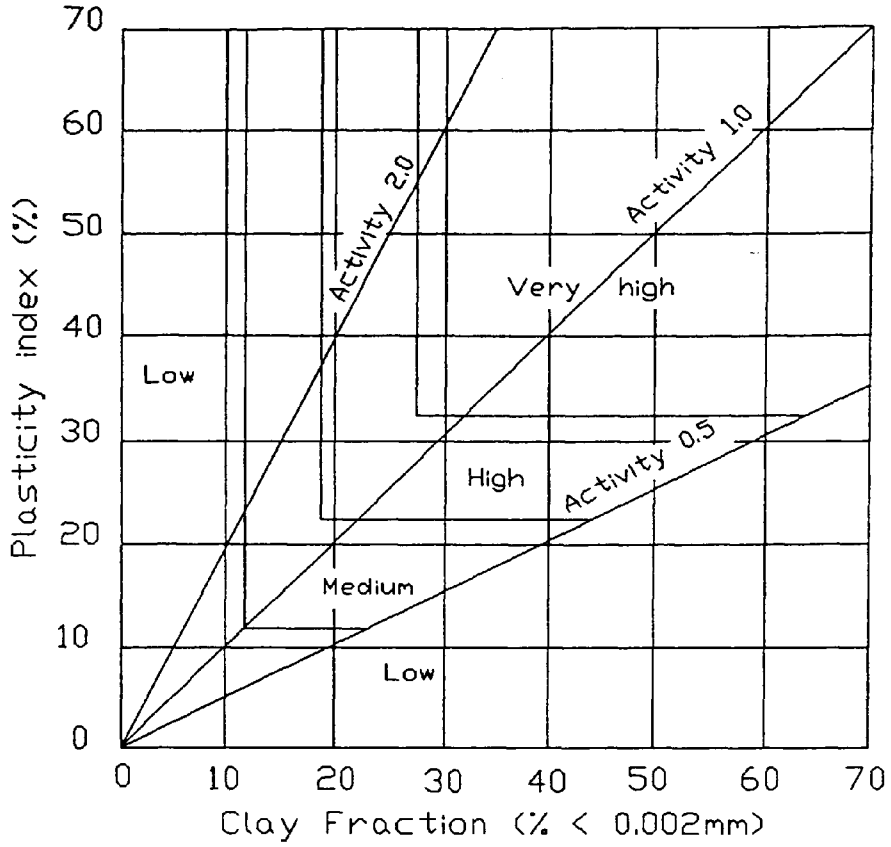

Figure 3.5 Determination of potential expansiveness of soils (After Van der Merwe (1964)).

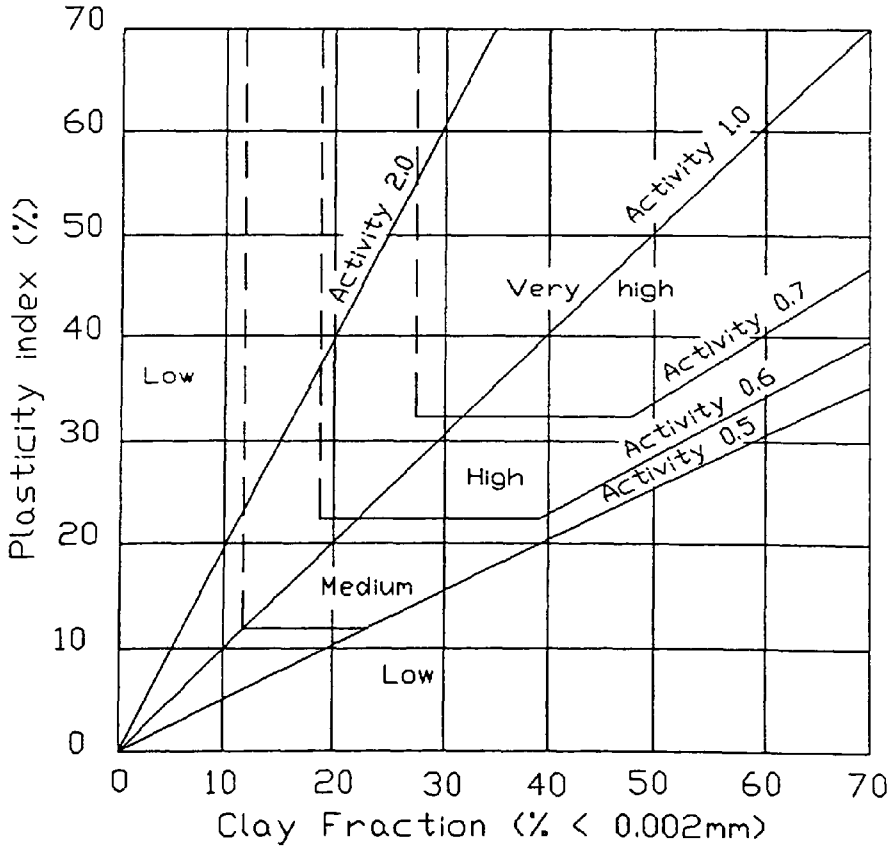

Figure 3.6 Proposed modified chart for determining expansiveness of soils.

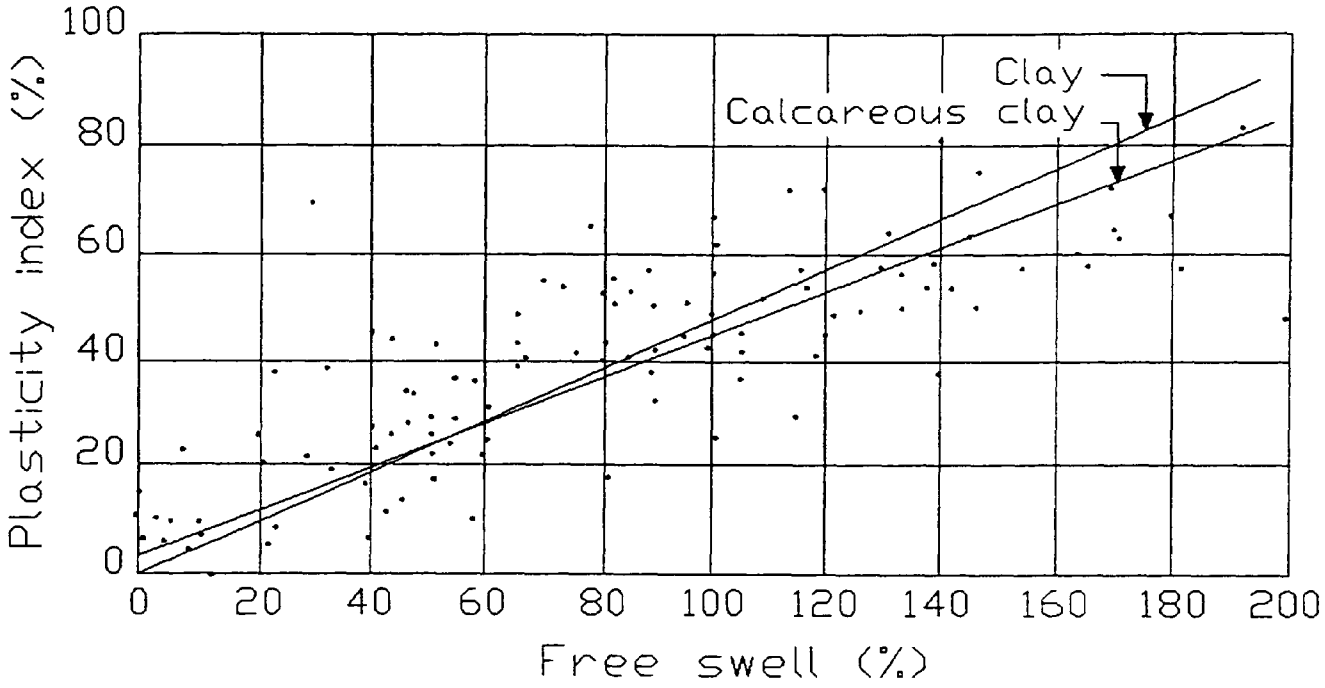

Figure 3.7 Relationship between Plasticity index and free swell (After Komornik and David (1969)).

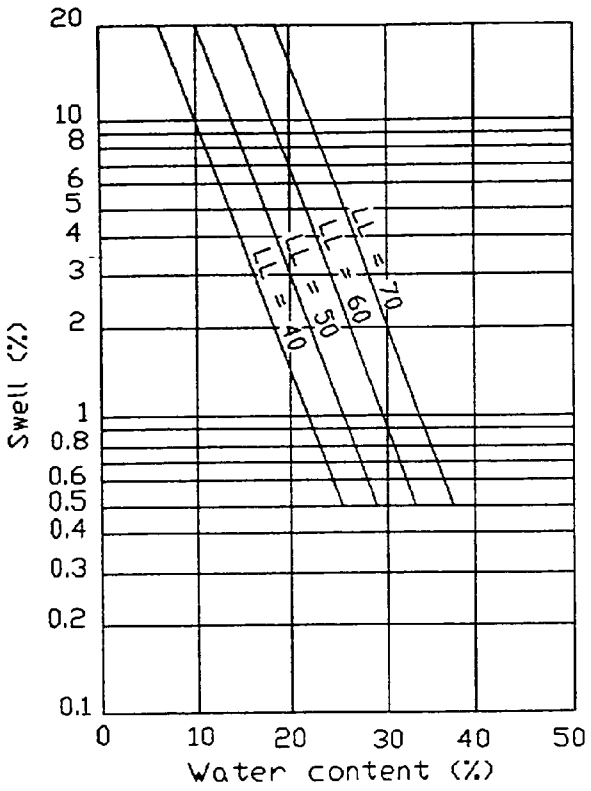

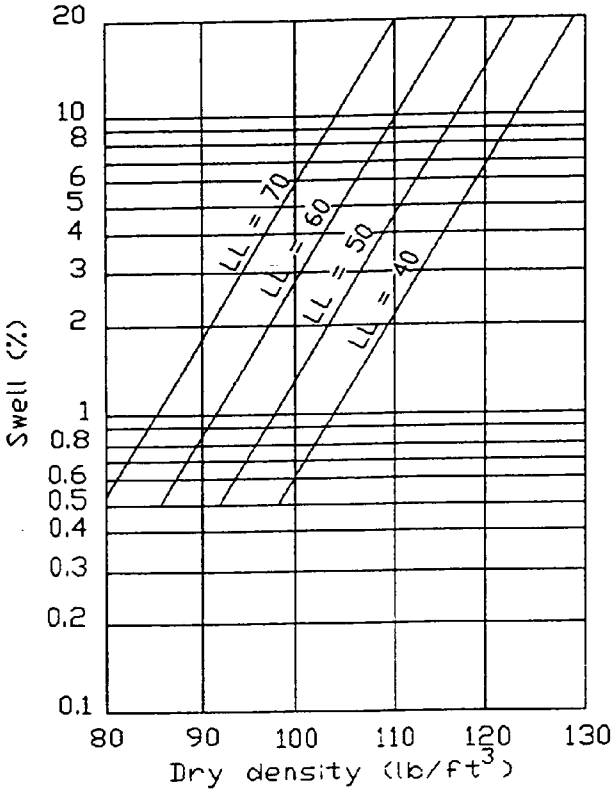

Figures 3.8 & 3.9 Correlations of percent swell with either liquid limit and water content or liquid limit and dry density (After Vijayvergiya and Ghazzaly (1973)).

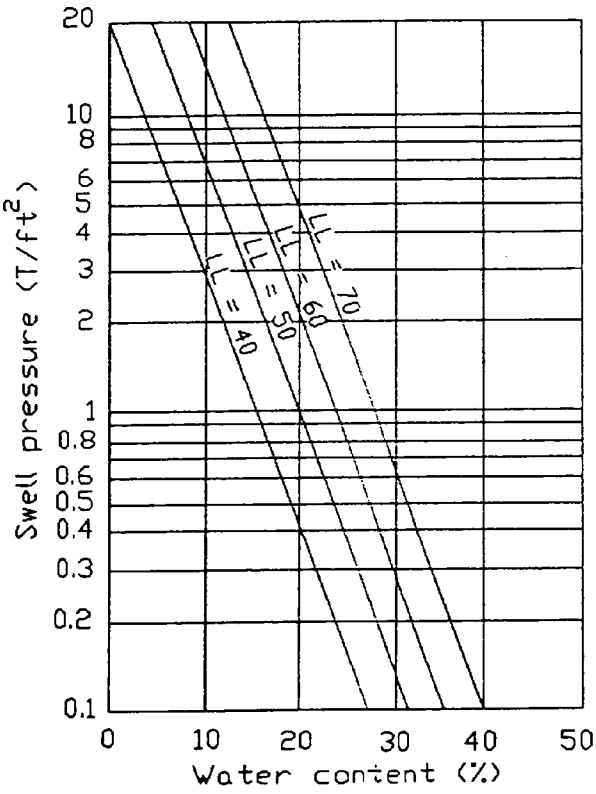

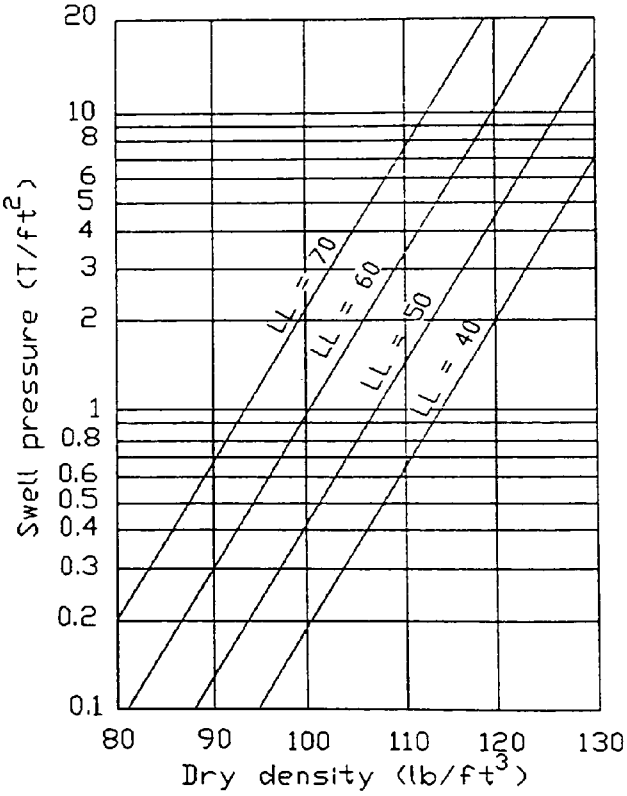

Figures 3.10 & 3.11 Correlations of swell pressure with either liquid limit and water content or liquid limit and dry density (After Vijayvergiya and Ghazzaly (1973)).

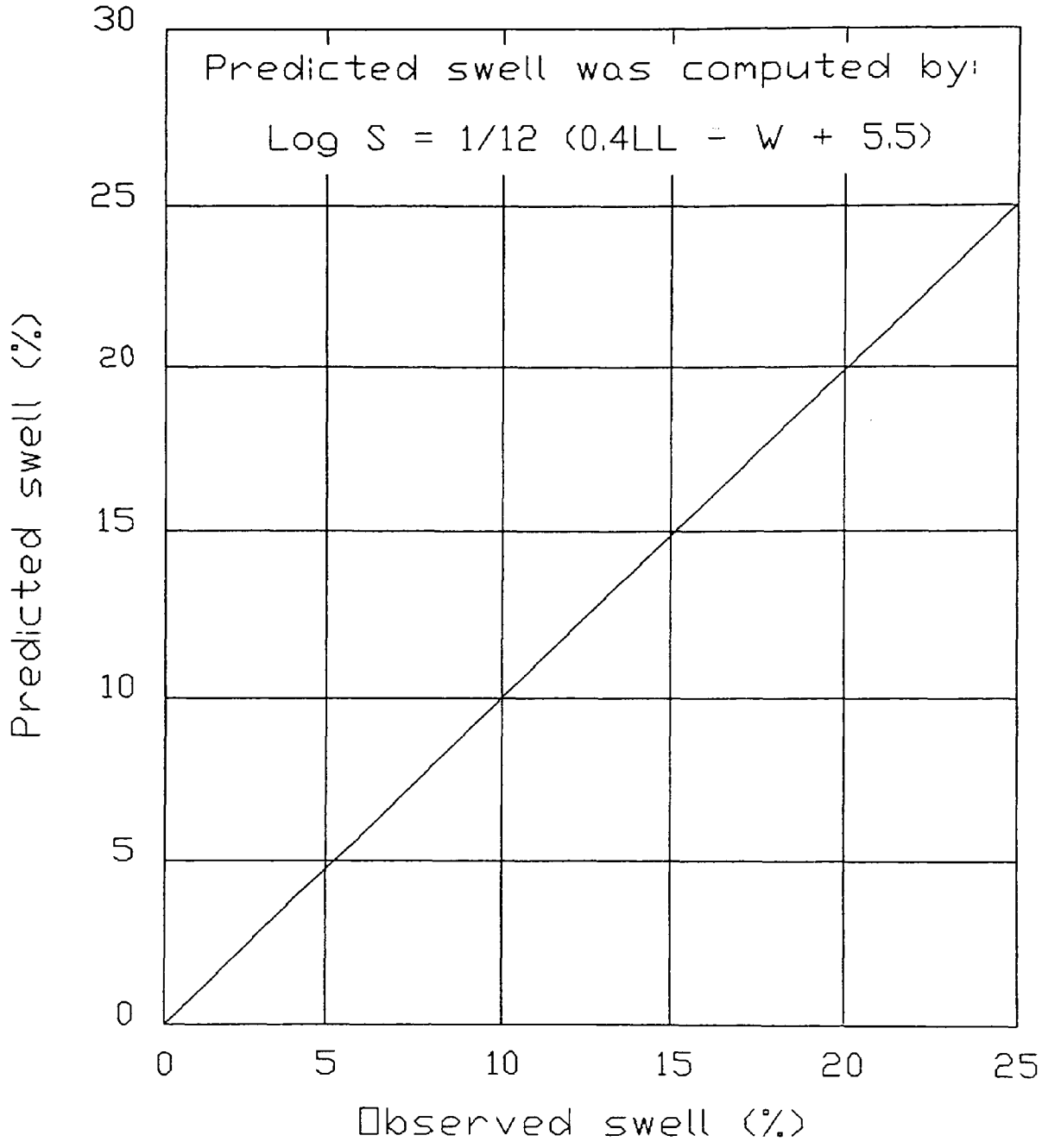

Figure 3.12 Comparison of predicted and observed swell (After Vijayvergiya and Ghazzaly (1973)).

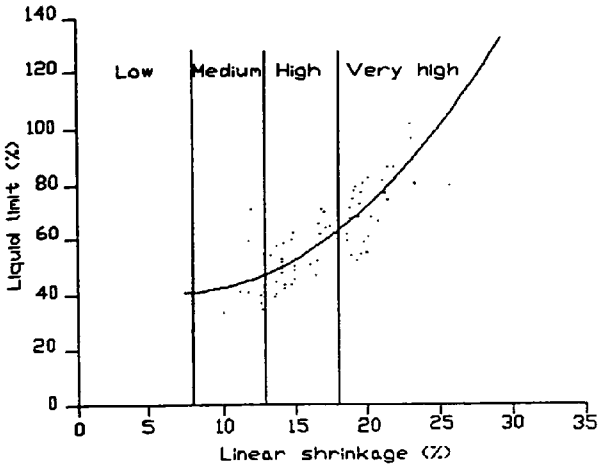

Figure 3.13 Liquid limit vs linear shrinkage

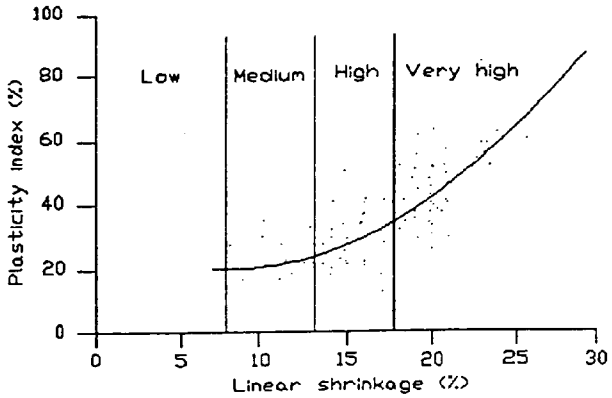

Figure 3.14 Plasticity index vs linear shrinkage

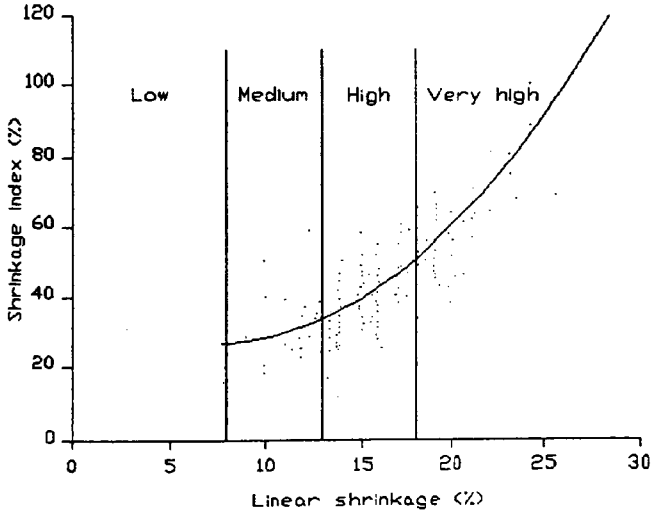

Figure 3.15 Shrinkage index vs linear shrinkage

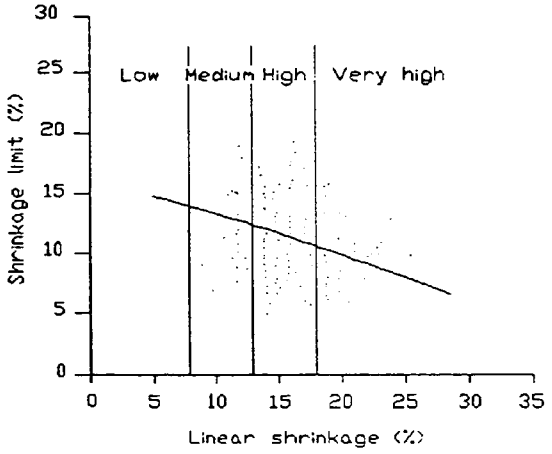

Figure 3.16 Shrinkage limit vs linear shrinkage

Figures 3.13 to 3.16 Liquid limit, plasticity index, shrinkage index and shrinkage limit vs linear shrinkage (After Tadanier and Nguyen (1984)).

CHAPTER FOUR

UNSATURATED SOILS

4.0 Introduction

A large portion of the earth's surface is covered with soils which can either be saturated or unsaturated.

Weathering processes have left over eighty percent of the earth's surface desiccated. As a result, cracks start to develop, and the soil becomes unsaturated.

4.1 Review of Unsaturated Soils

Lambe and Whitman (1969) stated that soil contains "three distinct phases: solid (mineral particles), gas and liquid (usually water)." However, according to Davies and Rideal (1963), the independent properties and continuous bounding surfaces of the air / water boundary (i.e. contractile skin) requires its consideration as a fourth Phase (Fredlund (1973) and Fredlund and Morgenstern (1976)). Fredlund and Morgenstern (1977) stressed that it is imperative to recognise an unsaturated soil as a four-phase system when performing a stress analysis on an element. An element of unsaturated soil can therefore be considered as a mixture, with two phases that come to equilibrium under applied stresses (i.e. soil particles and the contractile skin) and two phases that flow under applied pressure (i.e. air and water). However, from the stand point of the volume-weight relations for an unsaturated soil, Fredlund (1979) stated that it is possible to consider the soil as a three-phase system since the volume of the contractile skin is small and

its weight can be considered as part of the weight of water. Fredlund (1973) used the principle of superimposition of coincident equilibrium stress fields to isolate the stress state variables associated with the soil particles and the contractile skin.

In deriving the equilibrium analysis of unsaturated soil, Fredlund and Morgenstern (1977) used the water phase as a reference. However, if the air phase is to be used as a reference, the equilibrium equation would be of a slightly different form. The solid phase can also be used as a reference. In this case, the normal stress variables are: $(\sigma - U_a)$ and $(\sigma - U_w)$. Therefore, the stress analysis indicates that any two of three possible normal stress variables can be used to define the stress state. Possible combinations are (Fredlund (1979)):

i)	ii)	iii)
$(\sigma - U_a)$	$(\sigma - U_w)$	$(\sigma - U_w)$
and	and	and
$(U_a - U_w)$	$(U_a - U_w)$	$(\sigma - U_a)$

where: σ = total normal stress, U_a = air pressure, and U_w = water pressure.

It is desirable to develop an experimental technique to verify the theoretically proposed stress state variables. Fredlund (1973) proposed the following definition for independent stress state variables:

> "A suitable set of independent stress state variables are those that produce no distortion or volume change of an element when the individual components of the stress state variables are modified but the stress state variables themselves are kept constant. Thus the stress state variable for each phase should produce equilibrium in that phase when a stress point in space is considered."

After attempts to apply the stress state variables to volume change problems, Fredlund (1979) concluded that the $(\sigma - U_a)$

and (U_a - U_w) combination is the most satisfactory. The effects of total stress and pore water pressure changes can be separated; hence Fredlund's reason for adopting the above combination. Fredlund (1979) showed the stress state at a point as in Figure 4.1.

Fredlund (1979) called (σ - U_a) the total stress to represent σ relative to U_a and (U_a - U_w) the matrix suction. Continuity of the soil sample assures that the change in volume of the soil structure is equal to the sum of the changes in the air, water and contractile skin volumes (Fredlund (1973)).

$$\Delta V = \Delta V_a + \Delta V_w + \Delta V_c \qquad (4.1)$$

where: ΔV = change in volume of the soil structure or the overall sample,
ΔV_a = change in volume of the air phase,
ΔV_w = change in volume of the water phase, and
ΔV_c = change in volume of the contractile skin.

However, if the soil particles are assumed to be incompressible and the volume change of the contractile skin assumed internal to the element, the continuity requirement for an element reduces to:

$$\Delta V = \Delta V_a + \Delta V_w \qquad (4.2)$$

The measurement or prediction of any two of the above volume changes allows complete monitoring of the volume-weight change relationships (Fredlund and Morgenstern (1976)).

The volume change relationships for an unsaturated soil can be represented using the (σ - U_a) and (U_a - U_w) stress state variables and the volume-mass soil properties. The coefficient of compressibility can be defined for small stress increments. Fredlund (1979) defined the coefficient of compressibility with respect to the total stress as:

$$a_t = -de / d(\sigma - U_a) \qquad (4.3)$$

and the coefficient of compressibility with respect to matrix suction as:

$$a_m = -de / d(U_a - U_w) \qquad (4.4)$$

For corresponding stress ranges, a_t will approximately equal a_m when the degree of saturation is near 100%. As the degree of saturation decreases it has been found that a_t will become greater than a_m. This shows that a change in $(\sigma - U_a)$ is more effective in changing void ratio than a change in $(U_a - U_w)$.

A similar constitutive surface exists for the water phase. Fredlund (1979) defined the coefficient of water content with respect to total stress as:

$$b_t = -dw / d(\sigma - U_a) \qquad (4.5)$$

and the coefficient of water content with respect to matrix suction as:

$$b_m = -dw / d(U_a - U_w) \qquad (4.6)$$

At 100% saturation, b_t approaches b_m. At lower degrees of saturation, b_m will generally be greater than b_t since stress applied directly to the water phase will be more effective in removing water from the sample. Volumetric continuity requires that two independent relationships be written. One equation describes the deformation of the soil structure in terms of the change in void ratio, de:

$$de = a_t\, d(\sigma - U_a) + a_m\, d(U_a - U_w) \qquad (4.7)$$

where: e = void ratio, a_t = the coefficient of compressibility with respect to a change in $(\sigma - U_a)$, a_m = the coefficient of compressibility with respect to a change in $(U_a - U_w)$ (Fredlund and Rahardjo (1985)).

A second relationship describes the change in water content, dw:

$$dw = b_t\, d(\sigma - U_a) + b_m\, d(U_a - U_w) \qquad (4.8)$$

where: w = water content, b_t = the coefficient of water content change with respect to a change in $(\sigma - U_a)$, b_m = the coefficient of water with respect to change in $(U_a - U_w)$ (Fredlund and Rahardjo (1985)).

Although the uniqueness of the above relationships has been verified, to some extent, by several researchers (Matyas and Radhakrishna (1968), Barden et al (1969) and Fredlund and Morgenstern (1976)), the accurate quantifying of the coefficients a_t, a_m, b_t and b_m is of vital importance. Further work should therefore be undertaken to achieve as correct a value as possible for these coefficients. As quoted (Fredlund and Rahardjo (1985)), the above relationships have been verified for 100% saturation. No experimental data are available to verify the above relationships for low degrees of saturation.

4.2 Stress Path Method

The stress path method is a procedure that may be used to estimate either the strength or the deformation of representative soil elements in the field. The procedure followed in the stress path method is to remove a sample of the soil from the ground, and then subject it to the total and effective stress paths which are estimated to be applied to the soil element in the field. In general, the stress path method consists of two steps (Lambe (1967)):

1) estimating the history and variation of stress and strain for one or more elements of soil in the actual field structure. This obviously applies to unsaturated as well as saturated soils, and

2) using soil tests (laboratory or field, or both) and analytical techniques that approximate the field stress and strain conditions before, during and after construction.

In this study however, the samples are not from the field. The samples are artificially constituted and the stress history has to be created.

The stress history and stress variation involved in the field situation, soil test and analytical techniques are portrayed by stress paths. Since strain, pore water pressure and strength of a soil element depend on the stress path, this field stress path (or field strains, or both) should be used in the soil testing procedure and method of analysis for any given problem.

4.2.1 Definition of Stress Path

Lambe (1967) defined the stress path as:

> "A line drawn through points of stresses. The particular stress point used in the stress path method is that of maximum shear stress," (Figure 4.2).

Thus, a stress path is the locus of points of maximum shear stress experienced by an element in going from one state of stress to another.

The stress path method relies on the effective stress principle (Lambe and Marr (1979)). However, this principle does not apply to unsaturated soils very well. This is due to the fact that as the pore water pressure U_w decreases, the effective stress moves closer to total stress. Although Fredlund (1973, 1979) and Fredlund and Morgenstern (1976) have applied the stress path method in their works, they

chose (σ - U_a) and (U_a - U_w) as the best combination of stresses.

There are certain difficulties with the stress path method which must be faced. For example, it is extremely difficult to retrieve samples from the ground that are truly undisturbed. Disturbance of a sample will usually have the effect that the stiffness of the sample will be reduced, although the strength of the specimens is likely to be affected only slightly. It is also often difficult to estimate the changes in stress which will occur in a soil element in the ground as a boundary load is applied to the soil. It is usual to use an elastic analysis to estimate the distribution of stresses in the soil. However, this analysis can only be approximate, for soil is not perfectly elastic, and does not satisfactorily allow for any changes of total stresses which occur during dissipation of the excess pore water pressures (Atkinson and Bransby (1978)).

A further major difficulty is that the stress paths calculated to be imposed in the ground may be difficult, if not impossible, to simulate in the laboratory. For example, the stresses on the soil element predicted by an elastic analysis may be such as to cause failure of the element, even though the body of soil as a whole may be in a perfectly safe condition.

A common feature of the stress path method is the rotation of principal stress directions which accompanies changes in their magnitude. These rotations arise when principal stress increment directions do not coincide with the current principal stress directions. Under conditions of plane

strain, principal stress rotations are restricted to one plane. Similarly, in axisymmetric situations, rotations occur only in radial planes. In general, however, rotations of principal stress directions may occur about three axes. There are experimental difficulties in achieving controlled rotation of principal stress directions, referred to by Bishop and Henkel (1962). These have severely restricted investigations into the effects of principal stress rotation on soil behaviour.

Arthur et al (1980) claim to have developed a relatively inexpensive Directional Shear Cell at University College, London, in work on sand. They state that the cell was being further developed at the Massachusetts Institute of Technology for use with soft clays. Hight et al (1983) developed a hollow cylinder apparatus for investigating the effects of principal stress rotation on soils.

Bishop and Wesley (1975) designed a hydraulic triaxial apparatus (Figure 4.3) for controlled stress path testing. They claimed that any operator using the apparatus will generally desire to vary σ_a (the axial stress) and σ_r (the radial stress) in some controlled manner and measure the resulting deformation of the sample and the pore pressure response or volume change. However, the two pressures which can be controlled directly are the cell pressure (σ_r) and the pressure in the lower pressure chamber (P). The value of σ_a is dependent on both σ_r and P and the key to the operation of the apparatus is the relationship between σ_a, σ_r and P. While considering the equilibrium of the loading

ram, Bishop and Wesley (1975) deduced the following relationship:

$$\sigma_a = P \frac{a}{A} + \sigma_r \left(1 - \frac{a}{A}\right) - \frac{W}{A} \qquad (4.9)$$

where: A = the sample area, at the relevant stage of the test, a = the bellofram seal area, W = the weight of loading ram.

For any particular test it is easy to determine, from the above equation, the way in which the pressure P must be varied in relation to σ_r in order to produce the required stress path.

Unfortunately, this cell could not be used in the first phase of the present work due to the change in volume of the cell under pressure. When it became necessary to generate data on the shear strength of the samples, the Bishop Wesley cell was utilised. The volume change of the sample was measured directly by a radial strain measuring device using the Hall Effect method (see Chapter Six, Section 6.9.1).

4.3 Effective Stress Concept

Classical soil mechanics is primarily concerned with soils in which voids amongst soil particles are completely filled with water. It was for such saturated soils that Terzaghi (1936) proposed the effective stress equation:

$$\sigma' = \sigma - U_w \qquad (4.10)$$

where: σ' = effective stress,
σ = total stress, and
U_w = pore water pressure.

This equation proved to be of major significance in that the shear strength and compressibility of saturated soils were found to be uniquely determined by the effective stress defined by this equation.

Soils of the semi-arid and arid regions often exist in a state of partial saturation. Compacted soils in the "as compacted" state are also partially saturated (Satija (1978)). The engineering behaviour of partially saturated (unsaturated) soil has been observed to differ significantly from the behaviour of saturated soil. For example, upon being given access to free water a saturated soil swells whereas a partially saturated soil may exhibit either swell or a marked reduction in volume on account of a collapse in its structural arrangement (Jennings and Burland (1962)).

The partially saturated soils have not been subjected to extensive laboratory studies . This may be due to the fact that laboratory testing of soils in such a state is complex and time consuming. Most of the investigations are concerned with isolating the volume change behaviour of partially saturated soils or with establishing an effective stress equation for them. Aitchison (1956), Bishop et al (1960), Blight (1961), Donald (1961), Jennings and Burland (1962), M.I.T. (1963), Matyas and Radhakrishna (1968), Barden et al (1969), Gulhati (1972), Fredlund (1973) and Kawakami and Abe (1975), among others, have investigated the engineering behaviour of partially saturated soils.

Soil suction has been accepted in the past as a parameter similar to pore water pressure. As a result, many effective stress equations have been developed for partially saturated (unsaturated) soils. They include; Croney et al (1958), Bishop (1959), Lambe (1960), Aitchison (1961), Jennings (1961) and Richards (1967). All of these have attempted to

use suction as a negative pore pressure by the inclusion of a factor, the best known of which is X (see Equation 4.11). Bishop and Blight (1963) stated that the effective stress, by definition, is that function of total stress and pore pressure which controls the mechanical effects of a change in stress, such as volume change and a change in shear strength. Any form of the effective stress equation should satisfy the following requirements (Matyas and Radhakrishna (1968)):

a) the boundary cases for full saturation and for a completely dry state,
b) the behaviour (volume change and shear strength) of a soil element exposed to a change in stress should be independent of the manner in which the total stresses and the pore pressures change, and
c) the correctness of the form of such an effective stress equation should be verified experimentally.

In partially saturated soils it is practically impossible to satisfy all three requirements and therefore the use of any equation for the effective stress is necessarily limited to those cases which can be verified experimentally.
Difficulty in using effective stress concepts has led to several critical reviews of effective stress in partially saturated soils. Jennings and Burland (1962), for example, suggested that separate functions of the applied stress and a suction term, which includes the parameter X, govern soil behaviour. Bishop and Blight (1963) used a state surface in a three axes diagram of void ratio, applied stress and suction.

Attempts to link the deformation of an unsaturated soil with Bishop's effective stress equation have met with limited success. The available data (Matyas and Radhakrishna (1968)) indicate that there are important limitations to the use of effective stresses for predicting volume change behaviour. In order to develop an expression for defining effective stress in a partially saturated (unsaturated) soil, the assumption of identical behaviour of soil under external stresses and internal suction must be made. Such an assumption has shown to be misleading in predicting the behaviour of soils which tend to collapse on wetting (Jennings and Burland (1962)).

A qualitative explanation for the volume change behaviour of partially saturated soils was given by Burland (1965) in terms of grain stability. He used an idealised model of the soil structure. A similar concept was proposed by Newland (1965) who suggested that there were two parts to the effective stress in partially saturated soils:

i) a part due to forces arising at the point of contact between particles and acting normal to the tangent at the point of contact, and

ii) a part due to forces external to points of contact between particles and associated with tangential or shear forces.

Another assumption to be made in using effective stresses to predict volume change behaviour is that the compressibility of a soil in terms of effective stresses is independent of water content and degree of saturation (Blight (1965b)). No experimental justification for such an assumption is

available for a wide range of degrees of saturation. However, Matyas and Radhakrishna (1968) showed that the compressibility of the soil is a variable quantity which depends on the physical state of the soil (namely void ratio, saturation and stress). Bishop and Blight (1963) recognised these limitations and concluded that, "in the case of partly saturated soils it is not the effective stress path only, but the paths of the two components $(\sigma - U_a)$ and $(U_a - U_w)$ which must be considered." Burland (1965) also reiterated his dissatisfaction with Bishop's effective stress equation.

Brackley (1971) used two independent stress variables (i.e. $(\sigma - U_a)$ and $(U_a - U_w)$) in his study of partial collapse of unsaturated expansive clays. Difficulties were encountered in attempts to apply Bishop's effective stress equation. He listed several factors which appear to invalidate the principle of effective stress, or at least limit its use:

1) collapse of a soil upon inundation by water,
2) non-uniqueness of $(X : U_w)$ relationship,
3) the difference between final volume states of samples that pass between identical original and final stress states but follow different load saturation sequences,
4) the difference between apparent pre-consolidation pressure, determined from the compression curve of a free-swollen sample, and the swell pressure, which should be the pre-consolidation pressure of a normally consolidated sample, and
5) the cross-over of the virgin saturated compression line with the normal moisture content line, associated with

point 1) above.

Subsequently, the description of volume change behaviour for unsaturated soils was proposed as a function of the independent stress variables.

The success in describing the behaviour of saturated soils by using the effective stress equation, led the early investigators of partially saturated soils to seek an analogous effective stress equation for partially saturated soils.

Bishop (1959) suggested the following expression for effective stress in partially saturated soils which was based on the original effective stress Equation 4.10:

$$\sigma' = (\sigma - U_a) + X(U_a - U_w) \qquad (4.11)$$

where: σ' = effective stress,
σ = total stress,
U_a = pore air pressure,
U_w = pore water pressure, and
X = a function of saturation ranging from zero for dry soil to 1.0 for saturated soil.

This equation was not found to be satisfactory for portraying the compressibility behaviour of partially saturated soil. It was, however, believed to be valid for describing shear behaviour.

Other investigators (see Section 4.3.1) proposed other equations for effective stress in partially saturated soils. Cooling (1961) showed these equations to be equivalent to each other, differing in notation rather than in concept. None of these equations have been shown to be applicable in routine engineering practice or to predict the engineering behaviour of partially saturated soils.

Contrary to earlier belief, results of tests (Gulhati (1975)) indicate that Equation 4.11 is inadequate for

describing shear behaviour. This inadequecy manifests itself by producing:

i) X factors greater than 1.0,

ii) a reduction in X when the degree of saturation has been increased by increasing applied stress prior to shear,

iii) a marked increase in X when drainage is allowed during shear for samples at essentially the same saturation.

Jennings and Burland (1962) suggested that the expression for effective stress, as in Equation 4.11, would not be valid. This expression consists of two stress components: $(\sigma - U_a)$ and $X(U_a - U_w)$. The former component represents the externally applied stress whereas the latter originates on account of the tension in the pore water. When stress is applied externally at sample boundaries by increasing $(\sigma - U_a)$, it is transmitted to the sample interior by development of normal and shear stresses at particle contacts. The stresses induced at particle contacts cause failure at some contacts which produce slippage and particle reorientation which in turn result in volume reduction. On the other hand, when the stress component $X(U_a - U_w)$ is increased by increasing the tension in the pore water, the stress is not applied at sample boundaries but is induced internally. At each particle contact, since water pressure acts normally, the normal stress increases and the shear stress remains essentially unchanged. Instead of producing failure at particle contacts, particle rearrangement and volume reduction, an increase in $X(U_a - U_w)$ actually makes the particle contacts stronger thus imparting a rigidity to the soil skeleton. Some volume reduction occurs, perhaps, as

particles are pulled closer to each other by the increased suction in the pore water. On account of the different natures of the two stress components $(\sigma - U_a)$ and $X(U_a - U_w)$, it was suggested that they would influence compressibility behaviour of soil in different manners.

Bishop and Blight (1963) conceded that there is difficulty in using Equation 4.11 to describe volume change behaviour but insisted that this "equation can be used with much less difficulty in terms of shear strength, which is primarily controlled by the intergranular forces at the time of failure." Burland (1965) also agreed with this view when he observed that "unlike the case of volume change, the shear strength of soil depends mainly on the normal components of the interparticle forces" and as such "it appears quite reasonable that ... a change in total stress should be found to be equivalent to a change in some function of the pore pressure as far as shear strength is concerned."

Bishop and Donald (1961) performed drained triaxial tests on partially saturated silt. They claimed to demonstrate the validity of the form of the effective stress equation by varying cell pressure, pore water pressure and pore air pressure during the shearing process in such a way that both the terms $(\sigma_3 - U_a)$ and $(U_a - U_w)$ remained constant. These variations were found to have no effect on the stress-strain curve. However, when σ_3, U_a and U_w were changed without ensuring that $(\sigma_3 - U_a)$ and $(U_a - U_w)$ remained constant, the stress changes had a marked effect on stress-strain behaviour.

Jennings and Burland (1962) pointed out that such a demonstration is inadequate and that to show the correctness of the form of Equation 4.11, "it is necessary to show that the soil behaviour is unaffected by changes in $(\sigma - U_a)$ and $X(U_a - U_w)$ such that their sum, σ', is constant."

Gulhati (1972) highlighted the deficiency of Bishop and Donald's (1961) results in demonstrating the correctness of Equation 4.11. However, their work was demonstrated to be more applicable to the effective stress equation developed by Gulhati (1975). The balance of empirical evidence has been presented by Bishop and Blight (1963) in the form of relations between experimentally determined X factors and degree of saturation for four compacted soils. Using these results they demonstrated X and the degree of saturation "to be independent of the type of test used."

Jennings and Burland (1962), M.I.T. (1963) and Barden et al (1969), as a result of their respective studies on volume change behaviour of unsaturated soils, concluded that the component $(\sigma - U_a)$ induces both shear and normal stresses at particle contact because $(\sigma - U_a)$ and $(U_a - U_w)$ generate intergranular stress by essentially different mechanisms. They, therefore, proposed that the two components should be treated separately rather than combining them into a single stress as given by Equation 4.11.

Matyas and Radhakrishna (1968) treated applied stress $(\sigma - U_a)$ and suction $(U_a - U_w)$ as two independent variables and showed that the variations in void ratio and degree of saturation could be represented by unique surfaces in

stress/void ratio and stress/degree of saturation diagrams respectively.

It is generally agreed that the effective stress equations proposed by various researchers (see Section 4.3.1) are not valid for describing volume change behaviour of partially saturated soils. One should, therefore, consider the influence of the two stress components, that is, $(\sigma - U_a)$ and $(U_a - U_w)$ separately.

4.3.1 Extension of Effective Stress Equation to Partially Saturated Soils

In view of the utility of the effective stress principle in describing the behaviour of saturated soils, research workers investigating partially saturated soils were led into a search for a similar concept for partially saturated soils.

Hilf (1956) formulated an effective stress equation for partially saturated soils as:

$$\sigma' = \sigma - (U_a + U_c) \qquad (4.12)$$

where: U_c = capillary pressure.

This equation did not account for the fact that U_c does not act over the entire cross section of the soil.

Croney et al (1958) presented another modified effective stress equation:

$$\sigma' = \sigma - \beta' U_w \qquad (4.13)$$

where: β' = holding or bonding factor depending on degree of saturation.

Furthermore, β' is a measure of the number of bonds under tension, effective in contributing to the shear strength of the soil.

Bishop (1959) suggested the following expression for effective stress in partially saturated soils:

$$\sigma' = (\sigma - U_a) + X(U_a - U_w) \qquad (4.11)$$

Aitchison (1961) proposed an effective stress equation as follows:

$$\sigma' = \sigma + \text{¥}P'' \qquad (4.14)$$

where: ¥ = a parameter varying between zero and 1.0 for degree of saturation ranging from 0 to 1.0, and
P" = pore water pressure deficiency.

Jennings (1961) also proposed a modified effective stress equation for the partially saturated condition as:

$$\sigma' = \sigma + \text{ß}P'' \qquad (4.15)$$

where: ß = a statistical factor related to the ratio of contact areas of water and air along a plane passing through a soil mass, and
P" = soil's moisture tension , $-U_w$.

Expressions for effective stress suggested by Croney et al (1958), Aitchison (1961) and Jennings (1961) are identical with Bishop's (1959) expression when $U_a = 0$, that is, $\sigma' = \sigma - X\ U_w$, therefore, $X = \text{ß}' = \text{¥} = \text{ß}$.

During the Research Conference on "Shear Strength of Cohesive Soils" in June 1960, it was decided to adopt the parameter given by Bishop, that is X, and to express the effective stress equation for a partially saturated soil as:

$$\sigma' = \sigma + X(U_a - U_w) - U_a \qquad (4.11a)$$

Skempton (1961) suggested that the effective stress expressions derived for saturated soils could be extended to unsaturated soils and rocks. The specific equations proposed for the effective stress law with respect to shear strength and compressibility are respectively:

$$\sigma' = \sigma - \left(1 - \frac{a \tan \text{¥}}{\tan \phi'}\right) S_x\ U_w \qquad (4.16)$$

$$\sigma' = \sigma - \left(1 - \frac{C_s}{C}\right) S_x\ U_w \qquad (4.17)$$

where: σ' = effective stress,
σ = total stress,
a = contact area,
¥ = angle of intrinsic friction,
ϕ' = angle of shearing resistance,
C_s = compressibility of solids,
C = volume compressibility,
S_x = $1 + (1 - X)(U_a - U_w) / U_w$ which follows from Equation 4.11, and
U_w = pore water pressure.

Bishop and Blight (1963) expressed the law for partially saturated soils in a general form:

$$\sigma' = (\sigma - U_a) + f(U_a - U_w) \qquad (4.18)$$

They suggested that the volumetric changes, occurring due to application of an ambient stress, can be represented on a space diagram with axes e, $(\sigma - U_a)$ and $(U_a - U_w)$. The function $f(U_a - U_w)$ appeared to be very sensitive to stress path history.

Newland (1965) introduced the term endogenic, that is, stress components originating internally, σ_i and $X(U_a - U_w)$, and exogenic, that is, component arising from externally applied stress, $(\sigma - U_a)$ and suggested the following effective stress equation:

$$\sigma' = \sigma_i + X(U_a - U_w) + (\sigma - U_a) \qquad (4.19)$$

where: σ_i = the intrinsic stress arising from interparticle forces (originating from electrical, osmotic or van der Waals effects).

Richards (1967) postulated another effective stress equation based on the role played by solute suction:

$$\sigma' = \sigma - U_a + X_m (h_m + U_a) + X_s (h_s + U_a) \qquad (4.20)$$

where: X_m = effective stress parameter for matrix suction,
h_m = matrix suction,
X_s = effective stress parameter for solute suction,
h_s = solute suction.

Sridharan (1968) suggested an effective stress equation for partially saturated soils when the effect of admixtures or variation in pore fluid chemistry is of importance:

$$\sigma' = (\sigma - U_a) + a_w (U_a - U_w) + (A - R) \qquad (4.21)$$

where: a_w = ratio of area of water-mineral and water-water contact to total area of "wavy plane",
A = stress due to interparticle attractive forces,
R = stress due to interparticle repulsive forces.

Aitchison (1973) presented an effective stress equation slightly modified from that of Richards (1967):

$$\sigma' = \sigma + X_m P''_m + X_s P''_s \qquad (4.22)$$

where: P''_m = matrix suction $(U_a - U_w)$,
P''_s = solute suction, and
X_m and X_s = soil parameters, normally within the range of 0-1, which are dependent on the stress path.

Fredlund (1973) isolated the three stress state variables: $(\sigma - U_a)$, $(U_a - U_w)$ and $(\sigma - U_w)$ as being relevant in partially saturated soils. He further suggested that the engineering behaviour of partially saturated soils must be studied in terms of any of the combinations of stress state variables as in Section 4.1.

4.4 Shear Strength of Soils

The shear strength of a soil is defined as the maximum, or limiting, value of shear stress that may be induced within its mass before the soil yields. Under certain circumstances yielding will lead to the formation of a shear slip surface over which a significant amount of sliding movement may take place. Evaluation of the parameters of shear strength is a necessary part of analytical and design procedures in connection with foundations, retaining walls and earth slopes. Essentially, shear strength within a soil mass is due to the development of frictional resistance between adjacent particles.

The shear strength of a soil may be defined as the maximum resistance of the soil to shearing stress under any given

conditions. The conditions referred to are mainly concerned with the drainage properties of the soil. For a coarse-grained soil, drainage is normally good and occurs as the test proceeds. A fine-grained soil, however, will drain very slowly, and therefore the rate of testing is an important factor. There are several basic shear tests which may be carried out on a soil, which if carried out with the same drainage conditions, should give comparable results.

4.4.1 Shear Failure and Parameters

A simple equation and theory relating the shear strength of soil to the applied normal stress was first suggested by Coulomb in 1776. The cohesive resistance to shearing is assumed to be constant for a given soil and independent of the applied stress, while the frictional resistance varies directly with the magnitude of the normal stress developed on the shear slip surface. A straight line equation for the limiting shear stress γ_f is given by:

$$\gamma_f = C + \sigma_n \tan \phi \qquad (4.23)$$

where: C = cohesion,
σ_n = normal stress on slip surface, and
ϕ = angle of internal friction.

A graphical representation of Coulomb's equation is given in Figure 4.4a from which it will be seen that the value of the cohesion (C) is the intercept on the shear stress axis and the slope of the line is tanϕ.

It is generally accepted that soil shear strength is related to effective stress according to the expression (Figure 4.4b):

$$\gamma_f = C' + \sigma'_n \tan \phi' \qquad (4.24)$$

where: C' = cohesion referred to effective stress,
σ'_n = effective normal stress on the slip surface,

$= \sigma_n - U$,
U = pore pressure acting on the surface, and
ϕ' = angle of internal friction referred to effective stress.

The shear strength parameters C' and ϕ' would have constant values for a given soil, providing that the void ratio, density and pore pressures also remained constant for different values of normal stress. This cannot be the case, either in the field or during laboratory tests, since under drained loading the volume will change and under undrained loading the pore pressure will change. It is therefore necessary to refer measured values to the type of test and conditions under which they were measured.

4.4.2 Shear Strength Theory for Unsaturated Soils

Only a limited amount of work has been done on the shear behaviour of partially saturated soil with control and measurement of σ, U_a and U_w. This probably results from the fact that such testing of soil is complex, laborious and time consuming.

Previous studies of the shear strength of partially saturated clays have dealt with the examination and/or modification of the effective stress equation. This approach has been considered promising due to the demonstrated success of the use of the fundamental effective stress equation for fully saturated clays.

One of the first approaches is that by Bishop et al (1960):

$$\gamma = C' + (\sigma - U_a + X(U_a - U_w)) \tan \phi' \qquad (4.25)$$

where: γ = shear strength of the soil,
C' = effective cohesion,
σ = total stress,
U_a = pore air pressure,
U_w = pore water pressure,
X = a soil parameter with values between zero and unity depending on the degree of saturation,

the soil type, the moisture hysteretic state and the stress conditions, and
ϕ' = effective angle of shearing resistance.

The main disadvantage of this expression is the parameter X whose value depends on many factors. By analogy with saturated soil, the shear strength of partially saturated soil was hypothesised (Bishop (1959)) to be a function of effective stress (Equation 4.11). The shear strength of a partially saturated soil was hence expressed as (Gulhati and Satija (1981)):

$$\tau_f = \frac{(\sigma_1 - \sigma_3)_f}{2} = a' + ((\sigma_3 - U_a)_f + X(U_a - U_w)_f) \tan \alpha' \qquad (4.26)$$

where: a' = effective cohesion, and
α' = effective angle of shearing resistance.

Equation 4.26 neither yields a ready estimate of shear strength on account of the difficulty in assessing the magnitude of X nor, in fact, has it ever been shown to be a valid relationship.

The problems associated with the measurement of the pore air pressure, necessary for the modification of the effective stress equation for the case of partially saturated clays, are in most cases quite complex and thus render this approach quite difficult. Yong et al (1971) suggested an energy approach to the analysis of the shearing strength of partially saturated soils where the fundamental interaction forces within the system, that contribute to the shearing resistance of the material, are implicitly incorporated.

Lewis and Ross (1955) reportedly investigated the relationship between the shear strength of remoulded clays and soil suction (soil/water potential). Whilst the results of their studies showed that there was no simple

relationship between shear strength of remoulded cohesive soils and soil suction, it was demonstrated that the shear strength of such soils was a function of soil type, dry density and soil moisture suction. Croney and Coleman (1960), similarly, showed that the unconfined compressive strength of clay soils varied linearly with the suction of continuously puddled clay. This can be supported, in part, by the work of Towner (1961) who showed that the shear strength of clay soils can be considered to "vary linearly with initial suction" despite the fact that the values obtained show some scatter.

In partially saturated remoulded clays where volume changes occur because of changes in moisture regime and stress environment, corresponding changes in the shearing resistance of the material will be expected. This dependence of shear strength on moisture content for fully saturated clays is well known. In the case of partially saturated clays, considerations involving intrinsic energy lead to the conclusion that the shear strength of the soil may be examined in terms of the existent soil/water potential so long as the moisture (and/or stress) history of the soil is accounted for.

Since soil/water potential measurements describe the energy status of soils, these can be thought of as defining the integrity or stability of the system. The application of external work to shear a soil sample distorts the soil fabric and in turn causes a redistribution of moisture in the soil because of the presence of internal pressure or stress gradients.

Accepting that the soil/water energy relationship describes the system integrity for remoulded soils, a corresponding relationship between shear strength of remoulded soils and soil suction must therefore exist (Yong et al (1971)).

Prior to the 1960s unsaturated soils were tested in much the same manner as saturated soils, using conventional testing equipment. Strain rates for unsaturated soils were relatively high. In the early 1960s, high air entry ceramic discs were placed between the sample and the lower pedestal in an attempt to measure the pore water pressures separately from the pore air pressure. Empirical procedures were proposed for estimating the strain rate for testing (Bishop et al (1960)). The testing equipment and procedures were gradually modified such that the pore air and pore water pressures could be independently measured or controlled. The axis translation technique (Hilf (1956)) was used to overcome the limitations associated with the pore water pressure measuring system. A high air entry disc was commonly sealed onto the base pedestal while a coarse, low air entry disc was placed on the top of the soil sample. This allowed for the independent control or measurement of the pore water and pore air pressures respectively. Similar testing equipment has been used by Bishop and Donald (1961), MIT (1963), Gulhati and Satija (1981) and Ho and Fredlund (1982a).

The types of testing procedures that can be used for unsaturated soil testing are similar to the procedures used in saturated soil testing. First, the pore water and pore air pressures can be set and controlled while the sample is

loaded to failure. This is a consolidated drained type of test. Second, the soil sample can be allowed to come to equilibrium at a set of stresses and then the pore air and pore water pressures can be measured while the sample is loaded to failure. This is a consolidated undrained test with pore pressure measurements at constant water content. A third procedure was proposed by Bishop and Henkel (1962) in which the pore water pressure was controlled.

Researchers have realised the need to perform strength tests on unsaturated soils at an extremely slow rate in order to ensure equalisation or dissipation of induced pore pressures (Donald (1961) and Satija and Gulhati (1979)). However, no theoretical procedure is available for predicting satisfactory strain rates. Rather it seems most appropriate to assess a strain rate or time to failure by some trial and error procedure. Test data (Bishop and Henkel (1962)) showed the relationship between strain rate and deviator stress and illustrated a levelling off of deviator stress below a particular strain rate. This gives insight into an upper limit for failing an unsaturated soil sample but will not necessarily be sufficiently slow to ensure pore pressure equalisation or dissipation. Satija and Gulhati (1979) suggested that for constant water content tests, changes in matrix suction (U_a - U_w) would be a reasonable indicator of an appropriate strain rate.

4.4.2.1 Rate of Deformation

The rate of strain for shear strength testing should be sufficiently slow to avoid non-uniformity in the pore water distribution within the sample. This is true for testing

both saturated and unsaturated soils. The rate of deformation for shearing saturated soils under undrained conditions is selected so as to ensure at least 95% equalisation of induced pore water pressure. Similarly, under drained conditions, the rate of deformation is selected so as to ensure at least 95% dissipation of induced pore water pressure. Gibson and Henkel (1954) applied the consolidation theory to a triaxial sample and formulated a theretical method for approximating the time to failure required for a drained test. The procedure has been widely accepted for estimating the strain rate for triaxial testing (Bishop and Henkel (1962)).

The choice of a suitable strain rate for testing unsaturated soils is somewhat more complicated than for saturated soils. The first complication is the high air entry disc placed at the bottom of the soil sample. These discs have low coefficients of permeability. The discs are kept saturated and allow the passage of water but not air. However, the low coefficient of permeability of the disc results in impeded flow into or out of the soil sample. In 1963, Bishop and Gibson presented a solution to the problem of impeded flow from saturated triaxial and oedometer specimens as a result of a low permeability disc placed next to the soil. The second complication is the physical properties of the unsaturated soil. The two properties of primary concern are the coefficient of permeability and compressibility of the unsaturated soil.

Ho and Fredlund (1982b) presented a theoretical model to estimate the time required to shear an unsaturated soil.

They gave the relationship between the time required for a desired degree of pore pressure dissipation during a drained test. They concluded that the physical properties of the soil, that is the compressibility and the coefficient of permeability, along with the drainage boundary conditions are the main factors affecting the strain rate. They found that the high air entry ceramic discs with low coefficients of permeability, used to separate the pore air and pore water pressures during unsaturated soil testing, are a major factor affecting strain rate.

4.4.3 Experimental Review

Bishop and Donald (1961) conducted consolidated drained tests by varying σ_3, U_a and U_w in such a way that $(\sigma_3 - U_a)$ and $(U_a - U_w)$ remained constant to demonstrate the validity of the form of the effective stress Equation 4.11, through shear behaviour.

Blight (1961) worked on four different types of soils which he prepared by compaction and studied the influence on shear behaviour of the following variables:

a) water content at compaction, and

b) confinement, that is, by varying the magnitude of $(\sigma_3 - U_a)$.

His object was to compute X, as suggested by Bishop et al (1960), and to determine whether the relationship between X and the degree of saturation is unique. He conducted constant water tests and found that X values remained between 0 and 1.0. He concluded that the relationship between X and the degree of saturation is unique and is not dependent on water content or $(\sigma_3 - U_a)$.

Donald (1961) worked on Breahead silt samples prepared from saturated soil slurry with partial saturation attained by allowing drainage to occur under a controlled negative pore pressure of sufficient magnitude to draw air into soil voids. A nominal $(\sigma_3 - U_a) = 13.73$ kN/m^2 was applied so that the rubber membrane kept in close contact with the sample. The effect of $(U_a - U_w)$ up to a value of 147 kN/m^2 was observed during the process of shear under drained conditions. He computed X values and compared them with those calculated from Aitchison's (1961) equation. He also conducted constant water content tests in order to determine the effect of the type of test on X in conjunction with data of consolidated drained tests performed at various $(\sigma_3 - U_a)$ values ranging between 13.73 and 98.07 kN/m^2. He showed that X values were independent of the type of test, that is, drainage during shear and confinement.

Bishop and Blight (1963) conducted constant water content tests on compacted Talybont clay in order to validate the effective stress equation for partially saturated soils. They varied σ_3 and U_a during shear such that $(\sigma_3 - U_a)$ remained constant. They found that these changes in σ_3 and U_a did not have any influence on $(\sigma_1 - \sigma_3)$ versus axial strain or $(U_a - U_w)$ versus axial strain. But when $(\sigma_3 - U_a)$ was changed along with changes in σ_3 and U_a, then $(\sigma_1 - \sigma_3)$ versus axial strain and $(U_a - U_w)$ versus axial strain relationships were affected. They, therefore, concluded that the effective stress equation was valid.

Some data have been produced by M.I.T. (1963) in which compacted soil samples have been tested under constant water

content test condition to study the influence of the two stress state variables $(\sigma - U_a)$ and $(U_a - U_w)$ on shear behaviour. M.I.T. (1963) reported that "direct application of the effective stress equation to the shear tests yields values of X greater than one for degrees of saturation between 65% and 73%" which is inconsistent with the statement made by Bishop et al (1960), that is, values of X parameter lie between 0 and 1.0.

Sridharan (1968) studied the variation in strength of partially saturated soils with water content keeping other factors such as void ratio and soil structure constant. He also theoretically estimated the relative effect of electrical forces and pore water tensions on the magnitude of effective stress as defined in Equation 4.21. He found that the strength / effective stress relationship is "non-linear, void ratio dependent and relatively independent of soil structure." This study was conducted on soils at very low degrees of saturation with theoretically estimated, rather than measured, values of U_w.

Gulhati (1972) studied the effects of compaction, water content at compaction, drainage and confinement during shear, on shear behaviour through evaluation of X by Bishop et al's (1960) and Blight's (1967) methods. The study was made on Delhi silt and Dhanauri clay. The soil samples were prepared by compaction at water contents dry of optimum to optimum by either standard kneading, standard static or modified kneading compactions. The samples were either sheared at constant water content or under drained conditions. He concluded that the X factor, computed as

suggested by Bishop et al (1960), is not uniquely related to degree of saturation S but the X/S relationship is influenced by compaction conditions, conditions of drainage and confinement conditions during shear. X values for some samples were found to be greater than 1.0. He also observed that Blight's (1967) method for computing X gave values which do not lend themselves to any interpretation. He concluded that "Bishop et al's (1960) X factor, although not a fundamental parameter, is nevertheless useful in providing an insight into shear behaviour of partially saturated soils." It must be emphasised that the ranges of $(\sigma_3 - U_a)$ and that of pre shear $(U_a - U_w)$ used were quite narrow.

Gulhati (1975) presented results of triaxial shear tests on two compacted soils in the partially saturated state. The experimental results also yielded some X factors greater than 1.0. Blight (1967) carried out theoretical analyses and concluded that X can take on values far greater than unity at low suctions.

To compare volume change behaviour in unsaturated and saturated soils during triaxial shear and also in order to obtain the relationship between degree of saturation and X, Kawakami and Abe (1975) conducted constant water content tests on sandy silt samples compacted at two water contents dry of optimum (S = 48% and 64%). $(\sigma_3 - U_a)$ ranged from 67.67 to 362.86 kN/m^2 but the range of $(U_a - U_w)$ was limited from only 77.47 to 138.28 kN/m^2. Their data show that the X/S relationship is not affected by water content. X values, computed according to Bishop et al (1960), were found to be between 0 and 1.0.

It is apparent, from the above presentation, that there is no conclusive evidence that the equation for partially saturated soil, as suggested by Bishop (1959), is valid for shear behaviour of partially saturated soil.

During the past three dacades there has been an increasing use of two independent stress variables to describe the behaviour of unsaturated soils (Coleman (1962), Bishop and Blight (1963), Burland (1965), Aitchison (1967), Matyas and Radhakrishna (1968), Barden et al (1969), Brackley (1971), Fredlund (1974), Fredlund and Morgenstern (1976 and 1977), Murthy et al (1987) and Peterson (1992)). Most consideration has been given to describing the volume change behaviour and suitable constitutive relations for unsaturated soils. Several investigations have been made into the shear strength characteristics of unsaturated soils (Bishop et al (1960), M.I.T. (1963) and Sridharan (1968)). However, none has proven completely successful.

In 1978, Fredlund et al proposed a shear strength equation for unsaturated soils which was an extension of the commonly used Mohr-Coulomb (Terzaghi (1936)) equation for saturated soils. In the extended form of the Mohr-Coulomb equation, the effect of matrix suction, $(U_a - U_w)$, is assumed to yield a linear increase in shear strength. When $(\sigma - U_a)$ and $(U_a - U_w)$ are used as the stress state variables, the proposed unsaturated soil shear strength equation is as follows:

$$\gamma = C' + (\sigma - U_a) \tan \phi' + (U_a - U_w) \tan \phi^b \qquad (4.27)$$

The friction angle, ϕ^b, is equal to the slope of the diagram of matrix suction, $(U_a - U_w)$, versus shear strength when $(\sigma - U_a)$ is held constant.

The first stress state variables used by Fredlund et al (1978) were $(\sigma - U_w)$ and $(U_a - U_w)$. The advantage of this combination of variables is that it provides a transition from the unsaturated to the saturated case. The disadvantage arises in that when the pore water pressure is changed, two stress state variables are being affected. The relative significance of each variable must be borne in mind when considering the shear strength. This is also the disadvantage associated with utilising the $(\sigma - U_a)$ and $(\sigma - U_w)$ combination of stress state variables.

The second combination of stress state variables used was $(\sigma - U_a)$ and $(U_a - U_w)$. The advantage of this combination is that only one stress variable is affected when the pore water pressure is changed. Regardless of the combination of stress variables used to define the shear strength, the value of the shear strength obtained for a particular soil with certain values of σ, U_a and U_w must be the same.

The form of the equation describes a plane on a three dimensional plot as presented in Figure 4.5. Figure 4.6 shows the stress circles corresponding to the failure conditions plotted on a three dimensional diagram with the two stress state variables plotted on the horizontal axes and the shear strength as the ordinate.

There is a smooth transition from Fredlund et al's (1978) unsaturated soil shear strength equation to the conventional shear strength equation for saturated soils (Terzaghi

(1936)). As saturation is approached, the pore air pressure, U_a, becomes equal to the pore water pressure, U_w. At this condition, the proposed equation reverts to the conventional shear strength equation for a saturated soil.

In 1978, Satija initiated an extensive laboratory testing programme on statically compacted Dhanauri clay. Four series of constant water content (CW) and consolidated drained (CD) tests were conducted with pore air and pore water pressure measurements. The soil was compacted at two densities but with the same initial water contents. Both the constant water content and consolidated drained tests were performed at each of the compaction conditions. Although the samples for a particular series of tests were compacted at the same density and water content, they were allowed to equalise to various initial stress states to form an equally spaced grid of tests on a three dimensional surface. Figure 4.7 shows the failure stress circles for one series of the constant water content tests performed on samples with a high initial density. The shear strength versus matrix suction plot for all the constant water content tests on the high initial density samples is shown in Figure 4.8.

Murthy et al (1987) undertook drained triaxial compression tests on compacted specimens to investigate the variation of strength with changing degree of saturation keeping soil fabric and void ratio constant. They analysed their test results in terms of drained shear strength and the Mohr-Coulomb strength parameters as a function of the degree of saturation. They also attempted to estimate the effective

negative pore water pressure at failure by relating it to the cohesive intercept.

They found that at any degree of saturation, the drained compression strength increased linearly with the consolidation pressure and these relationships are parallel at different degrees of saturation. The test results also showed that for any consolidation pressure, the deviator stress at failure increased to a peak value at an optimum degree of saturation beyond which it decreased. The drained angle of shearing resistance remained almost constant but the cohesion intercept varied with the degree of saturation.

Peterson (1992) conducted a laboratory investigation to assess the influence of density and water content on the shear strength of unsaturated soil. Specimens were moulded to an initial density at water content wet or dry of optimum, consolidated to a range of densities by selected values of applied stress, and sheared as constant water content tests. Analysis of the data indicated the strength of unsaturated soil could be predicted by a modified Mohr-Coulomb strength relationship. The effect of density was to influence the friction angle, whereas the effect of water content was to influence the cohesion intercept. The effect of suction was to increase the cohesion intercept.

The results of the study indicated that the shear strength of unsaturated soil was dependent upon the water content and density of the specimen at failure. Peterson proposed the following equation, as a modified Mohr-Coulomb strength relationship, to predict the strength of the unsaturated soil.

$$\gamma = C' + (\sigma - U) \tan \phi' + C_{\psi} \qquad (4.28)$$

where: γ = shear strength,
$(\sigma - U)$ = applied stress, and
C_{ψ} = cohesion due to suction.

C' and ϕ' were determined in the conventional manner for saturated soils.

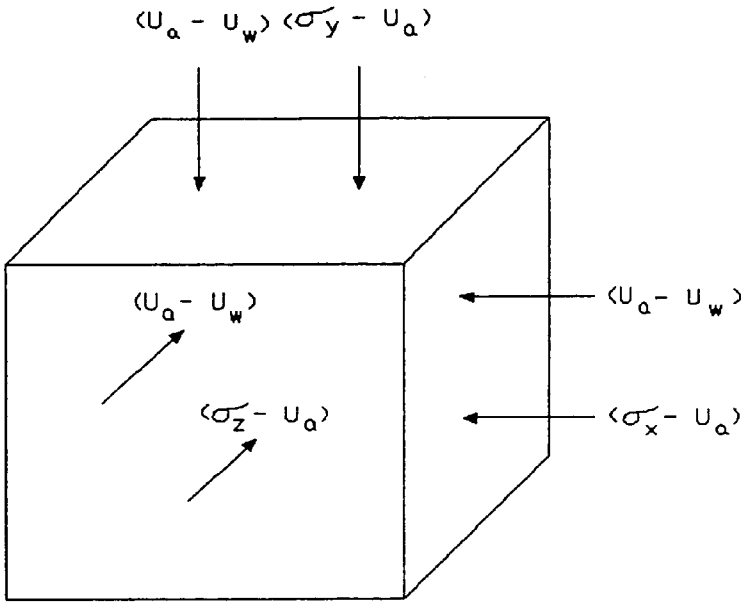

Figure 4.1 Stress state of soil particles for an unsaturated soil (After Fredlund (1979)).

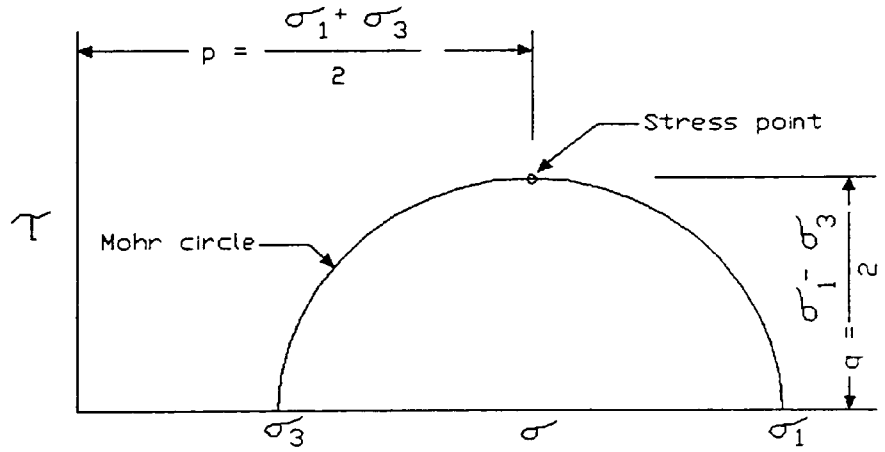

(a) Stress point

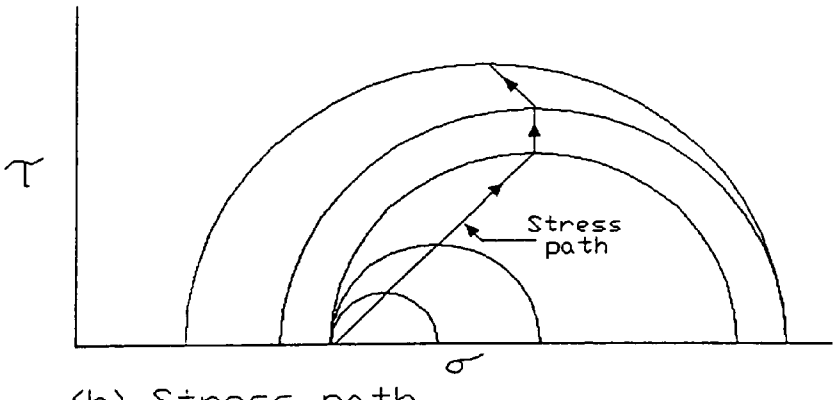

(b) Stress path

Figure 4.2 Stress point used in stress path method (After Lambe (1967)).

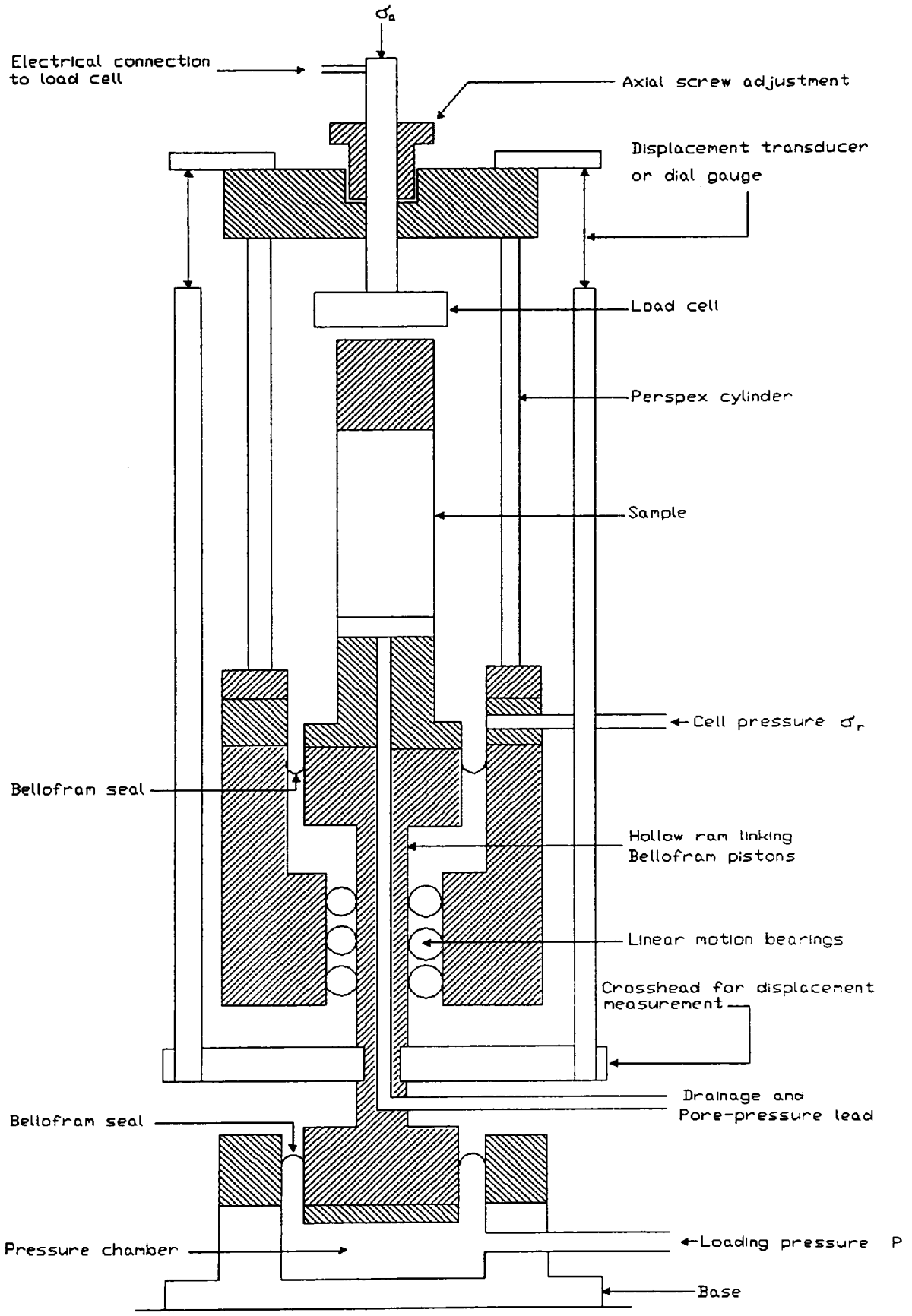

Figure 4.3 Diagrammatic layout of the hydraulic triaxial apparatus (After Bishop and Wesley (1975)).

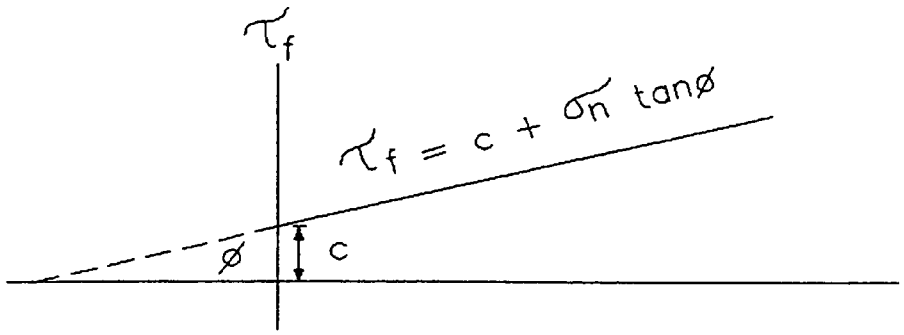

Figure 4.4a in terms of total stress.

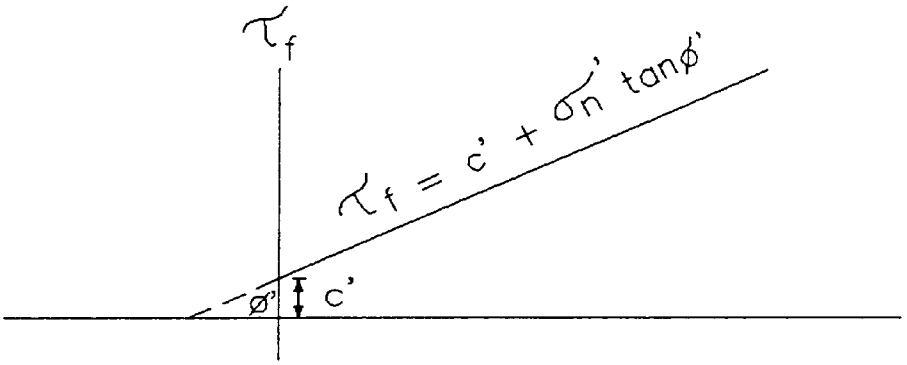

Figure 4.4b in terms of effective stress.

Figure 4.4 Coulomb's equation and failure envelope.

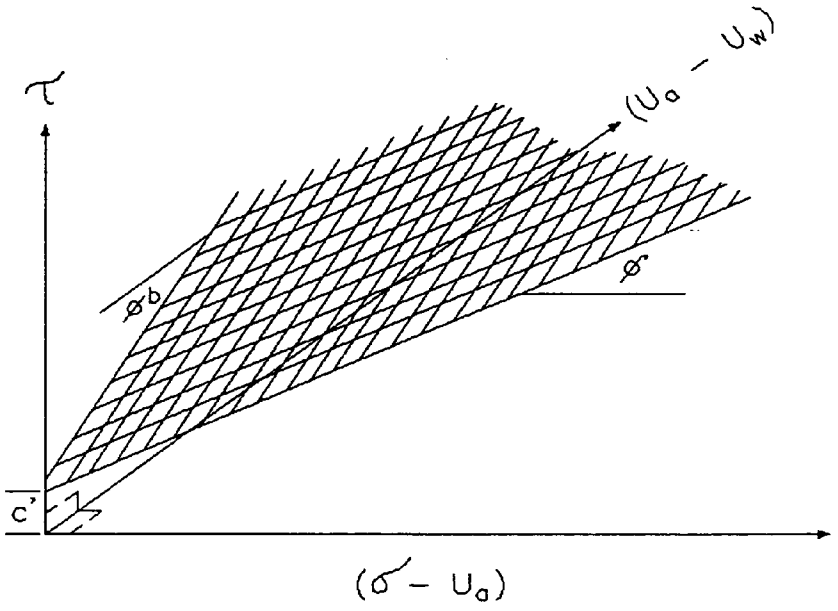

Figure 4.5 Graphical representation of the shear strength equation for unsaturated soils (After Fredlund et al (1978)).

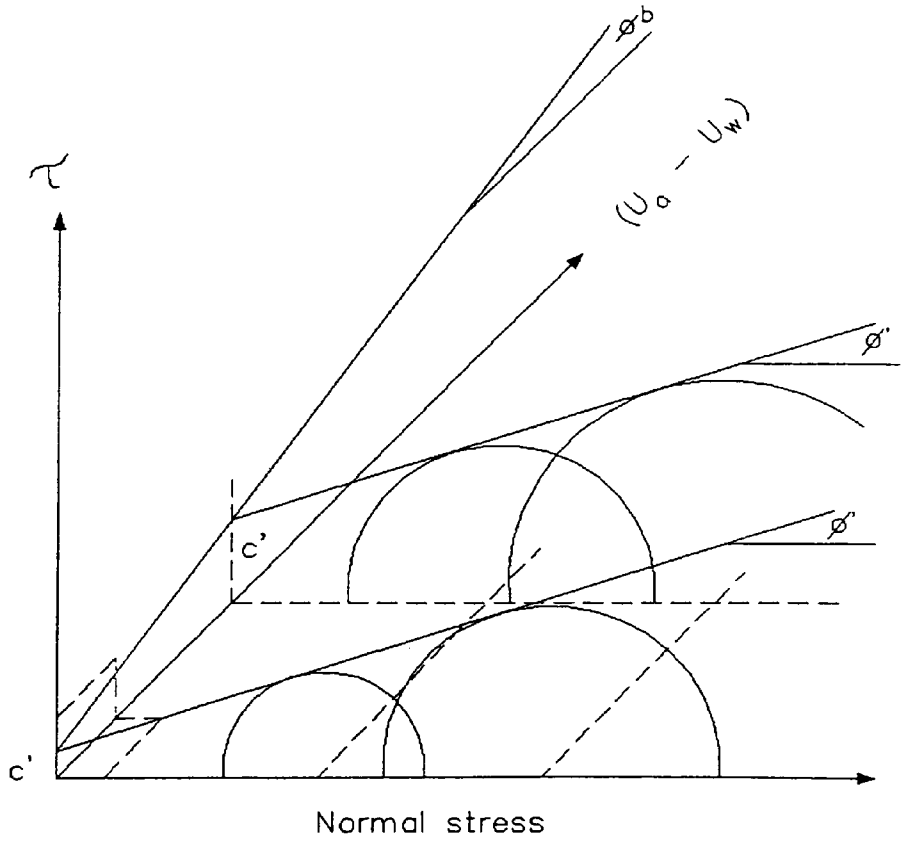

Figure 4.6 Three dimensional failure surface using stress variables ($\sigma - U_a$) and ($U_a - U_w$) (After Fredlund et al (1978)).

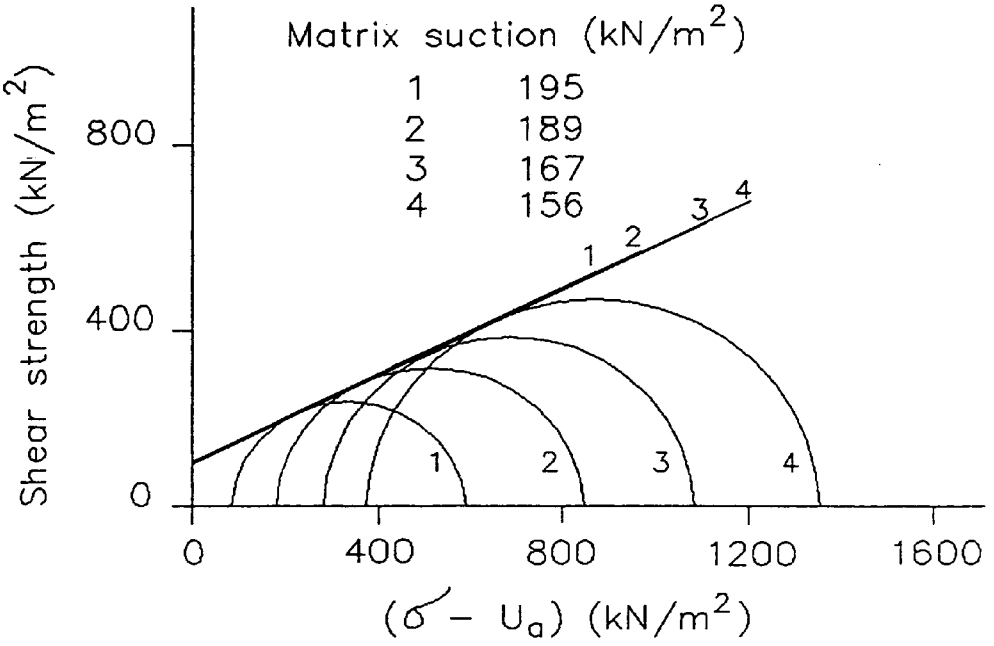

Figure 4.7 Mohr failure circles for Dhanauri clay with as compacted density (After Satija (1978)).

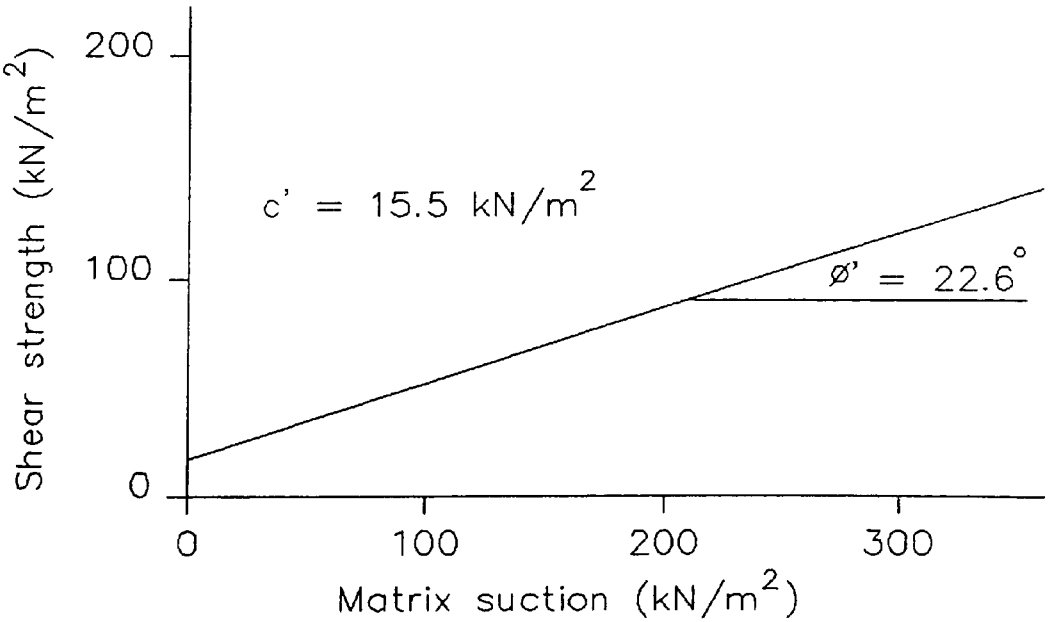

Figure 4.8 Shear strength versus matrix suction for Dhanauri clay with high as compacted density (After Satija (1978)).

CHAPTER FIVE

REVIEW OF SUCTION MEASUREMENT TECHNIQUES

5.0 Introduction

A large number of experimental techniques and pieces of apparatus have been developed over the past 40 years for the testing of expansive soils. They fall into three broad categories; swell and swell pressure, soil suction and field measurement techniques.

5.1 Swell and Swell Pressure Tests

Swell and swell pressure are dependent parameters; no attempt has been made to sub divide these into two different categories.

5.1.1 Methods Without Suction Control

The double oedometer technique may be used to monitor swell pressure and was initially developed by Jennings and Knight (1957) for collapsing soils. This technique involves placing soil samples in two oedometers each under a uniaxial pressure of 6.9 kN/m^2. Water is added to one sample through both top and bottom porous discs and the sample is allowed to swell until equilibrium is reached. The second sample is maintained at the field moisture content between non-absorbent discs. After equilibrium is reached both samples are subjected to a conventional consolidation test. The e-log p curves (Figure 5.1) are adjusted until the straight line portions, near the right hand limit on the pressure axis, coincide. The predicted void ratio swell under load

may then be read for any vertical pressure. Burland (1962) noted that the swell under load should be determined from a rebound curve not a reload one and proposed a technique of transferring a rebound curve to the estimated in situ (e-log p) point.

De Bruijn (1961) developed a volumnometer allowing vertical and horizontal swell under isotropic pressure. The soil sample is confined between two end plates and sealed by a rubber membrane. Water is admitted through one of the end plates. The sample is placed within a cell filled with water and pressure applied using a pressure coupler. Vertical movement is measured by a displacement transducer connected to a rod which passes through the top plate of the cell. Using this equipment, De Bruijn (1961) determined the potential expansiveness from a range of swelling moisture contents.

Sullivan and McClelland (1969) developed a technique in which the soil sample is allowed to wet up to equilibrium under constant volume conditions. The stress required to maintain the volume is the constant volume swell pressure. The sample is then unloaded in steps to determine the rebound curve and the swell pressure under load is measured at the estimated field vertical stress.

Schreiner (1988) reported on a laboratory manual in which MacIver and Hale (1970) dealt with both swell under load and constant volume swell pressure. The swell test is performed after obtaining the zero reading under a pressure of 6.9 kN/m^2 by adding the overburden pressure plus the expected design load and then allowing the sample to absorb

water. The load is then increased to maintain the sample height within 0.005 mm while the sample absorbs water.
Agarwal and Sharma (1973) described an automatic control system for performing constant volume swell pressure tests.

5.1.2 Methods Using Suction Plates

A hydraulic oedometer in which suction could be applied to the water below the bottom porous disc was developed by Rengmark and Eriksson (1953). The surcharge was applied hydraulically above a rubber membrane. The applied suction was limited to the cavitation suction of water of about 100 kN/m^2. This allowed measurement in the very wet range of partial saturation only.
Alpan (1957) used a similar technique to Rengmark and Eriksson (1953), but the surcharge was applied via a proving ring.
Didier et al (1980) developed a high pressure oedometer cell in which suction could be measured directly through the water. The apparatus is a further development of a previous cell (Didier (1973)) in which suction could be controlled by admitting air at a known humidity into the sample.
Chang (1969) developed a pressure plate apparatus (Figure 5.2). It consisted of a purpose built cell in which the laterally confined sample is placed on a high air entry porous plate. This permits air pressure above the sample to be raised to 200 kN/m^2 relative to the water below the plate. Testing can therefore be performed at suctions greater than those possible in a suction plate apparatus. The permissible suctions are governed by the air entry value of the porous disc. The measured suction is the matrix

suction, but if there is a significant salt content in the soil, there will then be uncontrolled change in the solute suction.

The major disadvantage of the pressure plate technique is that diffusion of salts can take place between the pore water in the sample above the porous disc and the pore fluid beneath the porous disc. This can cause long term changes in swell or swell pressure (Richards (1980)).

Escario (1969) introduced the pressure membrane oedometer. It functions similar to the pressure plate apparatus except that a semi-permeable membrane is placed between the sample and the porous disc. More advanced pieces of apparatus are described by Aitchison and Martin (1973) and Escario and Sáez (1973). However, none of these authors demonstrated that the membrane is actually semi-permeable with regard to salt and water. Richards (1980) claimed that salt diffusion was significant in tests that he performed using a pressure membrane apparatus. If the membrane is considered permeable to the salts, then the apparatus is no more than a pressure plate oedometer with an increased range (Schreiner (1988)).

5.1.3 Methods Using Osmotic Consolidometer

In the osmotic consolidometer developed by Kassiff and Ben-Shalom (1971), the matrix suction in the sample is controlled by the osmotic pressure difference across a semi-permeable membrane separating the sample from a solution of carbowax 6000 in water. The concentration of carbowax is varied to obtain the desired osmotic pressure difference. The apparatus was further developed by Kassiff et al in 1973 who found that carbowax 20,000 was required to prevent

leakage. Diffusion of salts from the soil sample into the carbowax solution is possible and may affect the validity of the results.

Komornik et al (1980) developed a hollow sample technique for measuring the effect of suction and lateral stress on swell in a triaxial cell. The suction is controlled by using carbowax within the central core, separated from the sample by a semi-permeable membrane. They used sodium decahydrate to prevent soil bacteria from destroying the membrane, which has been found to be a problem in the osmotic consolidometer.

5.1.4 Methods Using Controlled Wetting and Drying

Beal (1984) presented a method which permits controlled wetting and drying of an unconfined cylindrical sample. This is to determine vertical strain in terms of moisture content. Water may be added to the top of the sample at a controlled rate or removed by opening the plastic wrapping and gently warming the sample. A vertical load may be applied by mechanical means, allowing the determination of vertical strain versus moisture content curves under various surcharges.

A significant restriction on the test is the requirement that the surcharge be less than the unconfined compressive strength of the sample. This test permits the measurement of swell due to known suction changes in a soil under a set of stress conditions. The stress testing should not differ significantly from those to be expected in the field where the soil has previously cracked due to shrinkage.

Pile and McInnes (1984) developed a technique which uses a sample confined in a perforated ring which is dried in a vacuum desiccator under a surcharge applied by springs. Suction is measured using a Wescor thermocouple psychrometer, and the instability index is determined as vertical strain per unit log suction increase. Wetting tests are performed in the same way as swell under load tests in conventional oedometers with suction measured at the beginning and end of the test.

This test allows the measurement of the vertical swell of a soil in terms of measured suction changes. However, there may be some difficulties in interpretation of the results in terms of field conditions due to the variation in lateral confinement.

5.1.5 Discussion of Swell and Swell Pressure Tests

It is evident from Sections 5.1.1 to 5.1.4 that there is not a test method which can reasonably model the field stress and suction paths. The measurement of volume change due to known suction changes has also not yet been accepted as standard practice. This may be due to the complex and expensive apparatus required.

The techniques that show promise for routine testing for heave prediction are the pressure membrane oedometer, the osmotic oedometer and the pressure plate oedometer.

The pressure membrane oedometer has the significant benefit that salt diffusion may be eliminated if the membrane is correctly chosen. This is of particular importance where the salt content of the soil is high. The effect of diffusion of salts from the soil will be to reduce the salt concentration

of the pore fluid, which will increase the expansiveness of the soil.

All semi-permeable membranes are in fact permeable to salts. An alternative technique used to overcome the salt diffusion problem is the use of a water supply that has the same concentration as the pore fluid (Richards et al (1984)). However, if the water supply in the field is rainwater, with a low or zero salt content, then this technique will suppress the expansiveness of the soil in the laboratory compared with the soil in the field. However, where salt contents of the soil are low, this may not be a significant problem. The salt content of soils is seldom determined, and the problem has only been addressed in Australia where salt contents of up to 2% have been reported (Richards (1980)).

Of the remaining tests for measuring volume change, the swell under load technique, permitting complete wetting up in an oedometer, is the nearest to the field stress and suction paths (Brackley (1975a)). In the field the final moisture condition may exhibit a significant suction and this may make the test over predict the swell. Difficulty in obtaining full saturation may also exist, but could be reduced by the use of a Rowe oedometer in which a back pressure is applied.

All oedometer type tests in which the sample is laterally confined, will be affected by friction on the inside of the confining ring which will tend to restrict the swelling of the sample. The lateral stress has been measured and found to be large (e.g. Komornik and Zeitlen (1965) and Ofer et al (1984)). The friction on the inside of the ring is much

more significant for swell testing than for consolidation testing, since in swell testing the area of the contact surface tries to increase whereas in consolidometer testing, the contact area decreases. In addition, Fredlund (1969) noted that filter paper exhibited significant compressibility and hysteresis and that compressibility of the apparatus may be significant in constant volume swell pressure tests.

5.2 Soil Suction

The most simple and flexible way for defining soil suction is in terms of the thermodynamic potential. The International Society of Soil Science defined soil water potential as (Richards (1980)):

> "the work done per unit quantity of pure water in order to transport reversibly and isothermally an infinitesimal quantity of water from a pool of pure water out side the adsorptive force fields at a specified elevation and at atmospheric pressure to soil water (at the point under consideration)."

The International Society of Soil Science defined soil suction as (Richards (1980)):

> "the negative gauge pressure, relative to the external gas pressure on the soil water (normally atmospheric pressure), to which a pool of pure water at the same elevation and temperature must be subjected in order to be in equilibrium with the soil water."

Matrix and osmotic suctions have been defined as the two components of soil suction. The matrix suction of a soil can theoretically be independently measured or controlled in a soil sample, whereas osmotic suction cannot but can be obtained by indirect means. This is usually achieved by measuring or controlling both the total (i.e. matrix plus

osmotic) suction and the matrix suction, or by the measurement of suction on samples of pore fluid by dilution or high pressure squeezing.

A great variety of methods for measuring soil suction in the laboratory are reported in the literature. These methods include the pressure plate, pressure membrane, suction plate, centrifuge, freezing point depression, vacuum desiccator, electrical resistance gauge and thermocouple psychrometric technique (Croney et al (1952), Aitchison (1965) and Johnson (1974)). Among these methods, the pressure plate and pressure membrane devices appear to be the most commonly used methods for the laboratory measurement of soil suctions.

5.2.1 Total Suction

5.2.1.1 Vacuum Desiccator

This is generally accepted as one of the standard suction controlling devices which is often used for calibration of other techniques. It controls the total suction via the humidity of the air in which the sample is placed (Aitchison and Richards (1965)).

The principle of the vacuum desiccator is the establishment of equilibrium conditions between a soil sample and a standard solution of salt or acid in a closed container. The standard solution creates a known humidity within the container and the soil takes water from or loses water to the air in the container until it reaches equilibrium. Aitchison and Richards (1965) gave data for sulphuric acid and Baker et al (1973) for sodium chloride solutions. The

vacuum is applied to speed up the process of drawing water out of the soil.

A further technique using the vacuum desiccator for reducing the testing period is the null point method (Aitchison and Richards (1965)) which can be used with several other suction controlling techniques. Portions of a soil sample are placed in a series of vacuum desiccators for a fixed period, usually 24 hours. The humidity in each desiccator is chosen so that the series of desiccators cover the range of suction required.

5.2.1.2 Calibrated Filter Paper

This technique utilises the high standard of repeatability of moisture content versus suction for commercial grades of filter paper. Calibration may be performed using saturated salt solutions, pressure membrane or plate apparatus or soils at known distances above a water table. Discs of dry filter paper may then be placed in contact with or near a soil sample until the moisture content of the filter paper is in equilibrium with the suction of the soil. If the filter paper is in contact with the soil, then the suction that is measured is the matrix suction, as the water in the soil and in the filter paper are in contact and there will be no osmotic effects. Where the filter paper and soil are not in contact, the measured suction will be the total suction (McQueen and Miller (1968)).

5.2.1.3 Psychrometers

Two types of psychrometers, the thermistor and the thermocouple have been used in geotechnical engineering for

measurement of total suction. Both work on the same principle as the wet and dry bulb thermometer. The thermistor has been extensively developed in Australia by Richards (1965) and Peter and Martin (1973). One of two thermistors is cooled by evaporation of a water drop. The effect of the cooling is to change the resistance of the thermistor. The resistance change is measured as a voltage change in a four arm bridge and is calibrated against standard solutions as used in the vacuum desiccator.

The thermocouple has been developed for engineering use in the USA, largely at the Waterways Experiment Station (Snethen (1979)). The effect of cooling one of the thermocouples by evaporation of the water on it is to produce a measureable electric current. As above, the output current is calibrated against known suctions.

Psychrometers measure the suction via the humidity of the air in equilibrium with the soil. There should be little alteration of the soil suction by the moisture movement caused by the test procedure. Both types are sensitive to temperature changes, and must therefore be calibrated for various temperatures or be used in a constant temperature environment.

5.2.2 Matrix Suction

5.2.2.1 Suction Plate

The suction plate apparatus is used for measuring matrix suction (see Section 5.1.2). Due to its simplicity and reliable interpretation, this method is still one of the standards used for calibration of indirect methods. In order to measure matrix suction correctly, the water in and

beneath the porous plate must be identical to the soil water.

5.2.2.2 Pressure Plate

The mechanism of matrix suction control by a pressure plate was described by Chang (1969) (Figure 5.2). Details of a pressure plate cell, and a guide to calibration for compressibility of the cell were given by Mou and Chu (1981). This cell is intended for measurement of the soil suction by rapid adjustment of the air pressure to prevent the sample taking up or losing moisture. Bocking and Fredlund (1980) reviewed the limitations on the use of this technique with regard primarily to the null point cell in which the water pressure below the plate is measured with a pressure transducer. The suction is obtained from the difference between the air pressure above the sample and the water pressure below the sample. As the presence of occluded air bubbles may lead to an overestimate of the soil suction, it is important to have fully interconnected air voids.

The suction measured by both suction and pressure plates usually differs from the matrix suction. Matrix suction generally requires that the fluid in the soil and on the remote side of the porous wall or plate should be identical. This is not usually the case as distilled water is generally used beneath the plate, and may account for some of the apparent inconsistencies in the measurement of matrix and total suctions (Pile (1980) and Richards (1980)). Furthermore, both of these pieces of apparatus permit diffusion of salts between the pore fluid and the water supply.

5.2.2.3 Pressure Membrane

A pressure membrane may be used to monitor matrix suction. A detailed explanation of the apparatus is presented in Section 5.1.3.

5.2.2.4 Gypsum Block

The technique encompassing a gypsum block has been used widely in Australia (Aitchison and Richards (1965), South Africa (De Bruijn (1973)) and Israel (Kassiff et al (1967)). The resistance or conductivity of gypsum varies with the moisture content. Blocks of gypsum with electrodes installed during fabrication are calibrated under a range of moisture contents or suction conditions using standard suction control techniques. Each block must be individually calibrated, and may then be used for measuring the suction of a soil with which it is in equilibrium. Gypsum blocks are often used in boreholes for field measurement of matrix suction but are subject to inaccuracies due to temperature and soil salinity.

5.2.2.5 Osmotic Consolidometer

The osmotic consolidometer may be used to measure matrix suction and has been discussed in Section 5.1.3.

5.2.2.6 Calibrated Filter Paper

Calibrated filter paper may be used to measure matrix suction and has been discussed in Section 5.2.1.2.

5.2.2.7 Thermal Block

Lee and Fredlund (1984) described the calibration of a sensor which works on the rate of loss of heat from a porous

block. The rate of heat loss is sensitive to the moisture content of the block. It is accurate over the same range as the consolidometer, and moderately accurate up to a suction of 200 kN/m^2.

5.2.3 Summary of Soil Suction Measurement Techniques

A wide range of techniques is available for suction measurement in soils. The suction plate, pressure membrane and vacuum desiccator have been widely accepted as standard apparatus. Richards (1980) has raised significant doubt regarding salt diffusion that may affect all methods that require liquid transfer with the exception of the desiccator. Where the salt content of the soil is significant, the suction and pressure plates and pressure membrane apparatus will control the matrix suction in the soil. In these cases the matrix suction will be approximately equal to the total suction as the osmotic suction due to the salt content will be small. Where the salt content is high, it is suggested that the pressure membrane apparatus may measure a greater suction, that is, approaching the suction between pure water and soil water through a semi-permeable membrane, although it has generally been assumed to measure matrix suction (Richards (1980)).

In order to measure matrix suction correctly with the suction plate, pressure plate or pressure membrane, the fluid throughout the system should be identical to the initial pore fluid. This approach was used by Aitchison and Peter (1973) with a pressure membrane oedometer. The vacuum desiccator and saturated salt solutions appear to be the only reliable methods of controlling the total suction in a

soil sample. Where tests are of short duration, the pressure membrane may also be suitable for total suction control, and the suction plate and pressure plate for matrix suction control. Considerable care must still be exercised in determining the relevance of the measured suction to the field conditions.

5.3 Field Measurement Techniques

The measurement of soil heave and the associated suction changes at test sites have been performed since the 1950s. During the past 40 years more than 25 methods for the determination of the engineering characteristics of expansive soils and the prediction of heave have been proposed. Many of the proposed methods relate to laboratory or index tests whereas in situ tests, being more complex, have received less attention.

Valuable work was performed by (De Bruijn (1965, 1973), Donaldson (1965) and Blight and De Wet (1965)), among others, in the development of field tests for heave prediction.

Burland (1984) considered field testing to be perhaps "the most reliable and direct approach for evaluating the in situ characteristics of expansive soils." The primary requirement of a field test is to provide a profile of heave at various depths and corresponding moisture or suction changes. He suggested the use of surface heave points and depth heave points for obtaining the profile of heave. These should be located at the centre, the edge and at the third points on two orthogonal radii (Figure 5.3). Additional surface heave points should be located at half radius beyond the circular

test area on the same radii. Depth heave points should be located at strata boundaries and extend to at least 5 m. A stable datum point is needed and should be located below the lowest water table level or in some other stable soil or rock. Heave points located at depth may be either made of rods with anchor plates at the depth of interest and isolated along their length by a steel sleeve, or by wires anchored at depth and held in tension at the surface (Stevens and Matlock (1976)). They also used psychrometers in permanent access tubes to monitor soil suction.

Field tests are often used for evaluating the effect of techniques for minimising heave, particularly for roads. Little development has been made on instrumentation for measuring swell pressure in the field. Gupta et al (1983) devised a downhole swell pressure apparatus which may be used with wetting up of the whole test area. Ofer et al (1983, 1984) have developed a means for measuring lateral swell pressure using a probe that is pushed into a slightly undersize hole. Water is supplied to the soil via porous discs near the load cells which measure the lateral stress. Neither Gupta nor Ofer et al have tested their apparatus extensively in the field.

Baker et al (1973) developed a tensiometer which is a modification of the suction plate apparatus for field use. It consists of a saturated porous plate mounted in a water filled deaired cell. The porous disc is held in contact with the soil, and the soil exerts a suction on the water in the tensiometer. This suction is usually measured directly by a gauge.

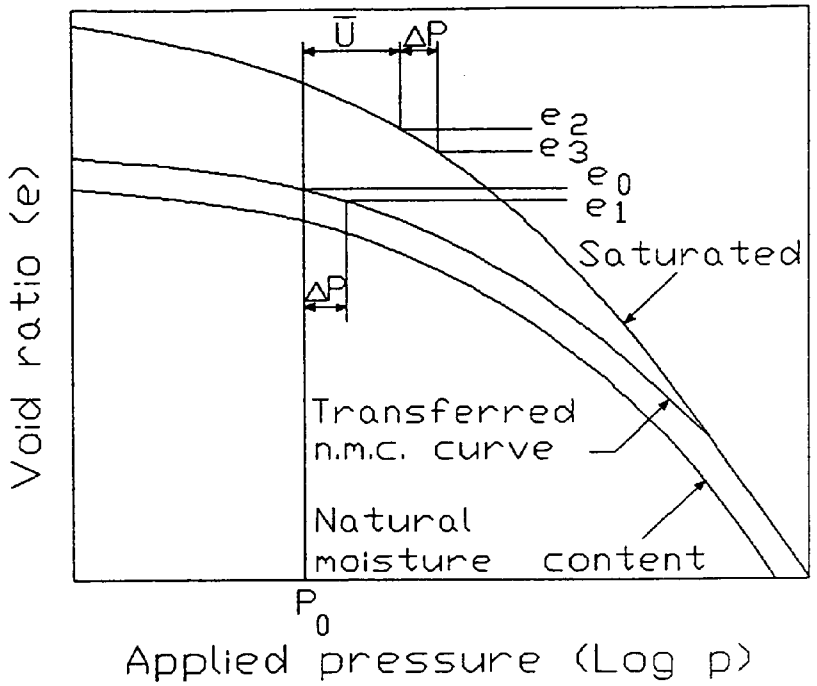

Figure 5.1 e-log p curves showing adjustment to bring straight line portions coincident (After Jennings and Knight (1957)).

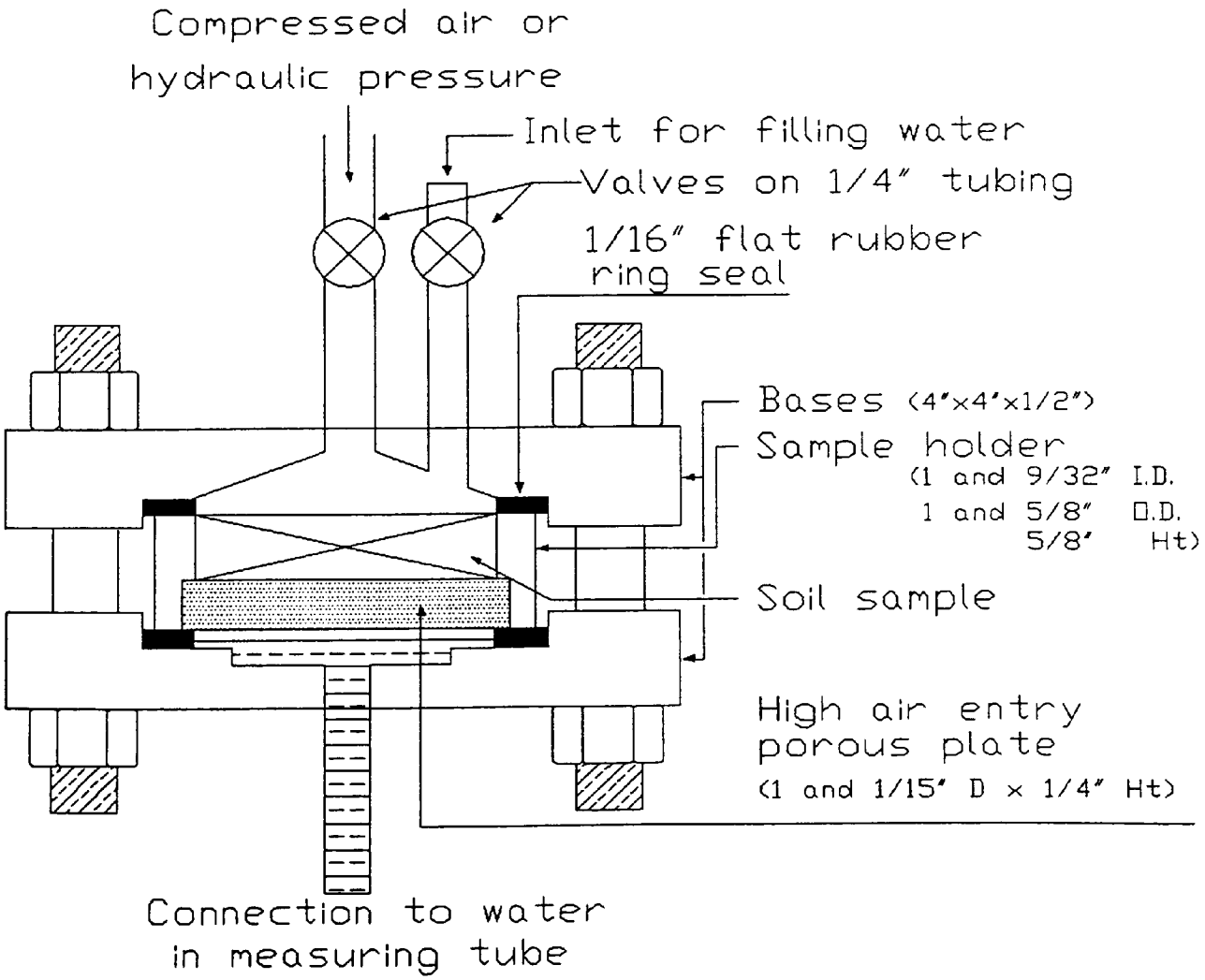

Figure 5.2 Details of pressure plate apparatus (After Chang (1969)).

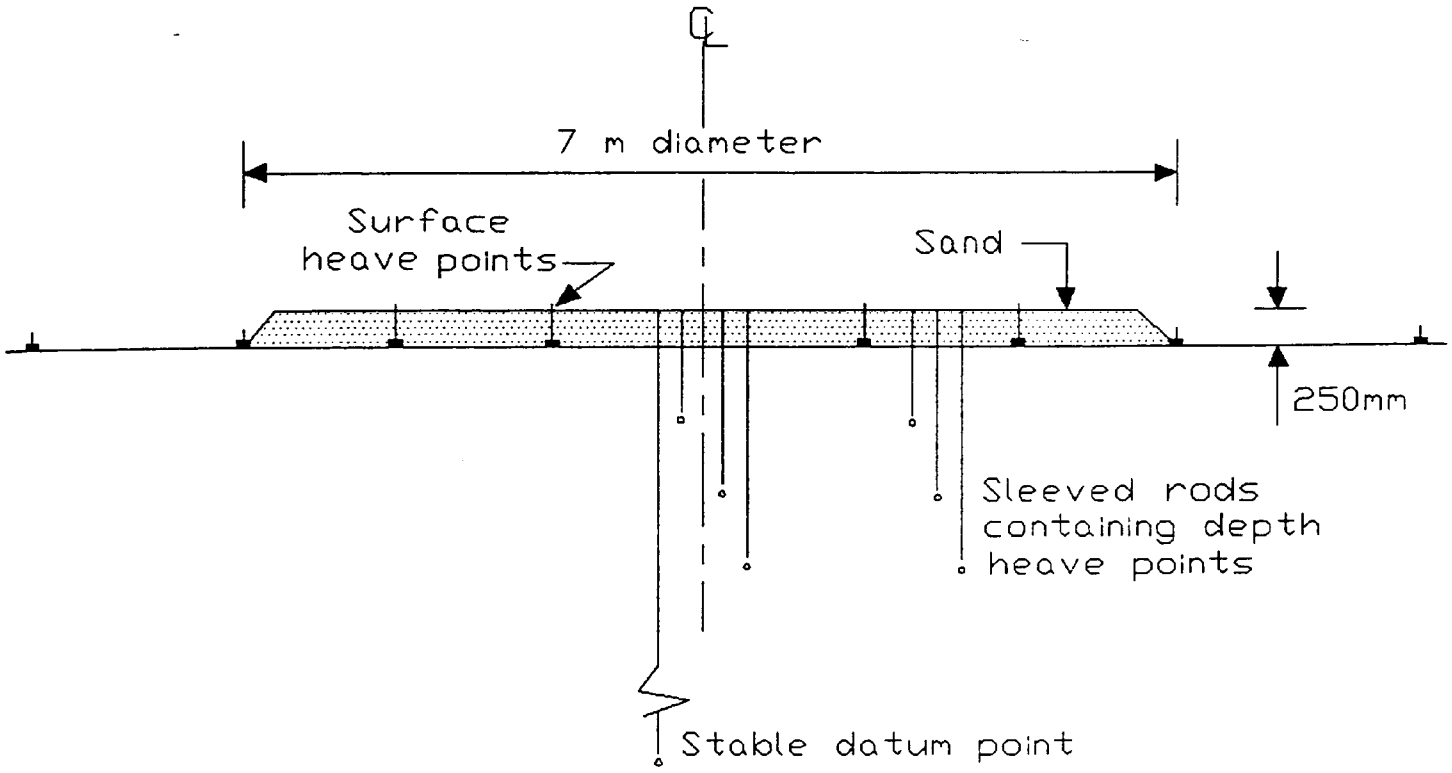

Figure 5.3 A simple direct field test using a 250 mm thick sand blanket which is previously irrigated (After Burland (1984)).

CHAPTER SIX

TESTING EQUIPMENT AND SAMPLE PREPARATION

6.0 Introduction

In order to study the behaviour of unsaturated expansive soils it is necessary to measure the flow of fluids and the deformation of solids. To achieve this, the soil testing system must operate in either of the following modes:

1) **Undrained:** no movement of air and/or water in or out of the specimen, or
2) **Drained:** the movement of air and/or water in and out of the specimen against a controlled pressure system.

The difficulty of separating the applied air and water pressures has long been recognised by soil scientists. This may be overcome by employing a pressure membrane or pressure plate technique within a triaxial system.

6.1 Development of Equipment

Many past researchers in the field of expansive soils engineering have based their experimental work on uniaxial (i.e. one dimensional) oedometer testing. They have restrained their samples from expanding laterally, by confining them in a ring, and allowing the soil to expand uniaxially. These researchers have omitted an important characteristic of unsaturated expansive soils, namely that the soil expands in all directions though with different magnitudes. In addition, an important disadvantage of one dimensional consolidometer testing is that the specimen is

subjected to lateral skin friction. In a triaxial cell the measured swell pressures would therefore be more realistic than swell pressures measured in a one dimensional consolidometer.

Komornik and Zeitlen (1965, 1970), Dudley (1971), Lewin (1971), Snethen (1972), Snethen and Haliburton (1973), Klementev (1974), El-Ruwayih (1976), Cole (1978), Ofer (1980), Attinger and Köppel (1983), Johnson (1987), Fourie (1989), Edil and Alanazy (1992) and Xin and Ling (1992), among others, have attempted to quantify the potential lateral expansion of soils.

The testing of unsaturated soils took a new direction as a result of Hilf's work in 1956. Prior to that, little attention had been paid to the difference between the air and water pressures in the pore fluid and their relationship to total stress.

Conventional volume change testing can be broadly sub-divided into one of two categories. The first category involves applying total pressures to a sample and monitoring the volume change of the sample. The second category involves applying various differential fluid pressures and monitoring the water volume change. Fredlund (1973) outlined the general basic requirements for testing unsaturated soils as:

1) **Pressure Requirement**

   The total, air and water pressures must either be measured in an undrained system or controlled in a drained system. The most versatile equipment would therefore incorporate the ability to either measure or

control all pressures.

2) **Deformation Requirement**

The volume change of the overall sample should be measured along with either the air or water phase volume change. The fluid phase volumes must be separable and must be accurately measured over long periods of time.

High air entry ceramic discs are generally used to separate the air and water pressures when testing unsaturated soils (Bishop and Henkel (1962)). Although saturated discs resist the passage of free air at differential pressures less than the air entry value, dissolved air diffuses through the water in the disc (Bishop and Donald (1961)). The diffused air then comes out of solution below the ceramic disc. This continues to be one of the main problems associated with testing unsaturated soils (Bishop (1969)). Unsaturated soils contain a relatively small amount of water and require lengthy periods of time for their testing. In order to accurately measure the water in the soil at any time, it is necessary to measure the amount of air that diffuses through the high air entry disc and apply a correction to the measured water volume change.

6.1.1 Double-Walled Triaxial Cell (Testing Station No. 1)

Bishop and Donald (1961) modified a four inch (100 mm) triaxial cell for performing shear strength tests on unsaturated Braehead silt. They used a high air entry ceramic disc built into the triaxial pedestal in conjunction with a closed circuit bubble pump and air trap. This permitted the removal and measurement of diffused air from

beneath the porous disc. It also enabled the correct determination of water volume change.

The water volume change was measured using a Bishop paraffin volume change indicator. To eliminate the diffusion of air through the rubber membrane, the specimen was surrounded by a perspex sleeve and the intervening space was filled with mercury. A cathetometer was used during the experiments for accurate measurements of vertical and lateral specimen displacements. The main disadvantage of this set up was the hazard associated with liquid mercury.

The equipment developed by Radhakrishna (1967) is similar in many respects to that developed by Bishop and Donald in 1961. An electrical lateral strain indicator was also incorporated into the design. The test system measured total volume change as well as those of the water and air. The air volume change within the specimen was measured using a Bishop type two limb water manometer located between the sample and the air source. No attempt was made to measure or even flush the diffused air from beneath the high air entry ceramic disc.

Gibbs and Coffey (1969) extended Hilf's (1956) testing system to accommodate shear strength testing in the triaxial cell. The air pressure and air volume change can both be measured at the base of the specimen. The water is similarly controlled from the top of the specimen. The total volume change was determined by measuring the change in water volume surrounding the specimen. There are a number of difficulties associated with the equipment developed by Gibbs and Coffey (1969). For example, the vertical and

lateral displacements of the soil sample cannot be measured separately and there is no facility for flushing diffused air from beneath the base high air entry ceramic disc. The measured water volume change is also subject to induced errors due to expansion of the cell wall.

The general shortcoming of the modified cells, as previously discussed, is their inability to accurately measure one of the fluid phase volume changes. For example, it is not sufficient to simply measure water volume change without correcting for the volume of diffused air. Fredlund (1973, 1975) highlighted the problem and arrived at a design for a diffused air volume indicator (Figure 6.1). In order to accurately assess the water volume change only, it is necessary to measure the diffused air volume and subtract it from the measured volume change.

Several devices have been developed and constructed to enable volume changes of samples in triaxial tests to be monitored by electronic logging equipment. Lewin (1971), Rowlands (1972), Klementev (1974), Menzies (1975, 1976) and Marchant and Schofield (1978) all relied on mechanical or electro-mechanical principles such as floats, levers or servo-mechanisms. Sharpe (1978), however, described a method for directly measuring the volume of electrolyte in a burette with a claim of sensitivity of volume change of +0.01 ml over a range of 25 ml.

Equipment by which changes in the sample volume can be measured by monitoring the cell fluid expelled or taken in had been developed at the Massachusetts Institute of Technology (M.I.T) in 1963. The limitation of this equipment

is the change in cell volume with changing pressure, a result of creep and deformation of the cell. The author has overcome this problem with the use of a double-walled triaxial cell. The water pressure on the outside of the inner cell balances the internal pressure, hence omitting creep (change in cell volume) due to pressure changes. A common base plate (Figure 6.2 and Plate 6.1) was designed to accommodate both cell chambers. The outline of the position of the two cells in relation to one another is shown in Figure 6.3 and Plate 6.2. There are two sources of friction in this modified cell due to two bushes, one on top of each cell. This necessitated the use of a load cell to monitor the expansive force exerted by the soil sample.

At the beginning of this project, during the design, manufacture and development of a double-walled triaxial cell, the author was not aware that similar cells were being developed by other workers. However, as a result of a continuing literature review, it became evident that research was currently in progress elsewhere using such units. To date two references have been located where double chamber triaxial cells have been employed for soil testing, though not used for quantifying the expansion of an unsaturated clay. Wheeler (1988) reported on the use of a double-walled triaxial cell to find the undrained shear strength of soils containing large gas bubbles. Johnson (1989), in a technical note, reported on the horizontal and vertical swell pressures developed in a triaxial test. The triaxial cells documented by Wheeler and Johnson have some features in common which are different from the cell

developed by the author. Wheeler (1988) used a ball guide for his loading ram whereas the author uses an ordinary sliding plunger. Johnson (1989) used a load cell located directly onto the sample.

A similarity between the two cells presented by the above two researchers is the connection between the inner and outer chambers. In their systems the two chambers are connected together through the same entry port so that they have a common pressure source and hence keep the pressure on either sides of the inner chamber constant. The author uses two separate ports to pressurise the two chambers. An advantage of having separate ports is that the equipment can be used as a single or double-walled unit.

One of the features of the equipment by Johnson (1989), which is different from the cell developed by the author and that of Wheeler (1988), is the use of aluminium for the inner chamber. The main disadvantage of this is that the specimen cannot be seen. The ability to view the sample during testing can at times be of great value.

Two methods for controlling piston friction in a triaxial chamber are rotation and the use of ball guides. Warlam first proposed rotation for the reduction of piston friction in 1942. Initially, he employed this principle in the form of a piston and then in the form of bushing rotation in 1944 and 1946 respectively and finally in the form of cylinder rotation (Warlam (1960)). Warlam (1944) claimed that ball bearing bushing reduces friction to as little as 4 to 8 percent of the friction in a sliding bush.

6.2 Unsaturated Soil Testing Equipment

The author's pressure and monitoring system (Plate 6.3) is based on work by Fredlund (1973). The overall system controls the total, air and water stresses and allows measurement of the total and water volume changes. In addition, the diffused air collecting under the ceramic porous disc is flushed away and quantified, thus enabling the true water volume change to be calculated. The whole equipment is located in a constant temperature chamber where the variation in temperature and humidity is minimised.

Initially, when only the magnitude of expansion was under consideration, the double-walled triaxial cell was held in a rigid loading frame (Figure 6.4 and Plate 6.3). However, to evaluate the shear strength parameters of the soil samples, the loading frame was replaced by a Wykeham Farrance Tritech shear frame (Plate 6.4).

The water back pressures are generated at pressurised reservoirs, which pass through "Bishop" water volume change indicators and finally enter the cell base.

Initially, there was direct contact between the air and water in the reservoir used for the sample back pressure. This allowed air to diffuse in the water under pressure. This was counter productive to the research, hence a rubber membrane (bladder) was introduced into the reservoir to prevent a direct contact between the air/water pressure system. The use of the bladder decreased the total volume of water in the pressure reservoir. This caused some concern since the soil testing occurred over a considerable period of time where a continued cycle of "air flushing" of the

base plate was conducted. However, during this period the reservoir was continuously monitored and when necessary recharged with de-aired, de-ionised water.

The water outlet from the base plate of the cell (Figure 6.5) is connected to a diffused air volume indicator through a brass transducer junction (T2 and V5). This enables measurement of the true base pressure which is needed for correcting the apparent water volume change of the measured diffused air.

The loading frame (Figure 6.4 and Plate 6.3), designed to hold the test cell, is a rigid steel assembly. It comprises upper and lower rectangular 25 mm thick steel plates, separated by four 40 mm diameter threaded studs located at the corners. Provision is made to monitor any vertical displacement of the specimen. It was anticipated that there would be no vertical movement in the loading frame. However, dial gauges were used to monitor any possible movement.

The general layout and schematic representation of testing station No. 1 are shown in Plate 6.3 and Figure 6.5 respectively.

To ensure an absolute airtight and watertight system push-in type connectors were used in the air system and brass compression rings for the waterpipes.

6.3 Pressure Control and Measurement

The test system requires an easily controlled air pressure source for the total, pore air, diffused air and pore water pressures.

The head of pressure is always maintained well above the maximum required for the experiment to prevent any

unnecessary fluctuation in pressure. Plate 6.3 shows the air supply board. The air supply first passes through a dirt/ moisture trap and is then fed to the main precision control air regulator valve. This valve dictates the magnitude of the maximum pressure in the release valves of the pressure controllers used during the experiment. The air flow is then split into four branches leading to the total, pore air, pore water and diffused air volume indicator back pressure supplies. The output from each branch is controlled by a further Norgren valve, and monitored by a pressure gauge. For accurate pressure measurement, a single pressure transducer (Figure 6.5, transducer T3) is linked into either of the four channels as required.

6.4 Measurement of Total Volume Change

The volumetric behaviour of an unsaturated soil is determined by the water pressure deficiency (suction). The specimen will swell provided suction is decreasing. Consequently, an increase in suction will result in an isotropic shrinkage of the specimen. It is apparent that under such circumstances the measured displacement will not be representative of the total volume change. The measurement of water volume change is achieved using a Bishop double tube, double acting water volume change indicator. The burettes have a full travel of the water/kerosene interface equal to 25 ml. Volume changes are recorded to within 0.05 ml. It is suggested that volume changes should always be recorded using the interface moving downwards, since this exhibits the best meniscus form and therefore the most consistent reading mark.

6.5 Diffused Air Volume Indicator

Although free air cannot pass through the ceramic disc at pressures below its high air entry value, diffused air can and does pass through and form as bubbles below the ceramic disc. The recorded water volume change is therefore in error, and must be adjusted for the volume of diffused air recorded over the same period of time. The volume of diffused air is measured using a purpose built indicator. It is flushed with water from beneath the ceramic disc to the indicator by creating a pressure gradient across the cell base. A diffused air volume indicator designed after Fredlund (1973) has been adopted. The design of the diffused air volume indicator (Figure 6.1) centres around an inverted 25 ml glass burette, partly filled with water and closed at the top. Water is flushed from the cell base and enters the diffused air volume change indicator into the lower end of the burette. At this point flushed bubbles float to the air/ water interface within the burette and due to its closed end air is thus diverted to an exit tube and finally into the main chamber. The amount of diffused air is registered as a change in the meniscus level.

6.6 Rubber Membrane

In normal triaxial testing of soil samples the triaxial cell is filled with water to transmit the desired all-round pressure to the soil sample. To have full control over volume and pore pressure changes in the sample it has been necessary to have a close fitting impermeable membrane as a barrier between the pore fluid in the sample and the water in the cell. Natural or synthetic rubbers are therefore

commonly used as membrane materials. However, the author has reservations about these since they resist lateral expansion of the soil sample and a correction has to be made; this is dealt with by Henkel and Gilbert (1952), Bishop and Henkel (1962), BS 1377 (1975, 1990a) and Head (1982).

In order to minimise errors in volumetric measurements, instead of clothing with rubber membranes, Marsal and Resines (1960) sealed their specimens with a special kind of rubber paint. After 12 hours of drying, the rubber film was protected with an acrylic coating. They claimed that permeability tests of the membranes obtained in this manner showed them to be as reliable as the manufactured rubber membranes.

When testing very soft sensitive material, for example quick clays, the placement of the membrane could be difficult and may result in disturbance of the sample. As previously stated the membrane itself would also influence the measured values of the strength parameters of the soil. Iversen and Moum (1974) of the Norwegian Geotechnical Institute put forward the idea that it should be possible to omit the use of a rubber membrane altogether if the triaxial cell is filled with a liquid immiscible with the pore water of the sample. The contact surface between the cell fluid and the soil sample could then sustain maximum pressure without permitting the cell fluid to enter the pores of the soil sample. The numerical value of this maximum pressure is related to the pore size of the soil under testing, the interfacial tension between the pore water and the cell fluid and the contact angle between the cell fluid and the

water/mineral system. They suggested the use of paraffin instead of a rubber membrane and listed the main advantages in using the paraffin method as:

1) There is a simpler building-in technique which saves considerable time.
2) By eliminating the rubber membrane the possibility of disturbing the sample during setting up is greatly reduced. This is most important for very soft clays and clays of high sensitivity.
3) There is no uncertainty concerning leakage through the rubber membrane or the seal between rubber membrane and the top and bottom platens.
4) Because paraffin does not mix with water, any leakage around the upper and lower platens or in the drainage connections can usually be seen and measured in the burette.
5) There is no correction for membrane stresses.
6) No extra oil is required in the cell for the piston bush.
7) The sample is fully visible, therefore the development of failure can be observed.
8) The paraffin method is of great advantage in testing samples with square cross-section and there is no trouble with air between the rubber and the sample.

6.7 Simultaneous Alteration of Stress Components

Fredlund (1973) noted difficulties in achieving an instantaneous stress change at the beginning of each test. This process involves changing the total stress, pore air

and pore water pressures simultaneously. Two distinct difficulties are encountered:

1) Due to the volume of the triaxial cell any change in pressure cannot be achieved instantaneously.

Fredlund (1973) overcame this by momentarily opening the air pressure valve in advance of the total cell and water pressure valves. This, he claimed, resulted in near instantaneous peaking of all stresses.

2) The simultaneous opening of the three valves is physically impossible for one operator and difficult to co-ordinate with more.

Williams (1988) simultaneously opened the total and air stress valves followed by the water stress valve though he did not elaborate further whether it was successful.

The author opens the total (V1) and water pressure (V2) valves simultaneously closely followed by the air stress (V4) valve shown in Figure 6.5. This combination is chosen because the total and water stresses have to pass through the Bishop water volume change indicators (2) and (1) respectively hence taking a longer time to be effective; the air however is connected directly through a larger bore tube.

A manual data logging procedure was adopted for this project. Readings were taken on the water volume, diffused air and specimen swell indicators. In addition, digital pressure readings were recorded as voltage output from the pressure transducers connected to the inner cell water, sample pore water and axial load cell.

6.8 Conventional Triaxial Cell (Testing Station No. 2)

The second phase of the experimental work involved studying the shear strength of the constituted test specimens before and after expansion. To accelerate generation of data, it was decided to set up additional test stations.

A conventional triaxial cell (Plate 6.5) was adopted to test samples containing 10% montmorillonite. It is appreciated that it suffers from the creep of perspex, due to its single-wall chamber, hence the decision to employ it for samples with least swelling potential.

An uninterrupted supply of pore water back pressure was produced by one of two ELE oil/water constant pressure systems. The other supplying the cell pressure.

In order to quantify the volume of water taken in by the sample and the displacement of water in the cell, due to expansion/shrinkage of the test specimen, two 100 ml capacity twin burette water volume change indicators were used. The burettes are graduated to read within 0.2 ml.

The general layout and schematic representation of the testing system are shown in Plate 6.5 and Figure 6.6 respectively.

The oil/water constant pressure system (a) in Figure 6.6 is connected to the twin burette water volume change indicator No. (1) which is connected to the cell. This maintains the cell pressure and allows the movement of water into or out of the cell to be quantified. The second oil/water constant pressure system (b) is connected to the twin burette water volume change indicator No. (2). This in turn is connected

to the underside of the porous ceramic disc and is used to saturate the soil sample.

The pore air back pressure is transferred from the air supply board (Plate 6.3) and connected to the drainage tube on top of the sample. In addition to the proving ring, a 3 kN capacity load cell is used to double check the deviator stress. It also allows overnight monitoring of the changes by connecting it to a Wykeham Farrance Autotech data logger.

Two major disadvantages of this testing station are:

1) creep due to single-wall cell, and
2) due to the restricted location of the testing equipment, difficulties were experienced with maintaining steady state temperature and humidity conditions.

6.9 Geotechnical Digital Systems (Testing Station No. 3)

The third testing equipment adopted is the Geotechnical Digital Systems Triaxial Testing Station (GDSTTS). It is used to test soil samples containing 20% montmorillonite. It is stated in Chapter Four, Section 4.2.1 that the Bishop Wesley cell (Figures 4.3 and 6.7, and Plate 6.8) could not be used because of the change in the volume of the cell due to variations in pressure. However, this problem may be overcome if a more direct means of measuring the volume change of the sample can be found. A number of devices have been developed at Imperial College but none has proven satisfactory. The Hall Effect Local Displacement Transducers, supplied by GDS Instruments Limited, are said to work satisfactorily (Clayton et al (1989)).

6.9.1 Radial Strain Measuring Device

The radial strain measuring device (Plate 6.6) comprises a caliper similar to that originally designed by Bishop and Henkel (1962). The caliper is mounted on the test specimen (Plate 6.7) by means of two diametrically opposed pads fixed to the test specimen by pins and bonded to the membrane by adhesive. The mounting block is shaped to fit the curvature of the cylindrical surface of the test specimen.

The Hall Effect transducer is positioned across the opening of the caliper where it measures the relative movement of the jaws.

The radial strain measuring device is connected to a voltmeter, for manual recording, and the Autotech data logger for continuous monitoring. The cell pressure, pore water back pressure and the rate of axial strain are delivered to the testing station through the GDS digital pressure controllers No. (1), (2) and (3) respectively. The general layout can be seen in Plate 6.8 and a schematic representation of the system is shown in Figure 6.7.

The pore air back pressure is transferred from the air supply board (Plate 6.3), and connected to the drainage tube on top of the sample.

The whole testing system is located in an isolated room with steady state temperature and humidity conditions.

6.10 Sample Preparation

The soil samples used in this work were artificially constituted. The main reasons for using such samples were:

1) the general unavailability of unsaturated expansive clays in the locality,

2) lack of control over the expansive nature of the soil samples, and

3) disturbance due to field soil sampling.

Hence the preparation of artificially constituted soil samples was considered more appropriate to provide consistent test specimens in terms of expansive nature, air / water content and density.

Sodium montmorillonite and kaolinite were used in the production of the test specimens.

6.10.1 Sodium Montmorillonite

The mineral used in this project originated from the Wyoming, South Dakota area of the United States. It has a very high liquid limit (see Tables 6.1 and 6.3) and is widely acknowledged as exhibiting extreme swell characteristics. It has been supplied by Steetley Mineral Limited in the form of light grey, fine ground powder with 72% passing the 300 μm BS Sieve.

The mineral is extremely hydroscopic, and although dry when supplied, it does contain up to 7% moisture when stored in atmospheric conditions. It was therefore dried and sealed in moisture proof containers for 24 hours prior to testing.

The properties of the mineral provided by the supplier are listed in Table 6.1.

Name : Sodium Montmorillonite (M) Trade Name : Wyoming Bentonite Origin : Wyoming, South Dakota, U.S.A. Colour : Grey	
Chemical Analysis % SiO_2 55.0 TiO_3 0.1 Al_2O_3 16.5 Fe_2O_3 5.1 CaO 1.9 MgO 2.0 Na_2O 1.2 K_2O 0.6 Mn_3O_4 0.1	Specific Gravity = 2.5 pH (5% suspension) = 9.3 Swelling Volume = 20-25 mls/2g Liquid Limit = 630% (BS 1377) Cation Exchange Capacity (Ammonium) = 70 meq/100g Bulk Density = 800-950 kg/m^3

Table 6.1 Properties of sodium montmorillonite.

6.10.2 Kaolinite

This white mineral originated from Cornwall in the United Kingdom where it is mined and sold as china clay.

The mineral has been supplied by Steetley Mineral Limited in a partially crushed and dried form with a maximum lump size of 20 mm and an average moisture content of 12%. It had been dried and crushed and its moisture content conditioned prior to laboratory use. Once dried, it retained a low moisture value for a considerably longer period than montmorillonite. The technical information given by the supplier for this mineral is presented in Table 6.2.

Name : Kaolinite (K) Trade Name : China Clay Origin : Par, Cornwall, U.K. Colour : White	
Chemical Analysis % SiO_2 47.4 Al_2O_3 37.2 Fe_2O_3 0.65 TiO_3 0.04 CaO 0.05 MgO 0.22 K_2O 1.6 Na_2O 0.06	pH = 5 Particle size distribution = 300 μm BSS = 0.03% max

Table 6.2 Properties of china clay.

6.10.3 Constituted Test Specimens

In addition to the chemical analysis data provided by the supplier, Williams (1988) found some impurities through the X-ray Diffraction (XRD) analysis. The XRD analyses of the Wyoming bentonite and china clay as reported by Williams (1988) are as follow:

Wyoming Bentonite = Na Montmorillonite + Illite + Feldspar

China Clay = Kaolinite + Illite + Feldspar

The technical data provided by the supplier omitted the Atterberg Limits. These were found in accordance with BS 1377 (1975, 1990b) and are presented in Table 6.3.

The maximum possible range of liquid limit was between 47% (kaolinite) and 550% (sodium montmorillonite). However, it was decided to employ a more modest range for the testing programme which would coincide with liquid limit and swell properties likely to be met in the field.

The required proportions of montmorillonite and kaolinite for the three main series of experimental tests are given in Table 6.3.

Test series	Soil type M%	K%	LL %	PL %	PI %	Specific gravity	Author
-	0	100	**47.0** 49.0	- 27.0	- 22.0	**2.63** 2.616	**Author** Williams
1	10	90	**84.2** 94.0	**36.2** 30.0	**48.0** 64.0	- -	**Author** Williams
2	20	80	**112.0** 120.0	**39.3** 33.0	**72.7** 87.0	- -	**Author** Williams
3	30	70	**141.25** 142.0	**41.9** 43.0	**99.35** 99.0	- -	**Author** Williams
-	100	0	**550.0** 530.0 630.0	- 43.0 -	- 487.0 -	**2.61** 2.27 2.5	**Author** Williams Supplier

Table 6.3 Liquid limit, plastic limit and plasticity index for the three main experimental series.

The quantities of the constituent materials (i.e. kaolinite, montmorillonite, air and water) for each test specimen were evaluated using Equations 6.1 and 6.2.

$$\rho_d = \frac{\rho_w (1 - A)}{\frac{n}{G_{sk}} + \frac{1 - n}{G_{sm}} + W} \qquad (6.1)$$

$$M_{st} = \rho_d \times V_t \qquad (6.2)$$

where:
ρ_d = dry density
ρ_w = density of water
A = percentage air
n = percentage of kaolinite
$1 - n$ = percentage of montmorillonite
G_{sk} = specific gravity of kaolinite
G_{sm} = specific gravity of montmorillonite
W = percentage of water
M_{st} = total mass of solid
V_t = total volume of sample

6.11 Mixing Procedure

The following procedure was employed in the mixing of the samples using both dry and wet mixing techniques:

1) Weigh dry samples of kaolinite and montmorillonite.
2) Place the weighed sample in a plastic bag and mix by hand.
3) Transfer the soil into a mixing bowl and dry mix using a spatula.
4) Add a third of the required water and mix in a six speed Kenwood excel chef mixer at speed 1 for one minute.
5) Hand mix the soil with a spatula for a further one minute.
6) Add an additional third of water and mix at speed 2 for one minute.
7) Repeat step 5.

8) Add the remaining water and mix with the mixer set at speed 3 for one minute.
9) Hand mix the soil using a spatula for a further two minutes.

6.12 Sample Compaction

A split mould (Figure 6.8 and Plate 6.9) was used for compaction purposes. Initially two other types of moulds were considered. They were straight cylinder and tapered moulds. They were both rejected because of high skin friction between the soil and the mould and disturbance of the specimen while extracting from the mould. The advantages of a split mould are:

1) the skin friction between the soil and the mould is much reduced,
2) disturbance due to extraction is eliminated,
3) the excess air within the sample escapes more readily during compaction due to the gap between the two limbs of the mould. This produces consistent voids throughout the sample.

The following procedure was found to yield the most consistent samples:

1) The pre-mixed soil was poured into the mould in one layer. If two or more layers were used, extra boundaries would have been introduced into the specimen which would have in turn interrupted the void pattern.
2) The end platens (Plate 6.9b) were kept apart using spacers. This provided more volume for the soil in the loose state. The mould was then placed in a rigid frame, the spacers removed and pressure applied to the end

platens using a hydraulic jack.

3) The sample was then ready for assembly in the modified triaxial cell for the commencement of the test.

6.13 Equipment Assembly

Prior to each test, the equipments were cleaned thoroughly and the pressure transducers and load cells calibrated. The porous ceramic discs were de-aired and kept saturated throughout the testing programme.

The soil samples were set up in a manner similar to a standard triaxial test (Bishop and Henkel (1962)). During the initial testing programme of the double-walled triaxial cell, it became evident that there was a leak in the drainage line connected to the platen on top of the soil sample. To overcome this problem the connection was sealed with a silicon rubber sealant and left to set for 12 hours before assembling the rest of the equipment and introducing the cell fluid. In view of continuous changes in soil suction immediately after compaction, this actually gave the sample time to equilibrate and the soil suction within the sample to reach a fairly constant level.

Once the testing stations were set up, the valves on the base plates were closed and the chambers were filled with de-aired, de-ionised water.

6.14 Test Initiation

The cell, pore air and pore water pressures were introduced into the soil samples by opening the appropriate valves on the base plates of the corresponding test stations.

Precision cut-in pressure transducers were used to check the pressures in the double-walled triaxial cell. The valves connected to the underside of the sample (V2) (Figure 6.5) and the inner cell (V1) were opened simultaneously closely followed by the pore air pressure (V4) (see Section 6.7). For the conventional and GDS triaxial test stations the pressures were monitored directly by precision gauges and pressure transducers respectively. At this stage the Bishop water volume change indicators were already in operational position for the double-walled and conventional triaxial test stations. The volume changes in the GDS test station were monitored by the pressure control units.

6.15 Routine Measurements For Double-Walled Triaxial Cell

Flushing and quantification of the diffused air from underneath the porous ceramic disc was exercised using a diffused air volume indicator. The water intake and total volume change of the sample were measured using the Bishop water volume change indicators (1) and (2) respectively (Figure 6.5). The actual pore water pressure and inner cell pressure were recorded using pressure transducers. The load exerted by the sample on the load cell was recorded using a digital read out unit.

The diffused air volume indicator was operated in the following manner:

1) The initial reading was taken on the graduated inner burette at atmospheric pressure.
2) A back pressure was applied across the base to create a pressure gradient of 30-70 kN/m^2.

3) The Bishop water volume change indicator number (1) was connected to the sample in a by pass mode.
4) The underside of the sample was flushed by opening the valve V5 from the underside of the sample on the base plate to the diffused air volume indicator (valve V6).
5) The connection valves V5 and V6 were closed again and the Bishop water volume change indicator was put back in operational mode.
6) The back pressure was released and the new level of water in the burette was recorded.

The **Bishop water volume change indicator** consists of two limbs which are filled with paraffin and water. The meniscus at the interface of the two fluids is read against a graduated burette. Once in operational mode, the two interfaces in the two limbs move relative to one another. The direction of water flow in the limbs relative to the position of the valves indicates whether the flow is into or out of the sample.

In order to achieve an almost **instantaneous stress change**, the base of the cell must be isolated. Once the changes are implemented, the valves are opened in the same order as stated in Sections 6.7 and 6.14.

Periodically throughout the testing programme, the **water reservoir** required **recharging** due to the water intake by the sample and water flushing beneath the ceramic disc as described in Section 6.2.

On completion of each test, the final set of readings was recorded. The pressures were removed and the equipment dismantled as rapidly as possible. The sample was removed and weighed, the height and diameter being measured using a micrometer. The diameter of the sample was measured at three cross sections; the top, middle and bottom. At each of these locations the moisture content was evaluated.

Where appropriate, this procedure was modified to suit each of the two additional test stations. Every effort was made to ensure that the testing technique was consistent throughout the whole testing programme.

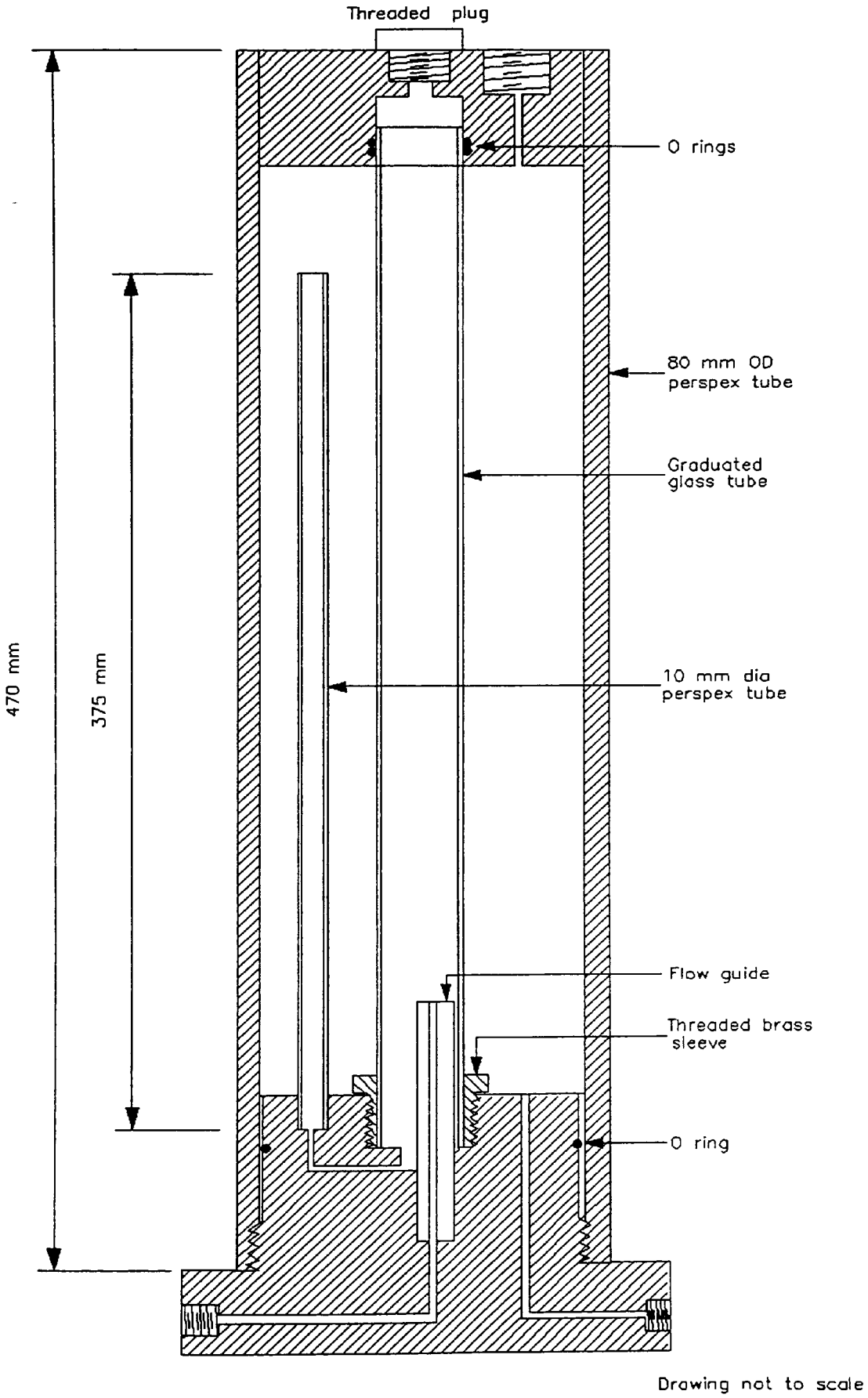

Figure 6.1 Diffused air volume indicator.

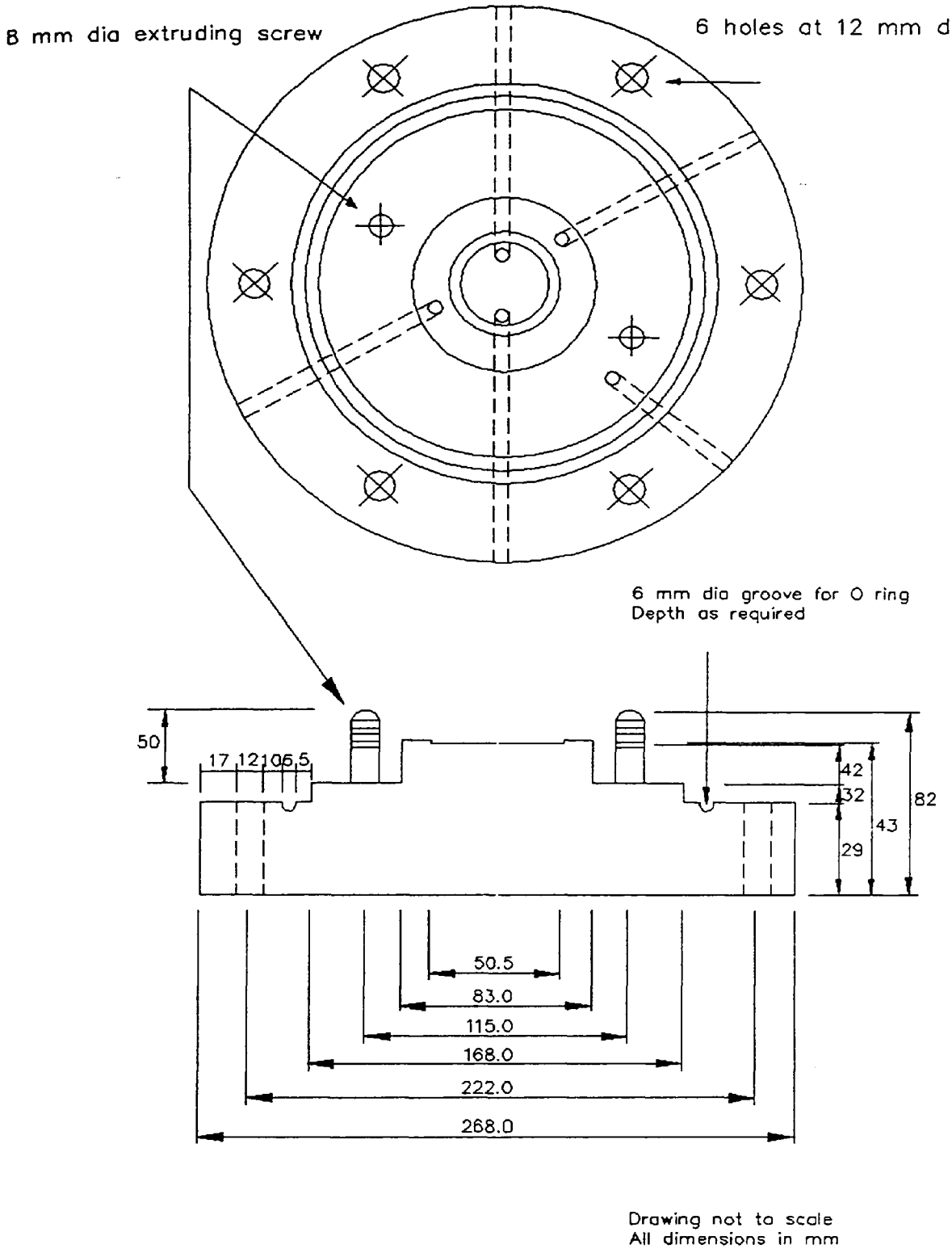

Figure 6.2 Common base plate for the modified triaxial cell.

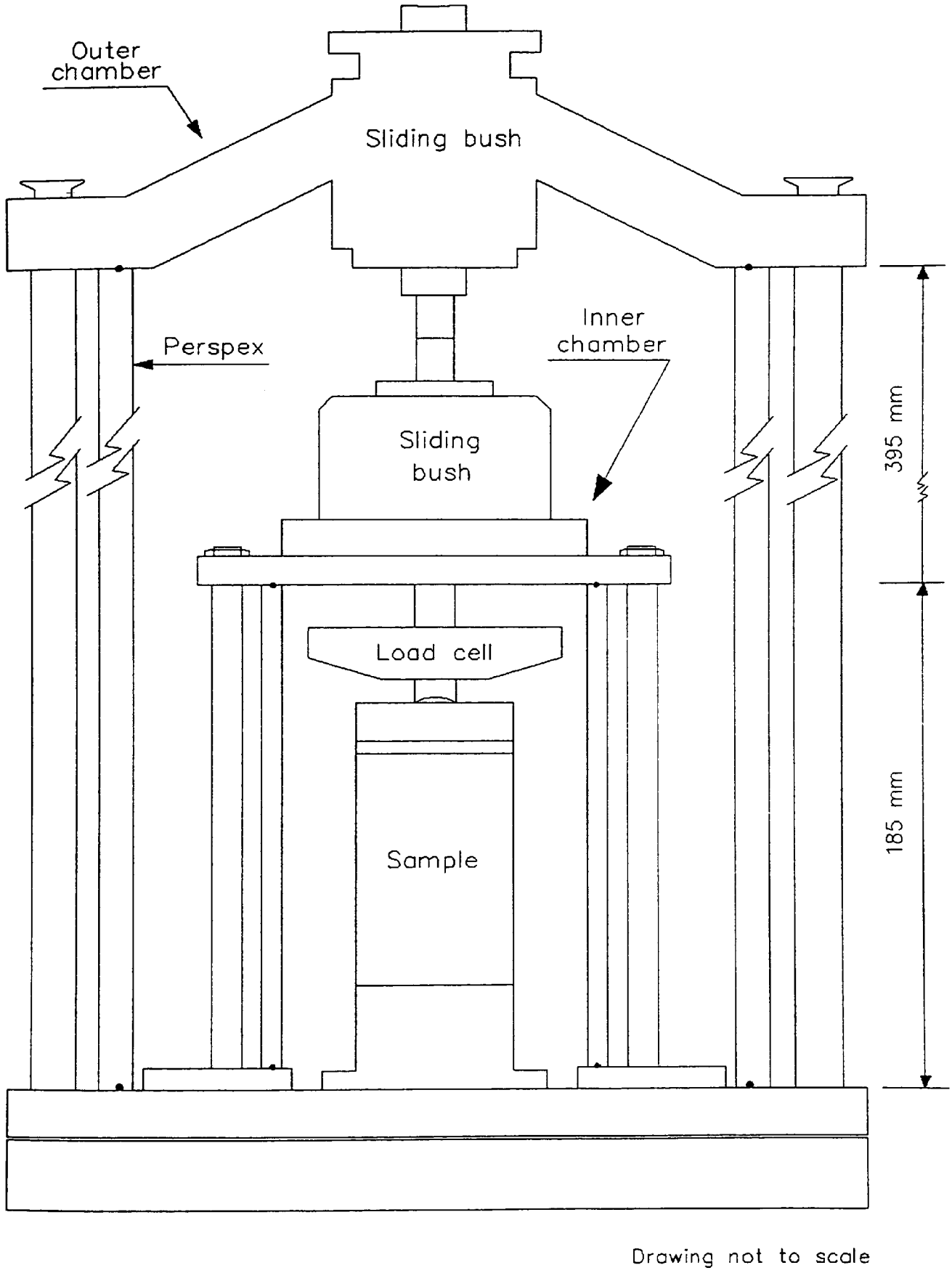

Figure 6.3 Outline of the two cell chambers.

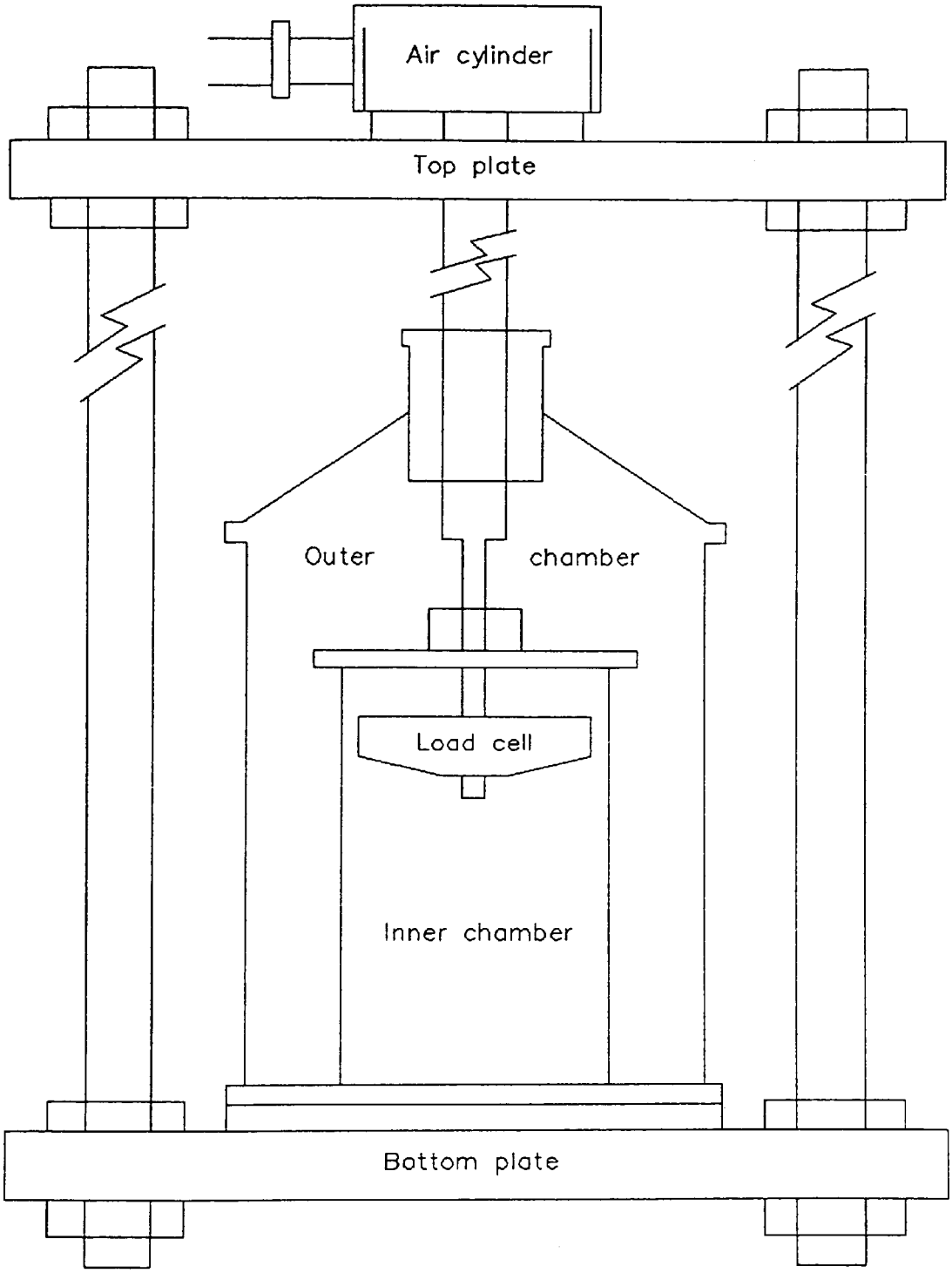

Figure 6.4 The loading frame.

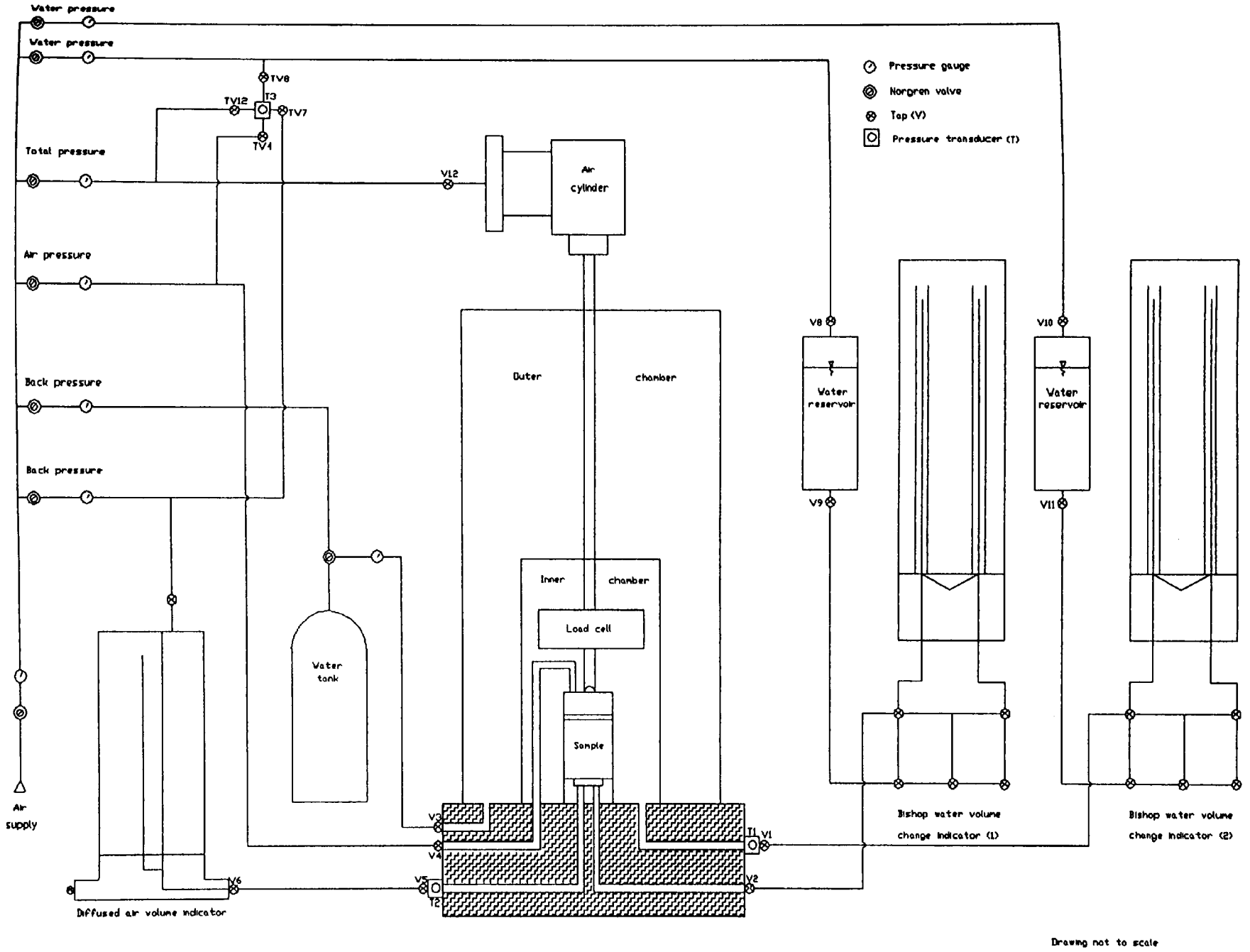

Figure 6.5 Schematic representation of testing station No. 1.

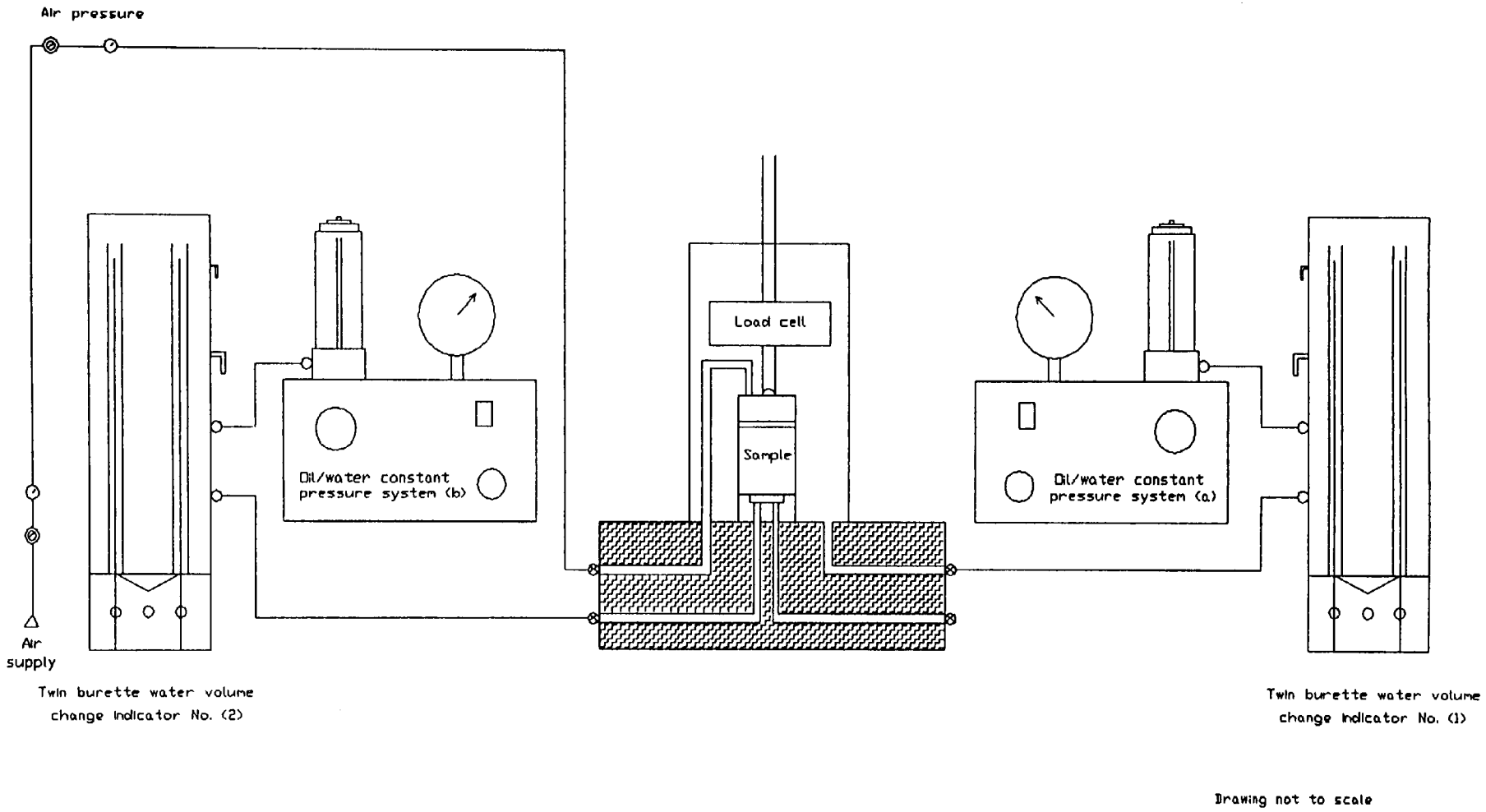

Figure 6.6 Schematic representation of testing station No. 2.

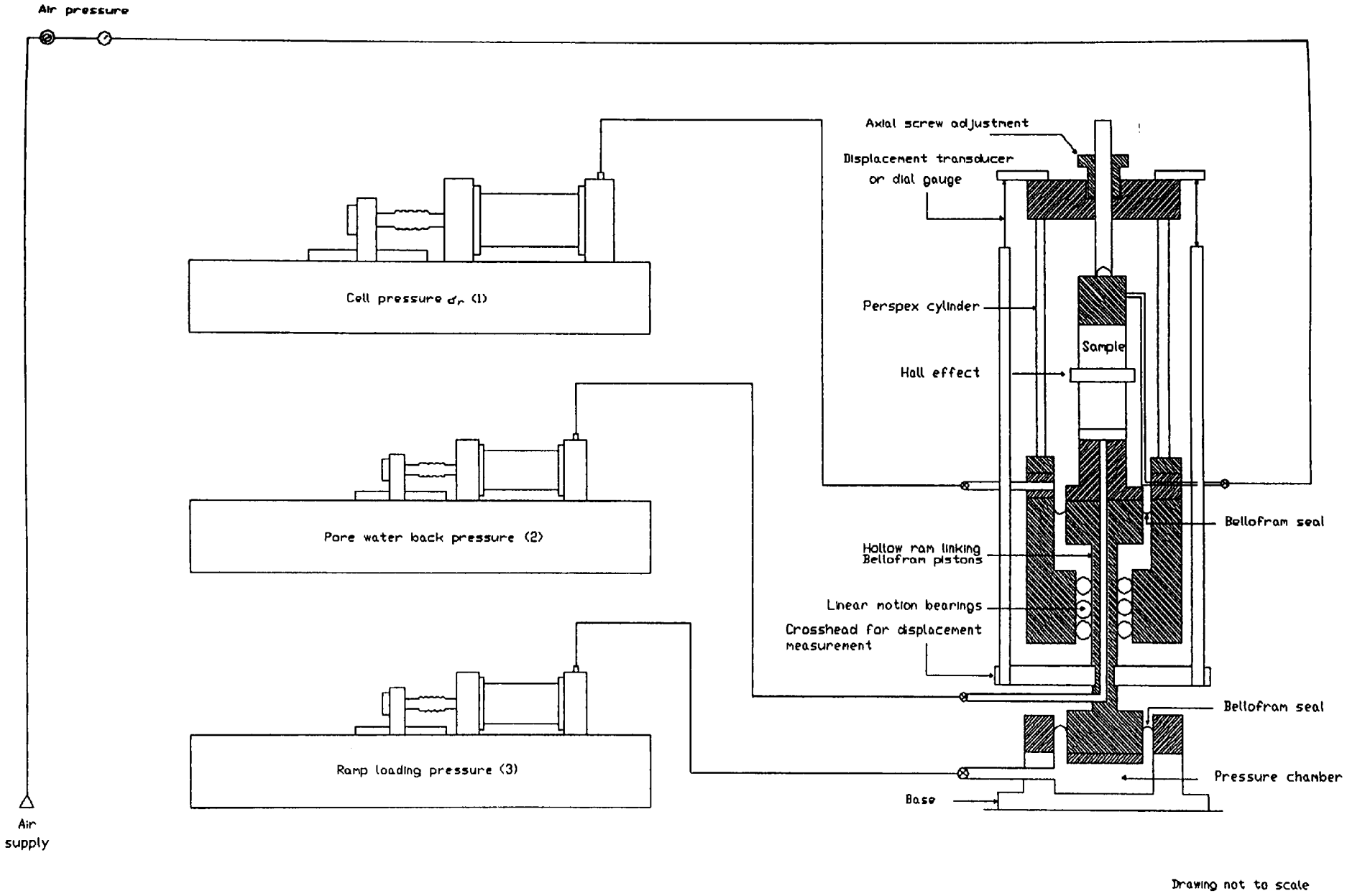

Figure 6.7 Schematic representation of testing station No. 3.

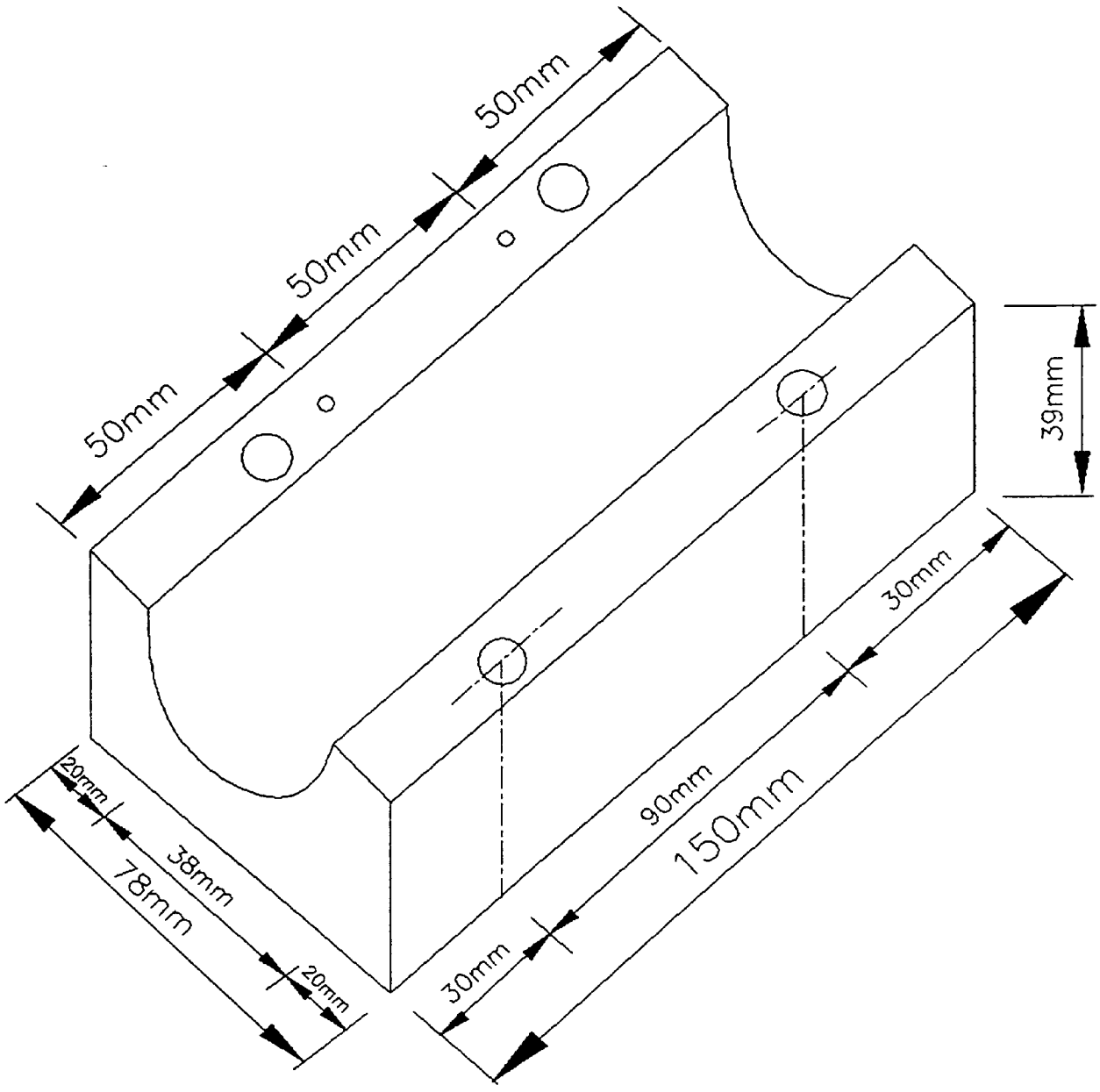

Figure 6.8 The split mould.

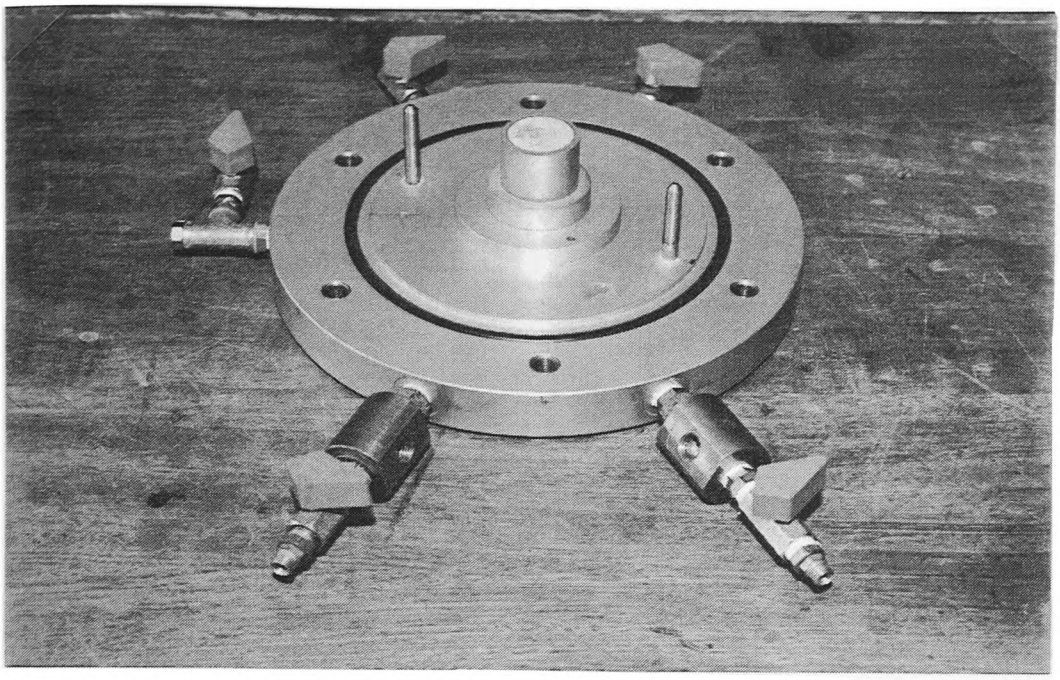

Plate 6.1 Common base plate for the modified triaxial cell.

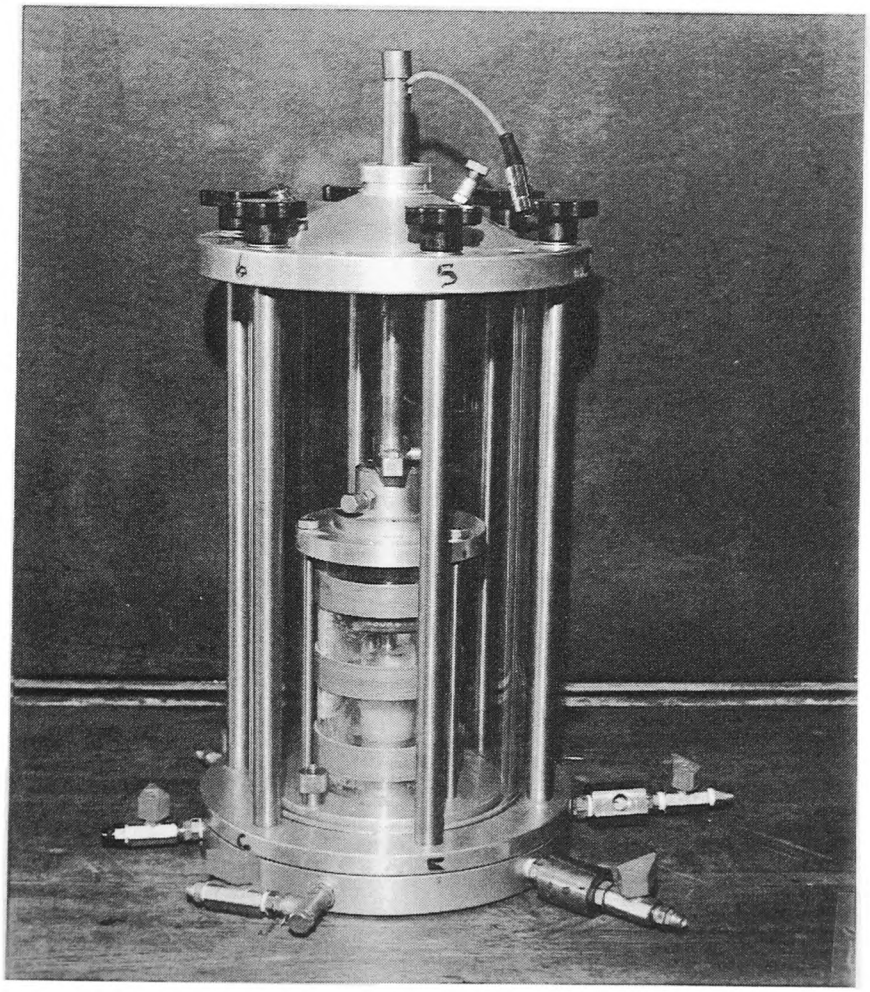

Plate 6.2 Outline of the two cell chambers.

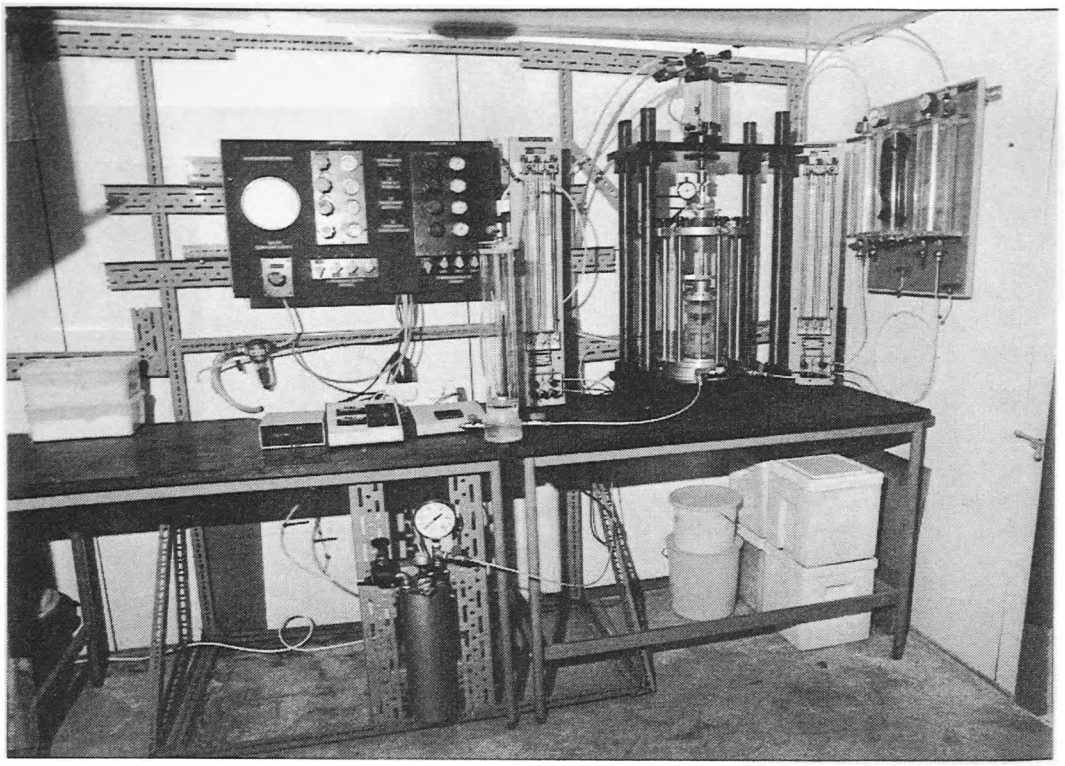

Plate 6.3 General layout of testing station No. 1.

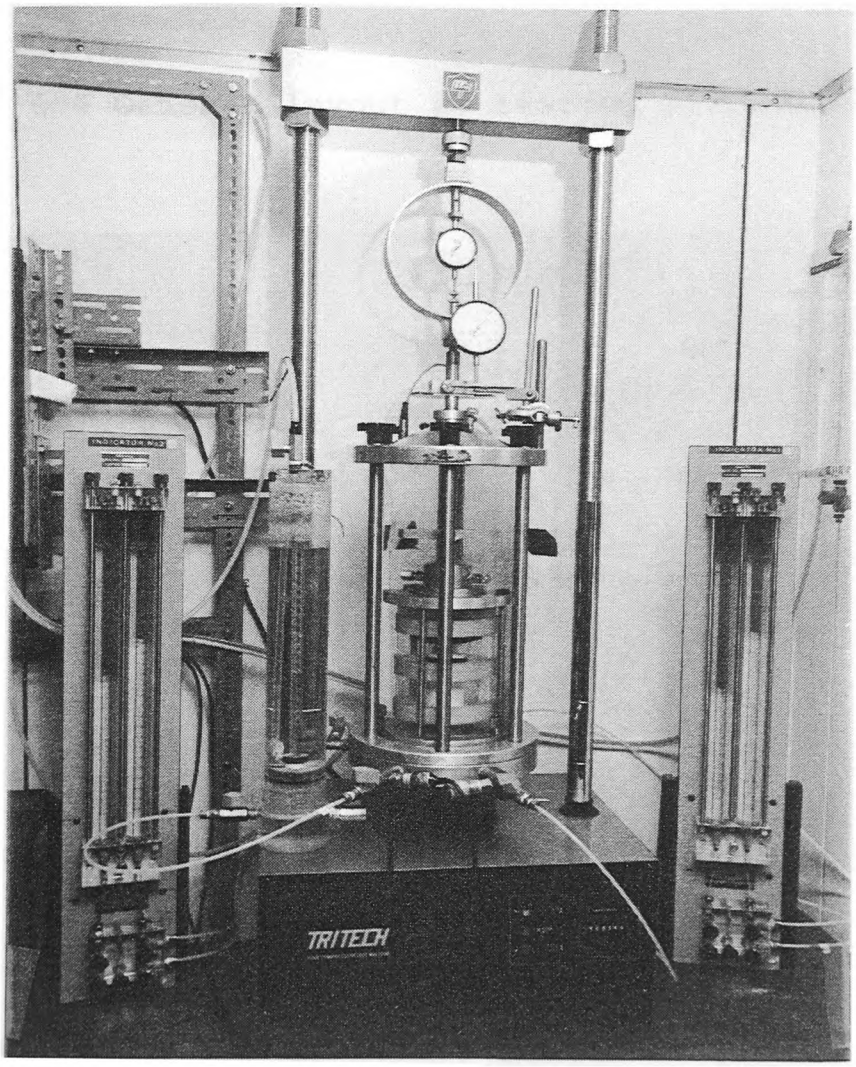

Plate 6.4 The modified triaxial cell in a shear frame.

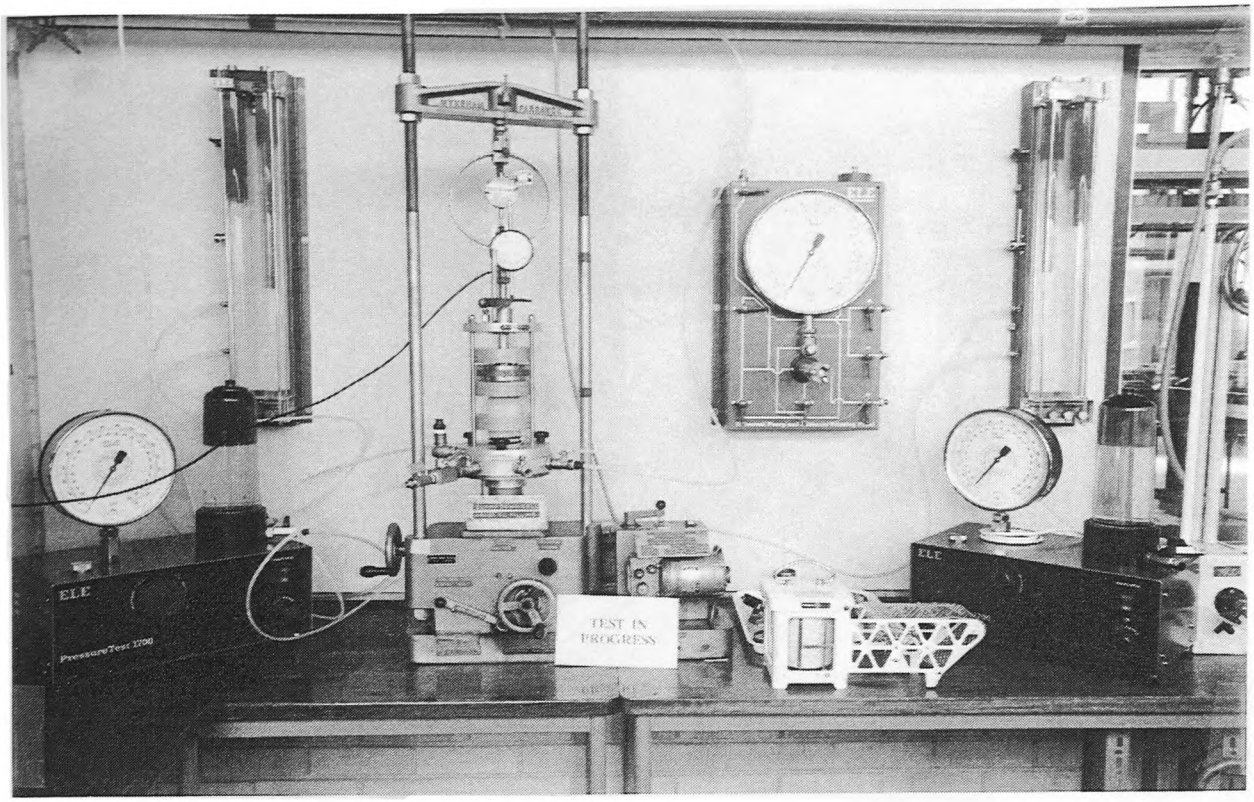

Plate 6.5 General layout of testing station No. 2.

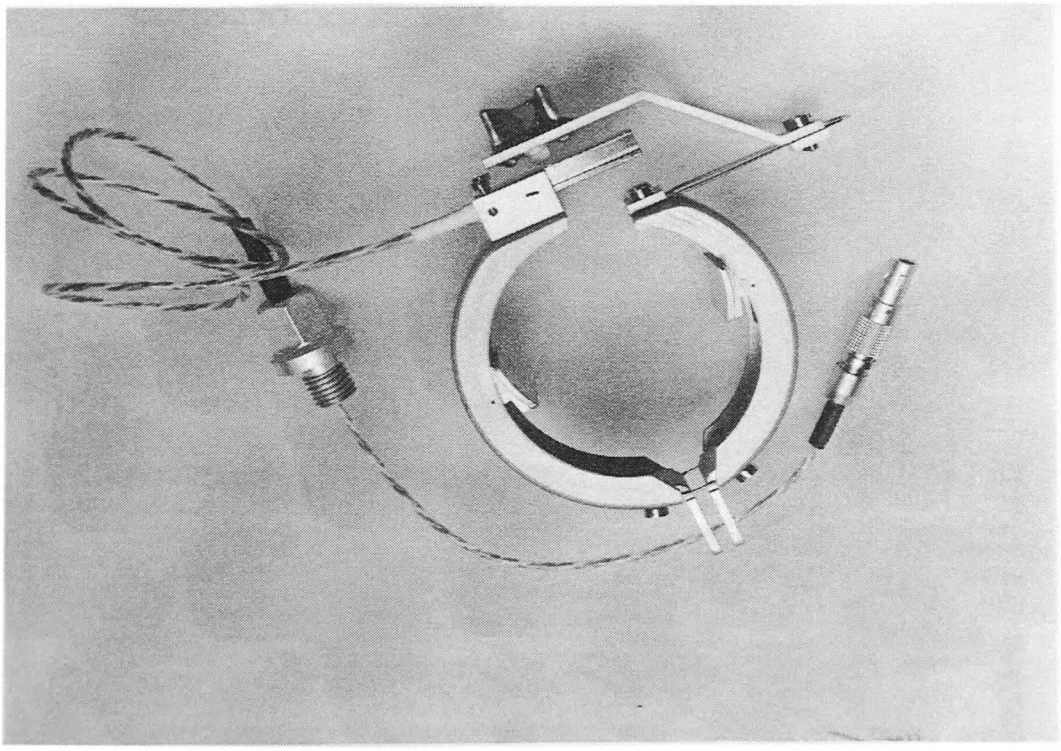

Plate 6.6 Radial strain measuring device.

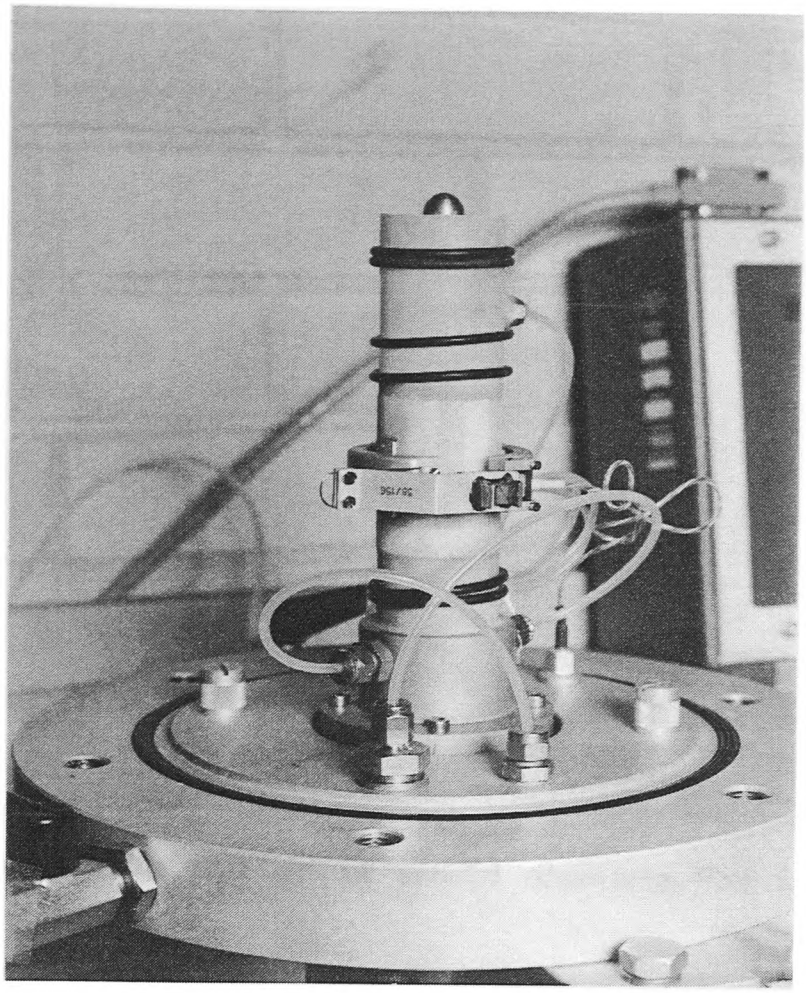

Plate 6.7 Radial strain measuring device mounted on a triaxial test specimen.

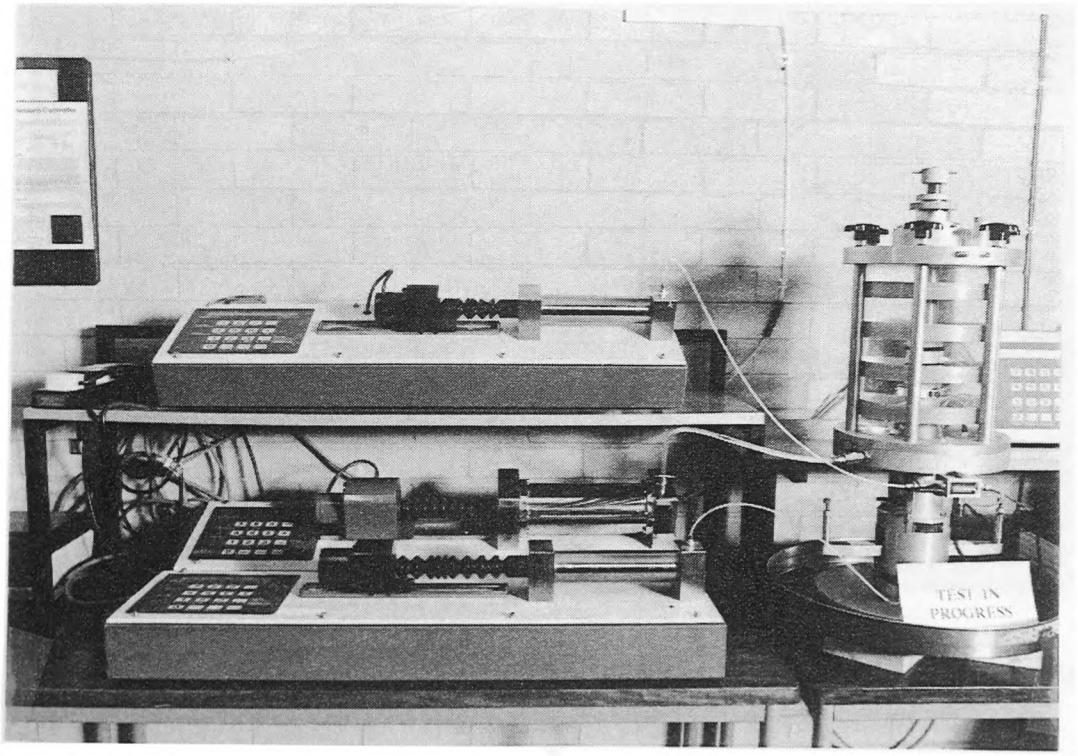

Plate 6.8 General layout of testing station No. 3.

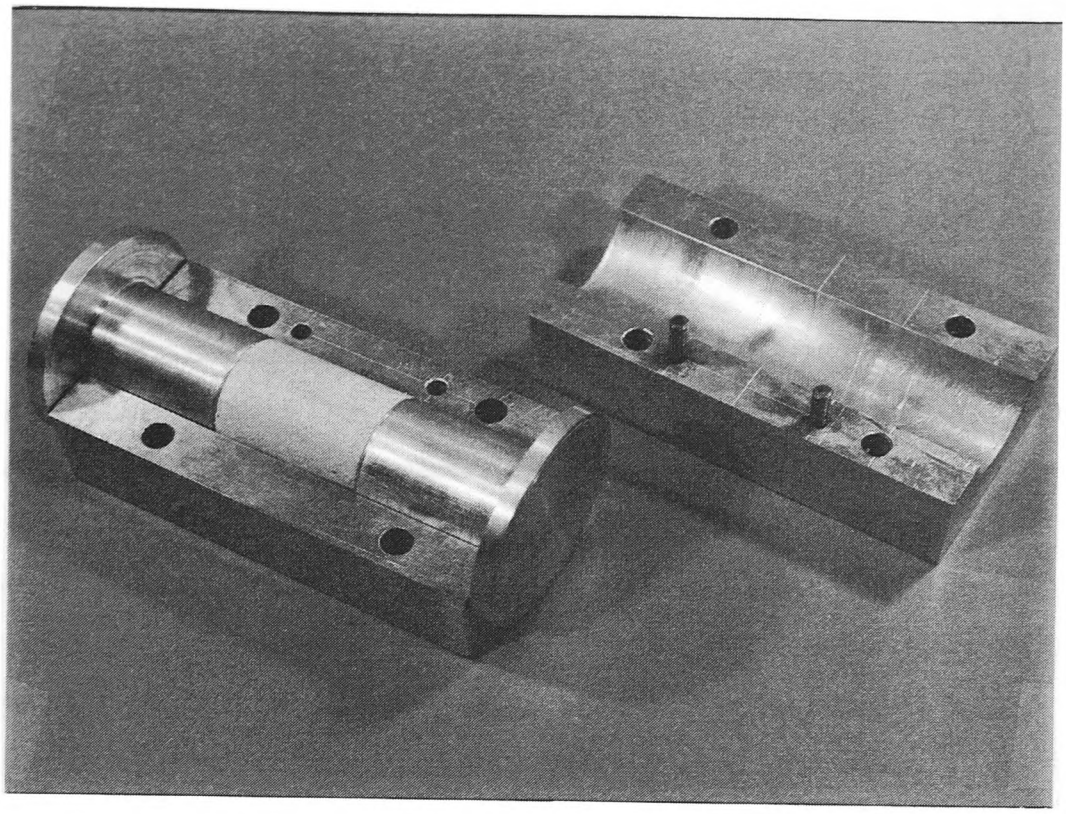

Plate 6.9a The split mould showing the sample.

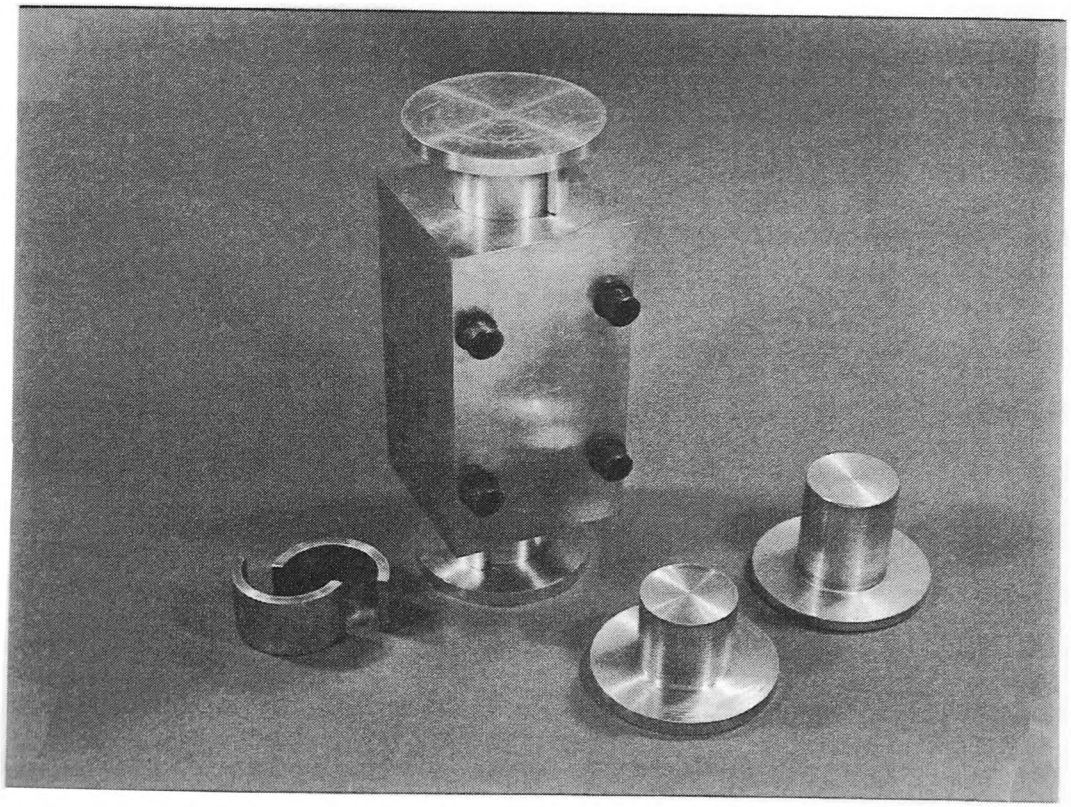

Plate 6.9b The split mould showing end platens and spacers.

Plate 6.9 The split mould.

CHAPTER SEVEN

PRESENTATION OF DATA AND ANALYSIS

7.0 Introduction

A summary of the experimental test programme and conditions is given in Tables 7.1 to 7.5.

The testing programme was conducted in two phases. For the first phase, where only the magnitude of expansion was being considered, the samples are numbered consecutively from CRS110 to CRS1430. The prefix CR refers to Cold Room (i.e. test station No. 1). S1 to S14 show the sample number and 10, 20 or 30, on the right, show the percentage of montmorillonite.

For the second phase, where the shear strengths of the samples were also considered, the data are referenced according to the test stations. For simplicity the samples containing 10%, 20% and 30% montmorillonite are grouped in separate tables.

Typically the following sample notations are used; CRS1130, GDSS2220, WFS3110 and W2FS3330. The prefix CR refers to Cold Room (i.e. test station No. 1), WF refers to Wykeham Farrance (i.e. test station No. 2), GDS refers to testing station No. 3 and W2F refers to the fourth station which was a conventional triaxial cell and was used for quick drained shear tests with no pore air or water back pressures. S1, S2 or S3, after the prefix, show the sample numbers in each category of testing. This is followed by a further digit which indicates the sample condition during testing. Number

1 means that the samples were saturated and allowed to swell and after reaching equilibrium they were sheared under drained conditions. Number 2 represents a test where the samples, with pore air and water back pressures, were sheared under drained conditions as soon as the equipment was assembled. Number 3 indicates that the samples were tested for shear, under drained conditions, immediately after equipment assembly but there were no pore air or water back pressures. Numbers 10, 20 or 30, on the right, indicate the percentage of montmorillonite. It must be emphasised that the second and third samples in the series are identical, in composition, to the first one, and tested under the same confining cell pressures.

The data and results of the analyses, from the experimental programme, are presented in Tables 7.6 to 7.51 and Figures 7.1 to 7.85.

Table 7.1a illustrates the initial stress conditions for each of the tests in the first phase. They include; σ, U_a and U_w along with the stress state variables $(\sigma - U_a)$, $(\sigma - U_w)$ and $(U_a - U_w)$.

Table 7.1b shows the stress state conditions of the samples in the first phase at the end of each test (i.e. final conditions). There are two test samples, namely CRS810 and CRS1210, in which the stress states were altered more than once. These changes are also shown in Table 7.1b.

Table 7.2 shows the stress changes between the final and initial conditions. The negative sign signifies a decrease in stress from the initial to the final condition. Tables

7.1 and 7.2 also show the stress state variables $(\sigma - U_a)$, $(\sigma - U_w)$ and $(U_a - U_w)$.

The stress conditions for samples containing 10%, 20% and 30% montmorillonite, used in the second phase of testing, are listed in Tables 7.3, 7.4 and 7.5 respectively. There were no confining or back pressure changes in samples tested in the second phase and the stresses remained constant throughout testing.

7.1 Liquid Limit, Plastic Limit and Plasticity Index Versus Montmorillonite Content

Figure 7.1 traces out the influence of montmorillonite content on liquid limit, plastic limit and plasticity index. This relates to the soil compositions used in this study. A linear relationship is clearly shown between the percentage montmorillonite content and the three indices.

7.2 Variation in Sample Moisture Content

Table 7.6 shows the moisture content of the samples after completion of each test in phase one of the experiments. It can be seen that in most cases the moisture content is highest at the bottom of the sample, which is closer to the source of water, and decreases towards the top. However, test samples CRS1210 and CRS430 experienced moisture gradients increasing from the bottom to the top.

There is a third group of samples in which the moisture content is highest at the middle. It is interesting to note that a comparison between Tables 7.6 and 7.10 reveals that these samples also experienced greater expansions at those positions. They were samples CRS810, CRS1210, CRS620 and CRS1430. This may be explained by the provision of filter

paper drains around the samples. The stiffness of the rubber membrane at the top and bottom, compared to the middle, may also have contributed to this phenomenon.

The final moisture contents of the samples tested in the second phase and containing 10%, 20% and 30% montmorillonite are presented in Tables 7.7, 7.8 and 7.9 respectively. As the samples were sheared, they were divided into two segments and are called top or bottom to indicate their proximity to the top or bottom plattens. The average moisture content for the whole sample is also shown.

When comparing Tables 7.7 to 7.9, the average final moisture contents of the samples increases as the amount of montmorillonite increases. This pattern is repeated in the average final moisture contents corresponding to the samples where there were no pore air or water back pressures or filter paper drain. The average final moisture contents corresponding to montmorillonite content and the state of back pressures are shown in the following table.

Back pressures	Montmorillonite content		
	10%	20%	30%
Yes	36.19	38.08	47.54
No	31.09	34.36	36.83

Average final moisture contents

7.2.1 Effects of Time on The Final Moisture Content

Table 7.6 shows that the duration of each test had an effect on the final moisture content of the samples. This was particularly significant for the samples with the filter paper drain which had a greater moisture content in the middle section of the samples. This phenomenon was more

significant in tests which extended past thirty days' duration.

From the results of the second phase for samples containing 10% to 30% montmorillonite given in Tables 7.7 to 7.9 respectively, no direct relationship between the duration of each test and the final moisture content could be established. This is true if all the values in each table are examined together. For example, if the final moisture contents corresponding to each of the series are considered some samples undergoing immediate shear exhibit greater final values than those undergoing saturation and expansion prior to shear.

If only the values for samples containing 10% montmorillonite, undergoing saturation and expansion prior to shear, are compared then a pattern similar to those in the first phase emerges. It shows that as the time of testing increases the final moisture contents increase too. Tables 7.8 and 7.9 for samples containing 20% and 30% montmorillonite, respectively, do not show the same trend. They indicate greater or smaller moisture contents as the time of testing varies. However, it seems clear, from the results, that there is a strong affinity for water by the samples, particularly those containing 30% montmorillonite. This apparent disparity between the final moisture contents of samples tested in the first and second phases may be attributed to the fact that in the second phase the samples underwent shear as well as saturation and expansion. It is also important to emphasise the effects of dilation during shear and the effect of overconsolidation.

7.3 Free Expansion of The Soil Samples

7.3.1 First Phase

The free radial and axial expansions, measured by a micrometer, are shown in Table 7.10. They were measured on completion of each of the experiments after all the triaxial pore air and pore water back pressures had been removed. These values represent the volume change as a percentage of the original dimensions of the soil samples. These volume changes are a combination of those experienced throughout testing, while the samples were under confining and back pressures, and the free expansion which is experienced by the sample after the removal of external stresses.

During testing, the samples were restrained at the bottom by the porous ceramic disc and at the top by the load cell. The inherent expansiveness was therefore suppressed while the samples were confined in the cell, but as soon as the equipment was dismantled, the samples showed an immediate axial expansion in conjunction with an increase in radial expansion. This rapid expansion is believed to be due to stress relief rather than a gradual process resulting from a progressive increase in the intake of water.

For most of the samples (71%), radial expansion was more evident at the bottom rather than at the top because that is where they had a more immediate access to water for the longest period of time. This pattern of decrease from the bottom to the top was also experienced when considering the final moisture contents (see Section 7.2). The remaining 29% of the samples showed greater expansion at the top compared

to the bottom. This is a reflection, in part, of a leak in the top drainage connection.

One notable feature is that in 50% of the samples, of all compositions, the swelling was greatest at the middle compared to the top and bottom portions hence producing a barrelling effect. This supports the author's reservation (see Chapter Six, Section 6.6) over the use of rubber membranes, where it seems apparent that the 'O' rings near the top and bottom of the samples have a stiffening effect on the membrane. In general this greater stiffness at the top and bottom of the soil sample has resulted in less expansion. This may resemble the loads of large structures founded on expansive clays which suppress much of the expansive force. It is clear that if the samples were longer the barrelling would be evident over a greater length.

7.3.2 Second Phase

Tables 7.11, 7.12 and 7.13 show the free radial and axial expansion of the soil samples containing 10%, 20% and 30% montmorillonite respectively. The radial expansions are shown as percentages of the initial diameter of the samples. The heights, on the other hand, have been left as magnitudes in mm because all the samples have undergone shear and therefore not only no expansion has been experienced, but all the new heights are shorter than the original.

Table 7.11, showing samples containing 10% montmorillonite, indicates that only one sample produced a perfect barrel with equal top and bottom diameters. It shows that two samples expanded more at the bottom than at the top and the

rest of the samples expanded more at the top. This pattern reverses as the montmorillonite content increases.

Table 7.12, showing samples containing 20% montmorillonite, indicates that in every case the samples expanded most at the middle as expected. In only one case the top and bottom diameters are the same. In half of the remaining samples the top expanded more than the bottom and in the other half the situation was reversed.

Table 7.13 shows the data for samples containing 30% montmorillonite. It can be seen that in one sample the amount of expansion is highest at the bottom and gradually decreases towards the top reaching zero. The other observation which can be made is that half the samples expanded more at the bottom than at the top and in the other half it expanded more at the top. With the exception of the one sample, mentioned above, all other samples expanded most at the middle.

These results cannot be realistically compared with those of the first phase as in the later phase shear was involved. This resulted in shortening of the heights of the soil samples due to axial deformation.

7.3.3 Diameter to Height Ratio

Though the initial diameter to height ratio of the samples is 0.76, Table 7.10 shows that in 71% of the samples tested in the first phase the ratio of percentage expansion radially to axially is greater than 1 and as high as 8.13. This is a reflection of high and low confining cell pressures, respectively, as well as the influence of montmorillonite content and changes in stress conditions.

There are some samples which could be excluded from the analysis. Samples CRS230 and CRS330, for example, suffered from leakage through the top drainage tube. This is reflected in much bigger than expected radial expansion in the top sections of the samples.

In the second phase, the ratio of radial to axial dimensions at the end of testing remained generally below one. This behaviour is, of course, expected as the soil samples have undergone axial deformation and cannot be directly compared to the results of first phase.

7.3.4 Axial and Radial Free Expansion

7.3.4.1 First Phase

Table 7.10 shows that the samples expanded axially as well as radially. The axial expansion ranged between 0.49 to 4.59 percent of the initial height. This phenomenon is explained by the fact that the rigid load cell on top of the sample suppressed the axial expansion during testing while radial expansion was able to take place. This may have resulted in a reorientation of the soil fabric. The potential axial expansion is also demonstrated by the load exerted on the axial load cell during testing (see Table 7.18); hence when the load is removed, expansion takes place rapidly. This is similar to the situation where the bottom of an excavation experiences swelling due to the removal of overburden. This in fact supports the view that in the field, if there is a large enough load on the susceptible area, there will not be any upward expansion experienced. However, this suppressed expansion, translated into horizontal movement, could be detrimental to buried structures and utilities.

7.3.4.2 Second Phase

Table 7.11 shows that samples containing 10% montmorillonite expanded radially between about 4% and 9% with two samples expanding about 14% and 19%. Table 7.12, similarly, shows that 9 out of 13 samples containing 20% montmorillonite expanded between 3% and 8% whereas the remaining 4 samples expanded between 10% and 15%. Table 7.13, too, shows that half the samples containing 30% montmorillonite expanded between 3% and 9% whereas the other half expanded between 10% and 13%.

7.3.5 Effect of Time on Free Expansion

Other than the effect of side filter paper drains, there is no apparent trend in the relationship between the duration of each experiment and the final expanded volume of each of the test samples in the first phase. This is true for all the three test series irrespective of the sample compositions. However, in the test series where samples contain 30% montmorillonite, there is a clear pattern between those samples tested under high confining cell pressures (i.e. 207 kN/m^2) and those tested under low confining cell pressures (i.e. 69 kN/m^2).

Samples CRS430 and CRS530 tested at higher confining cell pressures expanded more axially, during free expansion, than samples CRS1330 and CRS1430 tested at lower confining cell pressures. Similarly, higher radial expansions were recorded by samples tested under higher confining cell pressures than those tested under lower confining cell pressures. This indicates that, as there were greater confining cell

pressures, more expansive potential was stored in the test specimens.

In the second phase, a better pattern emerges. Tables 7.11 to 7.13 indicate that, with exceptions, the general pattern is that there is a relationship between duration and nature of testing and the percentage radial expansion. Samples left to expand and then sheared exhibit more expansion than those sheared immediately which in turn expand more than those with no pore air or water back pressures.

7.4 Water Intake Versus Expansion

Tables 7.14 to 7.17 show the water intake and its corresponding expansion for each of the test samples, preceding any axial deformation, under the stress conditions indicated in Tables 7.1 and 7.3 to 7.5 for the first and second phases respectively. Two sets of readings are recorded for samples CRS1110 and CRS1430. They correspond to changes in values as a result of a reduction in back pressures due to a malfunction in the compressor system. However, the values of water intake and expansion used in the subsequent analysis are based on those obtained before the compressor malfunctioned.

The magnitudes of expansion, recorded in Tables 7.15 to 7.17, are those from the beginning of testing upto the commencement of shear. For those samples sheared immediately after the start of the test this, of course, is not possible and the values represent the magnitude of expansion from the beginning of shearing process. Hence, they are combinations of expansion, due to grains absorbing water, and the shearing altering the geometry of the samples.

An attempt was made to relate expansion to water intake. Table 7.14 shows the relationships between expansion and water intake for samples tested in the first phase where no logical pattern emerged. In the second phase, however, a better pattern emerged. With the exception of one sample, containing 10% montmorillonite (Table 7.15), in all the other cases the ratio of expansion to water intake was greater for identical samples sheared immediately after equipment assembly compared to those undergoing expansion and then sheared.

7.5 Water Intake Versus Time

Figures 7.2 to 7.13 show the water intake (ml) against test duration in log hours for both phases of the experimental work. All the data have been adjusted to a common zero datum for ease of comparison between the individual tests.

7.5.1 First Phase

Results for the samples containing 10% montmorillonite are plotted on Figures 7.2 and 7.3. They had an initial confining cell pressure of 207 kN/m^2 (30 psi). The pore air back pressure was 138 kN/m^2 (20 psi) and the pore water back pressure was 69 kN/m^2 (10 psi).

Figure 7.2 shows the water intake of samples CRS910 and CRS1010 which experienced no changes in their stress histories. Samples CRS810, CRS1110 and CRS1210, where stresses were altered at certain stages, are shown in Figure 7.3. In all cases, where the stresses were changed, the pore water back pressure was increased from 69 kN/m^2 (10 psi) to 103.5 kN/m^2 (15 psi). In some cases an increase in

pore water back pressure was followed by a decrease in the confining cell pressure from 207 kN/m^2 (30 psi) to 172.5 kN/m^2 (25 psi). The times when the stresses were increased or decreased can be deduced from Figure 7.3.

Figure 7.4 traces the water intake by samples CRS620 and CRS720. These two samples, containing 20% montmorillonite, were tested under an initial confining cell pressure of 207 kN/m^2, 138 kN/m^2 pore air back pressure and 69 kN/m^2 pore water back pressure. Both samples experienced an increase in pore water pressure from 69 kN/m^2 to 103.5 kN/m^2 and a decrease in confining cell pressure from 207 kN/m^2 to 172.5 kN/m^2.

Samples CRS430 and CRS530 shown in Figure 7.5, containing 30% montmorillonite, were tested under an initial confining cell pressure of 207 kN/m^2, 138 kN/m^2 pore air back pressure and 69 kN/m^2 pore water back pressure.

Figure 7.6 shows the water intake by samples CRS1330 and CRS1430. These samples also contained 30% montmorillonite but were tested under an initial confining cell pressure of 69 kN/m^2, 48.3 kN/m^2 pore air back pressure and 20.7 kN/m^2 pore water back pressure. Both samples experienced an increase in pore water back pressures the times of which can be deduced from Figure 7.6.

Comparing the graphs in Figures 7.2 to 7.6, for samples with 10, 20 and 30 percent montmorillonite, it can be seen that in every case the gradient is shallowest for samples with least montmorillonite. The gradient increases with an increase in the amount of montmorillonite present in the

samples and reaches the steepest level with maximum montmorillonite (i.e. 30%).

There are certain positions where a sudden increased rate of water intake by the samples are observed. These are as a result of either an increase in pore water back pressure or a reduction in the confining cell pressure. When there is an increase in pore water back pressure, the suction term (U_a - U_w) decreases. This allows more water to be absorbed by the soil particles.

Reduction in the confining cell pressure allows easier access of water into the body of the sample. Figures 7.3, 7.4 and 7.6 have been annotated to show the effects of increase in pore water back pressure and reduction in confining cell pressure. Montmorillonite's affinity for water is therefore clearly demonstrated by the graphs.

Samples CRS1330 and CRS1430 were tested under lower confining cell pressures (i.e. 69 kN/m^2 as compared to 207 kN/m^2). Despite proportionally smaller pore water back pressures, the samples shown in Figure 7.6 absorbed water at an increased rate. The graphs show a very steep gradient.

This may also explain why in the field only light structures suffer damage. Conversely, the greater stresses imposed by larger and heavier structures on site will restrict the flow of water in a clay soil. This will in turn restrict the moisture variation and hence the area under consideration will have a more stable moisture regime.

7.5.2 Second Phase

The stresses under which the samples in the second phase were tested are listed in Tables 7.3, 7.4 and 7.5 for those

containing 10%, 20% and 30% montmorillonite respectively. The samples were tested under 70, 140 and 210 kN/m^2 confining cell pressures and their corresponding pore air and water back pressures. The stresses remained constant throughout testing except in sample CRS2130 where pore water back pressure was increased from 70 to 105 kN/m^2 which is clearly marked on Figure 7.13.

Figures 7.7 to 7.9 show the water intake (ml) versus test duration, in log hours, for samples containing 10% montmorillonite tested in stations No. 1 and 2. Each set of samples is illustrated by a different thickness line for ease of identification and comparison. The samples with an expansive phase prior to shear are clearly marked. Attention must be drawn to the trends in two different testing stations. The samples were tested in two different sets of equipment; double-walled and single-walled triaxial cells.

Two observations can be made when comparing the above-mentioned Figures. The first one is that the trends presented in Figure 7.7 are uniform whereas those in Figure 7.8 show great fluctuations. This does not imply greater intake of water by similar samples in test station No. 2 but that there was a lack of control over the testing environment. This is explained in Chapter Six, Section 6.8. The other observation is that magnitudes of water intake by samples in station No. 2 are greater than those in station No. 1.

An interesting observation, when comparing Figures 7.2 and 7.3, for samples tested in the first phase, and Figures 7.7 to 7.9, for samples tested in the second phase, is that the

trend and magnitude of water intake of samples are compatible when tested in station No. 1. This further confirms the confidence in design and use of the double-walled triaxial cell for this study.

Figures 7.10 and 7.11 show the water intake (ml) versus test duration, in log hours, for samples containing 20% montmorillonite and tested in stations No. 1 and 3 respectively. When comparing Figures 7.10 and 7.11, as mentioned above for samples containing 10% montmorillonite, certain observations can be made. Bigger magnitudes of water intake by samples tested in station No. 3 are obtained although the rate of increase is uniform in both test stations. However, when comparing Figures 7.4 with Figures 7.10 and 7.11, for samples tested in the first and second phases respectively, it can be deduced that there is compatibility between the magnitude of water intake by samples tested in station No. 1 in both phases.

The water intake (ml) versus test duration, in log hours, for samples containing 30% montmorillonite tested in station No. 1 are presented in Figures 7.12 and 7.13. It is interesting to compare Figures 7.5 and 7.13, for samples tested under high confining cell pressures, and Figures 7.6 and 7.12, for samples tested under low confining cell pressures, in the two phases. They both follow corresponding trends and magnitudes in the two phases.

7.6 Expansion Versus Time

7.6.1 First Phase

Figures 7.14 to 7.18 show expansion (ml) against test duration in log hours. These graphs are plotted using the

data from the Bishop water volume change indicator No. (2) (see Figure 6.5) connected to the inner chamber of the modified triaxial cell.

There seems to be a time delay, even for a short period of one hour, from the time that the samples have access to water up to the time when expansion is observed. This is true for three reasons:

1) **Adsorption of Water by Minerals**

   Minerals have a large surface area (see Chapter One, Section 1.5) which needs to be covered by water. For example, in the test sample with 30% expanding lattice, kaolinite and montmorillonite cover 841 m^2 and 19,210 m^2 respectively. The total surface area of the dry soil to be covered is therefore 20,051 m^2.

2) **Absorption of Water by Minerals**

   Once the surface area of the minerals is covered by water the water is then absorbed within the body of the particles and this takes time.

3) **Void Spaces**

   Once interparticle and intraparticle adsorption and absorption have taken place, the montmorillonite particles start to expand. The first wave of expansion would be internal where the void spaces are replaced by expanded particles. Once the voids are filled then external expansion takes place which would be observed by the Bishop water volume change indicator.

Figures 7.14 and 7.15 show the expansion (ml) of samples containing 10% montmorillonite under an initial confining cell pressure of 207 kN/m^2, 138 kN/m^2 pore air back pressure

and 69 kN/m^2 pore water back pressure. The positions where the stresses were either increased or decreased are marked in Figure 7.15.

The expansion experienced by samples CRS620 and CRS720 are traced out in Figure 7.16. These samples were also tested under an initial confining cell pressure of 207 kN/m^2, 138 kN/m^2 pore air back pressure and 69 kN/m^2 pore water back pressure. The increase in pore water pressure and decrease in confining cell pressure, in sample CRS720, are clearly indicated.

Figures 7.17 and 7.18 show the expansion of samples CRS430, CRS530, CRS1330 and CRS1430 all of which contained 30% montmorillonite. Samples CRS430 and CRS530 were tested under an initial confining cell pressure of 207 kN/m^2, 138 kN/m^2 pore air back pressure and 69 kN/m^2 pore water back pressure. Due to the fact that the magnitude of expansion experienced by other samples was smaller than anticipated, it was decided to test further samples at lower confining cell pressures. Samples CRS1330 and CRS1430 were therefore tested under an initial confining cell pressure of 69 kN/m^2 (i.e. 1/3 of others), 48.3 kN/m^2 pore air back pressure and 20.7 kN/m^2 pore water back pressure.

The magnitude of expansion did not increase as much as was anticipated. It is, however, evident that the reduction in cell pressure had a marked effect on the expansion. This substantiates the argument that when there is less confining pressure, the soil particles can expand more freely.

It had been envisaged that the testing would take place over rather long periods of time. After a few tests the author

decided to shorten the drainage path. This would, in theory, reduce the testing time. One option was to shorten the height of the sample. However, this would have been counter productive to the object of the exercise. Normally in expansive soil testing, especially in oedometer testing, the height to diameter ratio is much less than 1. There may be limitations in this as the sample may reach a state of equilibrium or saturation rather quickly. This may not give enough time for all the particles to develop full expansion. At the design stage it was decided to opt for a height to diameter ratio of greater than 1. The obvious choice would have been to follow the established ratio in shear strength testing, that is a height to diameter ratio of 2:1. As mentioned earlier it was obvious that this would take rather a long time for testing. It was therefore decided to have a sample with a height of 50 mm. Even this height required rather long periods of time for the samples to reach equilibrium or full saturation.

To avoid shortening the length of the specimen any further it was decided to use a side filter paper drain. This would shorten the drainage path because the sample would not only have access to water from the bottom but also from the periphery. This seemed successful in that it accelerated the water intake and resulted in a shorter reaction time between the water intake and the expanding lattices of montmorillonite. This is evident in Figures 7.2 to 7.6 where the water intake by the samples are shown. It can be seen that with the exception of sample CRS430, which had no side

filter paper drain and contained 30% montmorillonite, all other samples took up some water within the first hour.

The reaction time with expanding lattices may be divided into three groups based on their montmorillonite content.

Samples CRS810, CRS910, CRS1010 and CRS1110, containing only 10% montmorillonite, show a response time of between 4 and 30 hours after the initiation of each test, whereas sample CRS1210 with similar composition responded in the first hour. Sample CRS620, containing 20% montmorillonite, showed expansion after six hours whereas sample CRS720 with similar composition responded after just over an hour's exposure to water.

Samples CRS430, CRS530, CRS1330 and CRS1410 all contained 30% montmorillonite. Samples CRS430 and CRS530 were tested without any side filter paper drain and under an initial confining cell pressure of 207 kN/m^2; samples CRS1330 and CRS1430 were tested with side filter paper and under an initial confining cell pressure of 69 kN/m^2. Sample CRS430 reacted after one hour whereas sample CRS530, tested in similar circumstances, did not react until after a period of five hours. Samples CRS1330 and CRS1430 both responded to the reaction between water and the expanding lattices after about two hours. As there were smaller confining cell pressures surrounding these samples, shorter response times were anticipated. This anomally, which may be a function of the Bishop water volume change indicator, will be explored in greater detail in Section 7.10.

Water intake and expansion continued after this stage though at a slower rate. This is what the author terms "residual"

expansion. This may be very small compared to the main expansion obtained at a shorter time. However, it is important to be able to quantify this "residual" expansion because, over the lifetime of any structure, it might prove more damaging than the initial quick expansion.

7.6.2 Second Phase

In the second phase, when it was decided to study the shear strength of the unsaturated artificially constituted samples, the question of height to diameter ratio arose again. Traditionally, shear strength testing of samples are carried out using samples with a height to diameter ratio of 2:1. However, after careful consideration (Lade (1982), Lade and Tsai (1985)) and a private communication with Davies (1993) it was decided to keep the samples the same as those used in the first phase, that is, a height to diameter ratio of 1:1.32.

Figures 7.19 to 7.25 show the expansion (ml) against testing time, in log hours, for samples containing 10%, 20% and 30% montmorillonite and tested in stations No. 1, 2 and 3 respectively.

A comparison of Tables 7.15 to 7.17 and Figures 7.19 to 7.25 indicates that generally, as the confining cell pressures increase, the observed expansion reduces. This is of course expected and resembles the field situation where the level of damage reduces as the structure gets bigger. This is definitely true in the case of station No. 1 where there is very good control over the whole testing environment due to the modified double-walled triaxial cell. In other cases it is partly true, and if the same control could be excercised

in the case of stations No. 2 and 3, the same trends could probably be obtained.

7.7 Development of Axial Swell Pressures During Testing

The loads exerted by the samples during the first phase of testing, recorded on a load cell, are presented in Table 7.18. The loads shown are recordings after 1, 20, 50, 100, 500 and 1000 hours of testing.

Having found the loads exerted by the samples, they were then converted into pressures which actually showed how the swell pressures developed throughout testing. Equivalent swell pressures, recorded by the load cell, were calculated using the change in the diameter of each sample and are presented in Table 7.19; these are not the true swell pressures (loads) developed by the samples. The loads (swell pressures) developed by the samples should have first overcome the confining cell pressures before being effective on the load cell. The confining cell pressures were therefore calculated and added to the equivalent axial swell pressures recorded by the load cell and the final values obtained. For ease of comparison they are listed in Table 7.20 and each sample is traced out separately in Figures 7.26 to 7.29.

7.7.1 Axial Swell Pressure Versus Time

It is evident that the axial swell pressures exerted by each sample increased rapidly in the first few days. In fact, on average, about 90% of the total swell pressures developed in the first hour. Thereafter the pressures did not increase as rapidly. There were a few instances where there were

sudden drops or increases in the axial swell pressures. Any reduction in the axial swell pressure was generally due to a breakdown of the compressor as in the case of samples CRS1010, CRS1110 and CRS720 although there were instances, like in samples CRS810 and CRS1210, where there were reductions in the axial swell pressures without a satisfactory explanation.

There were other instances where a sudden increase in the axial swell pressure was recorded. This phenomenon was due to two reasons. The first was when there had been an increase in the pore water back pressure. The other was where there had been a decrease in the confining cell pressure. If the cell pressures were to reduce, the sample would be free to expand laterally with more ease.

Figure 7.26 shows the swell pressures (kN/m^2) developed by samples containing 10% montmorillonite. All the samples were tested under an initial confining cell pressure of 207 kN/m^2, 138 kN/m^2 pore air back pressure and 69 kN/m^2 pore water back pressure. The times where the pore water pressures increased or the confining cell pressures decreased can be deduced from Figure 7.26.

The swell pressures developed by samples CRS620 and CRS720, both containing 20% montmorillonite, are shown in Figure 7.27. The samples were tested under an initial confining cell pressure of 207 kN/m^2, 138 kN/m^2 pore air back pressure and 69 kN/m^2 pore water back pressure. The positions where the stresses were changed are indicated on the graphs.

Figures 7.28 and 7.29 show the swell pressures developed by samples CRS430 and CRS530, and CRS1330 and CRS1430

respectively. These samples contain 30% montmorillonite. The former two samples were tested under an initial confining cell pressure of 207 kN/m^2, 138 kN/m^2 pore air back pressure and 69 kN/m^2 pore water back pressure. Samples CRS1330 and CRS1430, for reasons previously explained (see Section 7.6.1), were tested under an initial confining cell pressure of 69 kN/m^2, 48.3 kN/m^2 pore air back pressure and 20.7 kN/m^2 pore water back pressure.

The swell pressures, developed after 100 hours of testing, are plotted against the montmorillonite content in Figure 7.30. It shows a direct relationship between the montmorillonite content and the rate of increase in axial swell pressure. As the montmorillonite content increases so does the axial swell pressure although the relationship is not linear. One hundred hours was chosen because all the samples were under test conditions for at least that duration. The swell pressures developed by samples containing 30% montmorillonite under high and low confining cell pressures are separated. It must be noted that samples tested under low confining cell pressures had side filter paper drains. It is envisaged that even lower swell pressures would have been obtained in the absence of side filter paper drains. The effect of side filter paper drains, in increasing the magnitude of swell pressure, is demonstrated in Figure 7.32.

Figure 7.30 shows that the rate of increase of swell pressures did not increase linearly when plotted against the montmorillonite content. It shows that the swell pressure increased more between 20% and 30% than between 10% and 20%

montmorillonite content. An important consideration in the field is the development of swell pressure which has a high potential for damage. Knowledge of swell pressure and hence potential for damage enables the designer to modify a design to withstand or even eliminate the threat of damage due to heave.

7.8 Swell Pressures Without Confining Pressures

Abdi (1992) set up a piece of apparatus (see Plate 7.1 and Figure 7.31) for measuring the swell pressures developed by a soil sample. There are no confining cell pressures around the samples and each one is confined only by a 5 mm thick perspex mould.

Figure 7.32 shows the swell pressures developed by two samples containing 10% montmorillonite. They were measured in the equipment devised by Abdi. It shows that 94% and 80% of swell pressures, by samples with and without side filter paper drains respectively, developed soon after the samples were allowed access to water. This rapid increase in swell pressure occurred in the first two or three days after which the swell pressures increased at a very slow rate.

One of the samples tested was wrapped in filter paper which affected the swell pressures. It can be seen that the sample with the side filter paper reached its peak value at a shorter time. It is also interesting to note that it experienced about 20 kN/m^2 more swell pressure than the sample without a filter paper.

The samples underwent two wetting and drying cycles and it is evident that the swell pressures in the second cycle reached the same level as in the preceding cycles.

The swell pressure developed by a sample containing 20% montmorillonite is presented in Figure 7.33. It underwent three wetting and drying cycles. It shows that the maximum swell pressure in each cycle is almost the same as those reached in the others. It can be seen that almost 98% of the maximum swell pressure was obtained in the first four days after which it increased at a much slower rate.

Figure 7.34a shows the swell pressure developed by a sample containing 30% montmorillonite. It shows that most of the swell pressure developed very early on after soaking. In fact it can be seen that about 75% of the total swell pressures developed within the first three days. The remaining 25% developed in the following 14 weeks. When the access of water to the sample ceased, the swell pressure dropped at a much faster rate than it had developed. It can be seen from the Figure that once the sample was in the drying cycle it took only 4.5 weeks for the swell pressure, developed over 14.5 weeks, to dissipate completely. Once the sample was rewetted, the swell pressure developed very rapidly but remained short of the pressures reached in the first wetting cycle. It also started to level off quickly. When the second drying cycle started the same behaviour was observed and the swelling pressure dissipated quicker than it had developed.

There may be a limitation in the use of the apparatus devised by Abdi (1992). A comparison of the swell pressures developed in this apparatus and those recorded by the load cell shows that the magnitude of swell pressures recorded were much less than those developed in the triaxial cell.

This is probably due to the flexibility of the proving ring allowing the samples to expand with a consequent drop in swell pressure.

For compatibility, the swell pressures developed after 20, 50, 100, 500 and 1,000 hours in the two pieces of apparatus were compared. They show that at high confining cell pressures (207 kN/m^2) the average swell pressures recorded by the load cell were greater by about 64%, 54%, 50%, 46%, and 40% respectively compared to those recorded by the proving ring in the new device (see Table 7.20 and Figure 7.34a). It is interesting to note that the swell pressures developed by samples CRS1330 and CRS1430, which were tested at a low (i.e. 69 kN/m^2) confining cell pressure, were almost the same as those recorded by the new apparatus designed by Abdi (1992).

The maximum swell pressure reached in the new device was 163.1 kN/m^2 after 2772 hours whereas the maximum recorded in the modified triaxial cell was 261.88 kN/m^2 after only 50 hours.

Figure 7.34a shows two cycles of wetting and drying. The second cycle of wetting shows a reduced swell pressure, with the maximum value developed in a much shorter time. One reason for this lower value of swell pressure in subsequent wetting cycles is due to the loss of fine particles through the access holes.

The swell pressure developed by another sample containing 30% montmorillonite is shown in Figure 7.34b. It shows that the two cycles peaked at about the same level of swell pressure. This is contrary to the behaviour of the other

sample shown in Figure 7.34a but follows those for samples containing 10% and 20% montmorillonite. It can be seen that almost 90% of the swell pressure was obtained in the first three days.

An interesting observation is that the magnitude of swell pressures increased as the montmorillonite content increased.

7.9 Percentage Volume Change by Micrometer

Tables 7.21 and 7.22 to 7.24 list the percentage volume change of the samples at the end of the first and second phases of testing respectively. They were obtained by physical measurement using a micrometer.

The final and initial heights, the final diameter, and the initial and final volumes of the samples from which the percentage volume changes are calculated, for samples tested in the first phase, are listed in Table 7.21. It shows that samples containing 10% and 20% montmorillonite experienced average values of free expansions of 2.7% and 5.8% respectively. Samples containing 30% montmorillonite, tested under low and high confining cell pressures, show average free expansions of 18.4% and 8.9% respectively. The samples tested under low confining cell pressures expanded by a much bigger magnitude. This further demonstrates the effect of confining cell pressures on the performance of expanding lattices.

Table 7.22 shows the free expansion of samples containing 10% montmorillonite, tested in stations No. 1, 2 and 4, in the second phase. It shows that the samples increased in volume by an average of about 3.6%. It also shows that one

sample experienced a reduction in volume. This was a quick shear test without prior saturation. The other samples which experienced reduction in volume are those tested in the fourth station where quick drained tests with no pore air or water back pressures were conducted. These samples were not allowed to expand prior to shear. The shearing process obviously consolidated the samples even further hence reducing the overall volume of the samples.

The free expansion of samples containing 20 percent montmorillonite, tested in stations No.1, 3 and 4, in the second phase are presented in Table 7.23. It shows that one set of samples, tested in station No. 3, expanded by an average of about 14% whereas the others expanded by an average of about 2%. This great difference in percentage volume increase of samples may be due to the fact that those experiencing highest increases were confined by only 70 kN/m^2 cell pressure whereas the others were confined by 140 and 210 kN/m^2. Two out of three samples tested in the fourth station, as a quick drained test with no pore air or water back pressures, decreased in volume by an average of about 2.5%. Four samples tested under different conditions, in stations No. 1 and 3, experienced an average decrease in volume of 0.41%. Two of these samples were sheared after they had been saturated and allowed to expand and the other two were quick drained tests with the appropriate back pressures. All of these samples were tested under higher confining cell pressures of 140 and 210 kN/m^2.

The free expansion of samples containing 30% montmorillonite, tested in stations No. 1 and 4, in the

second phase are presented in Table 7.24. It shows that only one sample, a quick drained test with no pore air or water back pressures, experienced a reduction in volume of 3.7%. All other samples experienced an average increase of about 5%. A set of samples, tested under the least confining cell pressure of 70 kN/m^2, expanded by an average of about 13.4%. The samples experiencing reduction in volume, in all the three compositions, have generally been tested in the fourth station. They were, therefore, quick drained tests where there were no pore air or water back pressures. Although minute amounts of water have been taken in by the samples, the confining cell pressures and the relatively short duration of testing prevented any expansion taking place as a result of reaction between water and the expanding lattices.

A comparison of the corresponding Tables indicates that samples tested in the first phase (Table 7.21) show bigger free volume changes than those in the second phase (Tables 7.22 to 7.24). The reason for this difference is that the first phase was an expansion only exercise whereas in the second phase the samples have, in addition to expansion, undergone shear which has caused further consolidation of the samples.

7.9.1 Volume Change (micrometer) and Time Versus Montmorillonite Content

7.9.1.1 First Phase

The relationships between volume change (%) and duration of testing (days) against the montmorillonite content, for samples tested in the first phase, are shown in Figure 7.35.

The Figure is based on information given in Tables 7.21 and 7.10. It generally shows that, as the montmorillonite content increases, so do the volume change and the time taken for pore pressures to stabilise.

A linear relationship between percentage volume change and percentage montmorillonite, contained in the samples tested under confining cell pressures of 207 kN/m^2, can be observed in Figure 7.35. It shows an increase in the duration of testing as the montmorillonite content increases. However, in contrast to the volume change, the relationship between duration of testing and the percentage montmorillonite is slightly curved. It shows that samples containing 30% montmorillonite took a longer time to stabilise than expected. The samples containing 30% montmorillonite were also tested under a low confining cell pressure of 69 kN/m^2 the results of which are not presented in the Figure.

The samples tested in the first phase experienced combined expansions of 2.7%, 5.8% and 8.9% for those containing 10, 20 and 30 percent montmorillonite respectively. They were all tested under 207 kN/m^2 confining cell pressures. However, when the confining cell pressures were reduced to 69kN/m^2, for samples containing 30% montmorillonite, the free expansion increased by 18.4%.

7.9.1.2 Second Phase

The relationships between volume change (%) and duration of testing (days) against the montmorillonite content, for samples tested in the second phase, are presented in Figure 7.36. The Figure is based on data given in Tables 7.22 to

7.24 and 7.11 to 7.13, for samples containing 10%, 20% and 30% montmorillonite, respectively.

Figure 7.36 shows that both volume change and duration of testing increased exponentially as the montmorillonite content increased. The curves presented are the averages of three values based on the confining cell pressures. The curves corresponding to volume changes, based on respective confining cell pressures, are also plotted to illustrate their effect.

It is evident that samples tested under the least confining cell pressures expanded considerably more than those under higher confining cell pressures.

The average values of expansion of the samples containing 10, 20 and 30 percent montmorillonite were 2.8%, 4.4% and 7.9% respectively. These values are the averages of figures for each composition but tested under different confining cell pressures of 70, 140 and 210 kN/m^2.

If there is greater overburden at a site underlain by a clay rich in montmorillonite, then it takes a longer time for the expansion to be completed whereas if there is a nominal surcharge present, then moisture movement stabilises and expansion takes place in a shorter time.

7.9.2 Three Dimensional Representation of Volume Change, Time and Montmorillonite Content

The volume change (%) and time to saturation (days) against montmorillonite content, plotted in three orthogonal planes for samples tested in the first and second phases, are illustrated in Figures 7.37 and 7.38 respectively. The resultants of the three planes are drawn with heavier prints

to show the true three dimensional representations of the three variables.

The three dimensional (the resultant) representation of the samples, tested in the first and second phases, show a near linear relationship.

7.10 Water Intake & Expansion Versus Montmorillonite Content

Water intake and expansion, as percentages of initial volume, against montmorillonite content for samples tested in the first and second phases are presented in Figures 7.39 to 7.42. They are obtained under test conditions using Bishop water volume change indicators.

7.10.1 First Phase

Figure 7.39 shows both water intake and expansion, as percentages of initial volume, against montmorillonite content. It illustrates that as the montmorillonite content of the soil samples increases there is a corresponding increase in the magnitudes of water intake and expansion. One notable feature is that the rate of increase in water intake and expansion follow the same trend. The rate of increase in water intake between samples containing 10% and 20% montmorillonite is 110% whereas between those containing 20% and 30% montmorillonite is only 17%. Similarly, the rate of increase in expansion between samples containing 10% and 20% montmorillonite is 97% whereas between those containing 20% and 30% montmorillonite is only 8%.

Figure 7.43 shows a linear relationship between the surface areas of dry samples as the montmorillonite content increases from 10 to 30 percent. It is expected that, in

perfect conditions, this linear relationship is reflected in the behaviour of the samples. However, the samples do not follow the same trend during soaking.

Samples containing 30% montmorillonite were tested under high and low confining cell pressures. Figure 7.39 shows the results for those tested under high confining cell pressures.

A sudden increase in water intake is experienced for the samples tested under low (69 kN/m^2) confining cell pressures (see Table 7.14). This behaviour follows the expectation that as there is less confining cell pressure the particles are in a less dense state and hence their ability to absorb water will be enhanced.

Figure 7.39 shows the expansion experienced by the samples under 207 kN/m^2 confining cell pressure. It is evident that in this case there is no linear relationship between expansion and increase in montmorillonite content. If linearity were to be maintained, a certain amount of expansion is expected between samples containing 10% to 30% montmorillonite. However, this is not the case.

The following table shows the expected and actual rates of increase in volume for samples containing between 10 and 30 percent montmorillonite.

Montmorillonite (%)	10 - 20 (%)	20 - 30 (%)	10 - 30 (%)
Expected	1.94	1.40	2.72
Actual	1.94	1.09	2.12

Expected and actual rates of volume increase

The samples containing 20% montmorillonite expanded about 1.94 times those containing 10%. If linearity is to be maintained, samples containing 30% montmorillonite should expand about 1.4 times those containing 20% or 2.72 times those with 10% montmorillonite. The actual expansion recorded for samples containing 30% montmorillonite, was in fact only 1.09 times those with 20% montmorillonite and 2.12 times those containing 10%.

An important factor is the suction term (U_a - U_w). Tables 7.1 and 7.2 list the stress changes at the beginning and throughout testing for samples tested in the first phase. Samples CRS430 and CRS530 containing 30% montmorillonite, were tested under high confining cell pressures. It is possible that because they were confined under high confining cell pressures and came against resistance due to suction they were prevented from experiencing bigger rates of expansion. Samples CRS1330 and CRS1430 were, however, tested under low confining cell pressures and the stresses were changed so that they would be tested under smaller suction forces (see Table 7.1b). Despite a reduction in these two inhibiting factors, they still did not experience as much expansion as was anticipated. This behaviour raises two questions:

1) Is it a natural fact that once the montmorillonite content exceeds a certain limit (may be greater than 25%) then the rate of expansion slows down?

This may be true for samples tested under different stresses and not in a free swell situation. It can be seen from Figures 7.35 and 7.51 that when free expansion was involved

the rate of increase in expansion was linear for samples containing between 10% and 30% montmorillonite.

Results of samples tested in the second phase (see Figures 7.41 and 7.42) discount this supposition although in Figure 7.42, if the results of two stations are used, the same trend follows. It shows that as the montmorillonite content increases from 10% to 30% so do the rates of increase in water intake and expansion.

2) Was there any limitation in the Bishop water volume change indicator recording expansion?

As question 1), above, is discounted, it only leaves this one as the most likely possibility.

Figure 7.44 shows the relationships between water intake and expansion, as percentages of original volume, versus the montmorillonite content in three orthogonal planes. Each point has been projected to present a true three dimensional representation of the planes. The real three dimensional curve, which falls in space and not in any one plane, is shown with a heavier print.

7.10.2 Second Phase

Figure 7.40 shows the relationship between water intake, as percentage of original volume measured by the Bishop water volume change indicator, and montmorillonite content. Three graphs are plotted to show the water intake by samples tested under different confining cell pressures, they are, 70, 140 and 210 kN/m^2.

Samples containing 30% montmorillonite and tested under the least confining cell pressure show a much bigger rate of water intake. To eliminate and compare the influence of

different pressures, two other graphs are presented. One is obtained by averaging the values from samples tested under highest confining cell pressures, namely, 140 and 210 kN/m^2. The other curve is produced by using the data from samples tested under all the confining cell pressures.

In both cases it shows an increased rate of water intake between samples containing 20% and 30% montmorillonite than those containing 10% and 20%.

The relationship between expansion and montmorillonite content is shown in Figure 7.41. The rate of expansion between samples have been separated by plotting them based on the confining cell pressures as was the case with water intake. In this case, the samples tested under the least confining cell pressure experienced most expansion. It can be seen that the relationship between rate of expansion and montmorillonite content is almost linear.

Although there are variations in the actual magnitudes between the two averaged curves, they generally follow the same trend. In fact it can be seen even better on the one with the two highest confining cell pressures. In both cases there is a much increased rate of expansion for samples containing 20% and 30% montmorillonite than those between 10% and 20%.

The relationship between water intake and expansion with montmorillonite content is further illustrated in Figure 7.42. This Figure is produced based on data obtained from two different test stations. It can be seen that those obtained from station No. 1 show similar trends to those plotted based on confining cell pressures. It certainly

proves the consistency in using one apparatus and the effect of equipment compressibility on the results.

Figures 7.45 and 7.46 show the relationships between water intake and expansion, as percentages of original volume, versus the montmorillonite content in three orthogonal planes. Each point on the planes has been projected to present a three dimensional representation of the values.

Figure 7.45 has been produced using data from samples tested under all three confining cell pressures whereas Figure 7.46 is based on information from two highest confining cell pressures. The effect of one set of test result on the outcome is better illustrated by these three dimensional presentations.

7.11 Initial Properties of Soil Samples

Tables 7.25 to 7.28 show the total, solid, air and water volumes for samples tested in the first and second phases. They also show the void ratios, dry densities and degrees of saturation for sample at the start of each test.

The preparation of artificially constituted soil samples was considered appropriate to provide more consistent test specimens in terms of expansive nature, air/water content and density. An examination of Table 7.25 and Figures 7.47 and 7.49, for the first phase, and Tables 7.26 to 7.28 and Figures 7.48 and 7.50, for samples tested in the second phase, proves the success of this operation.

The initial void ratios (e) and degrees of saturation (Sr), for samples tested in the first phase, fall within a narrow band where $e = 0.946 \pm 0.006$ and $Sr = 85.2\% \pm 0.5\%$. The initial void ratios for samples containing 10%, 20% and 30%

montmorillonite, tested in the second phase, are 0.941 ± 0.005, 0.941 ± 0.007 and 0.943 ± 0.01 respectively. The initial degrees of saturation for samples containing 10%, 20% and 30% montmorillonite, tested in the second phase, are 85.71% ± 0.5%, 85.54% ± 0.3% and 85.3% ± 0.5% respectively.

7.12 Final Properties of Soil Samples

The total, solid, gross water, water in filter paper, diffused air, net water and air volumes for samples tested at the end of the first and second phases are presented in Tables 7.29 and 7.30 to 7.32 respectively.

7.12.1 First Phase

It can be seen that the volume of air within two samples, calculated at the end of each test, shows a negative value. One assumption is that the samples reached 100% saturation and the volume of air should in fact read zero.

Samples CRS1330 and CRS1430, tested under low confining cell pressures, show negative volumes of around 7 and 13 cc of air. These high negative values produced degrees of saturation of about 126% and 143%. This rapid increase in the degree of saturation, for samples tested under low confining cell pressures, is clearly illustrated in Figure 7.49.

One explanation, for the negative volume of air, could be due to loss of material. If this were the case, the loss of solid particles at the sample preparation stage should be almost equal in every case. The effects of pressure on ion exchange were considered and were ruled out, as a

contributory factor, in the disparity between the samples tested under high and low confining cell pressures. The misreading or malfunctioning of the Bishop water volume change indicator may also have contributed to these eroneous readings.

The final hypothesis is that this is a physical phenomenon. This can only be validated or rejected with further tests on samples of different composition and under low confining cell pressures. If this is proved to be the case, then a whole new line of investigation should start. One major avenue of research would be whether the present definitions of the soil model and properties, like degree of saturation, are correct for unsaturated expansive clays tested under low confining cell pressures and containing considerable amounts of expanding lattices.

It must be pointed out that the volumes of air within the samples throughout testing were not quantified and these values were obtained through calculation. They were then used to calculate final void ratio (e) and degree of saturation (Sr)(%) for each sample which are presented in Table 7.33 and Figures 7.47 and 7.49 respectively.

The final void ratios of the samples increased by an average of 1.85% from the initial to the final conditions. If the results of the samples tested under high and low confining cell pressures are separated, different results will be deduced. The final void ratios, by samples tested under high confining cell pressures, and consisting of 10%, 20% and 30% montmorillonite increased by an average of 1.75%. Samples containing 30% montmorillonite and tested under low

confining cell pressures experienced an average increase of 2.24%.

Similarly, the final degrees of saturation increased by an average of 21.76% and when the effect of those samples tested under low confining cell pressures are eliminated, the average percentage increase reduces to 6.33%.

7.12.2 Second Phase

The volumes of different constituents, calculated at the end of the second phase of testing, are presented in Tables 7.30 to 7.32 for samples containing 10% to 30% montmorillonite respectively. Tables 7.30 and 7.31 show that there is no recorded volume of diffused air. This is as a result of lack of provision for diffused air volume measuring devices in stations No. 2 and No. 3.

Having found different volumes, the figures are used to calculate the final void ratios and degrees of saturation. They are presented in Tables 7.34, 7.35 and 7.36 for samples containing 10%, 20% and 30% montmorillonite respectively. The final void ratios and degrees of saturation are hence illustrated graphically in Figures 7.48 and 7.50 respectively.

For ease of comparison, the average percentage increases in the final void ratios and degrees of saturation, obtained from different testing stations, are presented in the following table. It is worth noting that the tests were conducted under three different confining cell pressures. They were; 70, 140 and 210 kN/m^2.

Test station	Montmorillonite content			Soil property
	10%	20%	30%	
No. 1	2.76 1.04			e S_r
No. 2	14.34 9.91			e S_r
Nos. 1 & 2	8.55 5.48			e S_r
No. 1		2.18 2.58		e S_r
No. 3		12.01 5.91		e S_r
Nos. 1 & 3		8.08 4.58		e S_r
No. 1			14.19 14.57	e S_r

Percentage increase in final properties of soil samples.

A closer examination of the table shows that the average percentage increases in the final values obtained by test stations No. 2 and 3 are generally bigger than those produced from test station No. 1 for identical samples tested in two different test stations.

Samples containing 30% montmorillonite were tested in station No. 1 only. These show large increases compared to those for 10% and 20% montmorillonite. This is due to large volume change experienced by the sample tested under the least confining cell pressure.

7.13 Weight/Volume Relationship

The initial and final weight/volume relationships, for samples tested in the first and second phases, are presented in columns 4 and 7 of Tables 7.37 and 7.38 to 7.40 respectively. The data presented have been measured by both micrometer and the Bishop water volume change indicator or the GDS pressure controller.

7.13.1 First Phase

The final weight/volume relationships, by the two methods, indicates that the ratios obtained by the micrometer decreased between 1.4% and 21% compared to those obtained by the Bishop water volume change indicator. Another point is that the final weight/volume relationships, measured by the micrometer, decreased by as much as 7.6% from the initial conditions whereas they increased between 3% and 15.5% when measured by the Bishop water volume change indicator.

7.13.2 Second Phase

A certain pattern emerges when the three Tables, representing data for samples containing 10%, 20% and 30% montmorillonite, are studied closely. For example, it can be seen that more than half of the samples in each group show decreases in the final weight/volume relationships when measured by micrometer rather than the Bishop water volume change indicator or the GDS pressure controller.

The other pattern emerging is that when the ratios between the initial and final conditions, obtained by the micrometer, are considered more than 50% of the samples in each group show an increase in the final condition. Similarly, when the Bishop water volume change indicator or the GDS pressure controller are considered the final ratios show an increase in more than half of the samples.

Table 7.38 shows that in 58% of the samples, containing 10% montmorillonite, the ratios obtained by the micrometer decreased by as much as 3.6% whereas in the remaining 42% it increased by as much as 10.7% compared to those obtained by

the Bishop water volume change indicator. It also shows that in 73% of the samples the weight/volume relationships, measured by the micrometer, increased by as much as 0.7% and decreased by as much as 0.6% in the remaining 27%. It can also be seen that in 67% of the samples, measured by the Bishop water volume change indicator, the ratio increased by as much as 0.9% and in the remaining 33% it decreased by as much as 0.08% from the initial to the final conditions.

Table 7.39 illustrates that in 50% of the samples containing 20% montmorillonite, the ratios obtained by the micrometer show decreases of as much as 0.6% and in the other 50% they increased by as much as 0.8% compared to those measured by the Bishop water volume change indicator or the GDS pressure controller. It also shows that in 85% of the samples the weight/volume relationships, measured by the micrometer, increased by as much as 0.7% and in the remaining 15% it decreased by as much as 0.07%. Table 7.39 also shows that in 50% of the samples the ratios, measured by the Bishop water volume change indicator or the GDS pressure controller, increased by as much as 0.5% and in the other 50% they decreased by as much as 0.9% from the initial to the final conditions.

The initial and final weight/volume relationships, for samples containing 30% montmorillonite, are presented in Table 7.40. It shows that in 80% of the samples the weight/volume relationships, obtained by the micrometer, show decreases of as much as 1%, and increases of 0.05% were achieved in the remaining 20% of the samples compared to those obtained by the Bishop water volume change indicator.

Table 7.40 also shows that in 50% of the samples the weight/ volume relationships, measured by the micrometer, increased by as much as 0.04% and in the other 50% decreased by as much as 0.5% from the initial to the final conditions. It can be seen that in 67% of the samples the ratios, measured by the Bishop water volume change indicator, increased by as much as 1% and in the remaining 33% they decreased by as much as 0.6%.

There are variations between the ratios for tests in the first and second phases of testing presented in Tables 7.37 and 7.38 to 7.40 respectively. This variation is due to the fact that those in the second phase of testing have undergone shear which reduces the physical volumes of the samples.

7.14 Difference in The Final Volumes by Two Methods

The final volumes of the samples, measured by both the micrometer and the Bishop water volume change indicator or the GDS pressure controller, are presented in Tables 7.41 and 7.42 to 7.44 for samples tested in the first and second phases respectively.

7.14.1 First Phase

Table 7.41 clearly shows that the final volumes measured by the micrometer are greater than those measured by the Bishop water volume change indicator. The extra expansion ranges from 1.4% to 21%.

Volume changes, as percentages of original volumes, measured by both micrometer and the Bishop water volume change

indicator, are plotted against montmorillonite content and liquid limit in Figure 7.51.

Liquid limit is a function of montmorillonite content. Hence when examining any site it is much easier and cheaper to perform liquid limit tests rather than a chemical analysis to determine the montmorillonite content. It can be seen that the rate of volume change, measured by the Bishop water volume change indicator, was greater for samples containing 10 to 20 percent montmorillonite than for those containing 20% to 30% montmorillonite. On the other hand the rate of volume change measured by the micrometer, shows an almost linear increase between samples containing 10 to 20 percent montmorillonite. It must be remembered that volume changes, measured by a micrometer, incorporate free expansion.

7.14.2 Second Phase

The difference in the final volumes measured by the micrometer and the Bishop water volume change indicator are presented in Tables 7.42 to 7.44 for samples containing 10% to 30% montmorillonite respectively.

The rate of increase in volumes, measured by the two methods in the second phase, do not follow the same trend as those in the first phase. In this phase, because the samples underwent shear as well as expansion, some samples show smaller volumes when measured by micrometer compared to those by the Bishop water volume change indicator or the GDS pressure controller. The negative signs in the Tables indicate smaller volumes measured by the micrometer.

Table 7.42, for example, shows that 42% of the samples containing 10% montmorillonite measured less when using the

micrometer. They range from 2.6% to 10% whereas in the remaining 58% of the samples the micrometer readings show increases of upto 3.6%, in volume, compared to those by the Bishop water volume change indicator.

The final volumes for samples containing 20% montmorillonite are presented in Table 7.43. It shows that 60% of the samples experienced smaller volumes when measured by the micrometer compared to those measured by the Bishop water volume change indicator. The reductions experienced range between 0.8% and 10% whereas the other 40% of the samples experienced increases of between 0.6% and 8%.

Table 7.44 shows the final volumes measured by the two methods for samples containing 30% montmorillonite. It shows that only one sample experienced a reduction in volume of 0.4%, when measured by the micrometer, whereas the others increased between 0.3% and 1.8%. The sample which shows a smaller volume, when measured by the micrometer, is a quick drained test without prior saturation and expansion.

The volume changes, as percentages of original volumes, measured by both the micrometer and the Bishop water volume change indicator, are plotted against montmorillonite content and liquid limit in Figure 7.52. It shows two different curves for volume changes measured by the Bishop water volume change indicator. One is the result of averages of the samples tested under the three confining cell pressures. The second is based on the averages obtained from two highest confining cell pressures, namely, 140 and 210 kN/m^2. The influence of samples tested under 70 kN/m^2 is quite evident from the two curves. As expected, the curve

has shifted further up. In other words, when there is less confining cell pressure more expansion is observed.
The free expansions, measured by the micrometer, are smaller than those measured in the first phase. This is due to the fact that the samples in this phase have undergone shear as well as expansion. Therefore, consolidation at the shear stage has reduced the heights of the samples.

7.14.3 Micrometer Versus Bishop Water Volume Change Indicator

An attempt was made to find a relationship between the volume changes measured by the two different methods. As evident from Figure 7.53, volume changes measured by the micrometer were plotted against those measured by the Bishop water volume change indicator for samples tested in the first phase. It can be observed that as the values measured by the micrometer increase so do those measured by the Bishop water volume change indicator up to 20% montmorillonite. From 20% to 30% montmorillonite the volume changes, measured by the micrometer, increase markedly.
Figure 7.54 shows the volume changes, measured by the micrometer, against the corresponding ones by the Bishop water volume change indicator for samples tested in the second phase.
Two relationships are presented in this Figure. One is based on the average of samples tested under 70, 140 and 210 kN/m^2 confining cell pressures. The other is based on those tested under 140 and 210 kN/m^2. It is evident that two different trends develop. When the averages of all the three different confining cell pressures are considered a linear

relationship develops between the volume changes measured by both the micrometer and the Bishop water volume change indicator. However, a different trend emerges when the results are based on the two higher confining cell pressures only. It can be seen that the rate of increase in volume, for samples containing between 10% and 20% montmorillonite, is quite steep and it decreases for samples between 20% and 30% montmorillonite. It is clear that as the volume changes measured by the micrometer increase so do those measured by the Bishop water volume change indicator.

7.14.4 Three Dimensional Representation of Volume Changes, Measured By Both Methods, and The Montmorillonite Content

A three dimensional representation of the volume changes, measured by the two methods, with montmorillonite content is shown in Figure 7.55 for samples tested in the first phase. The data presented are based on the soil samples tested under 207 kN/m^2 confining cell pressures. It can be seen that as the montmorillonite content increases so do the volume changes measured by either of the two methods.

The three dimensional representations of the percentage volume changes, measured by the two methods for samples tested in the second phase, with montmorillonite content are shown in Figures 7.56 and 7.57. The three points on the three curves are projected to produce the true three dimensional reflections which are shown in heavier black print.

Figure 7.56 is based on the results of tests conducted under 70, 140 and 210 kN/m^2 confining cell pressures. The results of the soil samples tested under 140 and 210 kN/m^2 confining

cell pressures are presented in Figure 7.57. Comparing Figures 7.56 and 7.57, samples tested under small confining cell pressures affect the overall performance. Figure 7.57 shows a concave resultant and a steeper rate of increase for samples containing between 10% and 20% montmorillonite than for those between 20% and 30%.

It is interesting to note that almost the same pattern has been established in Figures 7.55, for samples in the first phase, and in Figure 7.56 for samples in the second phase. However, more interesting is the comparison between Figures 7.55 and 7.57. Both of these Figures are plotted based on data from samples tested under high (140 and 210 kN/m^2) confining cell pressures. It can be seen that the resultant, on the former, is slightly convex whereas that on the latter is concave. The difference in the directions of the resultants is attributed to the type of testing. Figure 7.55 presents data for expansion only tests whereas samples presented in Figure 7.57 have undergone shear as well as expansion.

Despite the lack of a significant relationship between the volume changes measured by the micrometer and the Bishop water volume change indicator, for samples tested in the first phase, a pattern emerges when Figures 7.35, 7.39 and 7.51 are compared with Figure 7.53. There is a linear relationship between the volume changes, measured by the micrometer, and the montmorillonite content. In contrast, the water intake and volume change, measured by the Bishop water volume change indicator, are not linearly related to the montmorillonite content and liquid limit. The water

intake and volume change increase between samples containing 10% to 20% montmorillonite and continue non-linearly downward for samples containing 20% to 30% montmorillonite. However, when Figures 7.36, 7.40, 7.41 and 7.52 are compared with Figure 7.54, for samples tested in the second phase, a slightly different pattern emerges. They show that volume changes, measured by the micrometer, increase non-linearly with montmorillonite content and liquid limit. They also show that in all cases water intake and expansion, measured by the Bishop water volume change indicator, increased exponentially upward between 10% and 30% montmorillonite.

7.15 Hall Effect Local Displacement Transducer

In the second phase of the testing programme, it was necessary to set up another testing station (see Chapter Six, Section 6.9). This additional test station employed a conventional Bishop Wesley cell. This cell suffers from a similar problem, that is, a change in the volume of cell due to variation in cell pressures. To counteract this, a radial strain measuring device better known as the Hall Effect Local Displacement Transducer (see Chapter Six, Section 6.9.1) was used. This allows direct measurements to be made in order to determine expansion or otherwise of the samples and the magnitude of this change.

The data demonstrated in Figures 7.14 to 7.25 rely on the displacement of water in the cell to determine volume change. Apart from Figure 7.20, which shows fluctuating water movement from station No. 2, all others show a steady increase in the volumes of the samples as time of testing continues.

Figure 7.58 shows the volume of water, entering or leaving the Bishop Wesley cell, versus time. Normally, this Figure would have been used to determine the volume change of the samples. However, a closer examination of this Figure shows that this series of tests, in actual fact, took in a large volume of water. This intake of water by the cell could be representative of a case where the samples have decreased in volume and more water is needed to replace the newly created volume in the cell. In this study, however, the samples contain certain amounts of expansive lattices. This need for extra water therefore arises as a result of the cell itself increasing in volume, as testing continues, and creating the extra volume.

It was for this purpose that it was decided to employ a radial strain measuring device. The device, shown in Plates 6.6 and 6.7, is attached directly to the sample and indicates the changes in the diameter from which the overall volume change of the sample can be calculated. In contrast to Figures 7.14 to 7.22, Figure 7.23 has in fact been produced using the data from the Hall Effect rather than relying on the volume of water entering or leaving the cell.

7.16 Shear Strength of Unsaturated Soils

In the drained condition the pore fluid is allowed to enter or drain from the specimen to prevent any change of pore pressure during the shear process. It is common for a constant pore water back pressure to be maintained at a pre-determined rate of strain.

The shear strength at zero matrix suction is the strength due to the applied total stress. As the matrix suction is

increased, the shear strength increases to a peak value and then decreases to a fairly constant value. In a series of direct shear tests, on unsaturated fine sands and coarse silts, Donald (1956) found that as long as the specimens were saturated the strengths of the sands appeared to increase linearly with increasing confining pressure. When the sand was unsaturated, he found the rate of increase in strength decreased when the suction was increased beyond some limiting value.

Escario (1980) conducted a series of consolidated drained shear and triaxial tests on unsaturated Madrid gray clay. The tests were performed under controlled matrix suction conditions using the axis translation technique. A modified direct shear box, enclosed in a pressure chamber, was used to apply a controlled air pressure to the soil specimen. The specimen was placed on a high air entry disc in contact with water at atmospheric pressure. This arrangement is similar to the pressure plate system where the matrix suction is controlled by varying the pore air pressure while the pore water pressure is maintained constant. The results exhibited an increase in the shear strength as the matrix suction was increased.

A series of multistage triaxial tests on unsaturated, residual soils from Hong Kong was carried out by Ho and Fredlund (1982a). They were consolidated drained tests with the pore air and pore water back pressures controlled during shear. The assumption of an essentially planar failure surface was made by them in their analyses.

More recent experimental evidence using a higher range of matrix suction has shown some non-linearity in the failure envelope with respect to the matrix suction axis. Escario and Sáez (1986), for example, performed direct shear tests on three soils using a modified direct shear stress and matrix suction. The results exhibit curvature in the relationship between shear stress and matrix suction. Similarly, a re-analysis of the triaxial test results of Satija (1978) also revealed some non-linearity in the shear stress versus matrix suction failure envelope (Fredlund et al (1987)).

The shear strength of an unsaturated soil consists of an effective cohesion, C', and independent contributions from the net normal stress, $(\sigma - U_a)$, and a further contribution from the matrix suction, $(U_a - U_w)$. The mechanical behaviour of an unsaturated soil is affected differently by changes in net normal stress and changes in matrix suction (Jennings and Burland (1962)). The effective stress angle of internal friction, ϕ'', is associated with the shear strength contribution from the net normal stress state variable. Another angle, ϕ^b, is introduced (Fredlund (1979)) which is related to the shear strength contribution from the matrix suction stress state variable. For simplicity, in Section 7.16.1.1, ϕ_u and C_u are used to represent total angle of internal friction and total cohesion respectively. The effective stress angles of internal friction and effective stress cohesive intercepts, with respect to pore water $(\sigma - U_w)$, are represented by ϕ' and C' in Section 7.16.2.1. Similarly, ϕ'' and C'' are used to present the effective

stress angle of internal friction and effective stress cohesive intercept, with respect to pore air back pressure discussed in Section 7.16.2.2. Finally, ϕ^b and C^b are used to present values of effective stress angles of internal friction and effective stress cohesion with respect to matrix suction referred to in Section 7.16.2.3.

The rates of strain (mm/min) and time to failure (minutes) for samples, tested in the second phase of experimentation, containing 10%, 20% and 30% montmorillonite are presented in Tables 7.45 to 7.47 respectively. The maximum observed deviator stresses are also presented in these Tables.

The section headed "time to failure" includes three sub-headings; calc. (calculated), estim. (estimated), and actual. The figures under the sub-heading of calc. are those derived from the graphs of volume change versus square root of time. As the rate of strain and time to failure for unsaturated soils are not as certain and proven as those for saturated soils, the author has modified the rates in such a way to ensure that the tests are sufficiently slow to avoid any build up of pore water pressure. As evident from the Tables, the estimated times in some cases are almost twice as long as the calculated ones. In any case, none of the samples ran for the duration of the calculated or estimated times to failure. For ease of comparison, a column headed "actual" is also included. This is the actual time taken by the samples to reach shear failure.

As mentioned in Section 7.0, three different series of testing were undertaken in this phase. The first series comprised samples which were made and put into a saturation

phase with the appropriate confining cell pressures and pore water and pore air back pressures (see Tables 7.3 to 7.5). Once the samples had reached equilibrium, that is, when saturation had ceased and no further expansion was observed, the rate of deformation was calculated and the soil sample was then sheared. The second series comprised soil samples made with the same composition and sheared immediately after equipment assembly. The same values of confining cell pressure and pore air and pore water back pressures as in the previous series were used. In the third series, samples similar to the first two series were made and sheared as soon as the equipment was assembled but there were no pore air or pore water back pressures.

For compatibility and ease of comparison, the rate of strain used in the latter two cases were based on the former one. These are clearly shown in Tables 7.45 to 7.47.

7.16.1 Shear Failure Envelopes For Unsaturated Soils

The shear strength envelope is a measure of the ability of the soil to withstand applied shear stresses. The soil will fail when the applied shear stress exceeds the shear strength of the soil.

The shear failure envelopes for this study are presented, in four formats, in Figures 7.59 to 7.85. They are; total stress, effective stress using pore water back pressure, effective stress using pore air back pressure and effective stress using matrix suction. Each failure envelope is drawn using the Mohr circles relating to the three series of tests with 70, 140 and 210 kN/m^2 confining cell pressures. The Mohr circles are omitted for clarity. The soil samples

containing 10% and 20% montmorillonite were tested in two different stations.

The Mohr circles for an unsaturated soil are plotted in accordance with Fredlund's terminology. That is, the net normal stress axis, $(\sigma - U_a)$, is comparable to the effective stress axis, $(\sigma - U_w)$, for saturated soils. The location of the Mohr circle plot in the third dimension is a function of the matrix suction, $(U_a - U_w)$ (see Figure 4.6). In this presentation, however, the third axis has been omitted as the matrix suctions were maintained constant throughout the tests.

7.16.1.1 Total Stress

Figure 7.59 shows the failure envelopes of samples containing 10% montmorillonite, tested in stations No. 1 and 2, after the samples went through an initial saturation and expansion process. From the results the average total shear stress parameters ϕ_u and C_u, obtained from test stations No. 1 and 2, are 20.5° and 2.5 kN/m^2 respectively.

The second failure envelopes for samples containing 10% montmorillonite, tested in the two stations, are presented in Figure 7.60. In this series no saturation or expansion, prior to shear, was allowed. This new condition caused the average angle of internal friction to decrease from 20.5° to 16.5° whereas the average cohesive intercepts increased from 2.5 to 17.5 kN/m^2. This was expected because the soil had no opportunity to expand and draw in water prior to shear.

The third series of tests were those with no pore air or water back pressures nor a saturation or expansion phase prior to shear. This is illustrated in Figure 7.61. It is

evident that the Mohr circles fail to produce a unified failure envelope. In all probability the absence of back pressures has produced this variable set of Mohr circles resulting in a choice of three planar failure envelopes or a possible curved surface.

The presence of air in the soil samples generates soil suction which in turn produces cohesion. If a curved failure envelope is assumed it may pass through the origin which renders that supposition invalid. Two of the planar failure envelopes produce ϕ_u of 30° and 20°, and C_u of 20 and 45 kN/m^2 respectively whereas the third one produces values of 4° and 150 kN/m^2 respectively. If a certain trend, with the other two conditions (i.e. Figures 7.59 and 7.60), is to be maintained then it is more likely that the latter mentioned failure envelope would prevail.

The failure envelopes for samples with 20% montmorillonite content are plotted on Figures 7.62 to 7.64. The results shown in Figure 7.62 are for samples tested in stations No. 1 and 3 after an expansion phase had taken place. The average values of ϕ_u and C_u obtained from the results are 16.5° and 27.5 kN/m^2 respectively.

Figure 7.63 illustrates the resultant failure envelopes for samples tested, in stations No. 1 and 3, without any saturation or expansion prior to shear. The average values of internal friction angle and cohesion intercept obtained are 15° and 27.5 kN/m^2 respectively.

Figure 7.64 shows the failure envelope of samples, tested in station No. 4, with no pore air or water back pressures and where no saturation or expansion prior to shear was allowed.

Similar to the situation of samples containing 10% montmorillonite (Figure 7.61), two failure envelopes could be obtained from the presented Mohr circles. If the Mohr circle related to the sample tested under 210 kN/m^2 confining cell pressure is an underestimate, then an internal friction angle of 18° and a cohesive intercept of 37.5 kN/m^2 can be obtained. However, this does not follow the same trend as those in Figures 7.62 and 7.63. They show that as the amount of water entering the samples decreases, the cohesive intercept increases and the angle of internal friction decreases. If this pattern is to be repeated, it must be assumed that the sample tested under 140 kN/m^2, in Figure 7.64, is an overestimate. Once this disparity is adjusted the angle of internal friction reduces to 6.5° and the cohesive intercept increases to 65 kN/m^2.

The failure envelopes for samples containing 30% montmorillonite, tested in station No. 1, are presented in Figures 7.65 to 7.67. They illustrate the results of soil samples sheared in three different phases as defined in Section 7.16. They are; after expansion has been allowed, where no expansion prior to shear was allowed, and where no pore air or pore water back pressures nor prior saturation and expansion were allowed. Angles of internal friction of 15°, 14° and 4° for the three above-mentioned test series are recorded. Similarly, cohesive intercepts of 5, 20 and 90 kN/m^2, respectively, were obtained.

All the values of the cohesive intercepts and internal friction angles, based on total stress, for all test conditions and soil compositions are given in Table 7.48.

7.16.2 Pore Pressure Analysis

In a sealed unsaturated specimen the voids contain partly water and partly air. The air, U_a, and water, U_w, may increase in pressure as they compress. However, the water pressure is lower and may even be held negative as a result of the capillary suction of the water films in the small soil pores. The fluid pressures must be in equilibrium or there will be flow until this state is reached.

There are three series of effective failure envelopes for the shear strengths of unsaturated soils. They are: effective stress considering the pore water back pressure, effective stress considering the pore air back pressure and effective stress considering matrix suction.

7.16.2.1 Effective Stress Using Pore Water Back Pressure

The second series of failure envelopes, presented in Figures 7.68 to 7.73, are based on the values of effective stress using pore water back pressure. Figures 7.68 and 7.69 show the failure envelopes of samples containing 10% montmorillonite. Figure 7.68 shows the failure envelopes for samples sheared, after expansion had taken place, in stations No. 1 and 2. The average value of effective stress angle of internal friction, ϕ', is found to be 27° and an effective stress cohesive intercept, C', of zero is obtained for samples tested in both stations.

Similarly, Figure 7.69 shows the failure envelopes for samples sheared without prior expansion in stations No. 1 and 2. In this case, the average values of ϕ' and C', obtained from test stations No. 1 and 2 are 23° and 15 kN/m^2 respectively.

The failure envelopes for samples containing 20% montmorillonite are presented in Figures 7.70 and 7.71. Figure 7.70 shows the failure envelope for samples tested in stations No. 1 and 3 after a process of saturation and expansion. It produces an effective stress internal friction angle of 26° and an effective stress cohesive intercept of 10 kN/m^2, for samples tested in both stations.

The failure envelopes for samples sheared immediately after assembly, in stations No. 1 and 3, are presented in Figure 7.71. Average ϕ' = 22° and C' = 20 kN/m^2 can be obtained from these envelopes.

Figures 7.72 and 7.73 show the failure envelopes of samples with 30% montmorillonite tested in station No. 1. The samples undergoing saturation and expansion prior to shear produced an effective stress internal friction angle of 24° and an effective stress cohesive intercept of zero (see Figure 7.72). The effective cohesive intercept, for samples without expansion prior to shear (see Figure 7.73), increased to 10 kN/m^2 whereas the effective stress angle of internal friction decreased from 24° to 22°.

A summary of the values of ϕ' and C', considering pore water back pressure, for all three test conditions are given in Table 7.49.

7.16.2.2 Effective Stress Using Pore Air Back Pressure

The failure envelopes, based on the values of effective stress using pore air back pressure, are presented in Figures 7.74 to 7.79. Figure 7.74 shows the failure envelopes for samples containing 10% montmorillonite sheared, after saturation and expansion had taken place, in

test stations No. 1 and 2. An average value of ϕ'' = 38° was obtained whereas both test stations produced zero effective stress cohesive intercept.

Figure 7.75 presents the failure envelopes of samples containing 10% montmorillonite sheared without prior expansion in the two stations. In this case, the average ϕ'', obtained from stations No. 1 and 3, decreased to 32° whereas the average C'' increased to 20 kN/m^2.

The failure envelopes for samples containing 20% montmorillonite and tested in stations No. 1 and 3 are presented in Figures 7.76 and 7.77. Figure 7.76 shows the failure envelopes for samples after saturation and expansion had taken place. They indicate average ϕ'' and C'' of 31.5° and 20 kN/m^2 respectively. The failure envelopes for samples sheared immediately after assembly are presented in Figure 7.77. The average ϕ'' and C'' produced by the results are 30.5° and 25 kN/m^2 respectively.

The failure envelopes for samples containing 30% montmorillonite, tested in station No. 1, are presented in Figures 7.78 and 7.79. Figure 7.78 shows the failure enevlope for samples sheared after saturation and expansion had taken place. It produces ϕ'' and C'' of 31° kN/m^2 and zero respectively. The failure envelope for samples tested without prior saturation and expansion is illustrated in Figure 7.79. It results in an effective stress internal friction angle of 30° and effective stress cohesion of 10 kN/m^2. For ease of comparison the values of ϕ'' and C'', considering pore air back pressure, for all three test conditions are presented in Table 7.50.

7.16.2.3 Effective Stress Using Matrix Suction

The final set of failure envelopes, presented in Figures 7.80 to 7.85, are based on the values of matrix suction. Figure 7.80 shows the failure envelopes for samples containing 10% montmorillonite and sheared after initial saturation and expansion. Average values of 26° and 2.5 kN/m^2 for ϕ^b and C^b, respectively, are obtained for samples tested in stations No. 1 and 2.

The failure envelopes for samples containing 10% montmorillonite, where no prior saturation or expansion was allowed, are presented in Figure 7.81. They produce average ϕ^b and C^b of 22° and 22.5 kN/m^2, respectively, for samples tested in stations No. 1 and 2.

The failure envelopes for samples with 20% montmorillonite are presented in Figures 7.82 and 7.83. Figure 7.82 shows the failure envelopes for samples sheared after initial saturation and expansion. They show an average value of 23° as the effective stress angle of internal friction whereas an effective stress cohesive intercept of 20 kN/m^2 is found for samples tested in stations No. 1 and 3.

The failure envelopes for samples without prior saturation or expansion are presented in Figure 7.83. The average ϕ^b and C^b produced by the soil samples tested in stations No. 1 and 3 are 21.5° and 25 kN/m^2.

The failure envelopes of samples with 30% montmorillonite, tested in station No. 1, are presented in Figures 7.84 and 7.85. Figure 7.84 shows the failure envelope of samples sheared after initial saturation and expansion. It shows that values of ϕ^b = 23° and C^b = 0 are obtained. The failure

envelope for samples without prior saturation or expansion is presented in Figure 7.85. It produces an effective stress internal friction angle of 22° and an effective stress cohesive intercept of 10 kN/m^2.

The effective stress cohesive intercepts and effective stress internal friction angles, considering matrix suction, are shown in Table 7.51.

7.16.3 Discussion

The total stress across any interface through particle contact points in a soil mass is the sum of the pore water and pore air pressures in the soil's voids and the effective stress (which is equal to the summation of interparticle forces over a unit area).

The total stress and effective stress Mohr circles have the same radius, but are separated along the σ-axis by an amount equal to the pore pressures. Normally, shear stresses are not affected by pore pressures, that is, the values are identical whether expressed in terms of total stress or effective stress. The physical explanation for this is the inability of the pore water to resist shear, so that shear stresses are resisted entirely by contact forces between soil particles.

In a consolidated drained test the drainage valve is initially opened to allow the pore pressure to dissipate to zero, and is kept open while the specimen is taken to failure at a sufficiently slow rate to allow excess pore pressures to dissipate.

One of the ways in which a specimen, in the triaxial cell, may be taken to failure is axial compression. The specimen

can be compressed axially either by increasing the axial compressive stress or decreasing the radial stress (i.e. the cell pressure), or a combination of both.

The residual strength is usually considered to be of most significance in heavily overconsolidated clays, where a distinct failure plane or discontinuity is usually observed. Under large displacements, strong alignment of clay particles occur along the failure plane or within a thin failure zone.

For practical purposes failure envelopes are determined from a series of related tests. As far as possible three identical samples are obtained and tested at different cell pressures, giving three failure stress circles, and a failure envelope is drawn touching the three circles. Where three test specimens cannot be obtained, a multi-stage testing technique on one sample may be used (For example, Kenney and Watson (1961) and Parry and Nadarajah (1973) for saturated soils, and Nambiar et al (1985) and Gan and Fredlund (1988) for unsaturated soils).

In the consolidated drained tests it is basically easier to measure volume change than pore pressure, which can be greatly affected by small amounts of air in the soil voids or the measuring system. On the other hand, drained tests take longer to perform and provide only effective stress parameters.

For normally consolidated soil the envelope will usually be linear and pass through the origin. In the overconsolidated range the envelope will usually be essentially linear, but

deviating from the normally consolidated envelope to give a C' intercept.

When considering total stresses a clear pattern emerges. In all three compositions (10%, 20% and 30% montmorillonite) the angle of internal friction, ϕ_u, decreases as the test series change from saturation and expansion prior to shear to no saturation or expansion and no back pressure prior to shear.

Figures 7.59 to 7.61 show that ϕ_u decreases from 20.5° to 4° for samples containing 10% montmorillonite. Similarly, it decreases from 16.5° to 6.5° for samples containing 20% montmorillonite (see Figures 7.62 to 7.64). Figures 7.65 to 7.67 indicate that samples containing 30% montmorillonite show a decrease in the angle of internal friction from 15° to 4°. The effect of water (and/or air) on the cohesive intercepts is the reverse of that on the angle of internal friction. In other words, as the access to water is restricted the value of cohesion increases. The average values of cohesion intercept increased from; 2.5 to 150 kN/m^2, for samples containing 10% montmorillonite, from 27.5 to 65 kN/m^2, for samples with 20% montmorillonite, and from 5 to 90 kN/m^2, for samples with 30% montmorillonite. All these values are further summarised in Table 7.48 and described in detail in Section 7.16.1.1.

The effective stresses with respect to pore water back pressure ($\sigma - U_w$), illustrate the same trend. The effective stress angle of internal friction, ϕ', decrease as the access to water is restricted. They are 27° to 23° for samples containing 10% montmorillonite (Figures 7.68 and

7.69). The samples containing 20% montmorillonite (Figures 7.70 and 7.71) show a decrease in ϕ' from 26° to 22°. Those containing 30% montmorillonite (Figures 7.72 and 7.73) also show a reduction in the value of ϕ' from 24° to 22°. Conversely, the effective stress cohesive intercepts increase as access to water is restricted. They were from zero to 15 kN/m^2 for samples containing 10% montmorillonite, from 10 to 20 kN/m^2 for samples containing 20% montmorillonite and from zero to 10 kN/m^2 for samples containing 30% montmorillonite. These are discussed in detail in Section 7.16.2.1 and summarised in Table 7.49.

Similarly, the same trend occurs when evaluating the effective stresses based on the pore air back pressure ($\sigma - U_a$). It is evident, from Figures 7.74 to 7.79, that the effective stress cohesions increase as the soil samples have less access to water. They increase from zero to 20 kN/m^2 for samples containing 10% montmorillonite, from 20 to 25 kN/m^2 for those containing 20% montmorillonite and from zero to 10 kN/m^2 for samples containing 30% montmorillonite. These are summarised in Table 7.50 and further explained in Section 7.16.2.2. The effective stress internal friction angles decrease from 38° to 32° (10% montmorillonite), from 31.5° to 30.5° (20% montmorillonite) and from 31° to 30° (30% montmorillonite) as access to water is limited. The effective stress angles of internal friction, when considering effective stresses, may be attributed to the dilation of shear planes which merit further investigation. The values of the cohesive intecepts for these tests were also influenced by dilatancy. The water continued to be

drawn in by the soil samples during the shear process resulting in higher values of moisture content which is a further contributory factor in the dilation process.

The effective stresses with respect to matrix suction generally show a similar pattern to those with respect to pore water and pore air back pressures. The effective stress cohesive intercepts increase as access to water is restricted. They increase from 2.5 to 22.5 kN/m^2 for samples containing 10% montmorillonite (Figures 7.80 and 7.81), from 20 to 25 kN/m^2 for samples with 20% montmorillonite (Figures 7.82 and 7.83) and from zero to 10 kN/m^2 for samples containing 30% montmorillonite (Figure 7.84 and 7.85). A detailed discussion of these values is presented in Section 7.16.2.3 and a summary is given in Table 7.51. The effective stress internal friction angles decrease as access to water is restricted. The decreases were from 26° to 22°, from 23° to 21.5° and from 23° to 22° for samples containing 10%, 20% and 30% montmorillonite respectively.

The values of ϕ^b are found to be consistently less than ϕ'' with respect to pore air back pressures. This further emphasises the role that matrix suction plays in the behaviour of unsaturated soils. Therefore, it is not sufficient to determine values of ϕ'' alone in the case of unsaturated soils.

The values of ϕ^b are found to be higher than ϕ_u, with respect to total stresses, and ϕ' with respect to pore water back pressures. The following relationships were found to be generally applicable:

$$\phi'' > \phi' > \phi^b > \phi_u \qquad \text{and} \qquad C' < C'' \approx C^b < C_u$$

The values of effective stress angles of internal friction, with respect to pore air back pressure, are found to be higher than those with respect to pore water back pressure, matrix suction or the total stress. This is due to the fact that the magnitude of pore air back pressure is bigger than the pore water back pressure hence producing this great difference. As explained above it is not sufficient to evaluate the value of ϕ'' alone but ϕ^b should also be considered.

A significant point established from the tests is that the values of the angle of internal friction, whether total or effective, decreased as the amount of montmorillonite in the soil samples increased. This of course further indicates the affinity to water by montmorillonite. The bigger intake of water weakens the shearing resistance of soil samples. It is worth mentioning that the effective stress angles of internal friction obtained from the samples undergoing saturation and expansion prior to shear were generally greater than those sheared immediately after assembly. This is further indication that the soil samples after saturation and expansion are in a normally consolidated state, whereas those in the second series, where they were sheared immediately after assembly, appear to act as an overconsolidated clay due to the stress state.

7.17 Failure Geometry

In the second phase of testing, the shear strength of samples were also determined in addition to the swelling and shrinkage properties. The soil samples were sheared under three different conditions (see Section 7.0).

It is evident from the Plates 7.4 to 7.10 that the three possible modes of failure were obtained in the samples tested in this investigation. They are barrelling, single shear plane and cone failure.

A typical sample with a clear shear plane visible through the rubber membrane and a stripped sample can be seen in Plates 7.2 and 7.3 respectively.

7.17.1 Samples Containing 10% Montmorillonite

A total number of 15 samples containing 10% montmorillonite were tested in three stations; they were stations No. 1, 2 and 4. Plate 7.4 shows all the tested samples from which it can be seen that three samples failed with no shear plane forming. One of these samples was tested in station No. 2 without prior saturation or expansion. The other two were tested in station No. 4 where there were no back pressures or prior expansion.

The other samples generally failed with clear shear planes. However, three samples show conical failures. Two of these samples were sheared under 140 kN/m^2 confining cell pressure whereas the other one was under 210 kN/m^2 in station No. 2 (see Plates 7.9 and 7.10).

7.17.2 Samples Containing 20% Montmorillonite

Ten out of a total number of 13 samples containing 20% montmorillonite are shown in Plates 7.5 and 7.6. Most of the samples in this series failed with a barrel shape. Only five samples out of 13 show shear plane failures. It can be noted that all the plane failures occurred in samples sheared in station No. 3. Three samples failed after they had been

saturated and expanded whereas the other two samples were sheared in station No. 4 where there were no back pressures nor was there any prior expansion allowed.

7.17.3 Samples Containing 30% Montmorillonite

Six out of a total number of nine samples containing 30% montmorillonite are shown in Plates 7.7 and 7.8. Two samples tested in station No. 4, without any back pressure or prior expansion, show barrelling whereas the others failed with a clear shear plane. A conical failure can be seen in one of the soil samples sheared under 140 kN/m^2, after saturation and expansion had taken place (see Plates 7.9 and 7.10).

7.17.4 Conical Failure

Conical failure is rarely achieved in triaxial shear testing. Four samples failing in a conical manner, in this investigation, are shown in Plates 7.9 and 7.10. This mode of failure further supports the importance of a meticulous sample preparation technique. It indicates that the soil sample has been compacted in such a way that homogeneity along the length of the specimen has been achieved and sheared in an exact and controlled manner.

7.17.5 Shearing Without Confining or Back Pressures

A soil sample containing 30% montmorillonite was sheared in an unconfined compression mode where there were no cell fluid or cell pressure. A slow rate of strain of 0.0018 mm/min was adopted. The pore air and pore water back pressures had also been removed. Plates 7.11 and 7.12 show the formation of a clear shear plane for these test conditions.

Sample No.	Initial conditions (kN/m^2)					
	σ	U_a	U_w	$\sigma - U_a$	$\sigma - U_w$	$U_a - U_w$
CRS110	207	138	69	69	138	69
CRS810	207	138	69	69	138	69
CRS910	207	138	69	69	138	69
CRS1010	207	138	69	69	138	69
CRS1110	207	138	69	69	138	69
CRS1210	207	138	69	69	138	69
CRS620	207	138	69	69	138	69
CRS720	207	138	69	69	138	69
CRS230	207	138	69	69	138	69
CRS330	207	138	69	69	138	69
CRS430	207	138	69	69	138	69
CRS530	207	138	69	69	138	69
CRS1330	69	48.3	20.5	20.7	48.3	27.6
CRS1430	69	48.3	20.5	20.7	48.3	27.6

Table 7.1a

Sample No.	Final conditions (kN/m^2)					
	σ	U_a	U_w	$\sigma - U_a$	$\sigma - U_w$	$U_a - U_w$
CRS110	207	138	69	69	138	69
CRS810	172.5	138	103.5	34.5	69	34.5
	207	138	103.5	69	103.5	34.5
CRS910	207	138	69	69	138	69
CRS1010	207	138	69	69	138	69
CRS1110	172.5	138	103.5	34.5	69	34.5
CRS1210	172.5	138	103.5	34.5	69	34.5
	158.7	138	103.5	20.7	55.2	34.5
	138	138	138	0	0	0
CRS620	172.5	138	138	34.5	69	34.5
CRS720	172.5	138	138	34.5	69	34.5
CRS230	207	138	69	69	138	69
CRS330	207	138	69	69	138	69
CRS430	207	138	69	69	138	69
CRS530	207	138	69	69	138	69
CRS1330	51.8	48.3	48.3	3.45	3.45	0
CRS1430	69	48.3	41.4	20.7	27.6	6.9

Table 7.1b

Tables 7.1a and 7.1b Summary of stress changes for samples tested in the first phase.

Sample No.	Stress changes (kN/m^2)					
	σ	U_a	U_w	$\sigma - U_a$	$\sigma - U_w$	$U_a - U_w$
CRS110	0	0	0	0	0	0
CRS810	-34.5	0	34.5	34.5	69	34.5
	0	0	34.5	0	34.5	34.5
CRS910	0	0	0	0	0	0
CRS1010	0	0	0	0	0	0
CRS1110	-34.5	0	34.5	34.5	69	34.5
CRS1210	-34.5	0	34.5	34.5	69	34.5
	-48.3	0	34.5	48.3	82.8	34.5
	-69	0	69	69	138	69
CRS620	-34.5	0	34.5	34.5	69	34.5
CRS720	-34.5	0	34.5	34.5	69	34.5
CRS230	0	0	0	0	0	0
CRS330	0	0	0	0	0	0
CRS430	0	0	0	0	0	0
CRS530	0	0	0	0	0	0
CRS1330	-17.25	0	27.6	17.25	44.85	27.6
CRS1430	0	0	20.7	0	20.7	20.7

Table 7.2 Stress changes between the initial and final test conditions in the first phase.

Sample No.	Stress conditions (kN/m^2)					
	σ	U_a	U_w	$\sigma - U_a$	$\sigma - U_w$	$U_a - U_w$
CRS1110	70.00	49.00	21.00	21.00	49.00	28.00
CRS1210	70.00	49.00	21.00	21.00	49.00	28.00
W2FS1310	70.00	00.00	00.00	70.00	70.00	00.00
CRS2110	210.00	140.00	70.00	70.00	140.00	70.00
CRS2210	210.00	140.00	70.00	70.00	140.00	70.00
W2FS2310	210.00	00.00	00.00	210.00	210.00	00.00
CRS3110	140.00	98.00	42.00	42.00	98.00	56.00
CRS3210	140.00	98.00	42.00	42.00	98.00	56.00
W2FS3310	140.00	00.00	00.00	140.00	140.00	00.00
WFS1110	70.00	49.00	21.00	21.00	49.00	28.00
WFS1210	70.00	49.00	21.00	21.00	49.00	28.00
WFS2110	210.00	140.00	70.00	70.00	140.00	70.00
WFS2210	210.00	140.00	70.00	70.00	140.00	70.00
WFS3110	140.00	98.00	42.00	42.00	98.00	56.00
WFS3210	140.00	98.00	42.00	42.00	98.00	56.00

Table 7.3 Stress conditions for samples containing 10% montmorillonite tested in the second phase.

Sample No.	Stress conditions (kN/m^2)					
	σ	U_a	U_w	$\sigma - U_a$	$\sigma - U_w$	$U_a - U_w$
CRS1120	210.00	140.00	70.00	70.00	140.00	70.00
CRS1220	210.00	140.00	70.00	70.00	140.00	70.00
W2FS1320	210.00	00.00	00.00	210.00	210.00	00.00
CRS2120	140.00	98.00	42.00	42.00	98.00	56.00
CRS2220	140.00	98.00	42.00	42.00	98.00	56.00
OldGDSS120	70.00	00.00	62.00	70.00	8.00	-62.00
GDSS1120	70.00	49.00	21.00	21.00	49.00	28.00
GDSS1220	70.00	49.00	21.00	21.00	49.00	28.00
W2FS1G320	70.00	00.00	00.00	70.00	70.00	00.00
GDSS2120	140.00	98.00	42.00	42.00	98.00	56.00
GDSS2220	140.00	98.00	42.00	42.00	98.00	56.00
W2FS2320	140.00	00.00	00.00	140.00	140.00	00.00
GDSS3120	210.00	140.00	70.00	70.00	140.00	70.00
GDSS3220	210.00	140.00	70.00	70.00	140.00	70.00

Table 7.4 Stress conditions for samples containing 20% montmorillonite tested in the second phase.

Sample No.	Stress conditions (kN/m^2)					
	σ	U_a	U_w	$\sigma - U_a$	$\sigma - U_w$	$U_a - U_w$
CRS1130	68.95	48.26	20.69	20.69	48.26	27.57
CRS1230	68.95	48.26	20.69	20.69	48.26	27.57
W2FS1330	68.95	00.00	00.00	68.95	68.95	00.00
CRS2130	210.00	140.00	70.00	70.00	140.00	70.00
CRS2230	210.00	140.00	70.00	70.00	140.00	70.00
CRS1(2)330	210.00	00.00	00.00	210.00	210.00	00.00
CRS3130	140.00	98.00	42.00	42.00	98.00	56.00
CRS3230	140.00	98.00	42.00	42.00	98.00	56.00
W2FS3330	140.00	00.00	00.00	140.00	140.00	00.00

Table 7.5 Stress conditions for samples containing 30% montmorillonite tested in the second phase.

Sample No.	Moisture contents (%)					Time (Days)
	Top	Middle	Bottom	Average	Filter paper	
CRS110	51.10	52.20	55.40	52.90	-	59
CRS810	34.92	35.84	35.70	35.49	43.75	43
CRS910	33.47	33.79	34.41	33.89	26.47	13
CRS1010	35.64	37.23	37.85	36.91	41.18	6
CRS1110	41.77	43.05	42.39	42.40	51.50	47
CRS1210	41.39	41.63	40.34	41.12	32.35	34
CRS620	38.69	40.13	39.98	39.60	-	34
CRS720	38.45	40.03	40.15	39.54	-	40
CRS230	51.02	53.71	71.48	58.73	-	4
CRS330	67.24	74.57	95.29	79.03	-	6
CRS430	64.85	52.31	46.13	54.43	-	41
CRS530	39.97	40.95	43.27	41.40	-	59
CRS1330	48.85	51.51	54.89	51.75	25.71	20
CRS1430	56.86	59.67	58.07	58.20	64.00	61

Table 7.6 Final moisture contents (%) of the soil samples tested in the first phase.

Sample No.	Moisture contents (%)				Time (Days)
	Top	Bottom	Average	Filter paper	
CRS1110	37.15	39.71	38.43	41.17	25
CRS1210	38.72	39.59	39.16	34.28	2
W2FS1310	-	-	31.61	-	2
CRS2110	35.55	36.34	35.95	39.39	14
CRS2210	-	-	35.44	38.89	3
W2FS2310	31.39	31.51	31.45	-	2
CRS3110	35.77	36.15	35.96	47.06	17
CRS3210	36.35	36.52	36.44	34.21	5
W2FS3310	-	-	30.21	-	3
WFS1110	40.56	40.78	40.68	60.60	25
WFS1210	-	-	35.99	33.33	1
WFS2110	32.46	32.71	32.59	30.56	17
WFS2210	34.54	34.65	34.60	36.36	3
WFS3110	33.53	33.68	33.61	34.28	23
WFS3210	34.98	35.79	35.39	30.30	1

Table 7.7 Final moisture contents (%) of the soil samples containing 10% montmorillonite tested in the second phase.

Sample No.	Moisture contents (%)				Time (Days)
	Top	Bottom	Average	Filter paper	
CRS1120	-	-	36.04	44.10	16
CRS1220	-	-	37.58	70.00	7
W2FS1320	-	-	35.04	-	7
CRS2120	-	-	38.26	35.29	15
CRS2220	-	-	37.10	21.21	3
OldGDSS120	62.52	62.52	62.52	-	61
GDSS1120	42.07	42.12	42.09	40.54	17
GDSS1220	38.37	41.17	39.77	34.21	5
W2FS1G320	-	-	34.31	-	2
GDSS2120	35.78	36.19	35.99	57.57	27
GDSS2220	35.37	36.24	35.81	34.28	2
W2FS2320	-	-	33.74	-	2
GDSS3120	40.04	40.71	40.38	46.43	24
GDSS3220	-	-	37.82	33.33	2

Table 7.8 Final moisture contents (%) of the soil samples containing 20% montmorillonite tested in the second phase.

Sample No.	Moisture contents (%)				Time (Days)
	Top	Bottom	Average	Filter paper	
CRS1130	52.10	55.63	53.86	-	32
CRS1230	52.43	55.86	54.14	42.86	9
W2FS1330	-	-	36.16	-	3
CRS2130	43.45	45.03	44.24	-	36
CRS2230	41.37	44.65	43.01	54.28	6
CRS1(2)330	-	-	37.46	41.38	7
CRS3130	43.89	46.65	45.27	29.41	24
CRS3230	43.07	46.21	44.64	38.23	6
W2FS3330	-	-	36.86	-	7

Table 7.9 Final moisture contents (%) of the soil samples containing 30% montmorillonite tested in the second phase.

Sample No.	Radial expansion (%)				Axial expan. (%) (Ht)	Av/Ht	Time (Days)
	Top	Middle	Bottom	Average (Av)			
CRS110	8.29	12.10	13.42	11.27	3.03	3.72	59
CRS810	0.52	1.84	0.79	1.05	0.98	1.07	43
CRS910	0	0.26	0.66	0.31	1.17	0.26	13
CRS1010	0.66	1.84	1.32	1.27	0.49	2.59	6
CRS1110	1.05	4.89	6.45	4.13	1.86	2.2	47
CRS1210	2.68	3.6	1.58	2.62	3.13	0.84	34
CRS620	1.84	2.89	0.52	1.75	3.1	0.56	34
CRS720	0.79	2.76	1.32	1.63	1.57	1.04	40
CRS230	19.92	12.10	10.79	14.27	2.62	5.44	4
CRS330	29.39	18.42	11.76	19.85	4.59	4.32	6
CRS430	2.10	8.16	16.05	8.77	3.18	2.76	41
CRS530	2.37	2.89	3.16	2.79	3.02	0.92	59
CRS1330	3.68	9.47	6.84	6.66	1.75	3.08	20
CRS1430	7.36	13.29	7.63	9.43	1.16	8.13	61

Table 7.10 Free radial and axial expansion of the soil samples tested in the first phase.

Sample No.	Radial expansion (%)				Height (mm) Ht	Av/Ht	Time (Days)
	Top	Middle	Bottom	Average			
CRS1110	13.29	20.13	5.92	13.71	41.40	1.04	25
CRS1210	7.63	14.21	5.39	9.08	45.50	0.91	2
W2FS1310	0.39	7.84	2.89	3.71	46.50	0.85	2
CRS2110	7.37	13.68	7.24	9.43	44.00	0.94	14
CRS2210	22.84	25.79	7.63	18.75	38.60	1.17	3
W2FS2310	4.61	12.76	4.61	7.33	41.95	0.97	2
CRS3110	7.11	13.82	3.82	8.25	44.40	0.93	17
CRS3210	5.26	10.53	2.37	6.05	45.50	0.88	5
W2FS3310	2.24	9.03	1.45	4.24	44.50	0.89	3
WFS1110	6.58	13.42	3.68	7.89	48.10	0.85	25
WFS1210	1.05	7.11	2.63	3.61	49.30	0.80	1
WFS2110	4.47	10.13	2.11	5.58	44.80	0.90	17
WFS2210	6.05	9.87	1.32	5.74	46.60	0.86	3
WFS3110	4.21	10.61	2.89	3.61	49.30	0.80	23
WFS3210	7.89	9.21	1.32	6.13	46.80	0.86	1

Table 7.11 Free radial and axial expansion of the soil samples containing 10% montmorillonite tested in the second phase.

Sample No.	Radial expansion (%)				Height (mm) Ht	Av/Ht	Time (Days)
	Top	Middle	Bottom	Average			
CRS1120	8.95	16.05	5.26	10.08	43.30	0.97	16
CRS1220	7.37	11.58	5.53	8.16	45.00	0.91	7
W2FS1320	1.71	8.55	3.95	4.74	44.80	0.89	7
CRS2120	5.92	13.82	5.53	8.42	43.60	0.94	15
CRS2220	2.76	12.63	4.61	6.66	44.75	0.91	3
OldGDSS120	-	-	-	-	-	-	61
GDSS1120	13.16	12.37	6.71	10.74	48.25	0.87	17
GDSS1220	10.05	13.74	11.84	11.87	45.50	0.93	5
W2FS1G320	1.32	10.53	7.37	6.39	45.40	0.89	2
GDSS2120	13.16	18.42	11.84	14.47	41.60	1.04	27
GDSS2220	6.18	10.21	6.18	7.53	44.00	0.93	2
W2FS2320	0.21	5.92	2.63	2.92	47.50	0.82	2
GDSS3120	8.55	10.53	5.66	8.24	45.00	0.91	24
GDSS3220	4.74	10.79	6.97	7.50	44.40	0.92	2

Table 7.12 Free radial and axial expansion of the soil samples containing 20% montmorillonite tested in the second phase.

Sample No.	Radial expansion (%)				Height (mm) Ht	Av/Ht	Time (Days)
	Top	Middle	Bottom	Average			
CRS1130	11.05	17.11	10.79	12.97	46.00	0.93	32
CRS1230	9.21	17.11	10.53	12.29	45.50	0.94	9
W2FS1330	0.00	2.63	6.58	3.08	49.00	0.80	3
CRS2130	6.05	11.84	8.95	8.95	45.00	0.92	36
CRS2230	-	-	-	-	-	-	6
CRS1(2)330	7.37	15.26	11.18	11.26	43.50	0.97	7
CRS3130	9.21	14.47	6.58	10.08	44.00	0.95	24
CRS3230	4.21	11.84	6.84	7.63	48.50	0.84	6
W2FS3330	0.00	7.89	5.53	4.47	45.00	0.88	7

Table 7.13 Free radial and axial expansion of the soil samples containing 30% montmorillonite tested in the second phase.

Sample No.	Water intake (ml)	Expansion (ml)	Water intake / Expansion	Expansion / Water intake
CRS810	0.48	0.45	1.067	0.938
CRS910	0.37	0.25	1.480	0.676
CRS1010	1.82	0.10	18.200	0.055
CRS1110	1.99	0.35	5.686	0.176
Comp.off	1.37	0.65	2.108	0.474
CRS1210	2.07	0.60	3.450	0.289
CRS620	3.31	0.62	3.123	0.187
CRS720	2.46	0.75	3.280	0.305
CRS430	3.78	0.60	6.300	0.159
CRS530	2.95	0.90	3.278	0.305
CRS1330	12.33	0.40	30.825	0.032
CRS1430	18.24	0.90	20.267	0.049
Comp.off	18.44	1.01	18.257	0.055

Table 7.14 Water intake (ml) and expansion (ml) of the samples measured by the Bishop water volume change indicators in the first phase.

Sample No.	Water intake (ml)	Expansion (ml)	Water intake / Expansion	Expansion / Water intake
CRS1110	2.20	1.25	1.760	0.568
CRS1210	2.00	1.80	1.111	0.900
CRS2110	1.10	0.70	1.571	0.636
CRS2210	9.90	8.90	1.112	0.899
CRS3110	1.20	0.40	3.000	0.333
CRS3210	1.10	1.70	0.647	1.545
WFS1110	7.00	3.30	2.121	0.471
WFS1210	5.30	3.80	1.395	0.717
WFS2110	2.60	5.40	0.481	2.077
WFS2210	3.80	0.80	4.750	0.211
WFS3110	8.10	2.90	2.793	0.358
WFS3210	4.80	1.80	2.667	0.375

Table 7.15 Water intake (ml) and expansion (ml) of samples, containing 10% montmorillonite, measured by the Bishop water volume change indicators in the second phase.

Sample No.	Water intake (ml)	Expansion (ml)	Water intake / Expansion	Expansion / Water intake
CRS1120	1.95	0.50	3.900	0.256
CRS1220	0.70	1.50	0.467	2.143
CRS2120	1.45	0.75	1.933	0.517
CRS2220	4.10	2.60	1.577	0.634
GDSS1120	1.70	4.20	0.405	2.471
GDSS1220	4.45	4.10	1.085	0.921
GDSS2120	4.60	2.85	1.614	0.620
GDSS2220	2.50	6.05	0.413	2.420
GDSS3120	5.40	3.10	1.742	0.574
GDSS3220	5.35	5.65	0.947	1.056

Table 7.16 Water intake (ml) and expansion (ml) of samples, containing 20% montmorillonite, measured by the Bishop water volume change indicators in the second phase.

Sample No.	Water intake (ml)	Expansion (ml)	Water intake / Expansion	Expansion / Water intake
CRS1130	14.70	7.80	1.885	0.531
CRS1230	10.20	10.45	0.976	1.025
CRS2130	6.80	2.00	3.400	0.294
CRS2230	2.80	3.75	0.747	1.339
CRS3130	5.30	2.15	2.465	0.406
CRS3230	3.70	4.20	0.881	1.135

Table 7.17 Water intake (ml) and expansion (ml) of samples, containing 30% montmorillonite, measured by the Bishop water volume change indicators in the second phase.

Sample No.	Load (N)					
	1 hr	20 hrs	50 hrs	100 hrs	500 hrs	1000 hrs
CRS810	32.5	41.5	41.5	42.5	50.5	30.5
CRS910	26.5	37.5	38.5	38.5	-	-
CRS1010	10.5	34.5	37.5	17.5	-	-
CRS1110	16.5	44.5	46.5	49.5	56.5	25.5
CRS1210	7.5	19.5	22.5	32.5	54.5	56.5
CRS620	13.5	49.5	50.5	49.5	55.5	-
CRS720	24.5	48.5	48.5	33.5	43.5	45.5
CRS230	5.5	16.5	13.5	20.5	-	-
CRS430	11.5	59.5	63.5	63.5	54.5	-
CRS530	7.5	37.5	43.5	43.5	43.5	49.5
CRS1330	30.5	55.5	46.5	41.5	46.5	-
CRS1430	21.5	34.5	24.5	17.5	20.5	21.5

Table 7.18 Axial load reading recorded by the load cell in the first phase.

Sample No.	Swell pressure (kN/m^2)					
	1 hr	20 hrs	50 hrs	100 hrs	500 hrs	1000 hrs
CRS810	28.656	36.286	36.229	36.831	43.401	25.875
CRS910	23.366	32.926	33.698	33.504	-	-
CRS1010	9.258	30.420	32.995	15.301	-	-
CRS1110	14.548	39.073	40.743	43.258	48.482	21.478
CRS1210	6.613	17.050	19.632	28.165	45.692	46.934
CRS620	11.903	43.326	43.902	42.764	47.036	-
CRS720	21.602	42.207	42.031	28.791	36.866	37.643
CRS430	10.140	51.780	55.030	55.002	46.766	-
CRS530	6.613	32.926	38.035	37.856	37.057	41.458
CRS1330	26.893	48.552	40.658	35.965	39.613	-
CRS1430	18.957	30.118	21.210	15.001	17.169	17.643

Table 7.19 Equivalent swell pressures (kN/m^2) recorded by the load cell in the modified triaxial cell in the first phase.

Sample No.	Swell pressure (kN/m^2)					
	1 hr	20 hrs	50 hrs	100 hrs	500 hrs	1000 hrs
CRS810	235.506	243.136	243.079	243.681	250.251	232.725
CRS910	230.216	239.776	240.548	240.354	-	-
CRS1010	216.108	237.270	239.845	222.169	-	-
CRS1110	221.398	245.923	247.593	250.108	255.332	193.853
CRS1210	213.463	223.900	226.482	235.015	252.542	219.309
CRS620	218.753	250.176	250.752	249.614	253.886	-
CRS720	228.452	249.057	248.881	235.641	243.716	210.018
CRS430	216.990	258.630	261.880	261.852	253.616	-
CRS530	213.463	239.776	244.885	244.706	243.907	248.308
CRS1330	95.843	117.502	109.608	104.915	91.326	-
CRS1430	87.907	99.068	90.160	83.951	86.119	86.593

Table 7.20 Development of total axial swell pressure in the first phase.

Sample No.	Final ht. (mm)	Initial height (mm)	Final dia. (mm)	Initial volume x 10^{-5} m^3	Final volume x 10^{-5} m^3	Volume change (%)
CRS110	52.70	51.15	42.283	5.801	7.400	27.564
CRS810	51.50	51.00	38.400	5.784	5.964	3.112
CRS910	51.70	51.10	38.116	5.795	5.899	1.795
CRS1010	51.45	51.20	38.483	5.806	5.984	3.066
CRS1110	51.95	51.00	39.566	5.784	6.387	10.425
CRS1210	52.60	51.00	39.140	5.784	6.328	9.405
CRS620	53.00	51.40	38.666	5.829	6.223	6.759
CRS720	51.80	51.00	38.616	5.784	6.066	4.875
CRS230	52.50	51.45	43.423	5.835	7.775	33.247
CRS330	53.50	51.15	45.546	5.801	8.716	50.250
CRS430	52.85	51.22	41.333	5.809	7.091	22.069
CRS530	52.80	51.25	39.066	5.812	6.329	8.895
CRS1330	52.40	51.50	40.533	5.841	6.761	15.751
CRS1430	52.10	51.50	41.583	5.841	7.075	21.126

Table 7.21 Percentage volume change of the samples by physical measurement using a micrometer in the first phase.

Sample No.	Final ht. (mm)	Initial height (mm)	Final dia. (mm)	Initial volume x 10^{-5} m^3	Final volume x 10^{-3} m^3	Volume change (%)
CRS1110	41.40	51.15	42.98	5.801	6.006	+ 3.53
CRS1210	45.50	51.35	41.45	5.824	6.140	+ 5.43
W2FS1310	46.50	51.00	39.41	5.784	5.672	- 1.94
CRS2110	44.00	51.00	41.58	5.784	5.975	+ 3.30
CRS2210	38.60	50.90	45.13	5.773	6.175	+ 6.96
W2FS2310	41.95	51.15	40.78	5.801	5.479	- 5.55
CRS3110	44.40	51.00	41.13	5.784	5.899	+ 1.99
CRS3210	45.50	51.05	40.30	5.790	5.804	+ 0.24
W2FS3310	44.50	50.80	39.61	5.761	5.484	- 4.81
WFS1110	48.10	51.15	41.00	5.801	6.350	+ 9.46
WFS1210	49.30	51.05	39.37	5.790	6.002	+ 3.66
WFS2110	44.80	50.80	40.12	5.761	5.664	- 1.68
WFS2210	46.60	51.35	40.18	5.824	5.909	+ 1.46
WFS3110	45.30	50.70	40.24	5.750	5.761	+ 0.19
WFS3210	46.80	51.10	40.33	5.795	5.978	+ 3.16

Table 7.22 Percentage volume change of samples containing 10% montmorillonite by physical measurement using a micrometer in the second phase.

Sample No.	Final ht. (mm)	Initial height (mm)	Final dia. (mm)	Initial volume x 10^{-5} m^3	Final volume x 10^{-5} m^3	Volume change (%)
CRS1120	43.30	51.00	41.83	5.784	5.951	+ 2.89
CRS1220	45.00	51.00	41.10	5.784	5.970	+ 3.22
W2FS1320	44.80	51.00	39.80	5.784	5.574	- 3.63
CRS2120	43.60	51.00	41.20	5.784	5.813	+ 0.50
CRS2220	44.75	51.15	40.53	5.801	5.773	- 0.48
OldGDSS120	-	51.50	-	5.841	-	-
GDSS1120	48.25	51.05	42.08	5.790	6.710	+15.89
GDSS1220	45.50	51.00	42.51	5.784	6.458	+11.65
W2FS1G320	45.40	51.00	40.43	5.784	5.828	+ 0.76
GDSS2120	41.60	51.00	43.50	5.784	5.742	- 0.73
GDSS2220	44.00	51.00	40.86	5.784	5.770	- 0.24
W2FS2320	47.50	51.05	39.11	5.790	5.706	- 1.45
GDSS3120	45.00	51.00	41.13	5.784	5.979	+ 3.37
GDSS3220	44.40	51.40	40.85	5.829	5.819	- 0.17

Table 7.23 Percentage volume change of samples containing 20% montmorillonite by physical measurement using a micrometer in the second phase.

Sample No.	Final ht. (mm)	Initial height (mm)	Final dia. (mm)	Initial volume x 10^{-5} m^3	Final volume x 10^{-5} m^3	Volume change (%)
CRS1130	46.00	51.00	42.93	5.784	6.658	+15.11
CRS1230	45.50	51.40	42.67	5.829	6.506	+11.61
W2FS1330	49.00	51.00	39.17	5.784	5.905	+ 2.09
CRS2130	45.00	51.50	41.40	5.841	6.058	+ 3.72
CRS2230	-	51.00	-	5.784	-	-
CRS1(2)330	43.50	51.05	42.28	5.789	6.107	+ 5.49
CRS3130	44.00	50.90	41.83	5.773	6.047	+ 4.75
CRS3230	48.50	51.50	40.90	5.841	6.372	+ 9.09
W2FS3330	45.00	51.00	39.70	5.784	5.570	- 3.70

Table 7.24 Percentage volume change of samples containing 30% montmorillonite by physical measurement using a micrometer in the second phase.

Sample No.	Initial volumes (x 10^4 mm^3)				Void ratio (e)	Dry density (kg/m^3)	Sr (%)
	Total	Solid	Air	Water			
CRS110	5.801	2.982	0.414	2.405	0.945	1397.06	85.31
CRS810	5.784	2.982	0.397	2.405	0.940	1397.06	85.85
CRS910	5.795	2.982	0.408	2.405	0.943	1397.06	85.50
CRS1010	5.806	2.982	0.419	2.405	0.947	1397.06	85.16
CRS1110	5.784	2.982	0.397	2.405	0.940	1397.06	85.85
CRS1210	5.784	2.982	0.397	2.405	0.940	1397.06	85.85
CRS620	5.829	2.982	0.442	2.405	0.955	1395.01	84.47
CRS720	5.784	2.982	0.397	2.405	0.940	1395.01	85.85
CRS230	5.835	2.986	0.448	2.401	0.954	1395.01	84.28
CRS330	5.801	2.986	0.414	2.401	0.943	1395.01	84.29
CRS430	5.809	2.986	0.422	2.401	0.945	1395.01	85.05
CRS530	5.812	2.986	0.425	2.401	0.946	1395.01	84.96
CRS1330	5.841	2.986	0.454	2.401	0.956	1395.01	84.10
CRS1430	5.841	2.986	0.454	2.401	0.956	1395.01	84.10

Table 7.25 Total, solid, air and water volumes (mm^3), void ratio, dry density (kg/m^3) and degree of saturation (%) at the start of each test for samples tested in the first phase.

Sample No.	Initial volumes (x 10^4 mm^3)				Void ratio (e)	Dry density (kg/m^3)	Sr (%)
	Total	Solid	Air	Water			
CRS1110	5.801	2.982	0.414	2.405	0.945	1397.06	85.31
CRS1210	5.824	2.982	0.437	2.405	0.953	1397.06	84.62
W2FS1310	5.784	2.982	0.397	2.405	0.940	1397.06	85.83
CRS2110	5.784	2.982	0.397	2.405	0.940	1397.06	85.83
CRS2210	5.773	2.982	0.386	2.405	0.936	1397.06	86.17
W2FS2310	5.801	2.982	0.414	2.405	0.945	1397.06	85.31
CRS1310	5.784	2.982	0.397	2.405	0.940	1397.06	85.83
CRS3210	5.790	2.982	0.403	2.405	0.942	1397.06	85.65
W2FS3310	5.761	2.982	0.374	2.405	0.932	1397.06	86.54
WFS1110	5.801	2.982	0.414	2.405	0.945	1397.06	85.31
WFS1210	5.790	2.982	0.403	2.405	0.942	1397.06	85.65
WFS2110	5.761	2.982	0.374	2.405	0.932	1397.06	86.54
WFS2210	5.824	2.982	0.437	2.405	0.953	1397.06	84.62
WFS3110	5.750	2.982	0.363	2.405	0.928	1397.06	86.89
WFS3210	5.795	2.982	0.408	2.405	0.943	1397.06	85.50

Table 7.26 Total, solid, air and water volumes (mm^3), void ratio, dry density (kg/m^3) and degree of saturation (%) at the start of each test for samples containing 10% montmorillonite tested in the second phase.

Sample No.	Initial volumes (x 10^4 mm^3)				Void ratio (e)	Dry density (kg/m^3)	Sr (%)
	Total	Solid	Air	Water			
CRS1120	5.784	2.982	0.397	2.405	0.940	1395.01	85.83
CRS1220	5.784	2.982	0.397	2.405	0.940	1395.01	85.83
W2FS1320	5.784	2.982	0.397	2.405	0.940	1395.01	85.83
CRS2120	5.784	2.982	0.397	2.405	0.940	1395.01	85.83
CRS2220	5.801	2.982	0.414	2.405	0.945	1395.01	85.31
OldGDSS120	5.841	2.982	0.454	2.405	0.959	1395.01	84.12
GDSS1120	5.790	2.982	0.403	2.405	0.942	1395.01	85.65
GDSS1220	5.784	2.982	0.397	2.405	0.940	1395.01	85.83
W2FS1G320	5.784	2.982	0.397	2.405	0.940	1395.01	85.83
GDSS2120	5.784	2.982	0.397	2.405	0.940	1395.01	85.83
GDSS2220	5.784	2.982	0.397	2.405	0.940	1395.01	85.83
W2FS2320	5.700	2.982	0.313	2.405	0.911	1395.01	88.48
GDSS3120	5.784	2.982	0.397	2.405	0.940	1395.01	85.83
GDSS3220	5.829	2.982	0.442	2.405	0.955	1395.01	84.47

Table 7.27 Total, solid, air and water volumes (mm^3), void ratio, dry density (kg/m^3) and degree of saturation (%) at the start of each test for samples containing 20% montmorillonite tested in the second phase.

Sample No.	Initial volumes (x 10^4 mm^3)				Void ratio (e)	Dry density (kg/m^3)	Sr (%)
	Total	Solid	Air	Water			
CRS1130	5.784	2.986	0.397	2.401	0.937	1395.01	85.81
CRS1230	5.829	2.986	0.442	2.401	0.952	1395.01	84.45
W2FS1330	5.784	2.986	0.397	2.401	0.937	1395.01	85.81
CRS2130	5.841	2.986	0.454	2.401	0.956	1395.01	84.10
CRS2230	5.784	2.986	0.397	2.401	0.937	1395.01	85.81
CRS1(2)330	5.789	2.986	0.402	2.401	0.939	1395.01	85.66
CRS3130	5.773	2.986	0.386	2.401	0.933	1395.01	86.15
CRS3230	5.841	2.986	0.454	2.401	0.956	1395.01	84.10
W2FS3330	5.784	2.986	0.397	2.401	0.937	1395.01	85.81

Table 7.28 Total, Solid, air and water volumes (mm^3), void ratio, dry density (kg/m^3) and degree of saturation (%) at the start of each test for samples containing 30% montmorillonite tested in the second phase.

Sample No.	Final volumes (cc)						
	Total	Solid	Gross water	Filter paper	Diffused air	Net water	Air
CRS810	58.29	29.82	26.81	0.14	2.14	24.53	3.94
CRS910	58.20	29.82	25.05	0.09	0.54	24.42	3.96
CRS1010	58.16	29.82	26.17	0.14	0.16	25.87	2.47
CRS1110 Comp.off	58.19 58.49	29.82	27.50 27.96	0.17	1.29 2.37	26.04 25.42	2.33 3.25
CRS1210	58.44	29.82	27.40	0.11	1.17	26.12	2.50
CRS620	58.91	29.82	29.10	-	1.74	27.36	1.73
CRS720	58.59	29.82	28.45	-	1.94	26.51	2.26
CRS430	58.69	29.86	28.86	-	1.07	27.79	1.04
CRS530	59.02	29.86	28.85	-	1.89	26.96	2.20
CRS1330	58.81	29.86	36.71	0.09	0.28	36.34	- 7.39
CRS1430 Comp.off	59.31 59.42	29.86	43.41 43.81	0.16	1.00 1.20	42.25 42.45	-12.80 -12.89

Table 7.29 Total, solid, gross water, water in filter paper, diffused air, net water and air volumes at the end of each test measured by the Bishop water volume change indicator for samples tested in the first phase.

Sample No.	Final volumes (cc)						
	Total	Solid	Gross water	Filter paper	Diffused air	Net water	Air
CRS1110	59.26	29.82	26.25	0.14	0.50	25.61	3.83
CRS1210	60.04	29.82	26.05	0.12	0.08	25.85	4.37
CRS2110	58.54	29.82	25.15	0.13	0.28	24.74	3.98
CRS2210	66.63	29.82	33.95	0.14	0.06	33.75	3.06
CRS3110	58.24	29.82	25.25	0.16	0.48	24.61	3.81
CRS3210	59.60	29.82	26.00	0.13	0.10	25.77	4.01
WFS1110	61.31	29.82	31.05	0.20	-	30.85	0.64
WFS1210	61.70	29.82	29.35	0.11	-	29.24	2.64
WFS2110	63.41	29.82	29.56	0.11	-	29.45	4.14
WFS2210	59.04	29.82	27.85	0.12	-	27.73	1.49
WFS3110	60.40	29.82	30.30	0.12	-	30.18	0.40
WFS3210	59.75	29.82	28.85	0.10	-	28.75	1.18

Table 7.30 Total, solid, gross water, water in filter paper, diffused air, net water and air volumes at the end of each test measured by the Bishop water volume change indicator for samples with 10% montmorillonite tested in the second phase.

Sample No.	Final volumes (cc)						
	Total	Solid	Gross	Filter paper	Diffused air	Net water	Air
CRS1120	58.34	29.82	25.95	0.15	0.60	25.20	3.32
CRS1220	59.34	29.82	25.75	0.21	0.02	25.52	4.00
CRS2120	58.59	29.82	25.50	0.12	0.14	25.24	3.53
CRS2220	60.61	29.82	27.70	0.07	0.06	27.57	3.22
GDSS1120	62.10	29.82	25.95	0.15	-	27.80	4.48
GDSS1220	61.94	29.82	28.50	0.13	-	28.37	3.75
GDSS2120	60.69	29.82	28.65	0.19	-	28.46	2.41
GDSS2220	63.89	29.82	29.55	0.12	-	29.43	4.64
GDSS3120	60.94	29.82	29.45	0.13	-	29.32	1.80
GDSS3220	63.94	29.82	29.40	0.12	-	29.28	4.84

Table 7.31 Total, solid, gross water, water in filter paper, diffused air, net water and air volumes at the end of each test measured by the GDS pressure controller for samples containing 20% montmorillonite tested in the second phase.

Sample No.	Final volumes (cc)						
	Total	Solid	Gross water	Filter paper	Diffused air	Net water	Air
CRS1130	65.64	29.86	35.09	0.22	0.10	34.77	1.01
CRS1230	68.74	29.86	34.66	0.12	0.04	34.50	4.38
CRS2130	60.41	29.86	30.71	0.14	0.10	30.47	0.08
CRS2230	61.59	29.86	27.75	0.19	0.02	27.54	4.19
CRS3130	59.88	29.86	29.11	0.10	0.08	28.93	1.09
CRS3230	62.61	29.86	27.95	0.13	0.06	27.76	4.99

Table 7.32 Total, solid, gross water, water in filter paper, diffused air, net water and air volumes at the end of each test measured by the Bishop water volume change indicator for samples with 30% montmorillonite tested in the second phase.

Sample	e_i	e_f	Δe	Sr_i	Sr_f	ΔSr	Mc_f	ΔMc
CRS110	0.945	-	-	85.31	-	-	52.90	22.90
CRS810	0.940	0.955	0.015	85.85	86.16	0.31	35.49	5.49
CRS910	0.943	0.952	0.009	85.50	86.05	0.55	33.89	3.89
CRS1010	0.947	0.950	0.003	85.16	91.28	6.12	36.91	6.91
CRS1110	0.940	0.951 0.961	0.011 0.021	85.85	91.79 88.66	5.94 2.81	42.40	12.40
CRS1210	0.940	0.960	0.020	85.85	91.26	5.41	41.12	11.12
CRS620	0.955	0.976	0.021	84.47	94.05	9.58	39.60	9.60
CRS720	0.940	0.965	0.025	85.85	92.14	6.29	39.54	9.54
CRS230	0.954	-	-	84.28	-	-	58.73	28.73
CRS330	0.943	-	-	85.29	-	-	79.03	49.03
CRS430	0.945	0.966	0.021	85.05	96.39	11.34	54.43	24.43
CRS530	0.949	0.977	0.028	84.96	92.46	7.50	41.40	11.40
CRS1330	0.956	0.970	0.014	84.10	125.53	41.43	51.75	21.75
CRS1430	0.956	0.986 0.990	0.030 0.034	84.10	143.46 143.61	59.36 59.51	58.20	28.20

Table 7.33 Initial and final void ratios (e), initial and final degrees of saturation (%), final moisture content, differences between void ratios, degrees of saturation and moisture contents for samples in the first phase.

Sample No.	e_i	e_f	Δe	Sr_i	Sr_f	ΔSr	Mc_f	ΔMC
CRS1110	0.945	0.987	0.042	85.31	86.99	1.60	38.43	8.43
CRS1210	0.953	1.013	0.060	84.62	85.54	0.92	39.16	9.16
CRS2110	0.940	0.963	0.023	85.83	86.14	0.31	35.95	5.95
CRS2210	0.936	1.234	0.298	86.17	91.68	5.51	35.44	5.44
CRS3110	0.940	0.953	0.013	85.83	86.59	0.76	35.96	5.96
CRS3210	0.942	0.999	0.057	85.65	86.53	0.88	36.44	6.44
WFS1110	0.945	1.056	0.111	85.31	97.97	12.66	40.68	10.68
WFS1210	0.942	1.069	0.127	85.65	91.72	6.07	35.99	5.99
WFS2110	0.932	1.126	0.194	86.54	87.67	1.13	32.59	2.59
WFS2210	0.953	0.980	0.027	84.62	94.90	10.28	34.60	4.60
WFS3110	0.928	1.025	0.097	86.89	98.69	11.80	33.61	3.61
WFS3210	0.943	1.004	0.061	85.50	96.06	10.56	35.39	5.39

Table 7.34 Initial and final void ratios (e), initial and final degrees of saturation (%), final moisture content, differences between void ratios, degrees of saturation and moisture contents for samples with 10% montmorillonite in the second phase.

Sample No.	e_i	e_f	Δe	Sr_i	Sr_f	ΔSr	Mc_f	ΔMc
CRS1120	0.940	0.956	0.016	85.83	88.36	2.53	36.04	6.04
CRS1220	0.940	0.990	0.050	85.83	86.45	0.62	37.58	7.58
CRS2120	0.940	0.965	0.025	85.83	87.73	1.90	38.26	8.26
CRS2220	0.945	1.033	0.088	85.31	89.54	4.23	37.10	7.10
GDSS1120	0.942	1.082	0.140	85.65	86.12	0.47	42.09	12.09
GDSS1220	0.940	1.076	0.136	85.83	88.33	2.50	39.77	9.77
GDSS2120	0.940	1.035	0.095	85.83	92.19	6.36	35.99	5.99
GDSS2220	0.940	1.143	0.203	85.83	86.38	0.55	35.81	5.81
GDSS3120	0.940	1.044	0.104	85.83	94.21	8.38	40.38	10.38
GDSS3220	0.955	1.144	0.189	84.47	85.81	1.34	37.82	7.82

Table 7.35 Initial and final void ratios (e), initial and final degress of saturation (%), final moisture content, differences between void ratios, degrees of saturation and moisture contents for samples with 20% montmorillonite in the second phase.

Sample No.	e_i	e_f	Δe	Sr_i	Sr_f	ΔSr	Mc_f	ΔMc
CRS1130	0.937	1.198	0.261	85.81	97.18	11.37	53.86	23.86
CRS1230	0.952	1.302	0.350	84.45	88.73	4.28	54.14	24.14
CRS2130	0.956	1.023	0.067	84.10	99.74	15.64	44.24	14.24
CRS2230	0.937	1.063	0.126	85.81	86.79	0.98	43.01	13.01
CRS3130	0.933	1.005	0.072	86.15	96.37	10.22	45.27	15.27
CRS3230	0.956	1.097	0.141	84.10	84.76	0.66	44.64	14.64

Table 7.36 Initial and final void ratios (e), initial and final degrees of saturation (%), final moisture content, differences between void ratios, degrees of saturation and moisture contents for samples with 30% montmorillonite in the second phase.

Sample No.	Initial weight (kg)	Initial volume x 10^{-5} m^3	Initial wt./vol. (kg/m^3)	Final wt. (kg)	Final volume x $10^{-5}m^3$	Final wt./vol. (kg/m^3)
CRS110	0.101	5.801	1741.079	0.119	7.400	1608.108
CRS810	0.103	5.784	1780.774	0.107	5.964	1794.098
Bwvci					5.829	1835.649
CRS910	0.103	5.795	1777.394	0.107	5.899	1813.866
Bwvci					5.820	1838.488
CRS1010	0.103	5.806	1774.026	0.107	5.984	1788.101
Bwvci					5.816	1839.752
CRS1110	0.103	5.784	1780.774	0.111	6.387	1737.905
Bwvci					5.849	1897.760
CRS1210	0.103	5.784	1780.774	0.110	6.328	1738.306
Bwvci					5.844	1882.272
CRS620	0.103	5.829	1767.027	0.108	6.223	1735.497
Bwvci					5.891	1833.305
CRS720	0.103	5.784	1780.774	0.108	6.066	1780.415
Bwvci					5.859	1843.318
CRS230	0.103	5.835	1765.210	0.123	7.775	1581.993
CRS330	0.103	5.801	1775.556	0.136	8.716	1560.348
CRS430	0.103	5.809	1773.110	0.118	7.091	1664.081
Bwvci					5.869	2010.564
CRS530	0.103	5.812	1772.195	0.108	6.329	1706.431
Bwvci					5.902	1829.888
CRS1330	0.102	5.841	1746.276	0.116	6.761	1715.722
Bwvci					5.881	1972.453
CRS1430	0.103	5.841	1763.396	0.121	7.075	1710.247
Bwvci					5.942	2036.351

Table 7.37 Initial and final weight/volume relationships measured by micrometer and the Bishop water volume change indicator (Bwvci) in the first phase.

Sample No.	Initial weight (kg)	Initial volume $x10^{-5}m^3$	Initial wt./vol. (kg/m^3)	Final wt. (kg)	Final volume $x10^{-5}m^3$	Final wt./vol. (kg/m^3)
CRS1110 Bwvci	0.103	5.801	1775.556	0.108	6.006 5.926	1798.202 1822.477
CRS1210 Bwvci	0.104	5.824	1785.714	0.109	6.140 6.004	1775.244 1815.456
W2FS1310	0.103	5.784	1780.775	0.104	5.672	1833.568
CRS2110 Bwvci	0.103	5.784	1780.775	0.106	5.975 5.854	1774.059 1810.728
CRS2210 Bwvci	0.103	5.773	1784.168	0.106	6.175 6.663	1716.599 1590.875
W2FS2310	0.103	5.801	1775.556	0.103	5.479	1879.905
CRS3110 Bwvci	0.103	5.784	1780.775	0.107	5.899 5.824	1813.866 1837.225
CRS3210 Bwvci	0.103	5.790	1778.929	0.107	5.804 5.960	1843.556 1795.302
W2FS3310	0.103	5.761	1787.884	0.103	5.484	1878.191
WFS1110 Bwvci	0.103	5.801	1775.556	0.110	6.350 6.131	1732.283 1794.161
WFS1210 Bwvci	0.102	5.790	1761.658	0.107	6.002 6.170	1782.739 1734.198
WFS2110 Bwvci	0.103	5.801	1775.556	0.104	5.664 6.341	1836.158 1640.120
WFS2210 Bwvci	0.103	5.824	1768.544	0.106	5.909 5.904	1793.874 1795.393
WFS3110 Bwvci	0.102	5.750	1773.913	0.105	5.761 6.040	1822.600 1738.411
WFS3210 Bwvci	0.103	5.795	1777.394	0.107	5.978 5.975	1789.896 1790.795

Table 7.38 Initial and final weight/volume relationships measured by micrometer and the Bishop water volume change indicator (Bwvci) for samples containing 10% montmorillonite in the second phase.

Sample No.	Initial weight (kg)	Initial volume $x10^{-5}m^3$	Initial wt./vol. (kg/m^3)	Final wt. (kg)	Final volume $x10^{-5}m^3$	Final wt./vol. (kg/m^3)
CRS1120 Bwvci	0.102	5.784	1763.485	0.106	5.951 5.834	1781.213 1816.935
CRS1220 Bwvci	0.102	5.784	1763.485	0.106	5.970 5.934	1775.544 1786.316
W2FS1320	0.102	5.784	1763.485	0.105	5.574	1883.746
CRS2120 Bwvci	0.103	5.784	1780.775	0.107	5.813 5.859	1840.702 1826.250
CRS2220 Bwvci	0.103	5.801	1775.556	0.107	5.773 6.061	1853.456 1765.385
OldGDSS120	0.103	5.841	1763.396	0.126	-	-
GDSS1120 GDS	0.102	5.790	1761.658	0.110	6.710 6.210	1639.344 1771.337
GDSS1220 GDS	0.102	5.784	1763.485	0.108	6.458 6.194	1672.344 1743.623
W2FS1G320	0.102	5.784	1763.485	0.105	5.828	1801.647
GDSS2120 GDS	0.101	5.784	1746.196	0.105	5.742 6.069	1828.631 1730.104
GDSS2220 GDS	0.102	5.784	1763.485	0.106	5.770 6.389	1837.088 1659.102
W2FS2320	0.102	5.790	1761.658	0.104	5.706	1822.643
GDSS3120 GDS	0.102	5.784	1763.485	0.109	5.979 6.094	1823.047 1788.645
GDSS3220 GDS	0.102	5.829	1749.871	0.107	5.819 6.394	1838.804 1673.444

Table 7.39 Initial and final weight/volume relationships measured by micrometer, the Bishop water volume change indicator and the GDS pressure controller for samples containing 20% montmorillonite in the second phase.

Sample No.	Initial weight (kg)	Initial volume $x10^{-5}m^3$	Initial wt./vol. (kg/m^3)	Final wt. (kg)	Final volume $x10^{-5}m^3$	Final wt./vol. (kg/m^3)
CRS1130 Bwvci	0.103	5.784	1780.775	0.118	6.658 6.564	1772.304 1797.684
CRS1230 Bwvci	0.103	5.829	1767.027	0.118	6.506 6.874	1813.710 1716.613
W2FS1330	0.102	5.784	1763.485	0.104	5.905	1761.219
CRS2130 Bwvci	0.103	5.841	1763.397	0.111	6.058 6.041	1832.288 1837.444
CRS2230 Bwvci	0.103	5.784	1780.775	0.109	- 6.159	- 1769.768
CRS1(2)330	0.102	5.789	1761.962	0.105	6.107	1719.338
CRS3130 Bwvci	0.102	5.773	1766.846	0.110	6.047 5.988	1819.084 1837.007
CRS3230 Bwvci	0.103	5.841	1763.397	0.111	6.372 6.261	1741.996 1772.880
W2FS3330	0.102	5.784	1763.485	0.102	5.570	1831.239

Table 7.40 Initial and final weight/volume relationships measured by micrometer and the Bishop water volume change indicator (Bwvci) for samples containing 30% montmorillonite in the second phase.

Sample No.	Initial volume x 10^{-5} m^3 (Mic)	Volume change (%) (Bwvci)	Final volume x 10^{-5} m^3 (Bwvci)	Final volume x 10^{-5} m^3 (Mic)	Difference in volume x 10^{-5} m^3 (both methods)
CRS110	5.801	-	-	7.400	-
CRS810	5.784	0.780	5.829	5.964	0.135
CRS910	5.795	0.430	5.820	5.899	0.079
CRS1010	5.806	0.170	5.816	5.984	0.168
CRS1110	5.784	1.120	5.849	6.387	0.538
CRS1210	5.784	1.037	5.844	6.328	0.484
CRS620	5.829	1.060	5.891	6.223	0.332
CRS720	5.784	1.290	5.859	6.066	0.207
CRS230	5.835	-	-	7.775	-
CRS330	5.801	-	-	8.716	-
CRS430	5.809	1.030	5.869	7.091	1.222
CRS530	5.812	1.550	5.902	6.329	0.427
CRS1330	5.841	0.680	5.881	6.761	0.880
CRS1430	5.841	1.730	5.942	7.075	1.133

Table 7.41 Initial volume, volume change (%), final volumes measured by both Bwvci and micrometer (Mic) and the difference in the final volumes measured by both methods in the first phase.

Sample No.	Initial volume x 10^{-5} m^3 (Mic)	Volume change (%) (Bwvci)	Final volume x 10^{-5} m^3 (Bwvci)	Final volume x 10^{-5} m^3 (Mic)	Difference in volume x 10^{-5} m^3 (both methods)
CRS1110	5.801	2.15	5.926	6.006	0.080
CRS1210	5.824	3.09	6.004	6.140	0.136
CRS2110	5.784	1.21	5.854	5.975	0.121
CRS2210	5.773	15.42	6.663	6.175	-0.488
CRS3110	5.784	0.69	5.824	5.899	0.075
CRS3210	5.790	2.94	5.960	5.804	-0.156
WFS1110	5.801	5.89	6.131	6.350	0.219
WFS1210	5.790	6.56	6.170	6.002	-0.168
WFS2110	5.761	9.37	6.301	5.664	-0.637
WFS2210	5.824	1.37	5.904	5.909	0.005
WFS3110	5.750	5.04	6.040	5.761	-0.279
WFS3210	5.795	3.11	5.975	5.978	0.003

Table 7.42 Initial volume, volume change (%), final volumes measured by both Bwvci and micrometer (Mic) and the difference in the final volumes measured by both methods for samples containing 10% montmorillonite in the second phase.

Sample No.	Initial volume x 10^{-5} m^3 (Mic)	Volume change (%) (Bwvci)	Final volume x 10^{-5} m^3 (Bwvci)	Final volume x 10^{-5} m^3 (Mic)	Difference in volume x 10^{-5} m^3 (both methods)
CRS1120	5.784	0.86	5.834	5.951	0.117
CRS1220	5.784	2.59	5.934	5.970	0.036
CRS2120	5.784	1.30	5.859	5.813	-0.046
CRS2220	5.801	4.48	5.827	5.773	-0.054
GDSS1120	5.790	7.25	6.210	6.710	0.500
GDSS1220	5.784	7.09	6.194	6.458	0.264
GDSS2120	5.784	4.93	6.069	5.742	-0.327
GDSS2220	5.784	10.46	6.389	5.770	-0.619
GDSS3120	5.784	5.36	6.094	5.979	-0.115
GdSS3220	5.829	9.69	6.394	5.819	-0.575

Table 7.43 Initial volume, volume change (%), final volumes measured by both Bwvci and micrometer (Mic) and the difference in the final volumes measured by both methods for samples containing 20% montmorillonite in the second phase.

Sample No.	Initial volume x 10^{-5} m^3 (Mic)	Volume change (%) (Bwvci)	Final volume x 10^{-5} m^3 (Bwvci)	Final volume x 10^{-5} m^3 (Mic)	Difference in volume x 10^{-5} m^3 (both methods)
CRS1130	5.784	13.49	6.564	6.658	0.094
CRS1230	5.829	17.93	6.874	6.506	-0.368
CRS2130	5.841	3.42	6.041	6.058	0.017
CRS2230	5.784	6.48	6.159	-	-
CRS3130	5.773	3.72	5.988	6.047	0.059
CRS3230	5.841	7.19	6.261	6.372	0.111

Table 7.44 Initial volume, volume change (%), final volumes measured by both Bwvci and micrometer (Mic) and the difference in the final volumes measured by both methods for samples containing 30% montmorillonite in the second phase.

Sample No.	Rate of strain (mm/min)	Time to failure (minutes)			Max. deviator stress (kN/m^2)
		calc.	estim.	actual	
CRS1110	0.00284	2,500	4,320	1,380	102.21
CRS1210	0.00284	2,500	4,320	1,590	170.87
W2FS1310	0.00240	2,500	4,320	2,400	232.91
CRS2110	0.00437	1,600	2,880	1,620	296.36
CRS2210	0.00437	1,600	2,880	2,970	275.05
W2FS2310	0.00400	1,600	2,880	2,610	431.78
CRS3110	0.00191	6,400	6,400	3,960	222.57
CRS3210	0.00191	6,400	6,400	2,820	213.10
W2FS3310	0.00180	6,400	6,400	4,200	404.13
WFS1110	0.00240	3,025	4,320	1,320	69.05
WFS1210	0.00240	3,025	4,320	1,230	92.06
WFS2110	0.00180	5,760	5,760	3,090	248.15
WFS2210	0.00180	5,760	5,760	2,880	238.10
WFS3110	0.00180	5,760	5,760	4,245	142.86
WFS3210	0.00180	5,760	5,760	1,515	164.55

Table 7.45 Effect of rate of strain on shear strength of identical samples containing 10% montmorillonite in the second phase.

Sample No.	Rate of strain (mm/min)	Time to failure (minutes)			Max. deviator stress (kN/m^2)
		calc.	estim.	actual	
CRS1120	0.00094	6,400	12,960	8,160	260.45
CRS1220	0.00094	6,400	12,960	8,640	269.92
W2FS1320	0.00080	6,400	14,400	9,600	224.93
CRS2120	0.00169	7,225	7,225	4,770	203.23
CRS2220	0.00169	7,225	7,225	3,720	217.83
OldGDSS120	0.00158	22,500	22,500	12,315	115.00
GDSS1120	0.00500	900	7,200	2,790	165.00
GDSS1220	0.00500	900	7,200	3,360	138.00
W2FS1G320	0.00180	900	7,200	2,730	187.18
GDSS2120	0.00500	7,225	7,225	5,520	168.00
GDSS2220	0.00500	7,225	7,225	3,210	204.00
W2FS2320	0.00180	900	7,200	1,950	247.79
GDSS3120	0.00667	5,476	5,476	1,620	307.00
GDSS3220	0.00667	5,476	5,476	2,220	290.00

Table 7.46 Effect of rate of strain on shear strength of identical samples containing 20% montmorillonite in the second phase.

Sample No.	Rate of strain (mm/min)	Time to failure (minutes)			Max. deviator stress (kN/m^2)
		calc.	estim.	actual	
CRS1130	0.00085	10,000	14,400	4,650	74.52
CRS1230	0.00085	10,000	14,400	2,160	92.34
W2FS1330	0.00080	10,000	14,400	3,360	211.10
CRS2130	0.00172	3,600	7,200	11,700	205.82
CRS2230	0.00172	3,600	7,200	3,705	235.19
CRS1(2)330	0.00172	3,600	7,200	5,685	315.70
CRS3130	0.00094	6,400	12,960	4,470	178.37
CRS3230	0.00094	6,400	12,960	6,000	188.63
W2FS3330	0.00080	6,400	14,400	8,160	253.11

Table 7.47 Effect of rate of strain on shear strength of identical samples containing 30% montmorillonite in the second phase.

Sample ratio	Condition	Test station	Cohesion (C_u) each	Cohesion (C_u) average	Friction angle (ϕ_u) each	Friction angle (ϕ_u) average
K/M 90/10	After expansion	No. 1	5	2.5	21	20.5
		No. 2	0		20	
	No prior expansion	No. 1	30	17.5	14	16.5
		No. 2	5		19	
	No back pressures	No. 4	150	-	4	-
K/M 80/20	After expansion	No. 1	25	27.5	15	16.5
		No. 3	30		18	
	No prior expansion	No. 1	30	27.5	16	15
		No. 3	25		14	
	No back pressures	No. 4	65	-	6.5	-
K/M 70/30	After expansion	No. 1	5	-	15	-
	No prior expansion	No. 1	20	-	14	-
	No back pressures	No. 4	90	-	4	-

Table 7.48 Cohesion (kN/m^2) and angle of internal friction (ϕ_u), for samples in the second phase, based on total stress.

Sample ratio	Condition	Test station	Effective cohesion (C') each	Effective cohesion (C') average	Friction angle (ϕ') each	Friction angle (ϕ') average
K/M 90/10	After expansion	No. 1	0	0	29	27
		No. 2	0		25	
	No prior expansion	No. 1	25	15	22	23
		No. 2	5		24	
K/M 80/20	After expansion	No. 1	10	10	26	26
		No. 3	10		26	
	No prior expansion	No. 1	25	20	22	22
		No. 3	15		22	
K/M 70/30	After expansion	No. 1	0	-	24	-
	No prior expansion	No. 1	10	-	22	-

Table 7.49 Effective cohesion (kN/m^2) and effective angle of internal friction (ϕ'), for samples in the second phase, with respect to ($\sigma - U_w$).

Sample ratio	Condition	Test station	Effective cohesion (C'') each	Effective cohesion (C'') average	Friction angle (ϕ'') each	Friction angle (ϕ'') average
K/M 90/10	After expansion	NO. 1	0	0	40	38
		No. 2	0		36	
	No prior expansion	No. 1	30	20	30	32
		No. 2	10		34	
K/M 80/20	After expansion	No. 1	25	20	29.5	31.5
		NO. 3	15		33.5	
	No prior expansion	No. 1	35	25	28	30.5
		No. 3	15		33	
K/M 70/30	After expansion	No. 1	0	-	31	-
	No prior expansion	No. 1	10	-	30	-

Table 7.50 Effective cohesion (kN/m^2) and effective angle of internal friction (ϕ''), for samples in the second phase, with respect to ($\sigma - U_a$).

Sample ratio	Condition	Test station	Effective cohesion (C^b) each	Effective cohesion (C^b) average	Friction angle (ϕ^b) each	Friction angle (ϕ^b) average
K/M 90/10	After expansion	No. 1	5	2.5	27	26
		No. 2	0		25	
	No prior expansion	No. 1	40	22.5	19	22
		No. 2	5		25	
K/M 80/20	After expansion	No. 1	30	20	20	23
		No. 3	10		26	
	No prior expansion	No. 1	30	25	20	21.5
		No. 3	20		23	
K/M 70/30	After expansion	No. 1	0	-	23	-
	No prior expansion	No. 1	10	-	22	-

Table 7.51 Effective cohesion (kN/m^2) and effective angle of internal friction (ϕ^b), for samples in the second phase, with respect to $\sigma - (U_a - U_w)$.

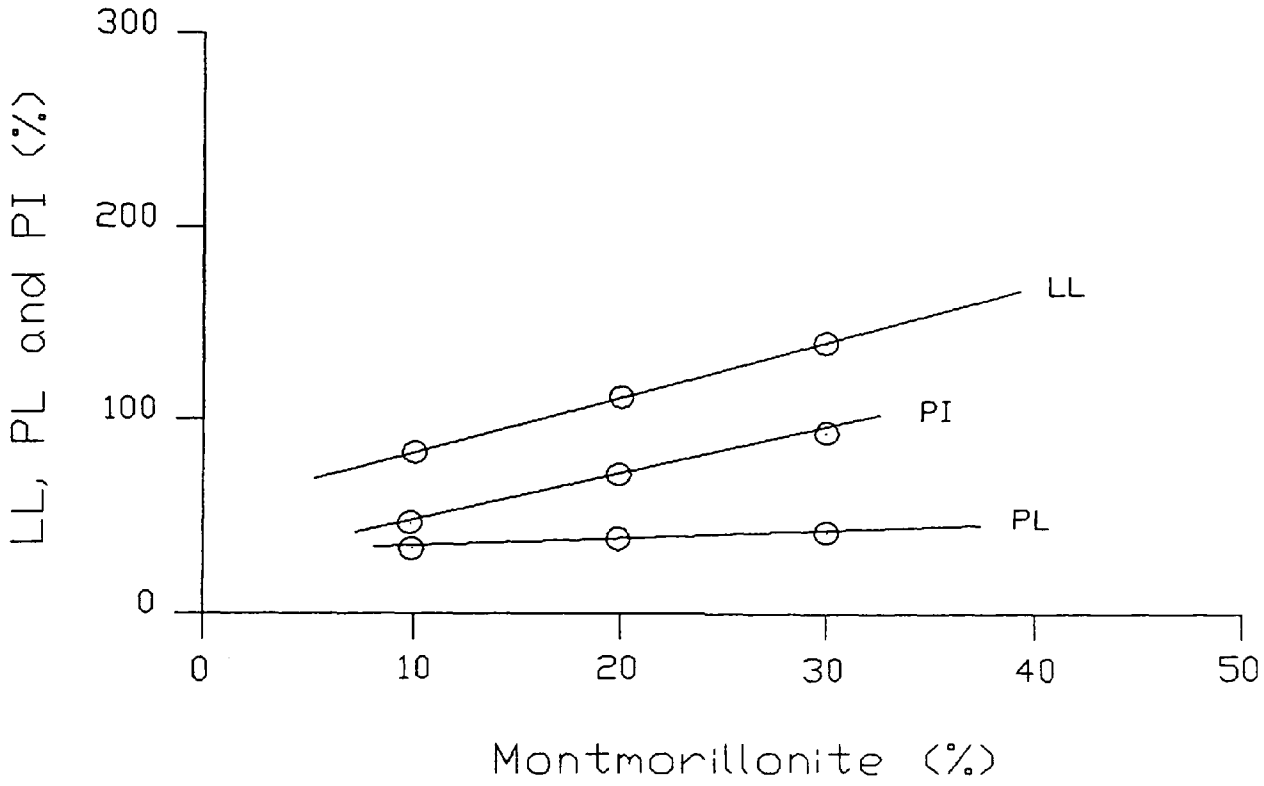

Figure 7.1 Influence of montmorillonite on liquid limit, plastic limit and plasticity index.

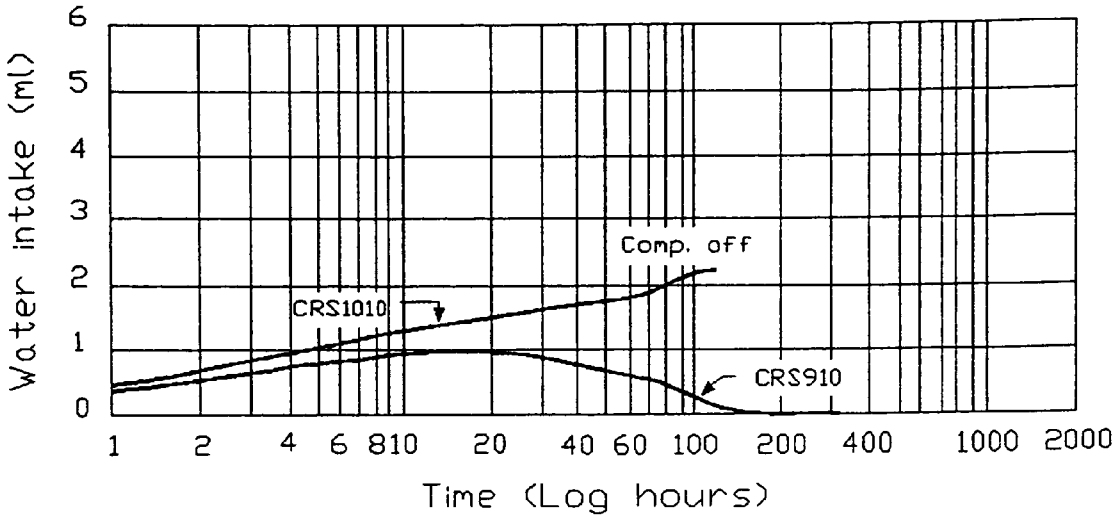

Figure 7.2 Water intake versus time by samples containing 10% montmorillonite tested, under initial confining cell pressures of 207 kN/m^2, in the first phase.

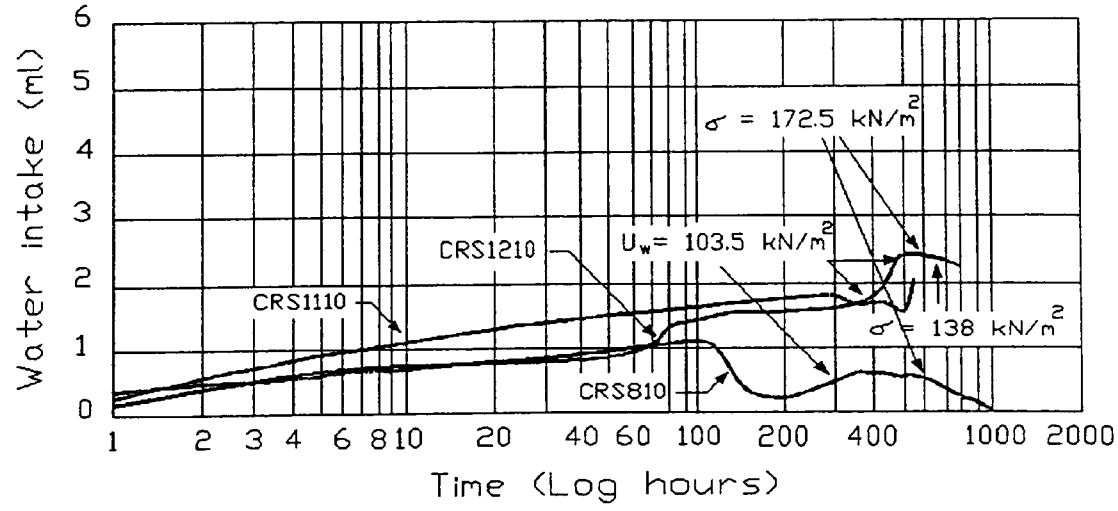

Figure 7.3 Water intake versus time by samples containing 10% montmorillonite tested, under initial confining cell pressures of 207 kN/m^2, in the first phase.

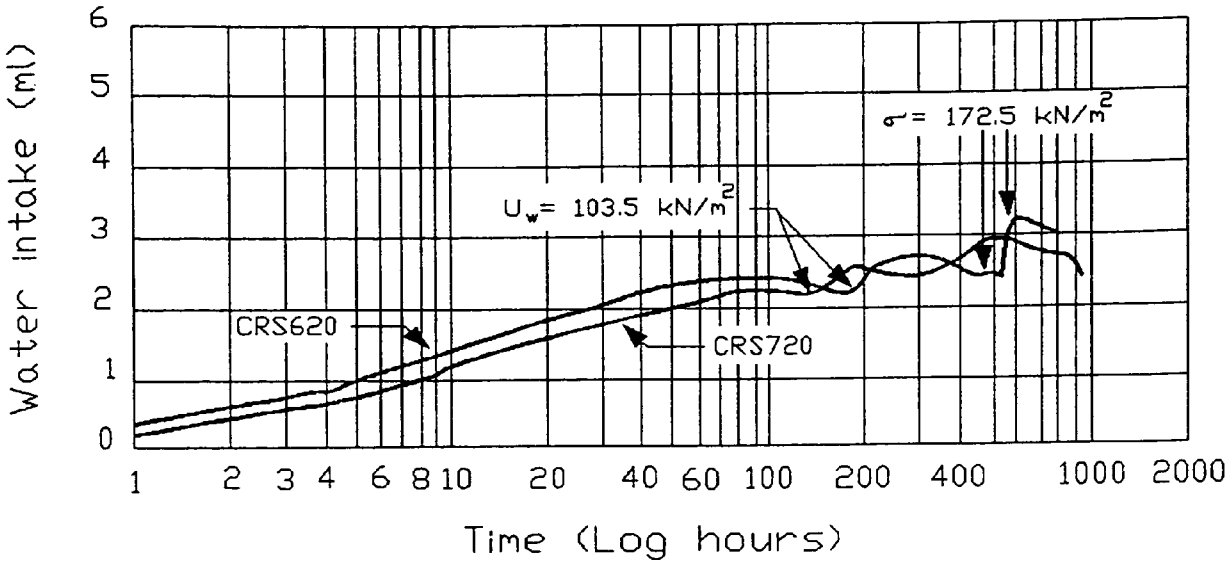

Figure 7.4 Water intake versus time by samples containing 20% montmorillonite tested, under initial confining cell pressures of 207 kN/m^2, in the first phase.

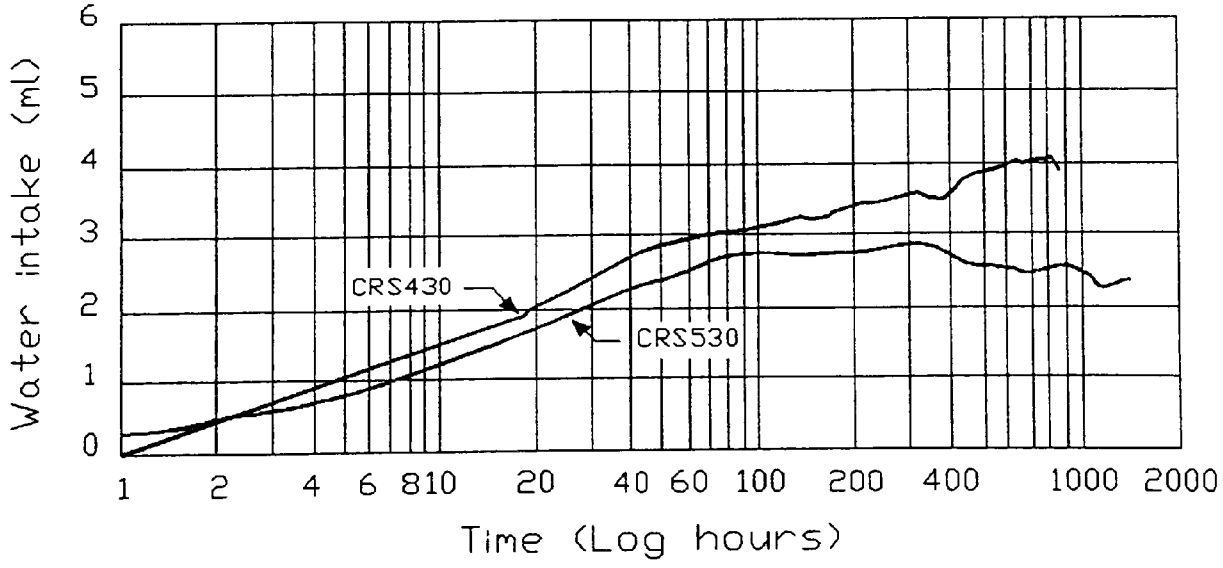

Figure 7.5 Water intake versus time by samples containing 30% montmorillonite tested, under initial confining cell pressures of 207 kN/m^2, in the first phase.

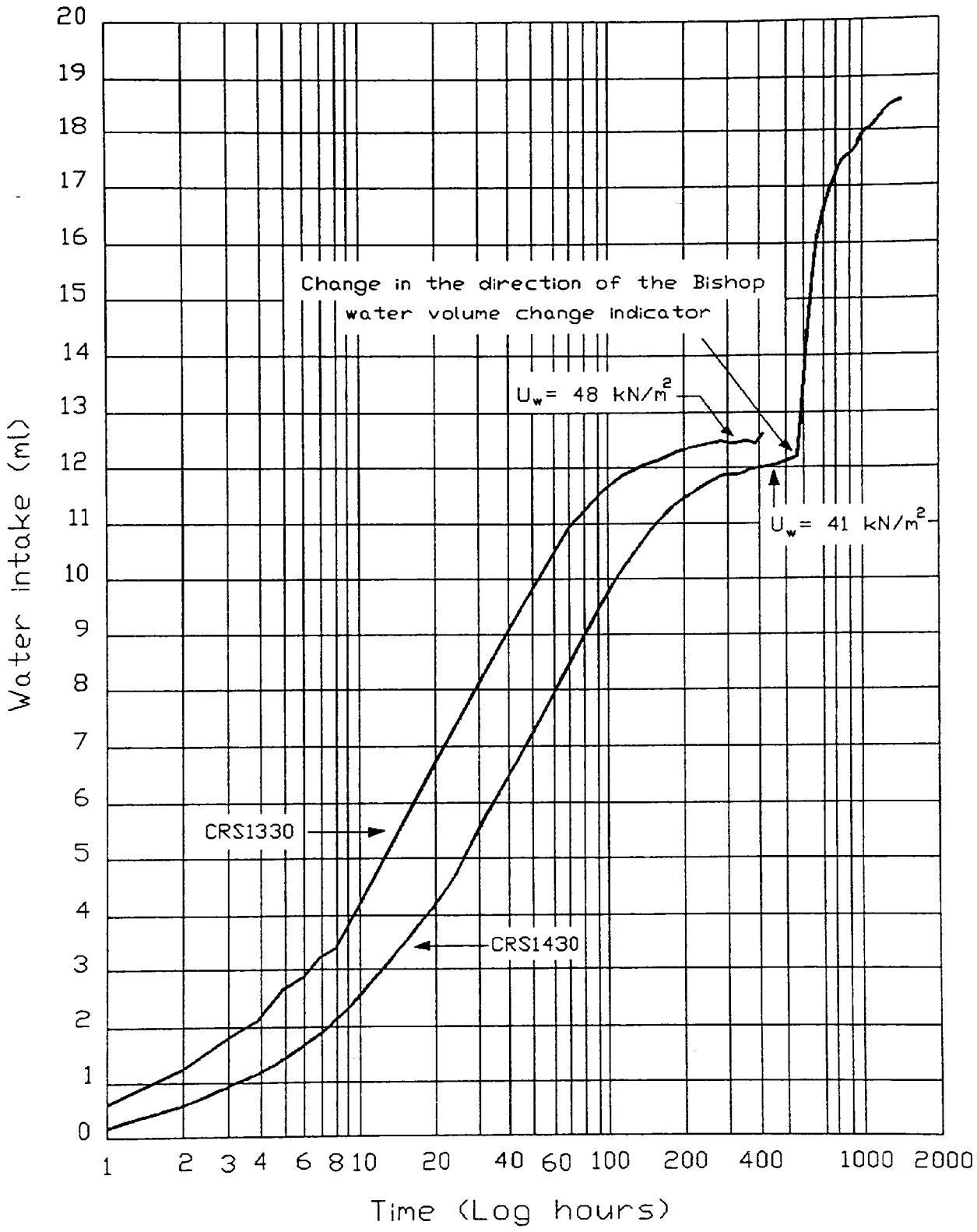

Figure 7.6 Water intake versus time by samples containing 30% montmorillonite tested, under initial confining cell pressures of 69 kN/m^2, in the first phase.

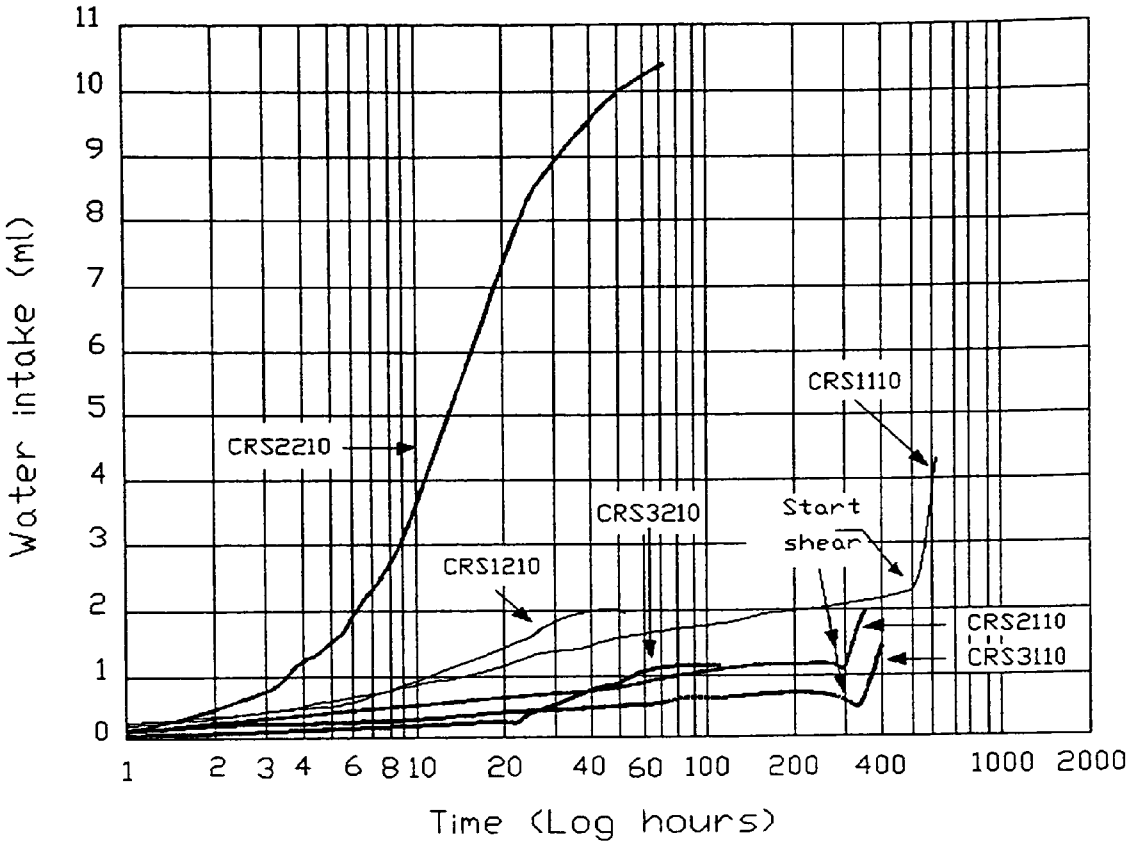

Figure 7.7 Water intake versus time by samples containing 10% montmorillonite tested in the second phase in station No. 1.

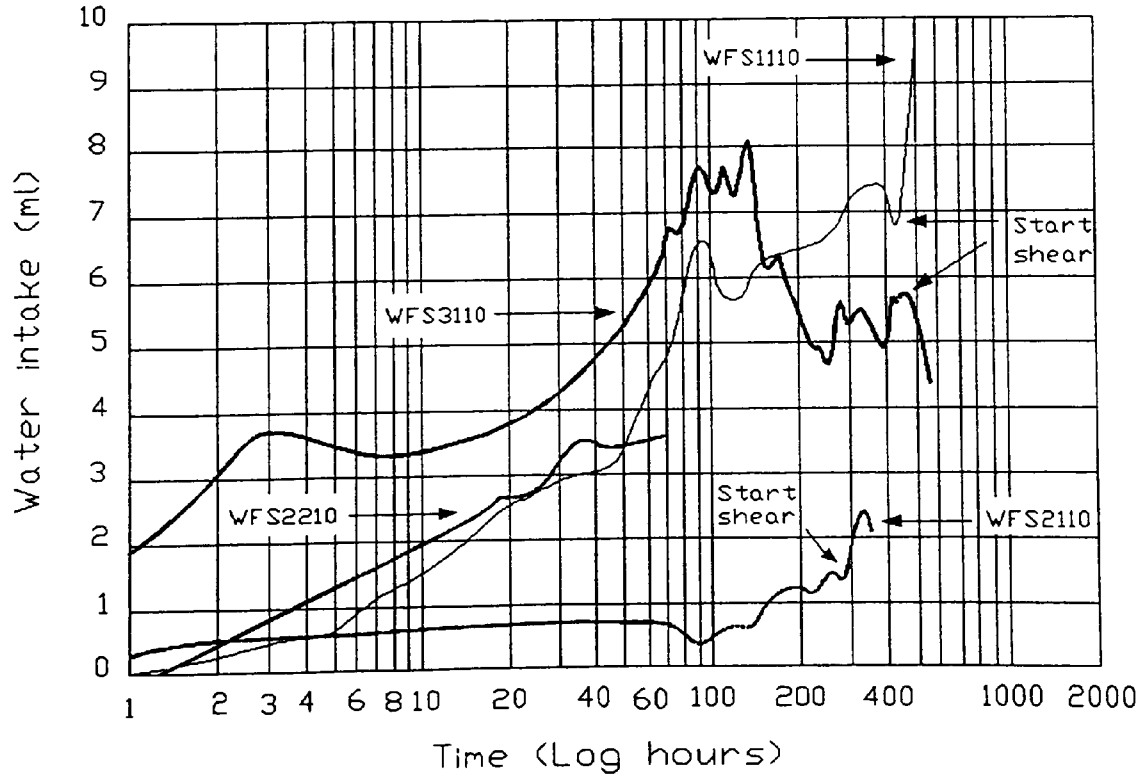

Figure 7.8 Water intake versus time by samples containing 10% montmorillonite tested in the second phase in station N0. 2.

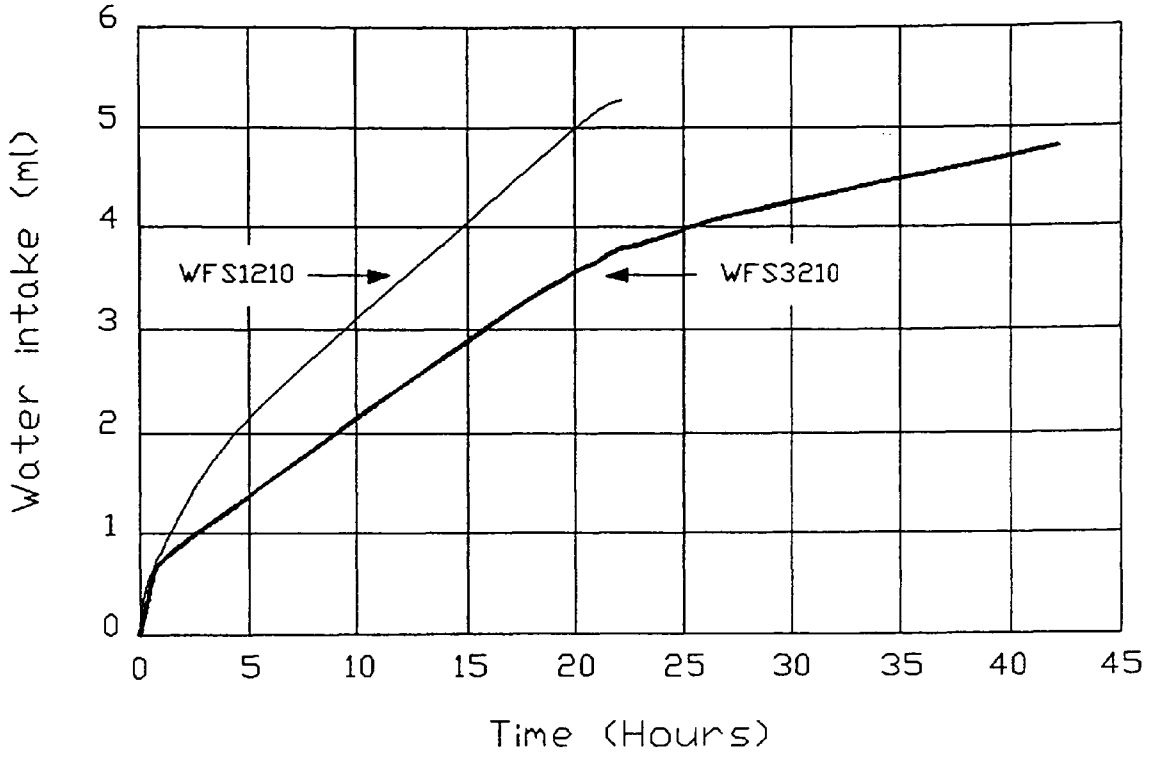

Figure 7.9 Water intake versus time by samples containing 10% montmorillonite tested in the second phase in station No. 2.

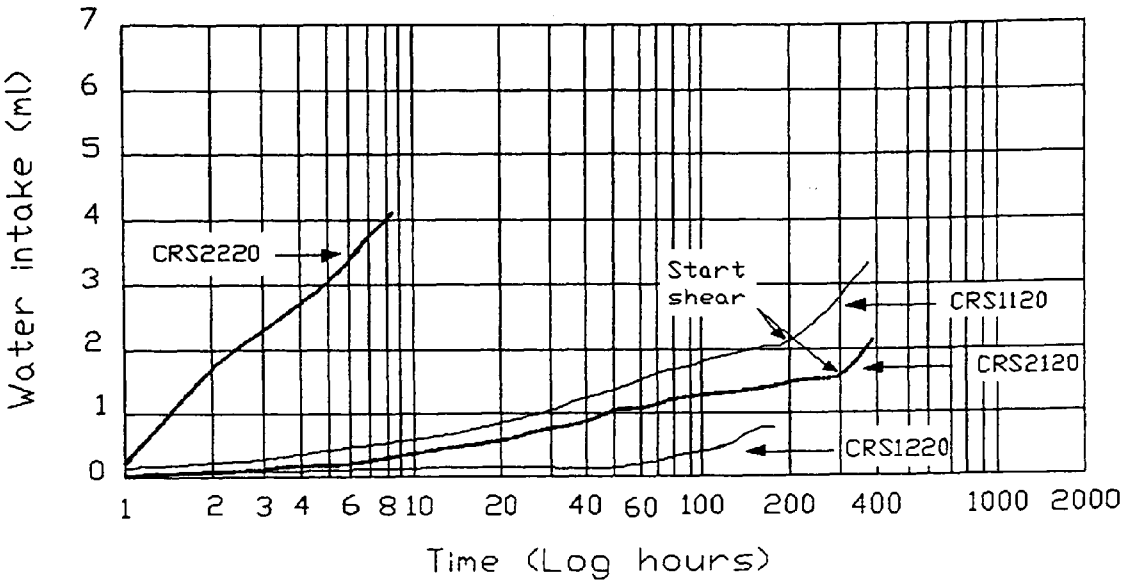

Figure 7.10 Water intake versus time by samples containing 20% montmorillonite tested in the second phase in station No. 1.

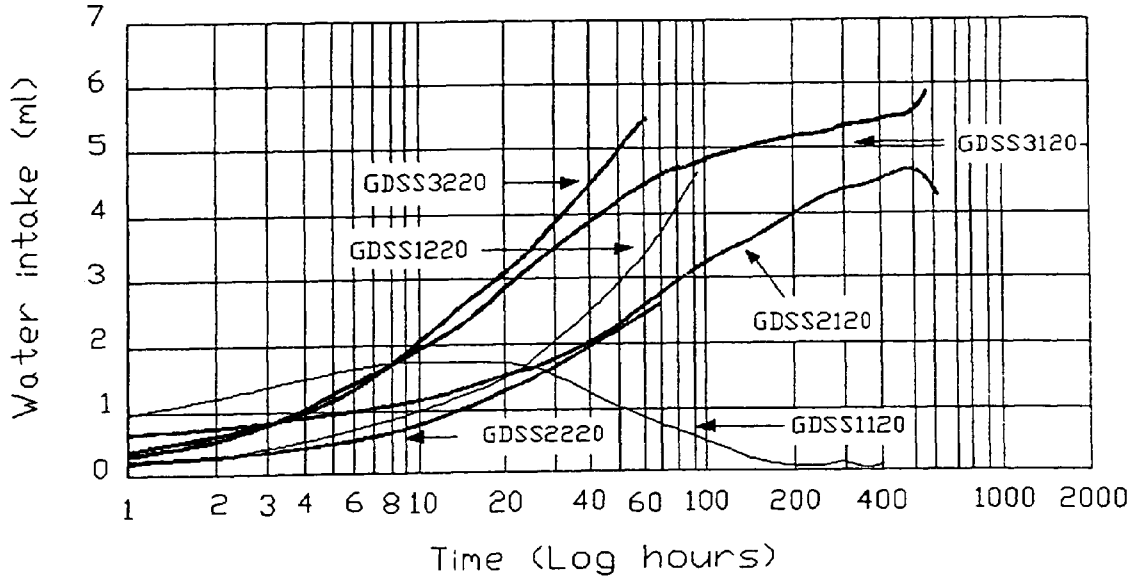

Figure 7.11 Water intake versus time by samples containing 20% montmorillonite tested in the second phase in station No. 3.

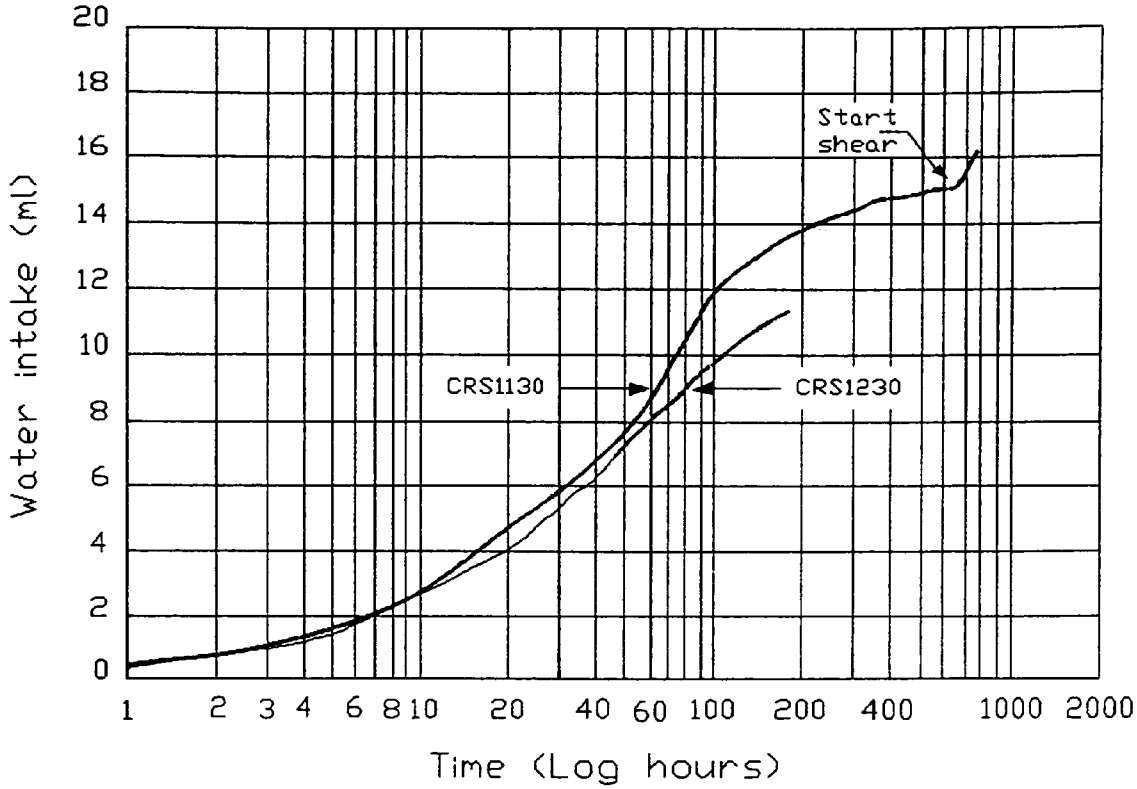

Figure 7.12 Water intake versus time by samples containing 30% montmorillonite tested in the second phase in station No. 1.

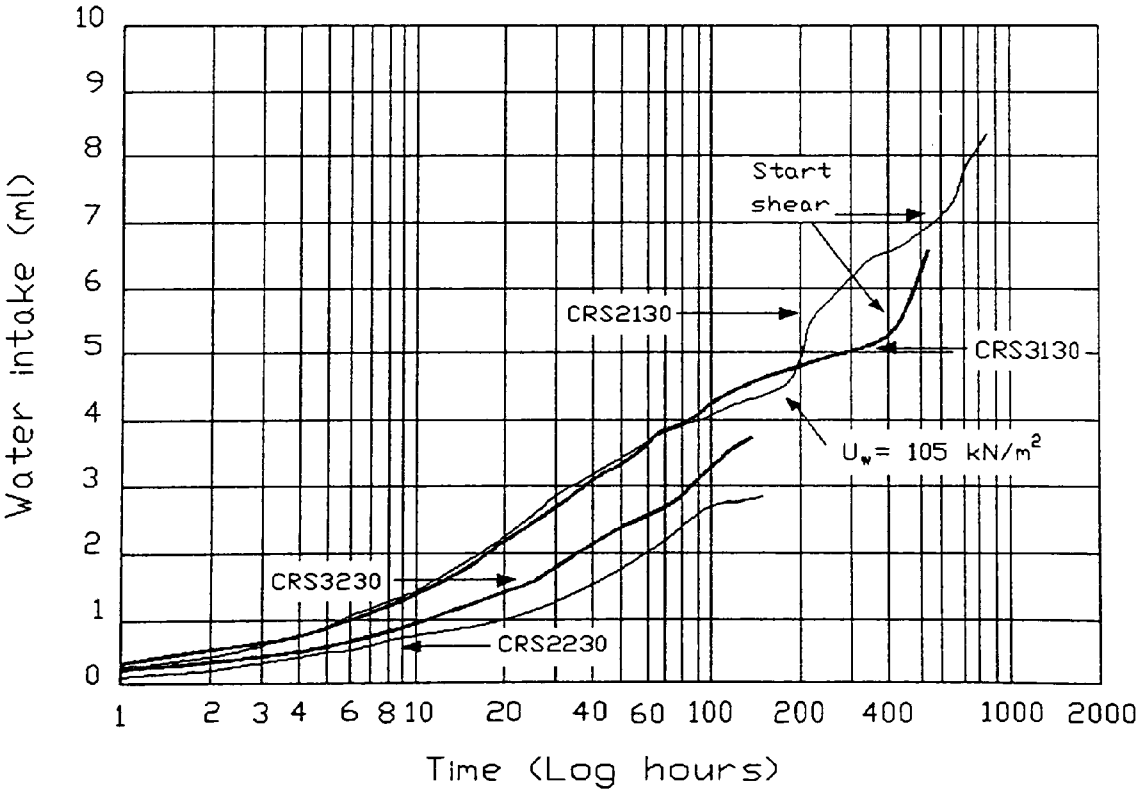

Figure 7.13 Water intake versus time by samples containing 30% montmorillonite tested in the second phase in station No. 1.

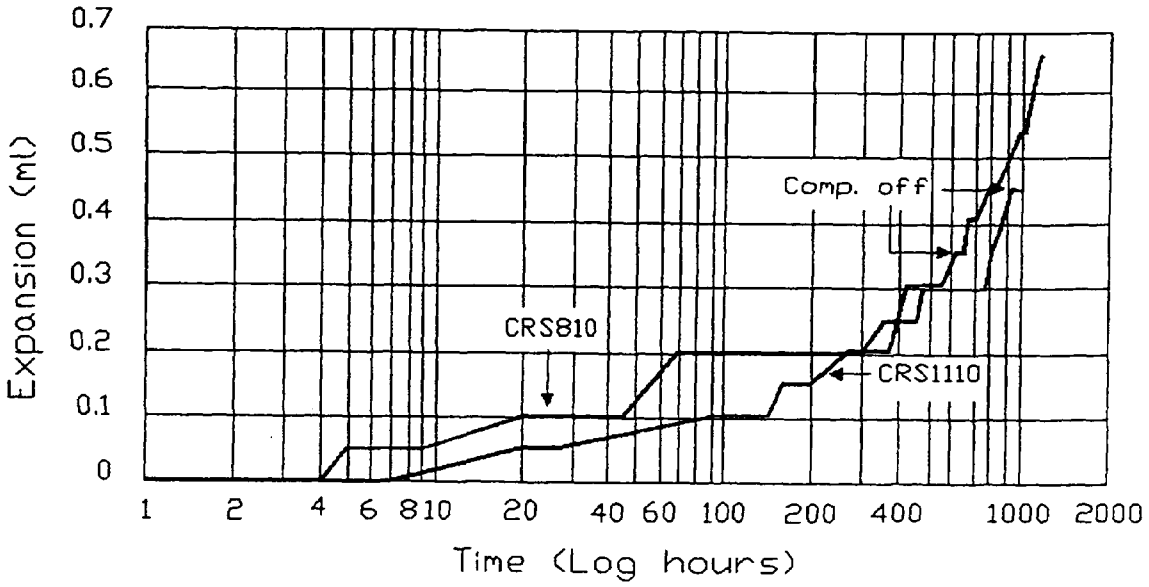

Figure 7.14 Expansion versus time by samples containing 10% montmorillonite tested, under initial confining cell pressures of 207 kN/m^2, in the first phase.

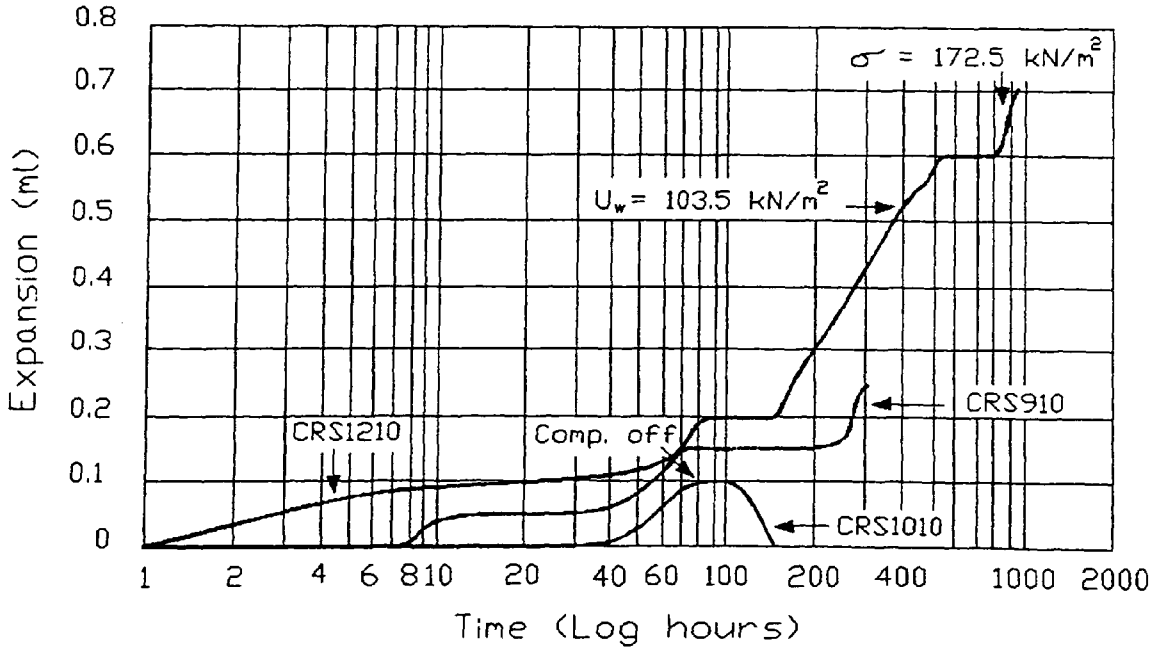

Figure 7.15 Expansion versus time by samples containing 10% montmorillonite tested, under initial confining cell pressures of 207 kN/m^2, in the first phase.

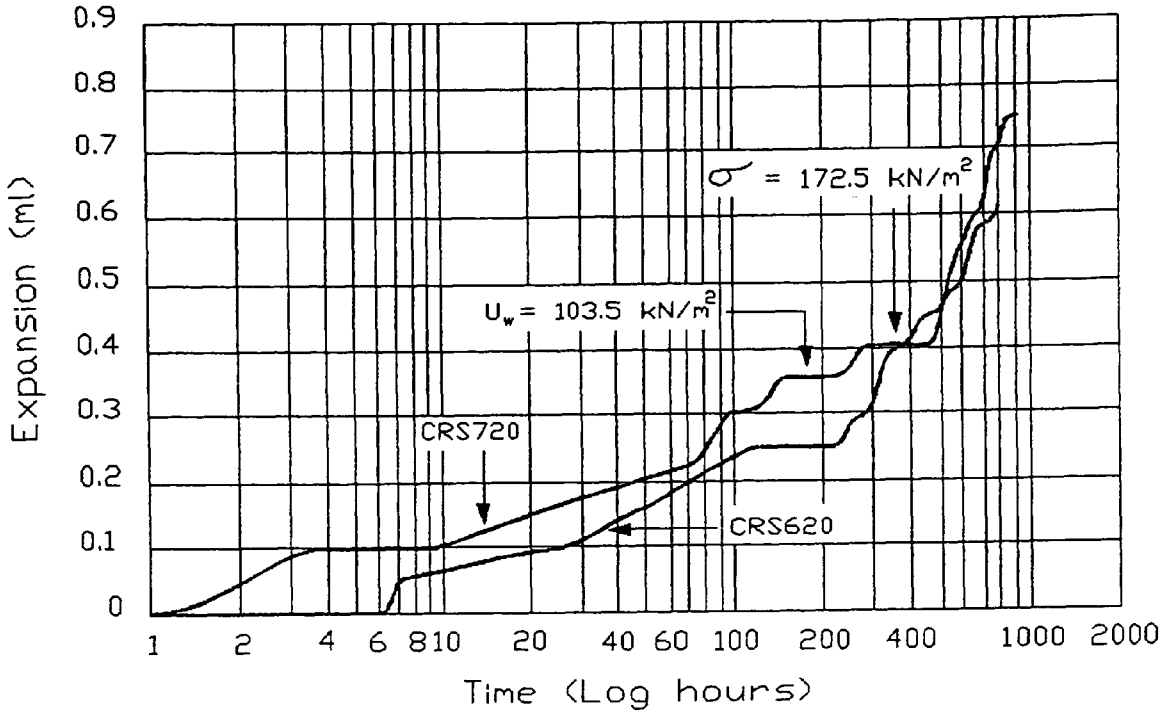

Figure 7.16 Expansion versus time by samples containing 20% montmorillonite tested, under initial confining cell pressures of 207 kN/m^2, in the first phase.

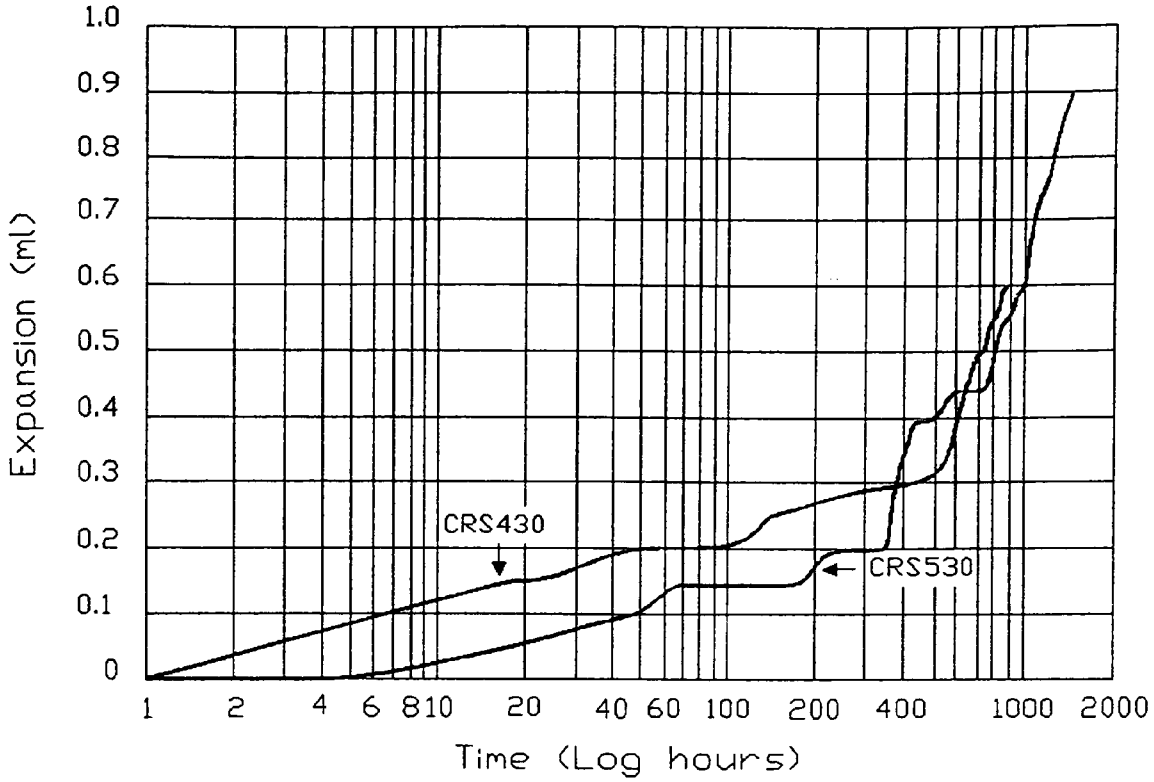

Figure 7.17 Expansion versus time by samples containing 30% montmorillonite tested, under initial confining cell pressures of 207 kN/m^2, in the first phase.

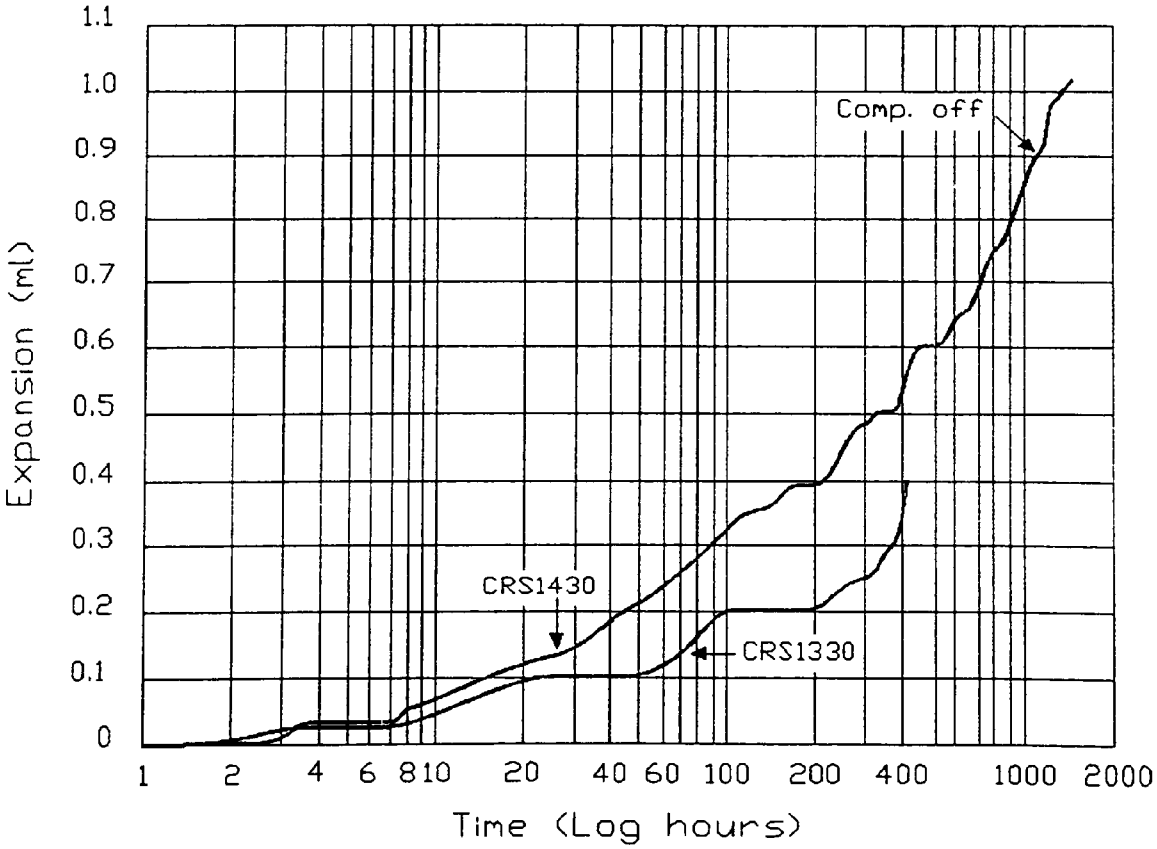

Figure 7.18 Expansion versus time by samples containing 30% montmorillonite tested, under initial confining cell pressures of 69 kN/m^2, in the first phase.

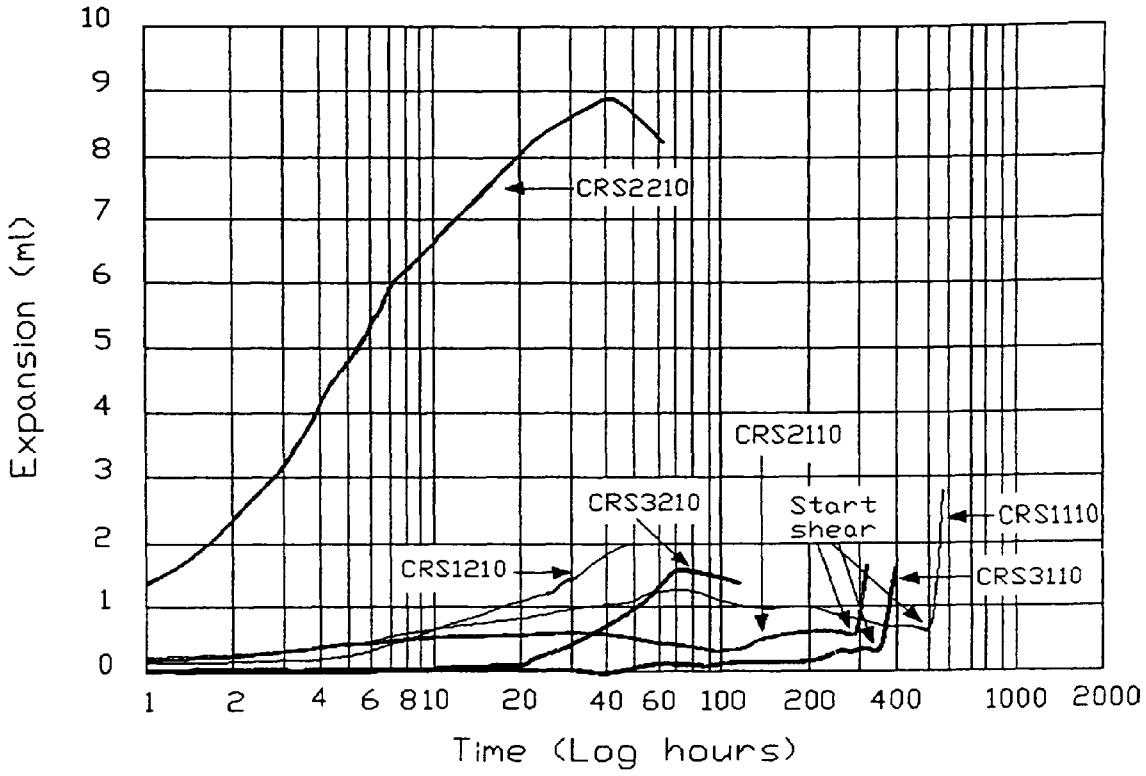

Figure 7.19 Expansion versus time by samples containing 10% montmorillonite tested in the second phase in station No. 1.

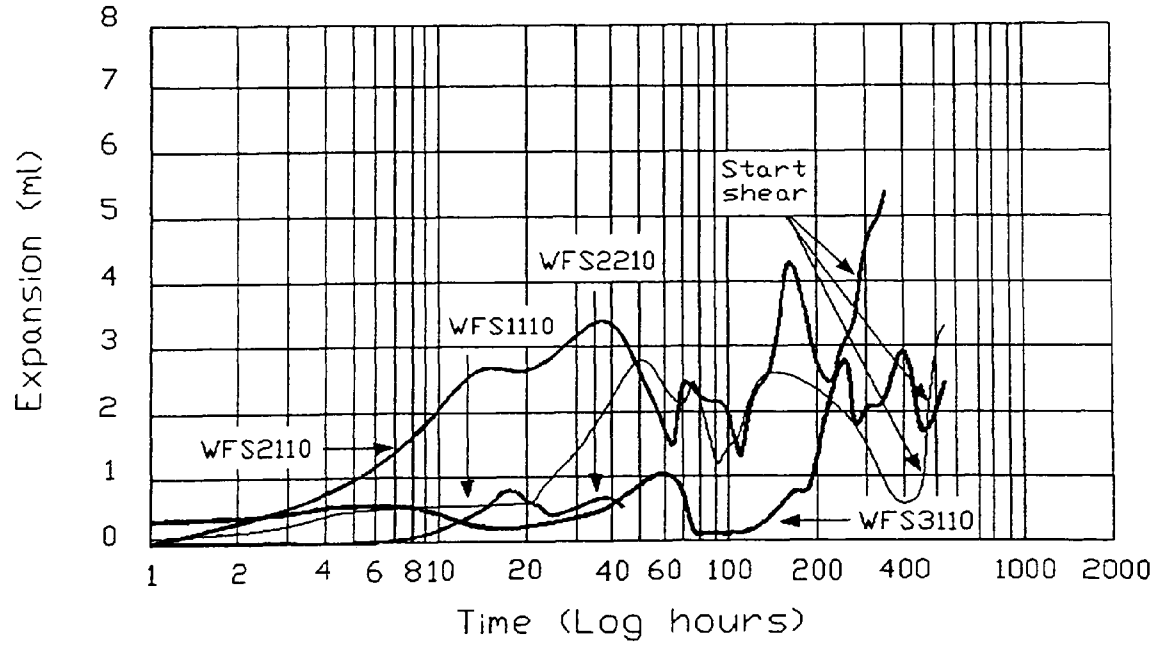

Figure 7.20 Expansion versus time by samples containing 10% montmorillonite tested in the second phase in station No. 2.

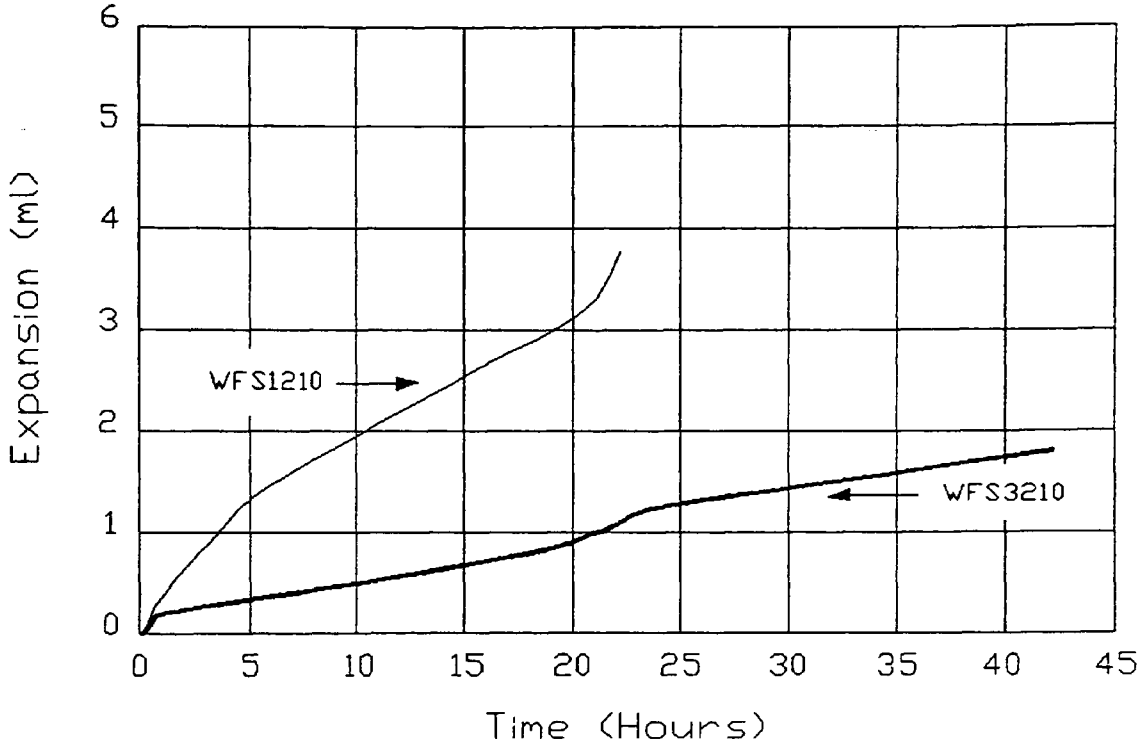

Figure 7.21 Expansion versus time by samples containing 10% montmorillonite tested in the second phase in station No. 2.

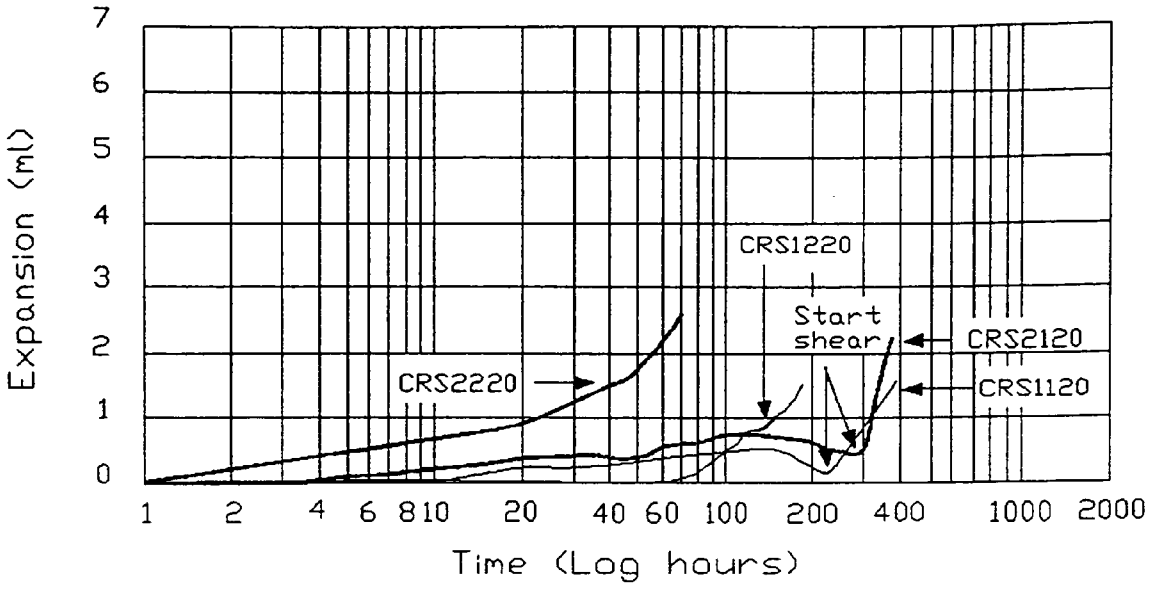

Figure 7.22 Expansion versus time by samples containing 20% montmorillonite tested in the second phase in station No. 1.

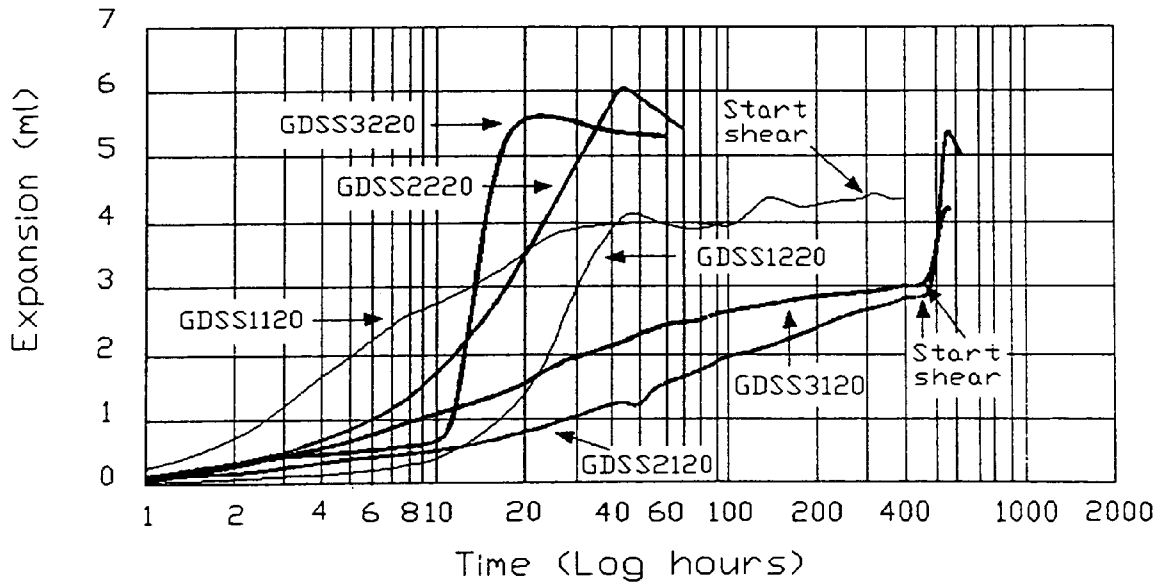

Figure 7.23 Expansion versus time by samples containing 20% montmorillonite tested in the second phase in station No. 3.

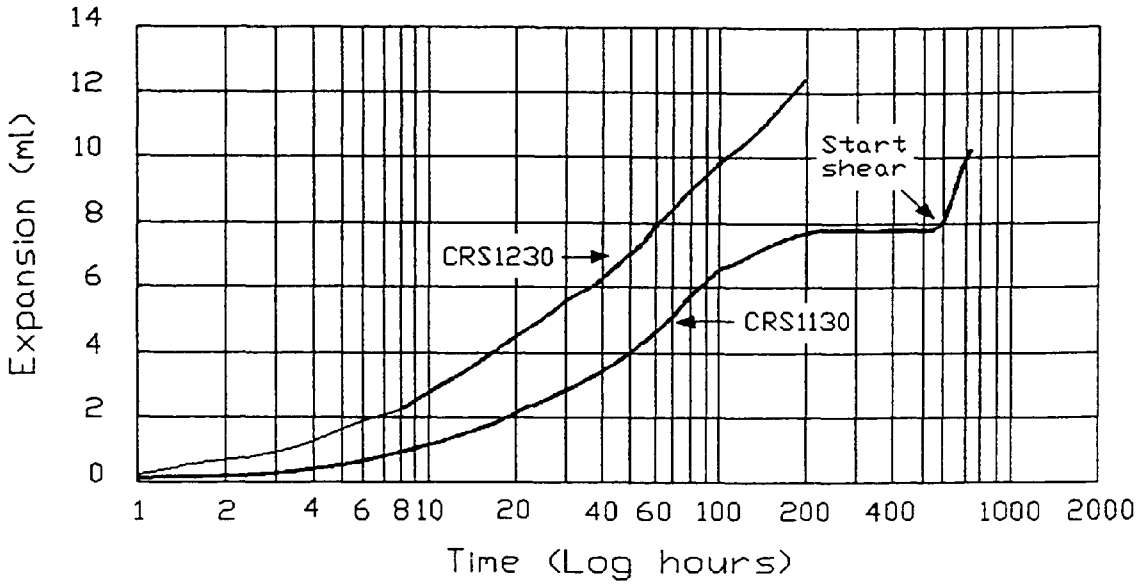

Figure 7.24 Expansion versus time by samples containing 30% montmorillonite tested in the second phase in station No. 1.

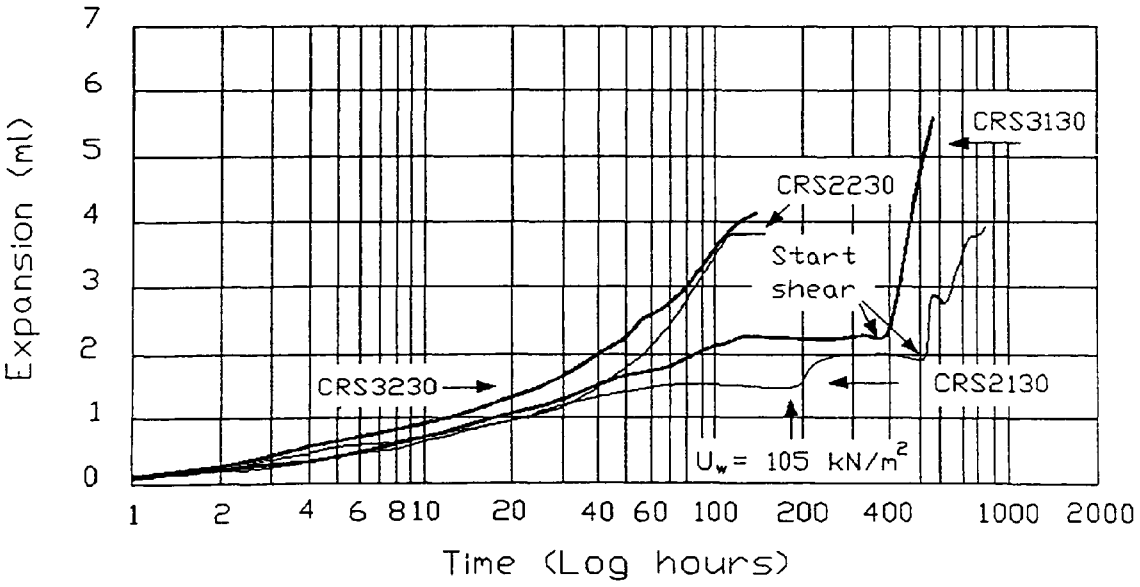

Figure 7.25 Expansion versus time by samples containing 30% montmorillonite tested in the second phase in station No. 1.

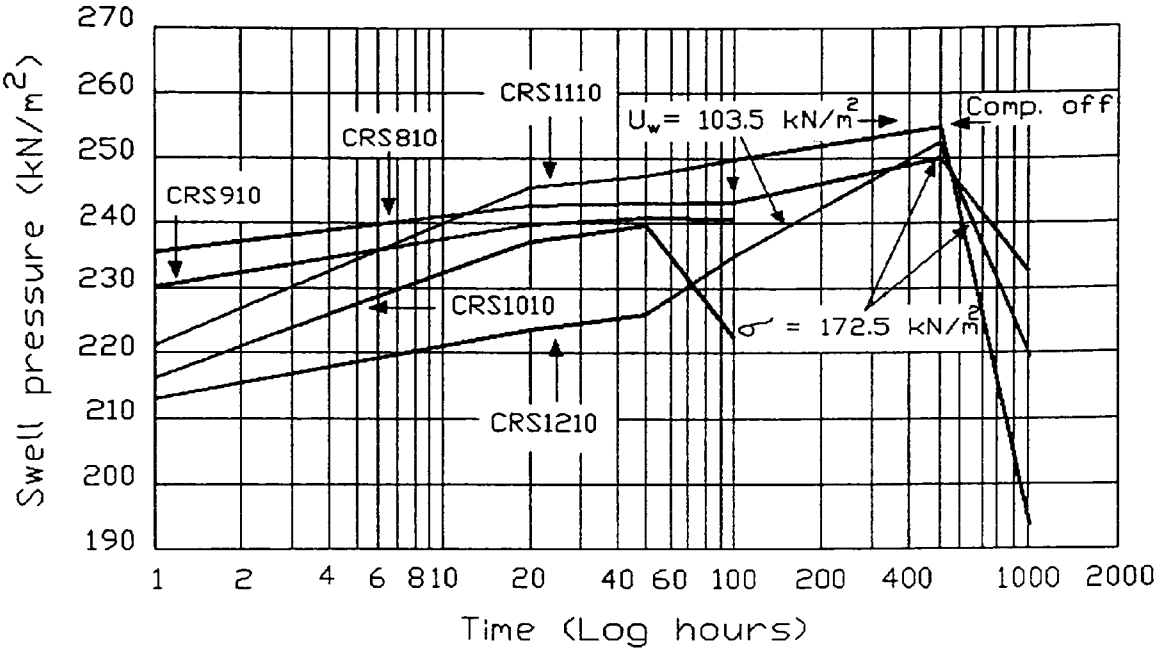

Figure 7.26 Swell pressures developed by samples containing 10% montmorillonite tested, under initial confining cell pressures of 207 kN/m^2, versus time in the first phase.

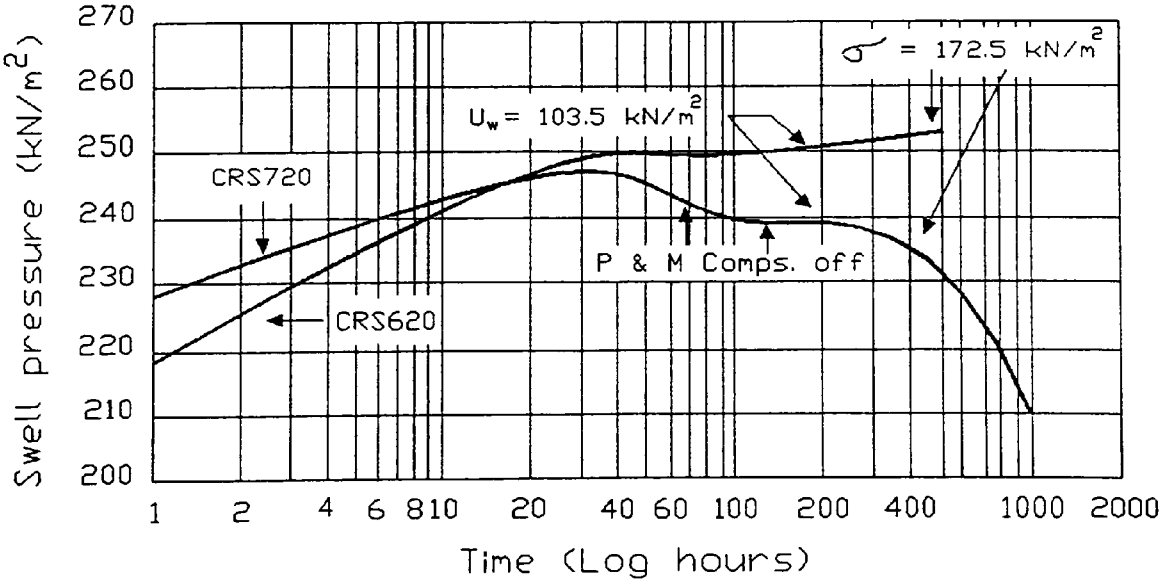

Figure 7.27 Swell pressures developed by samples containing 20% montmorillonite tested, under initial confining cell pressures of 207 kN/m^2, versus time in the first phase.

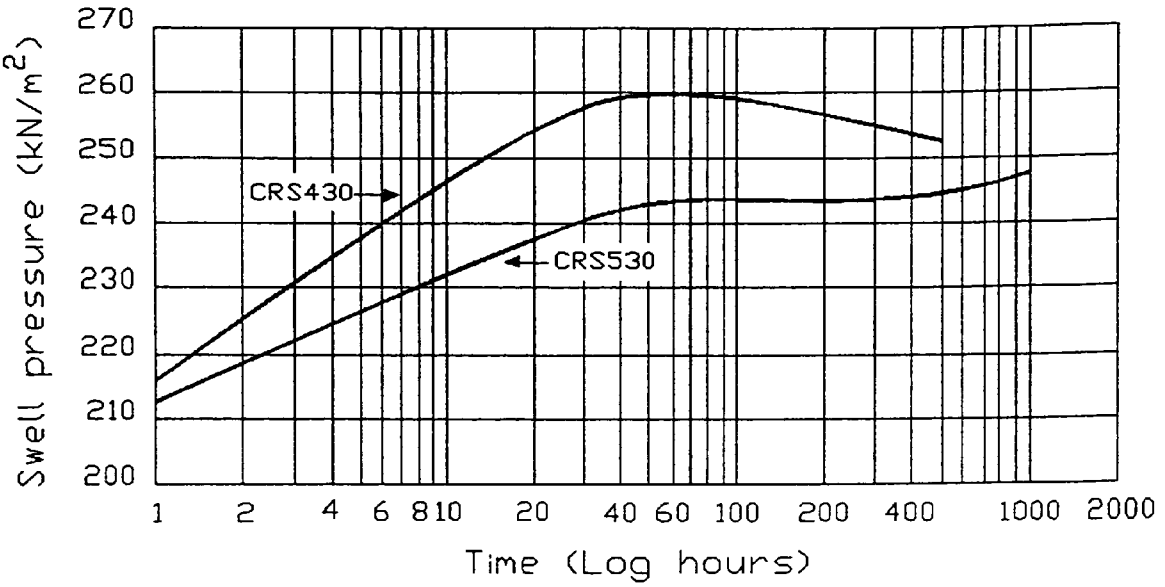

Figure 7.28 Swell pressures developed by samples containing 30% montmorillonite tested, under initial confining cell pressures of 207 kN/m^2, versus time in the first phase.

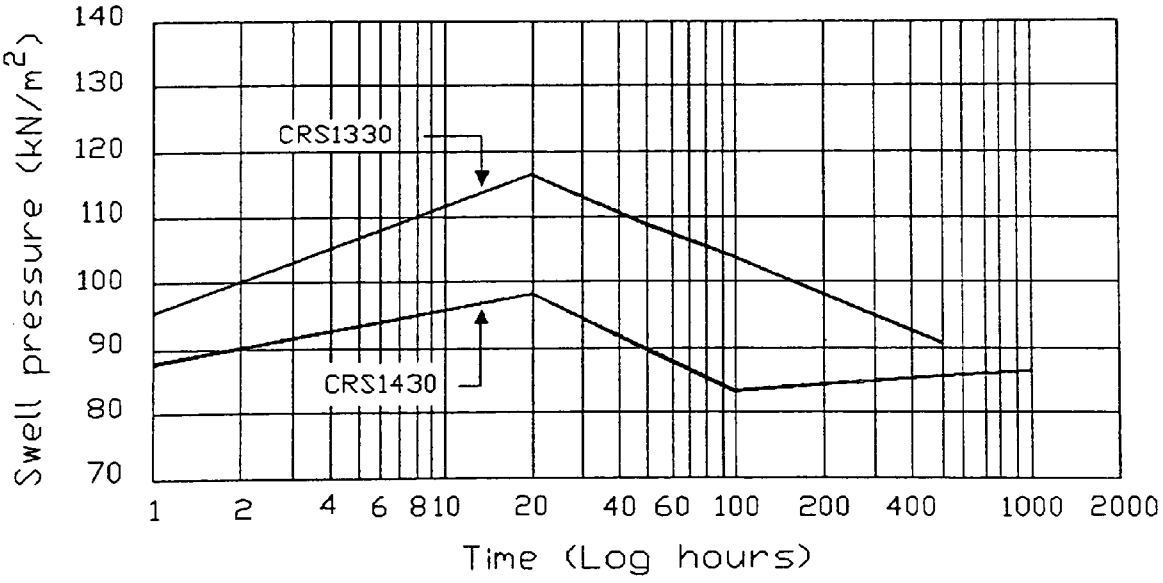

Figure 7.29 Swell pressures developed by samples containing 30% montmorillonite tested, under initial confining cell pressures of 69 kN/m^2, versus time in the first phase.

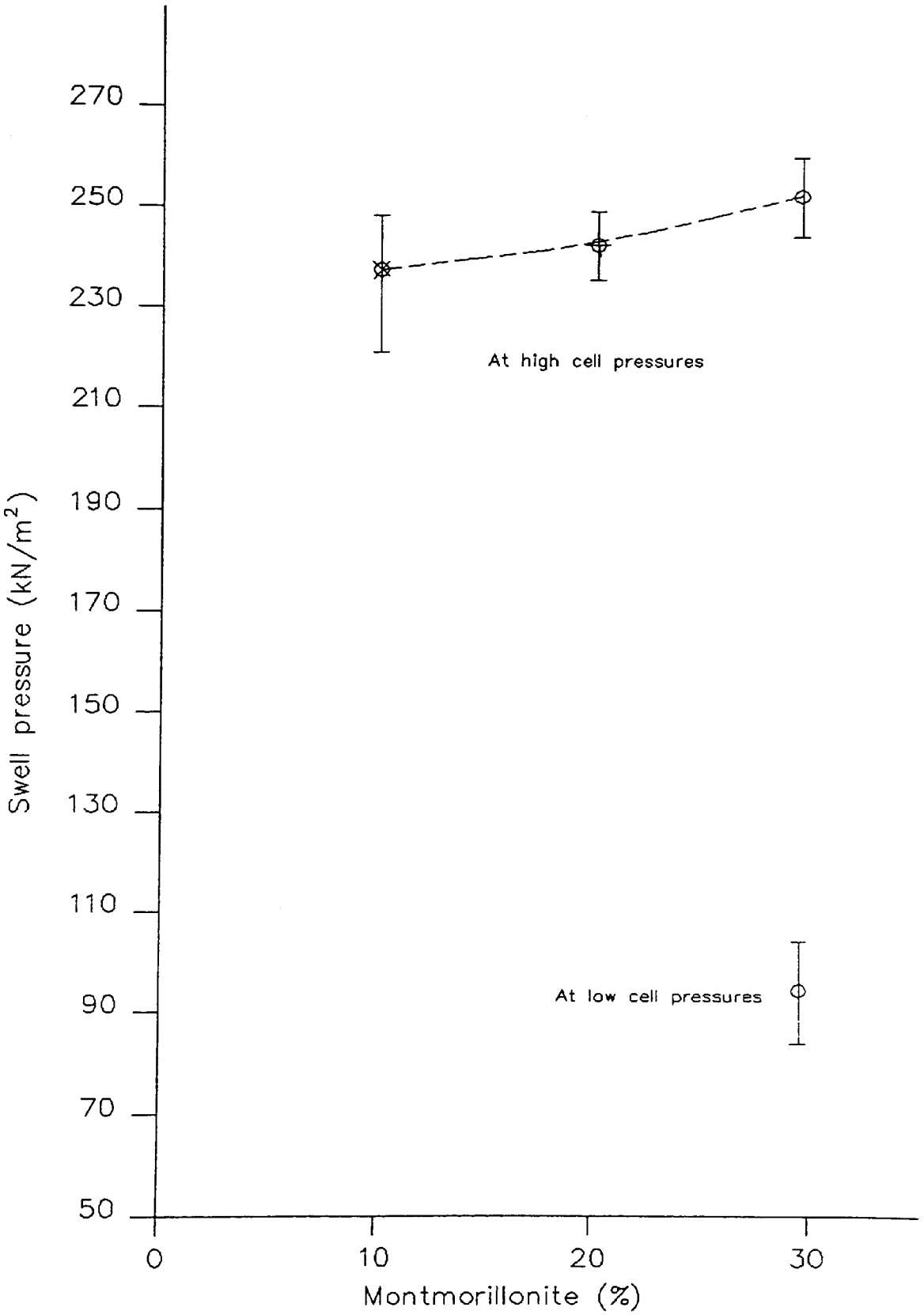

Figure 7.30 Swell pressures after 100 hours for 10%, 20% and 30% montmorillonite content tested under initial confining cell pressures of 207 and 69 kN/m^2 in the first phase.

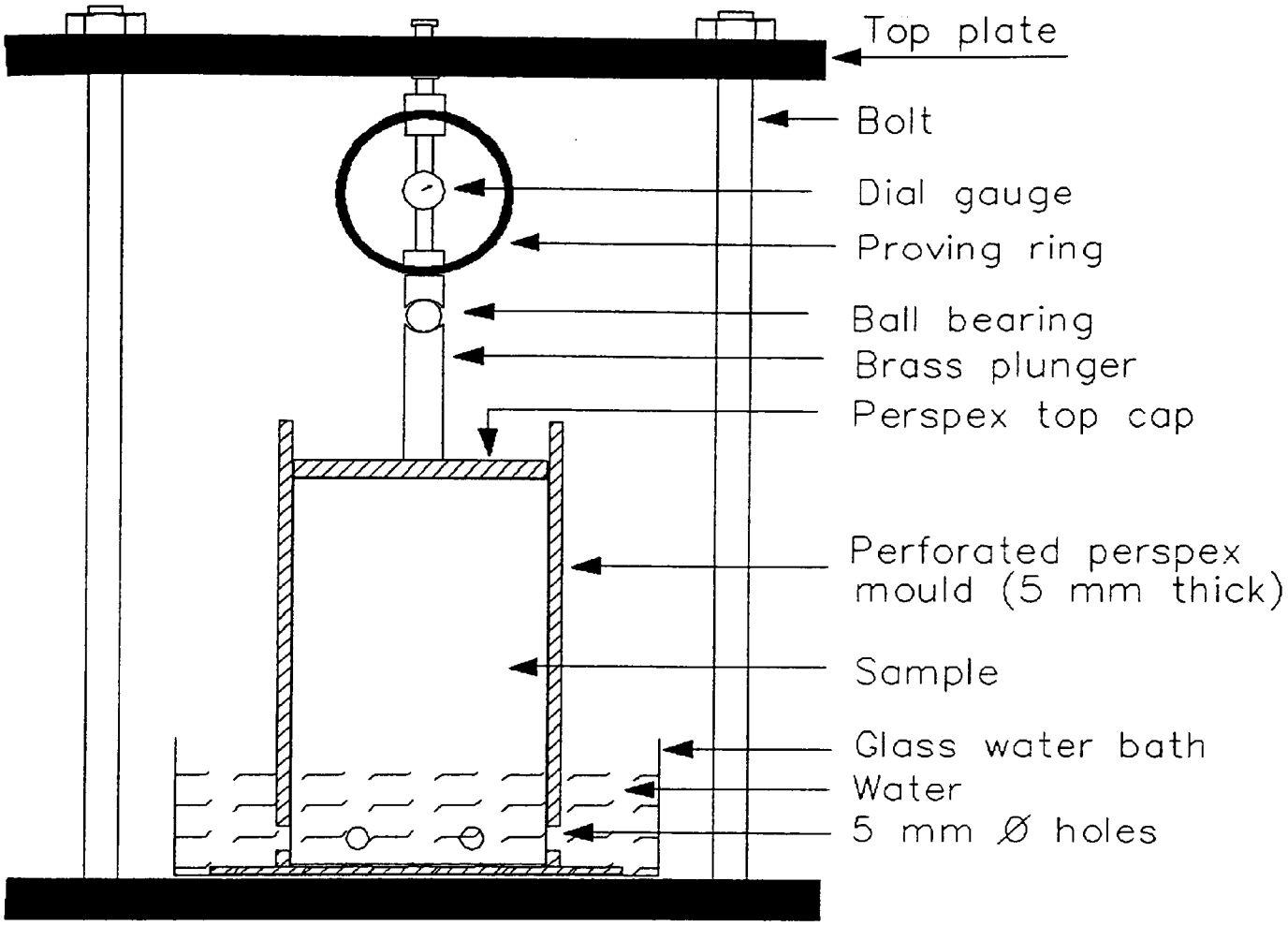

Figure 7.31 Apparatus for the measurement of swell pressure under no confining pressure (After Abdi (1992)).

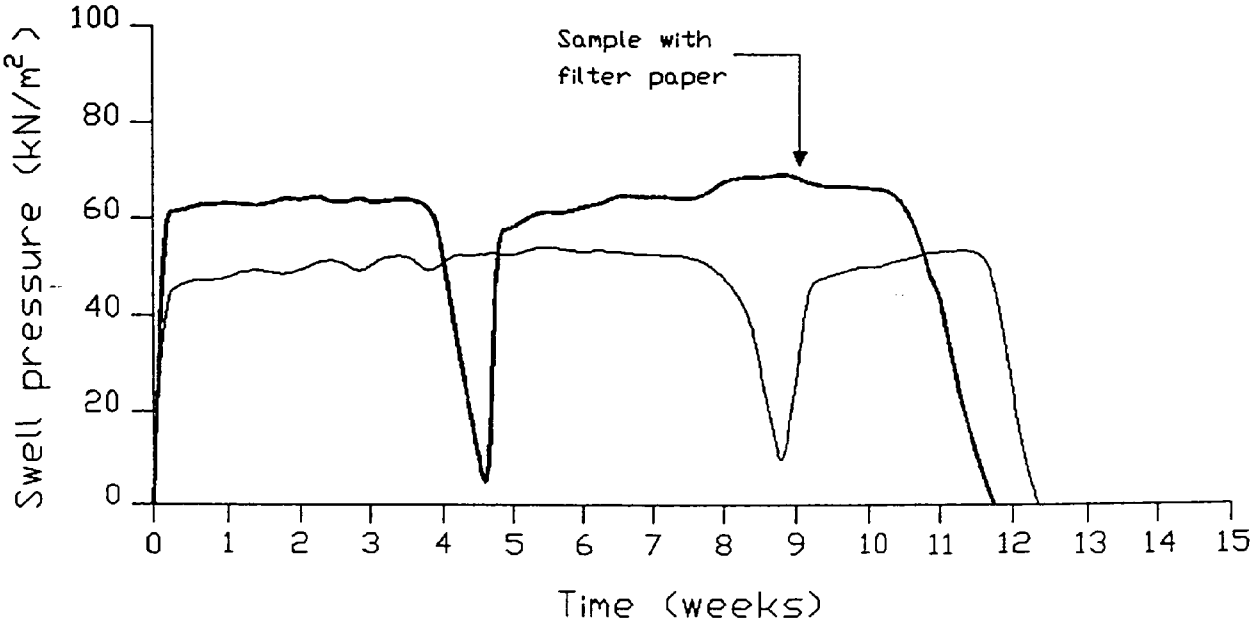

Figure 7.32 Swell pressures developed by two samples containing 10% montmorillonite, using Abdi's (1992) apparatus, under no confining pressure.

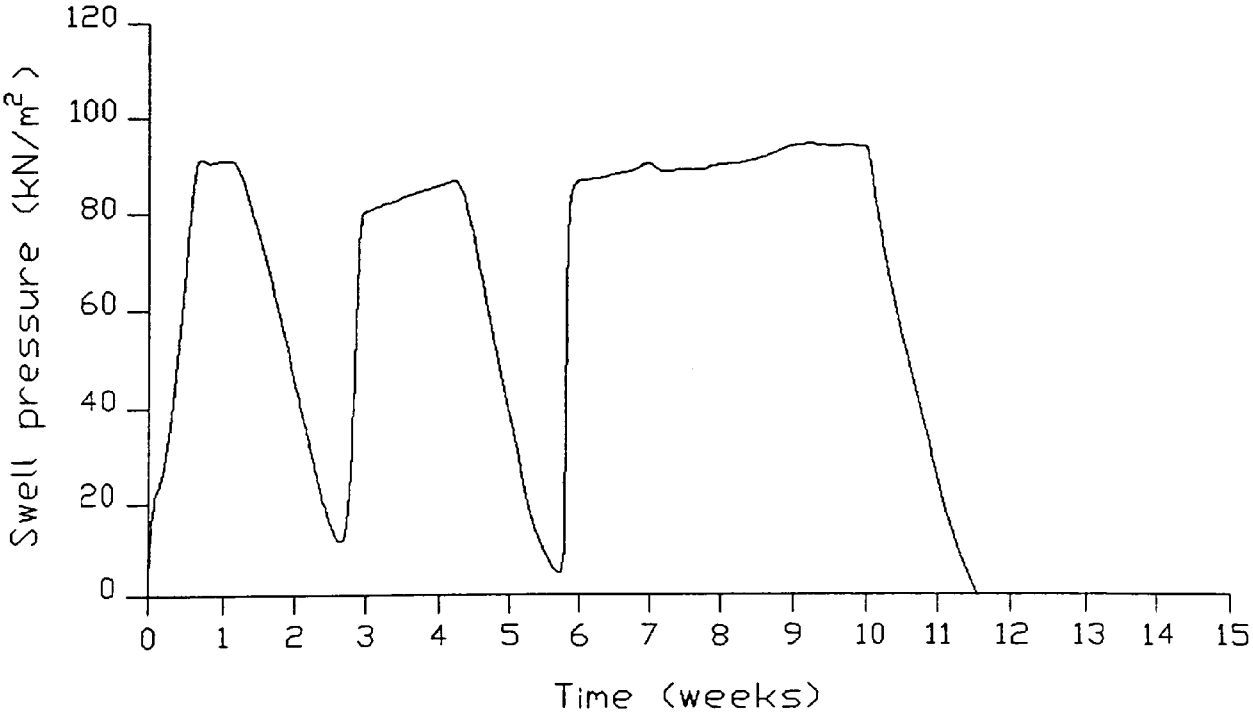

Figure 7.33 Swell pressure developed by a sample containing 20% montmorillonite, using Abdi's (1992) apparatus, under no confining pressure.

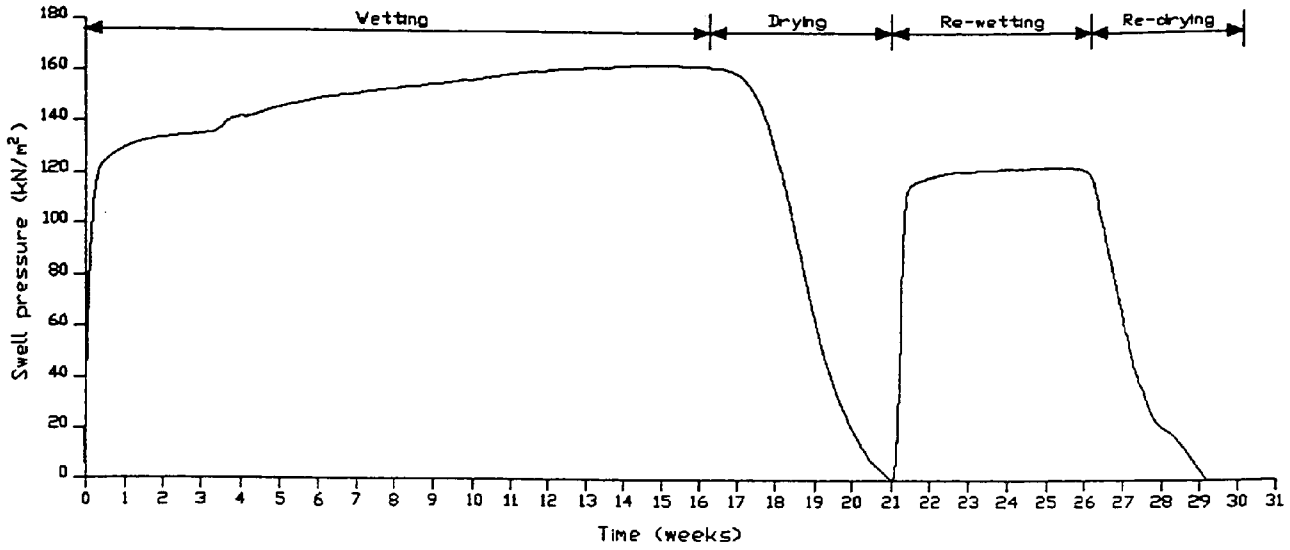

Figure 7.34a

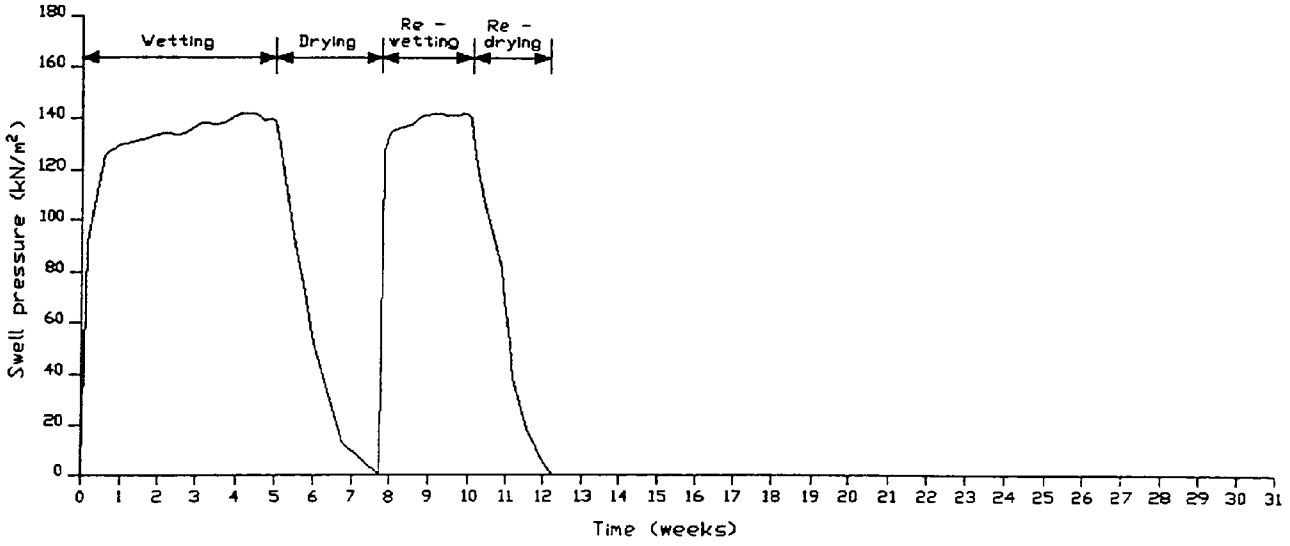

Figure 7.34b

Figures 7.34a and 7.34b Swell pressures developed by two samples containing 30% montmorillonite, using Abdi's (1992) apparatus, under no confining pressure.

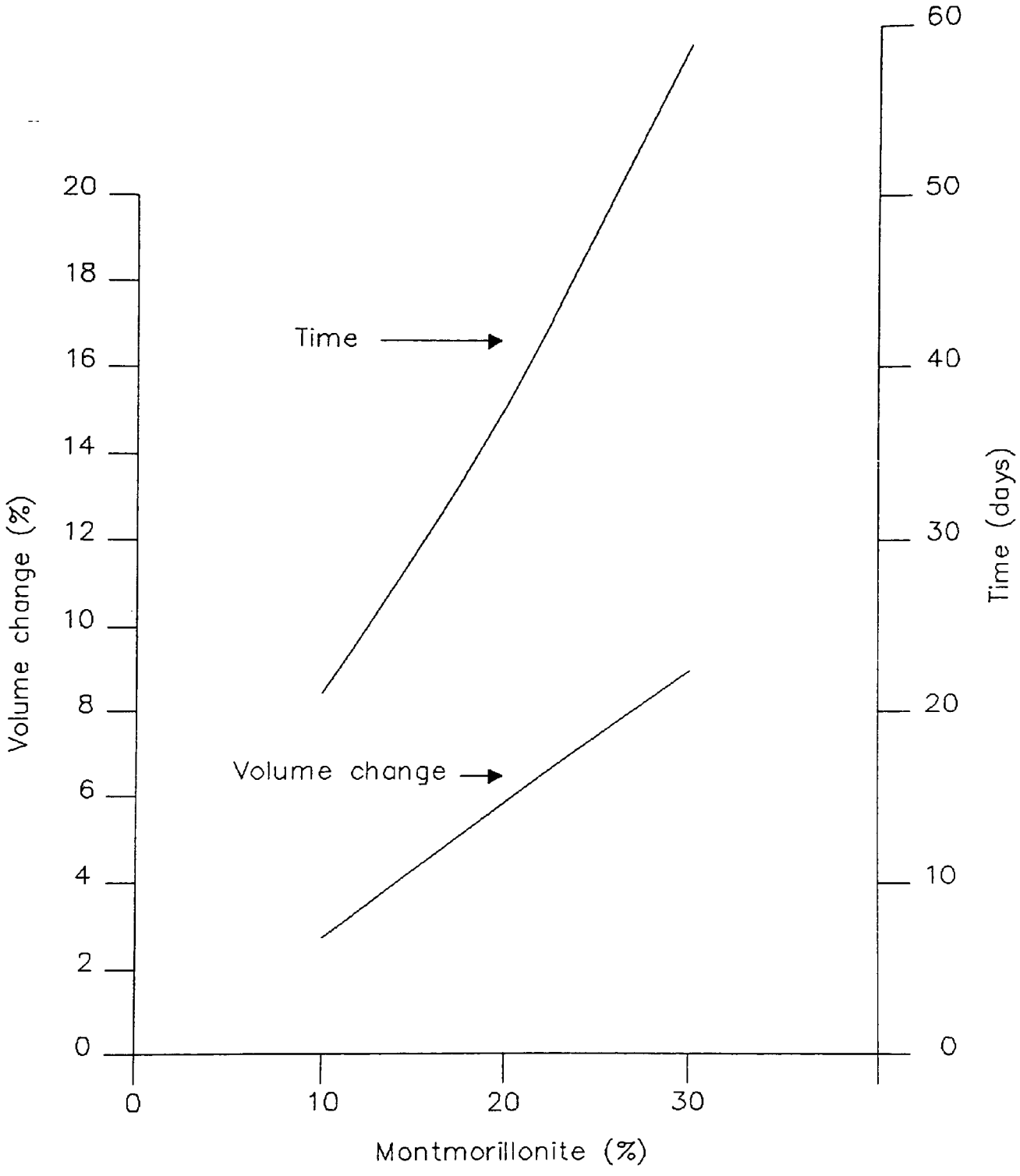

Figure 7.35 Volume changes and duration by samples containing 10%, 20% and 30% montmorillonite tested in the first phase. The volume changes were measured after the samples were removed from the cell and free swell occurred.

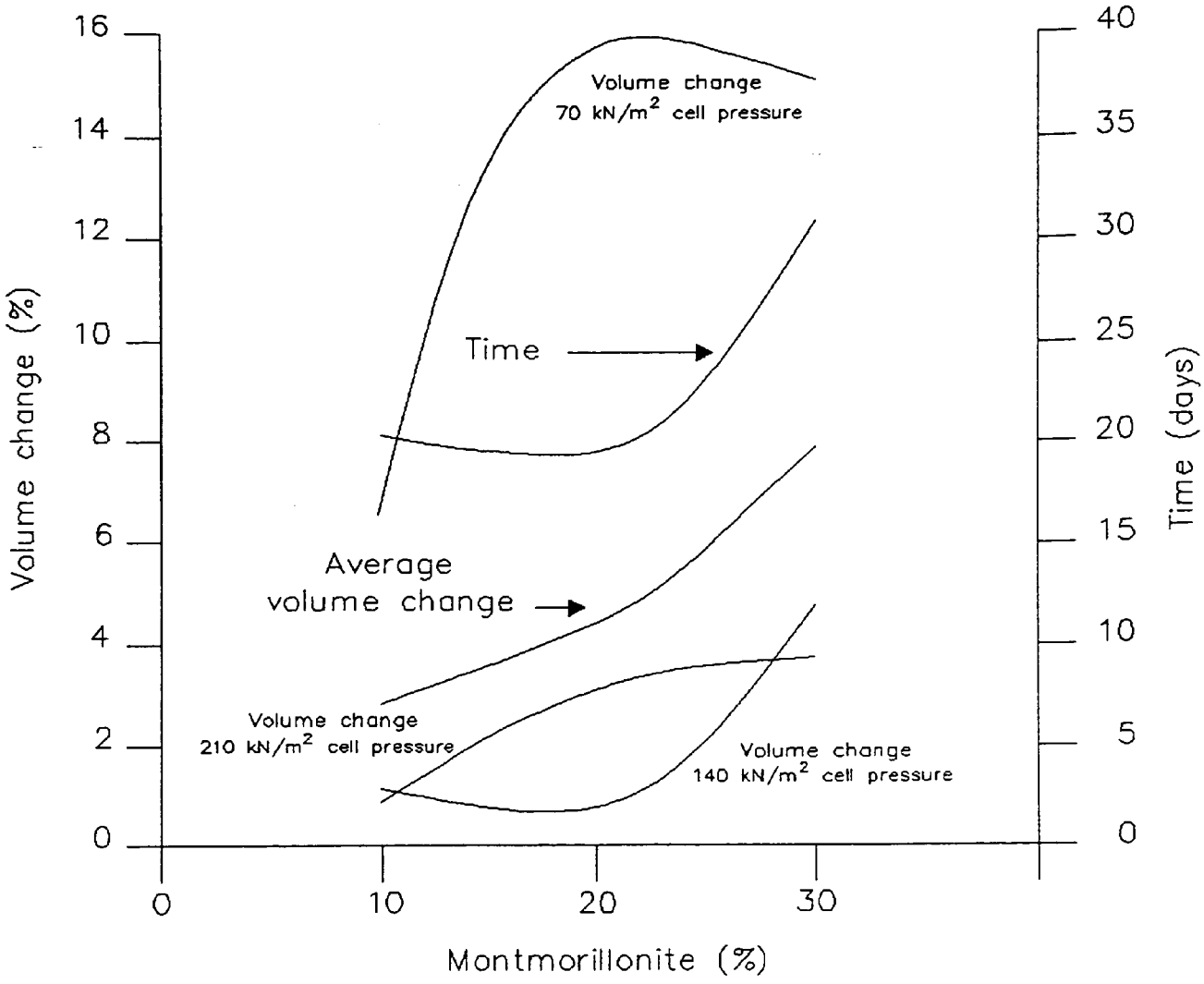

Figure 7.36 Volume changes and duration by samples containing 10%, 20% and 30% montmorillonite tested in the second phase. The volume changes were measured after the samples were removed from the cell and free swell occurred.

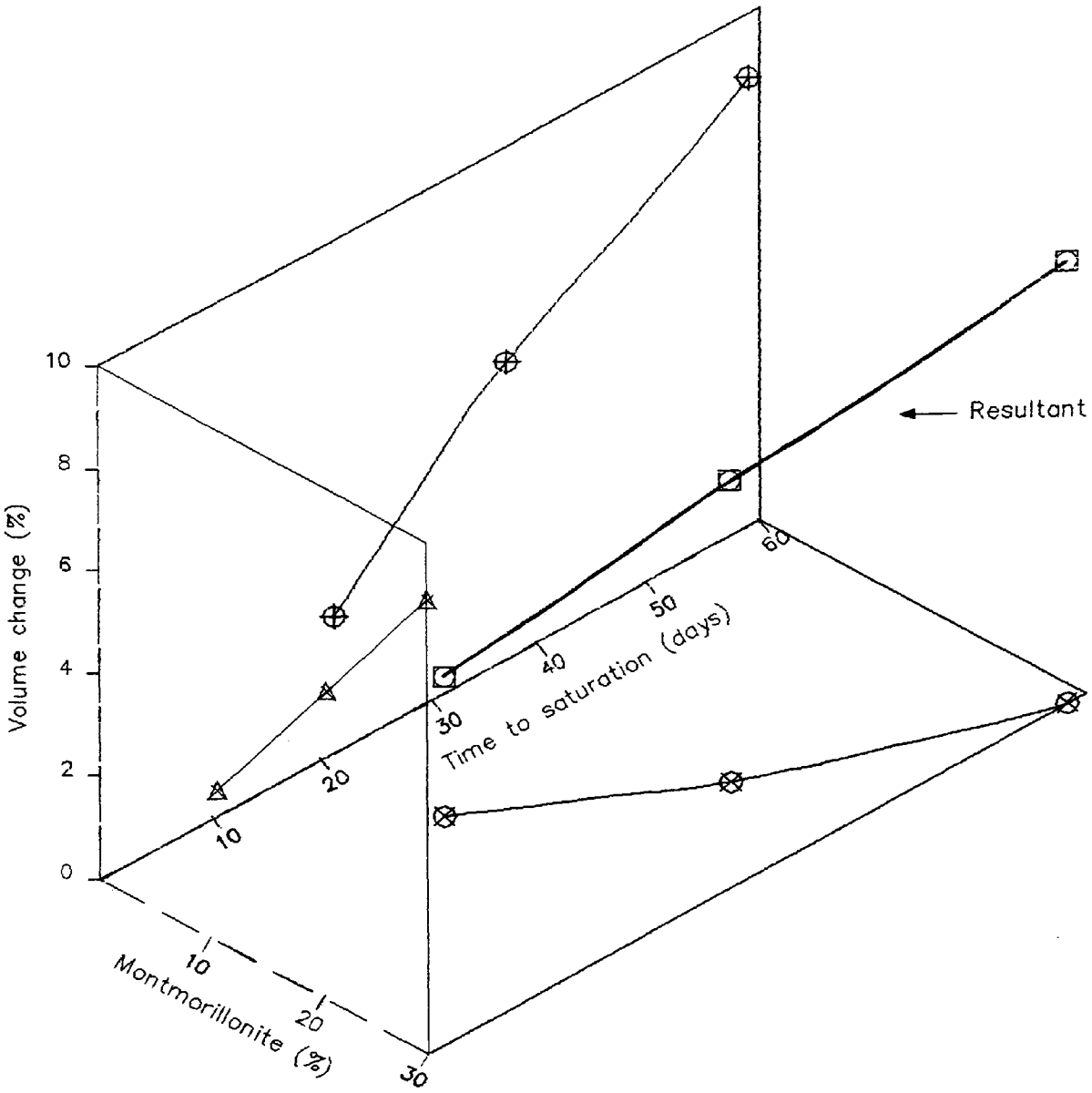

Figure 7.37 Three dimensional relationship of average volume changes, time to saturation and the montmorillonite content of samples tested in the first phase. The volume changes were measured after the samples were removed from the cell and free swell occurred.

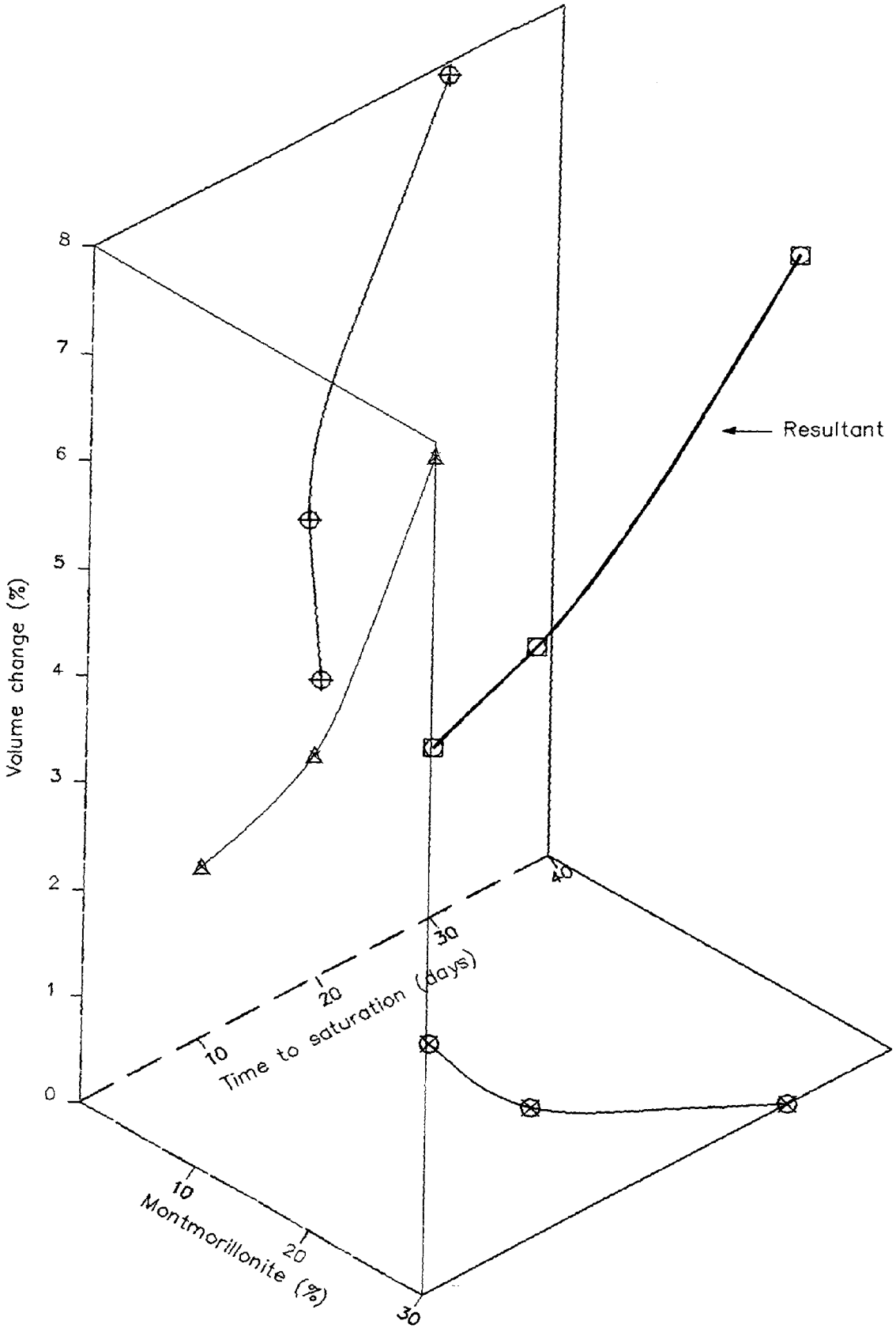

Figure 7.38 Three dimensional relationship of average volume changes, time to saturation and the montmorillonite content of samples tested in the second phase. The volume changes were measured after the samples were removed from the cell and free swell occurred.

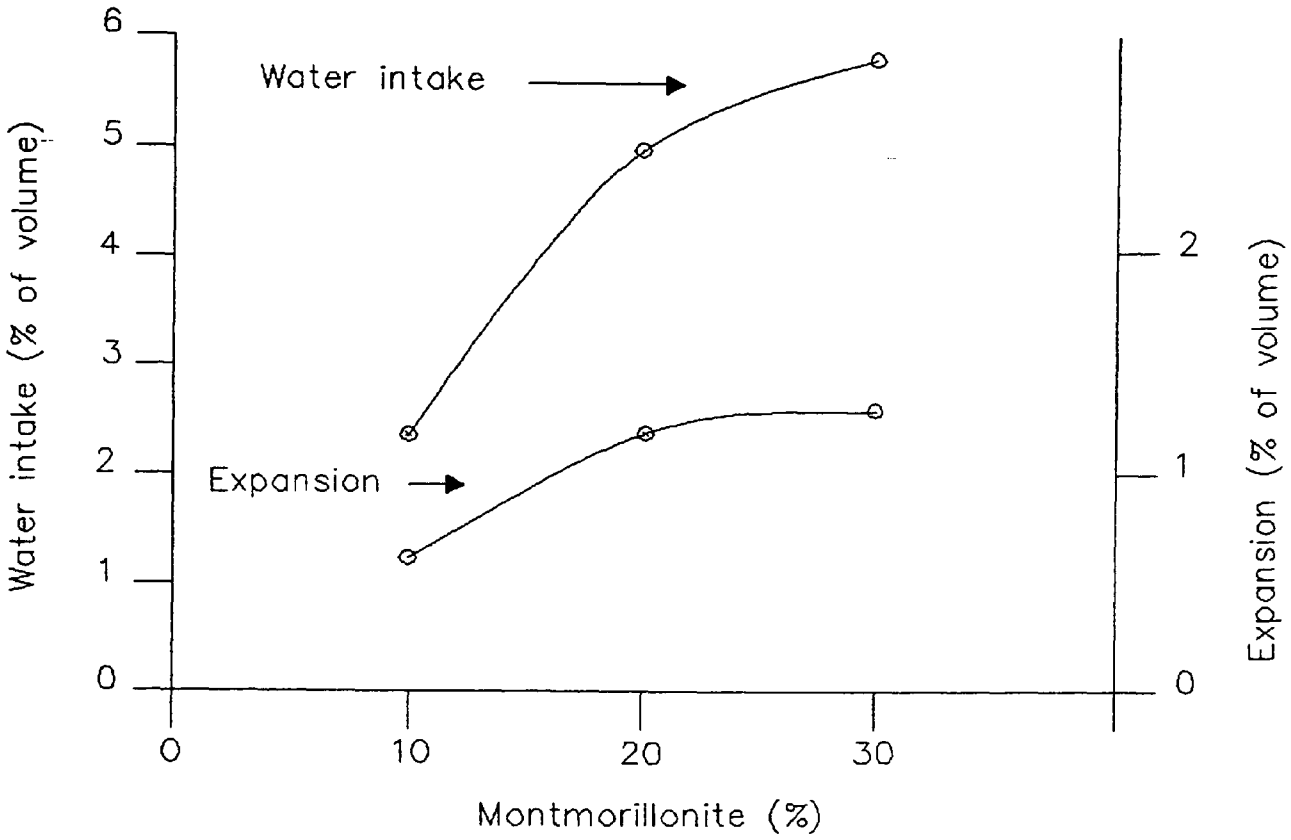

Figure 7.39 Water intake and expansion, measured by the Bishop water volume change indicators, by samples in the first phase under 207 kN/m^2 confining cell pressures.

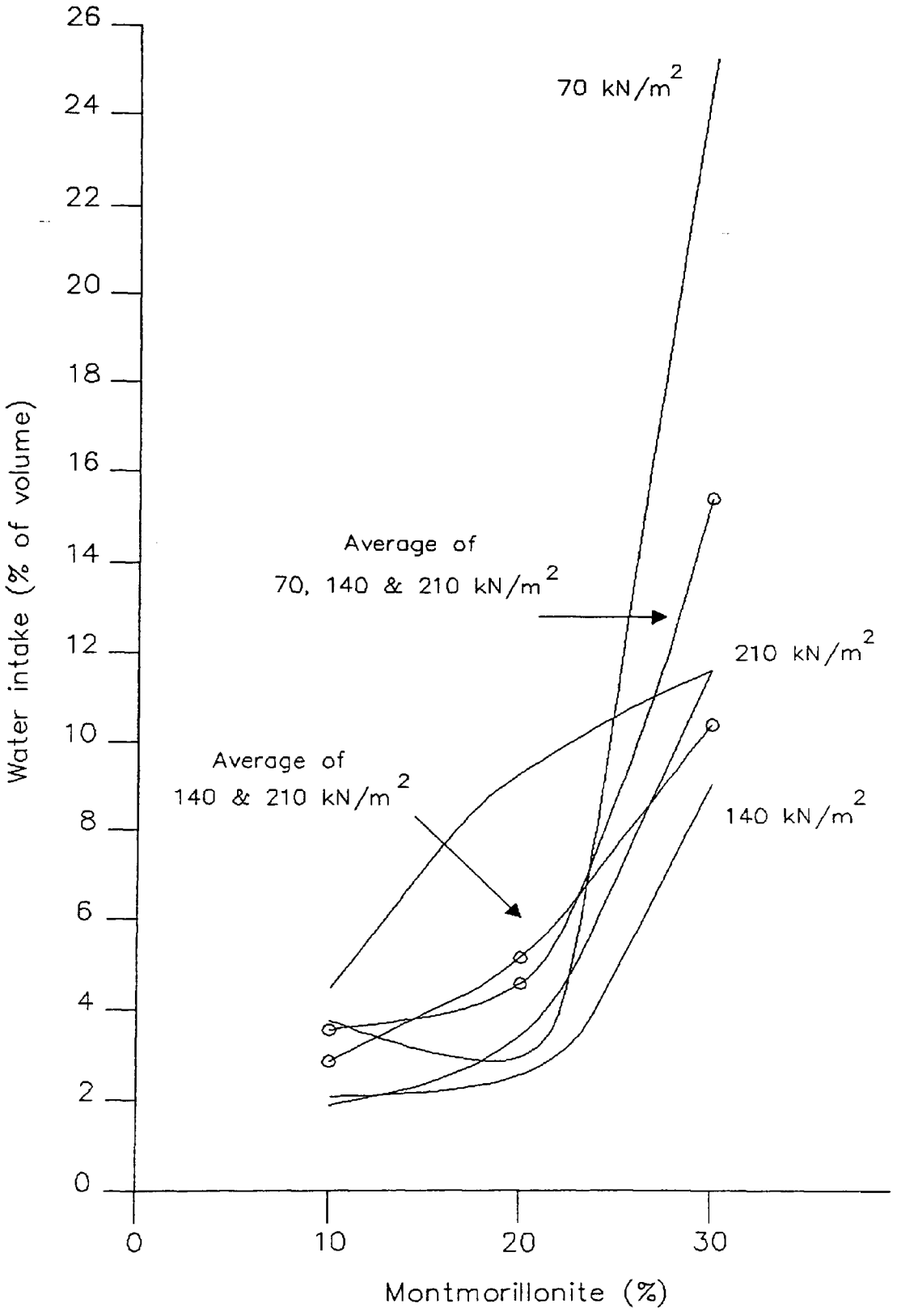

Figure 7.40 Water intake, measured by the Bishop water volume change indicator, by samples in the second phase.

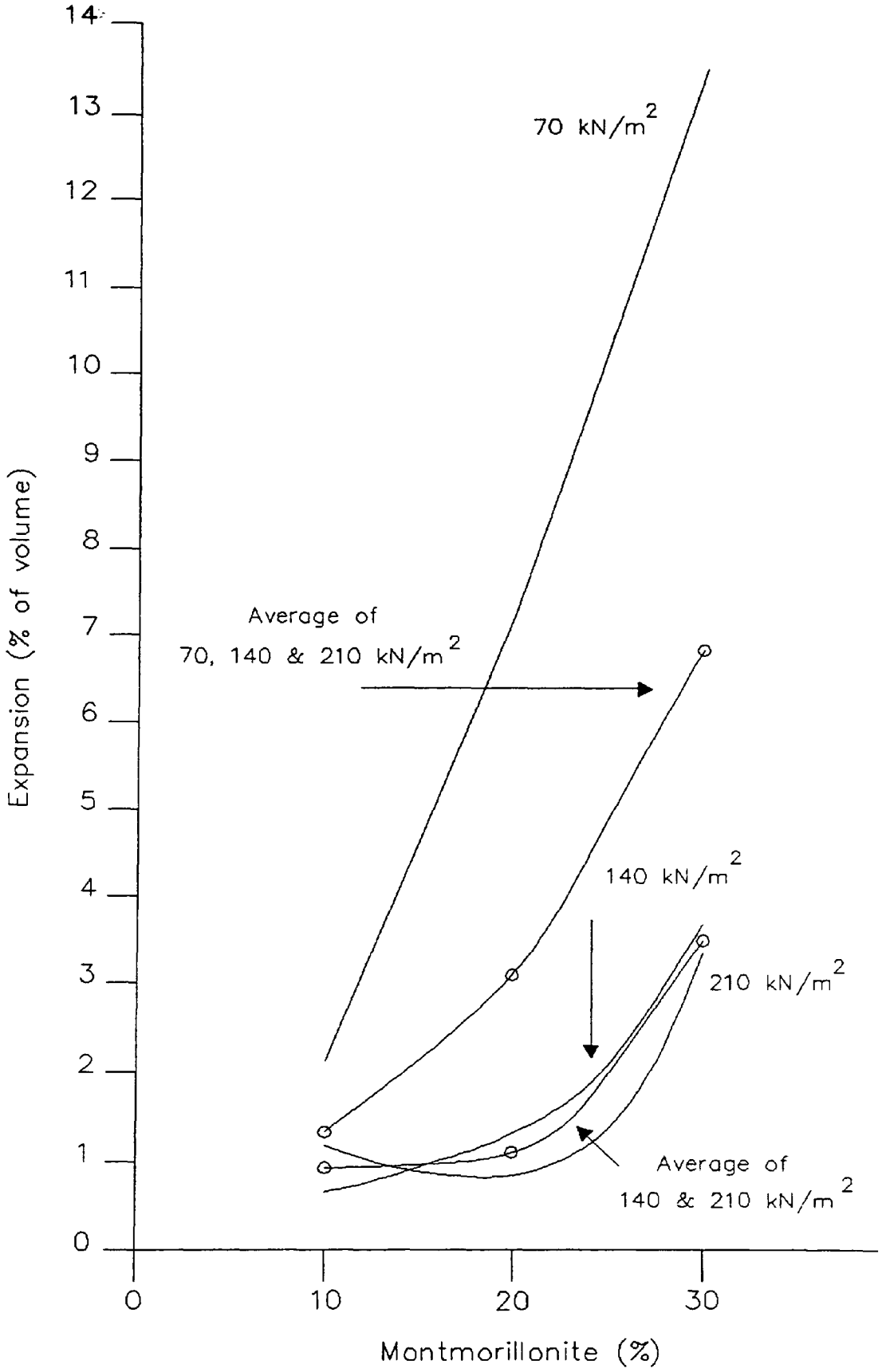

Figure 7.41 Expansion, measured by the Bishop water volume change indicator, by samples in the second phase.

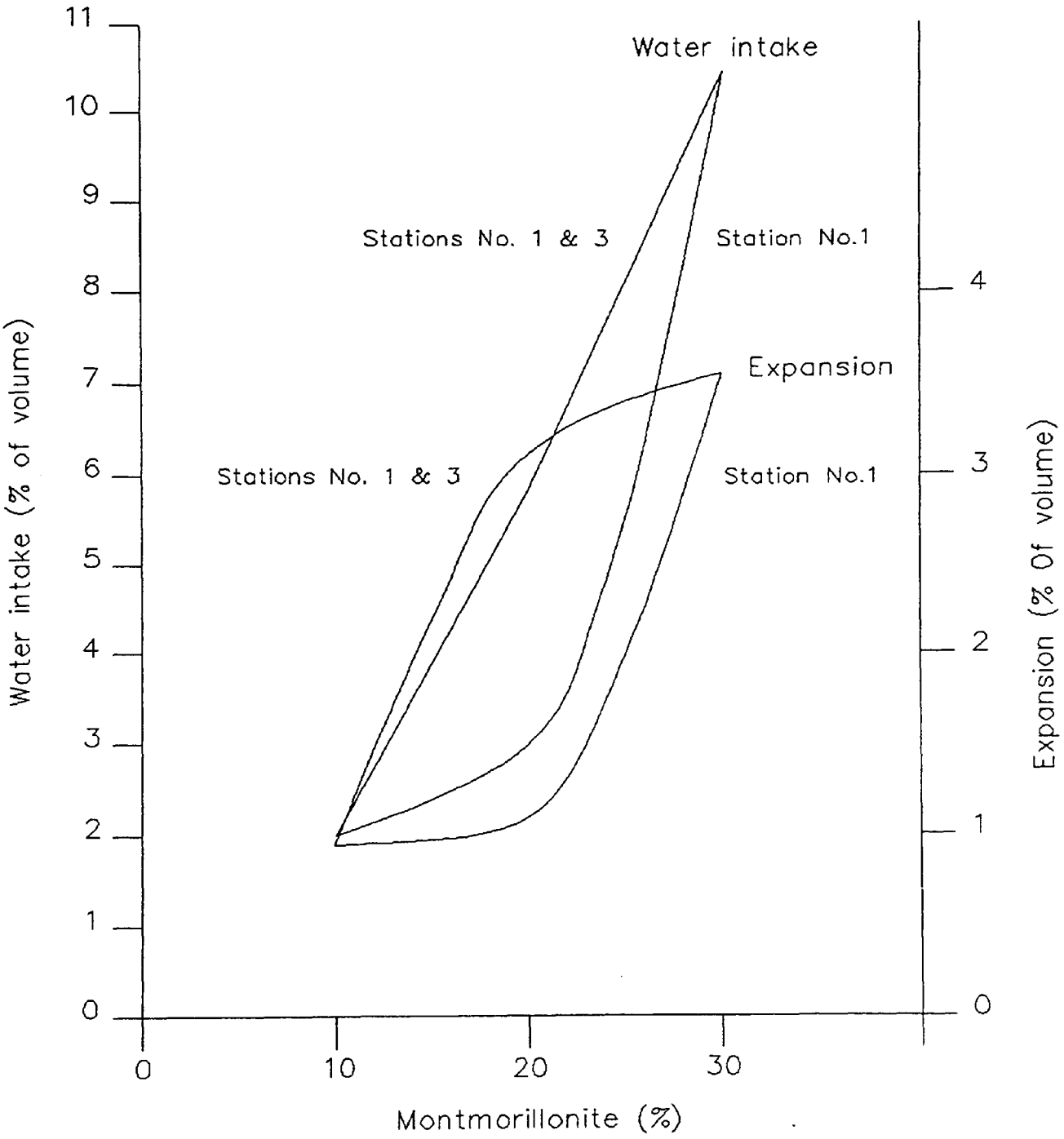

Figure 7.42 Water intake and expansion, measured by the Bishop water volume change indicators, by samples tested in the second phase.

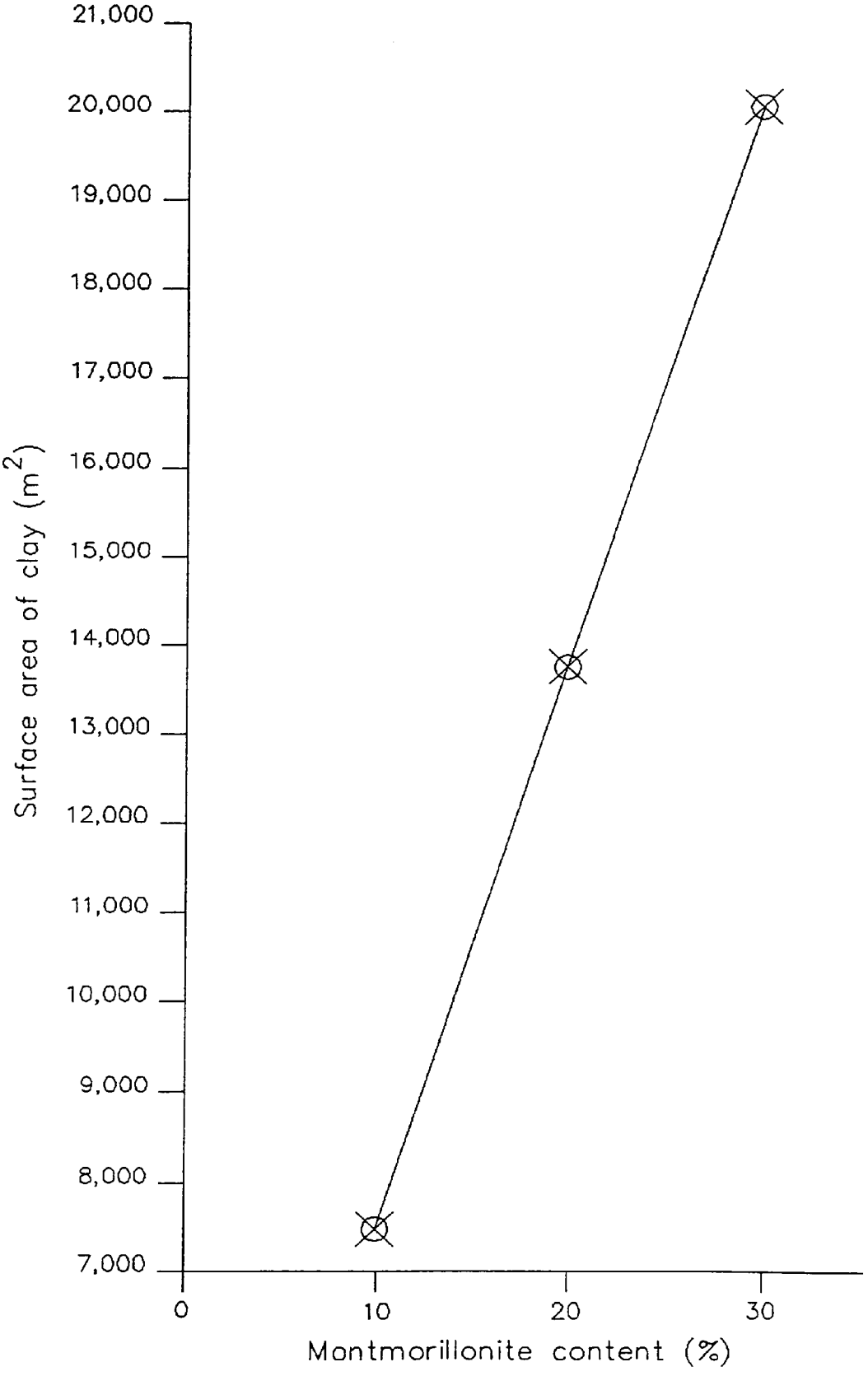

Figure 7.43 Linear relationship between the dry surface area of kaolinite and montmorillonite versus the increasing proportions of montmorillonite.

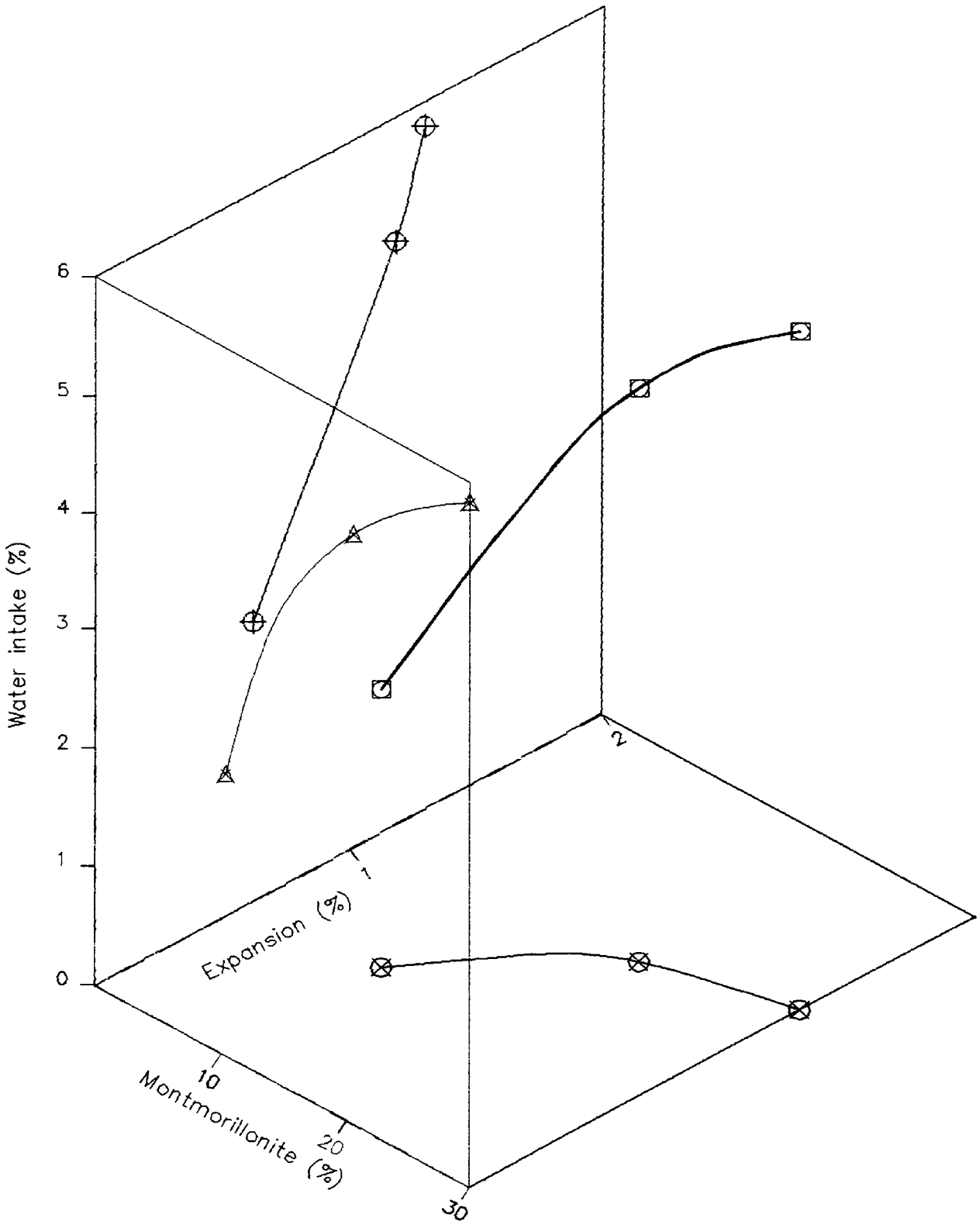

Figure 7.44 Three dimensional relationship of water intake and expansion, measured by the Bishop water volume change indicators, and the montmorillonite content by samples in the first phase under 207 kN/m^2 confining cell pressures.

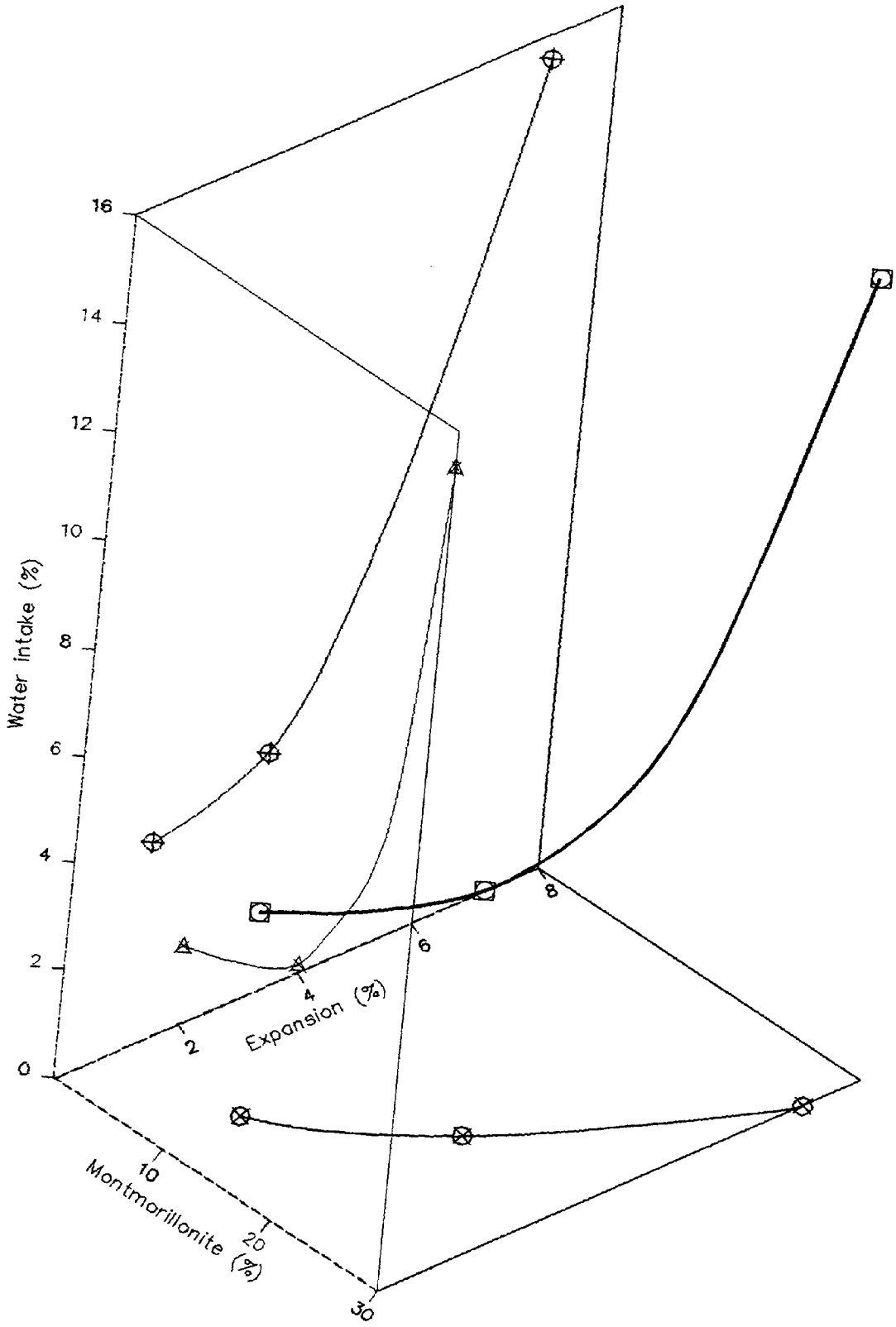

Figure 7.45 Three dimensional relationship of water intake and expansion, measured by the Bishop water volume change indicators, and the montmorillonite content by samples in the second phase. The values represent averages of 70, 140 and 210 kN/m^2 confining cell pressures.

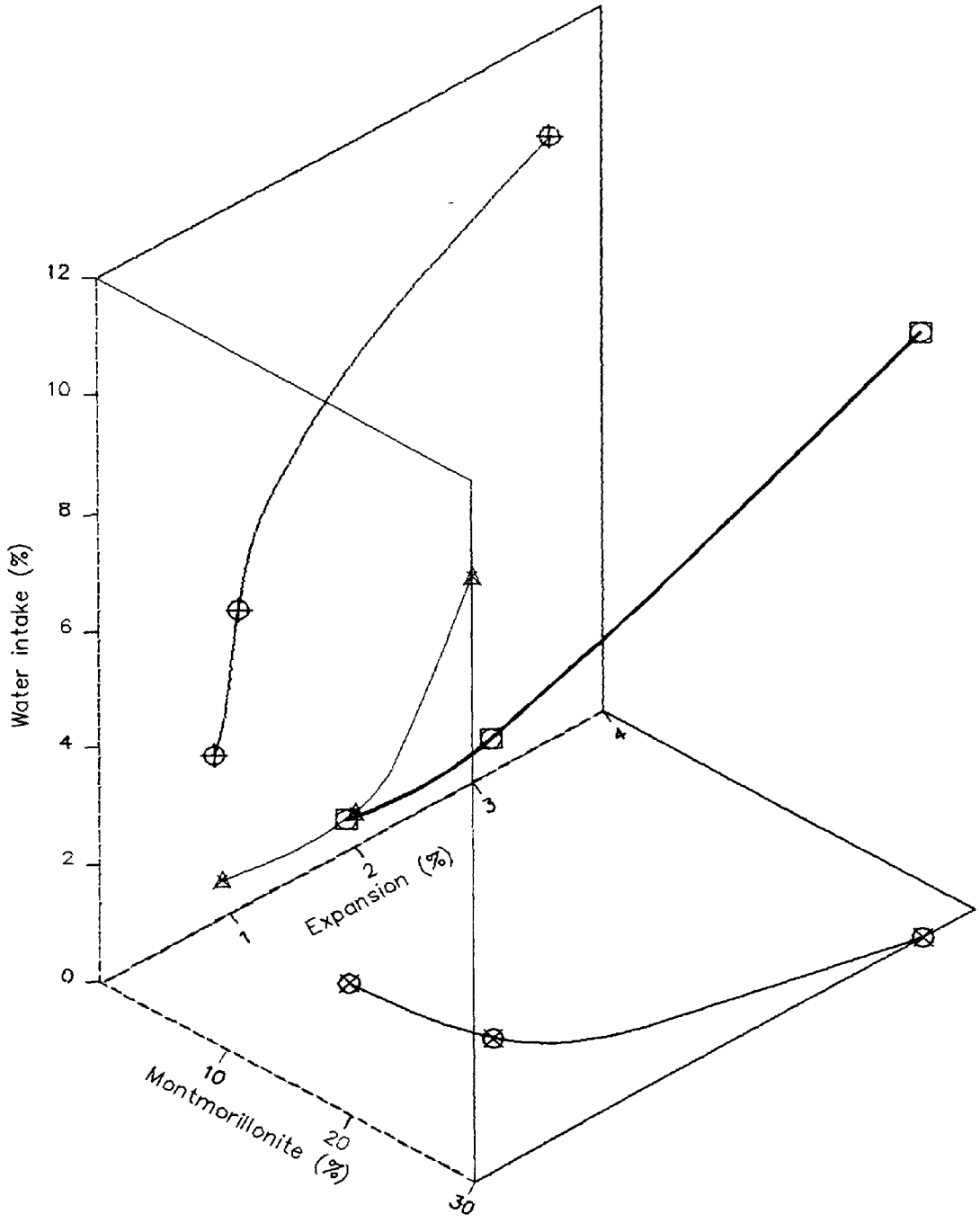

Figure 7.46 Three dimensional relationship of water intake and expansion, measured by the Bishop water volume change indicators, and the montmorillonite content by samples in the second phase. The values represent averages of 140 and 210 kN/m^2 confining cell pressures.

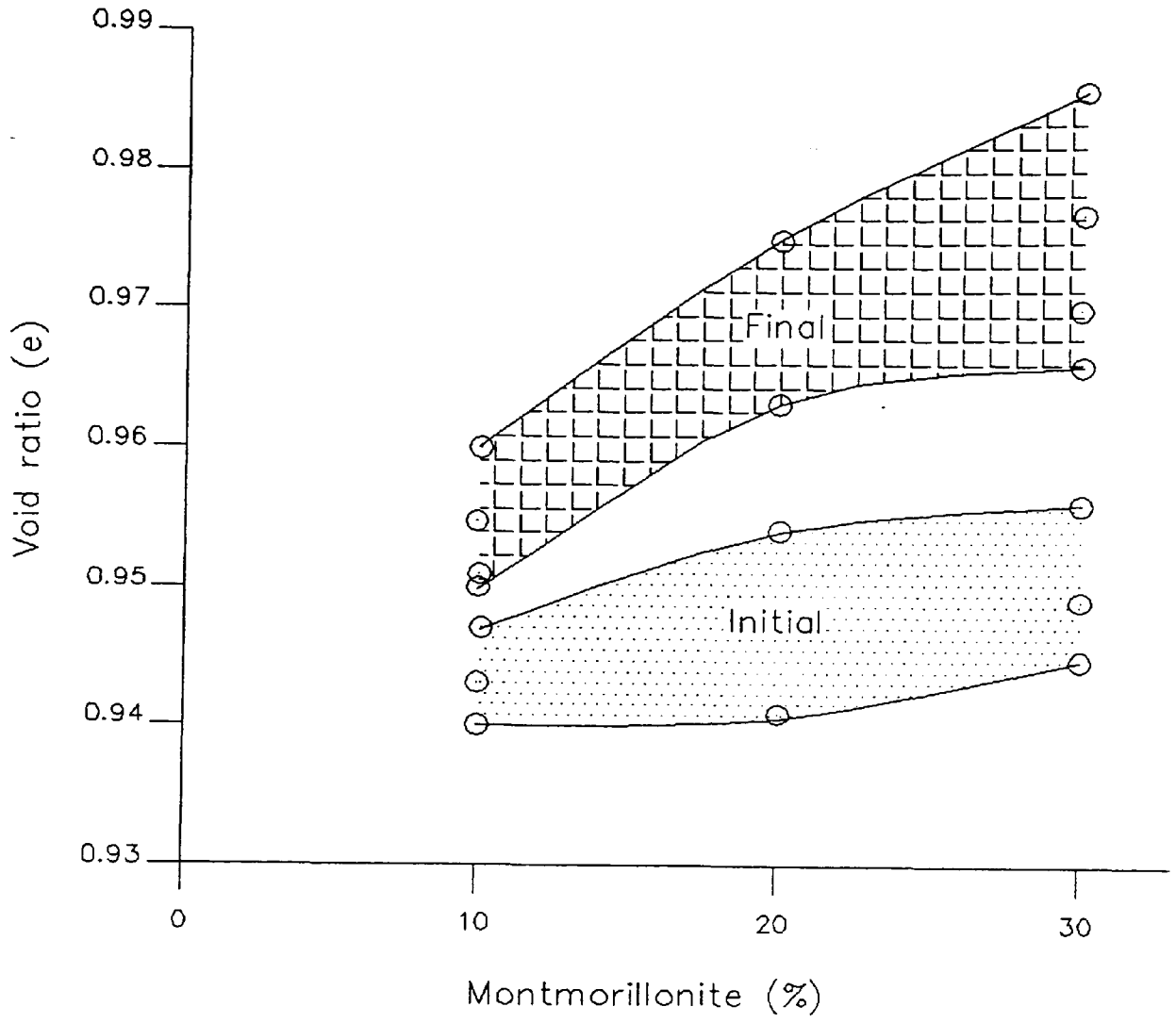

Figure 7.47 Initial and final void ratios for samples tested in the first phase.

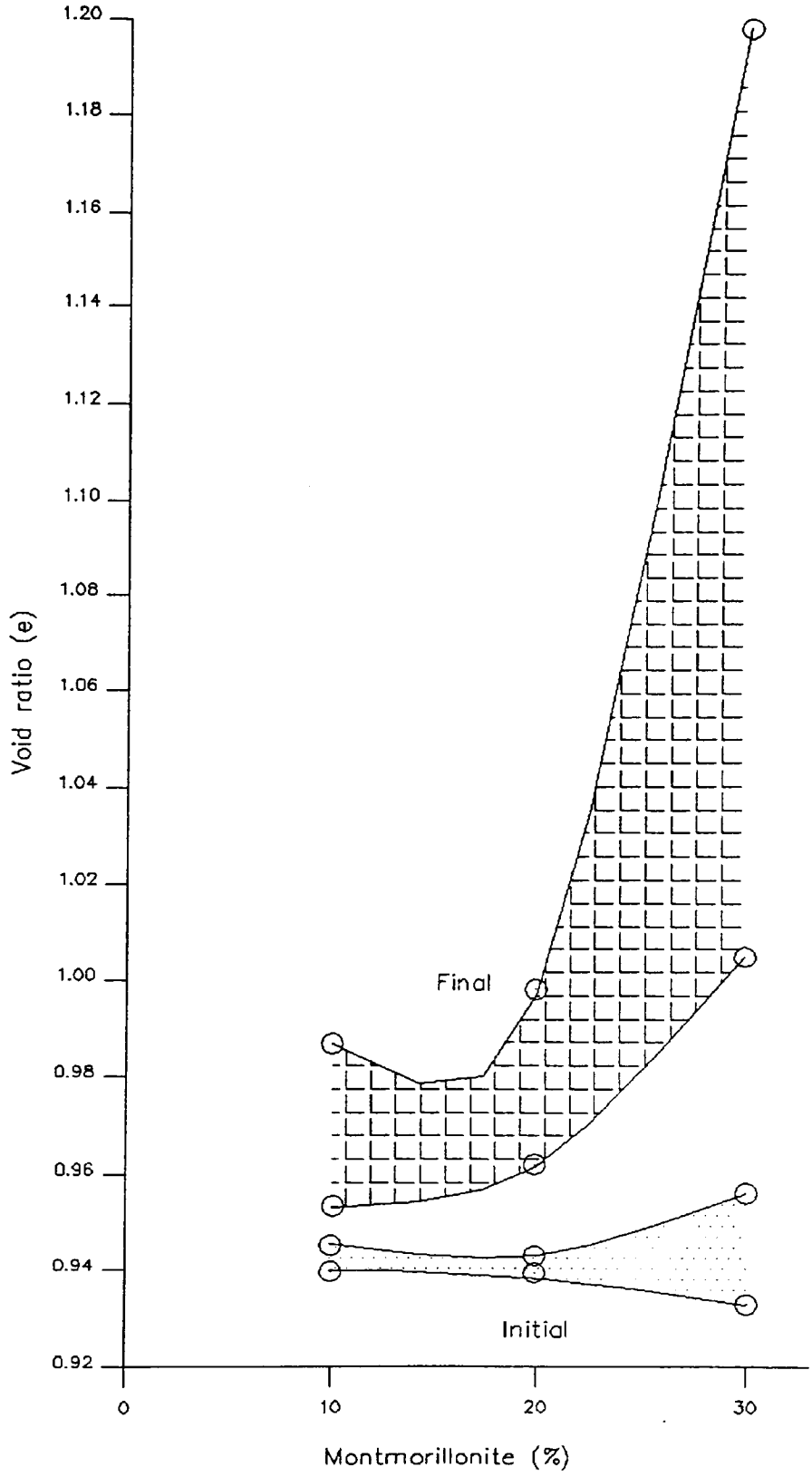

Figure 7.48 Initial and final void ratios for samples tested in the second phase.

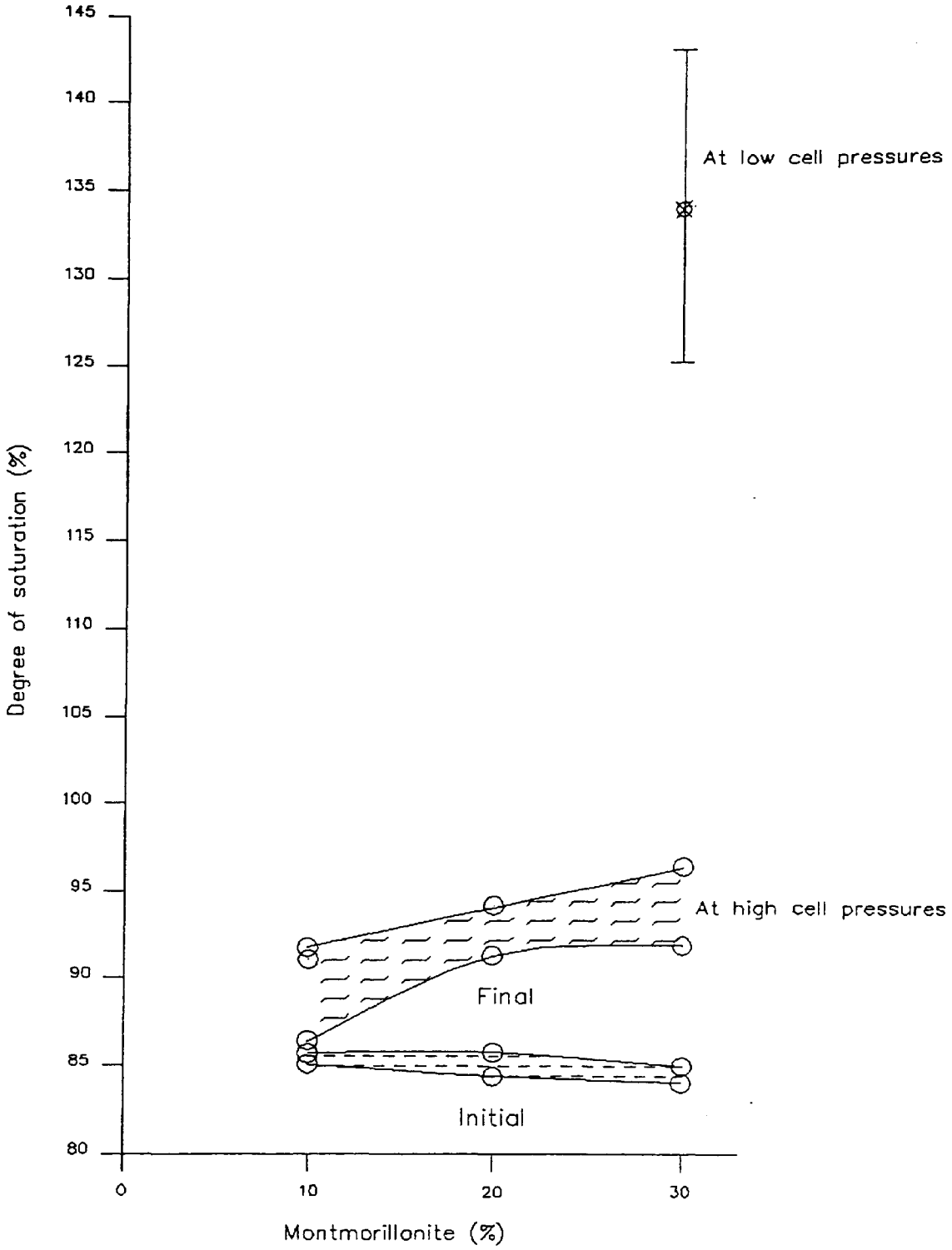

Figure 7.49 Initial and final degrees of saturation for samples tested in the first phase.

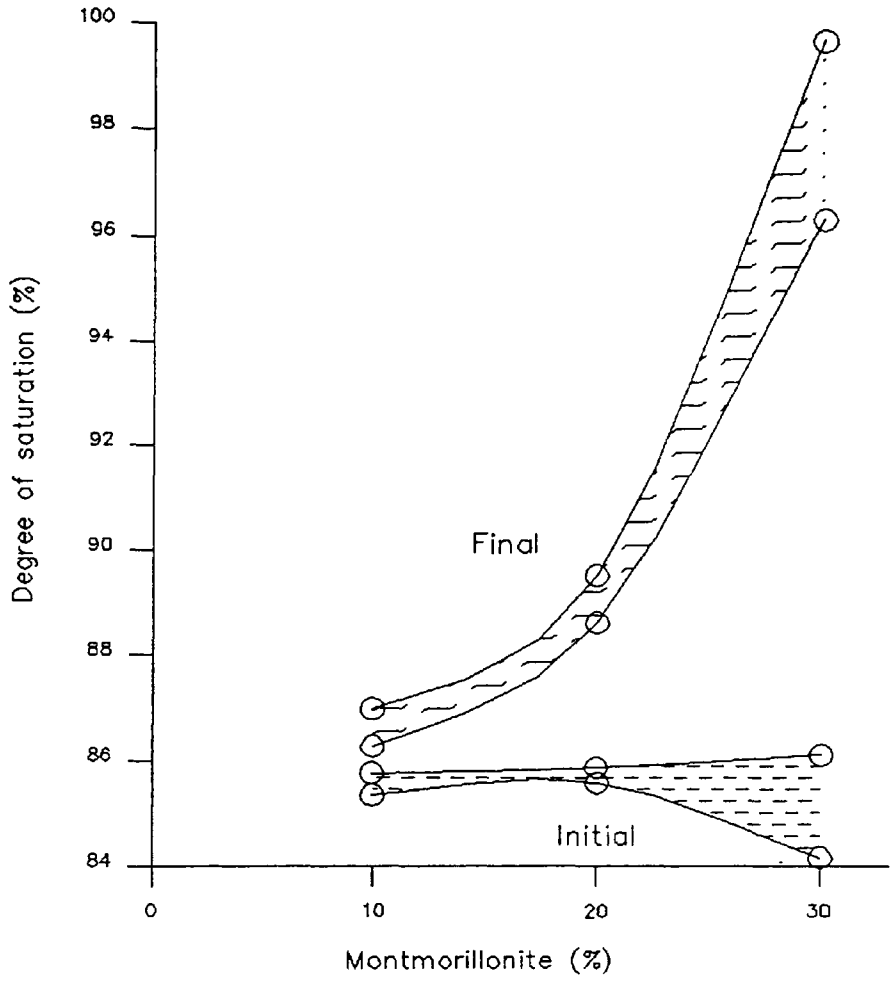

Figure 7.50 Initial and final degrees of saturation for samples tested in the second phase.

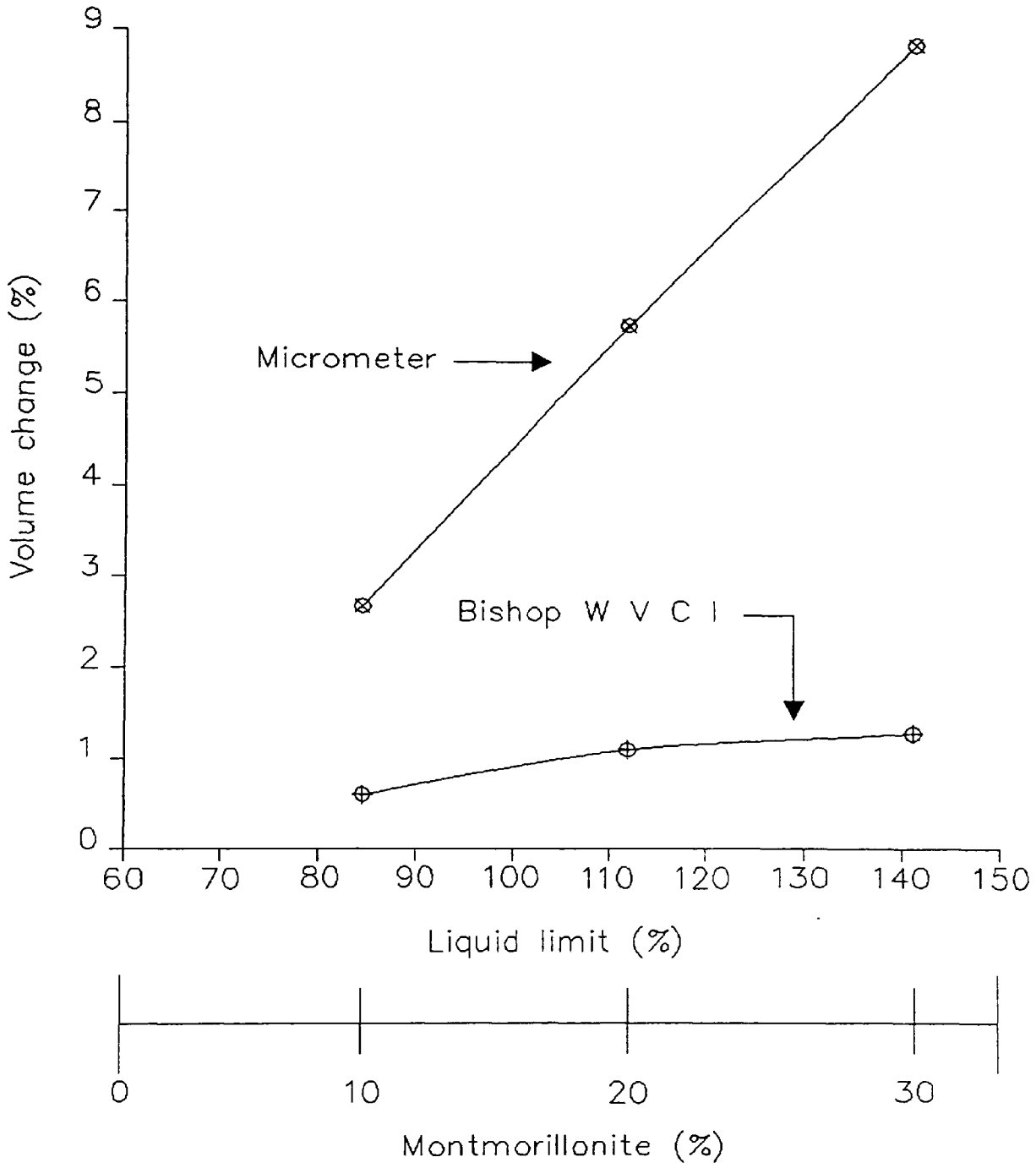

Figure 7.51 Volume changes measured by micrometer and the Bishop water volume change indicator, by samples in the first phase, versus montmorillonite contents and their corresponding liquid limits.

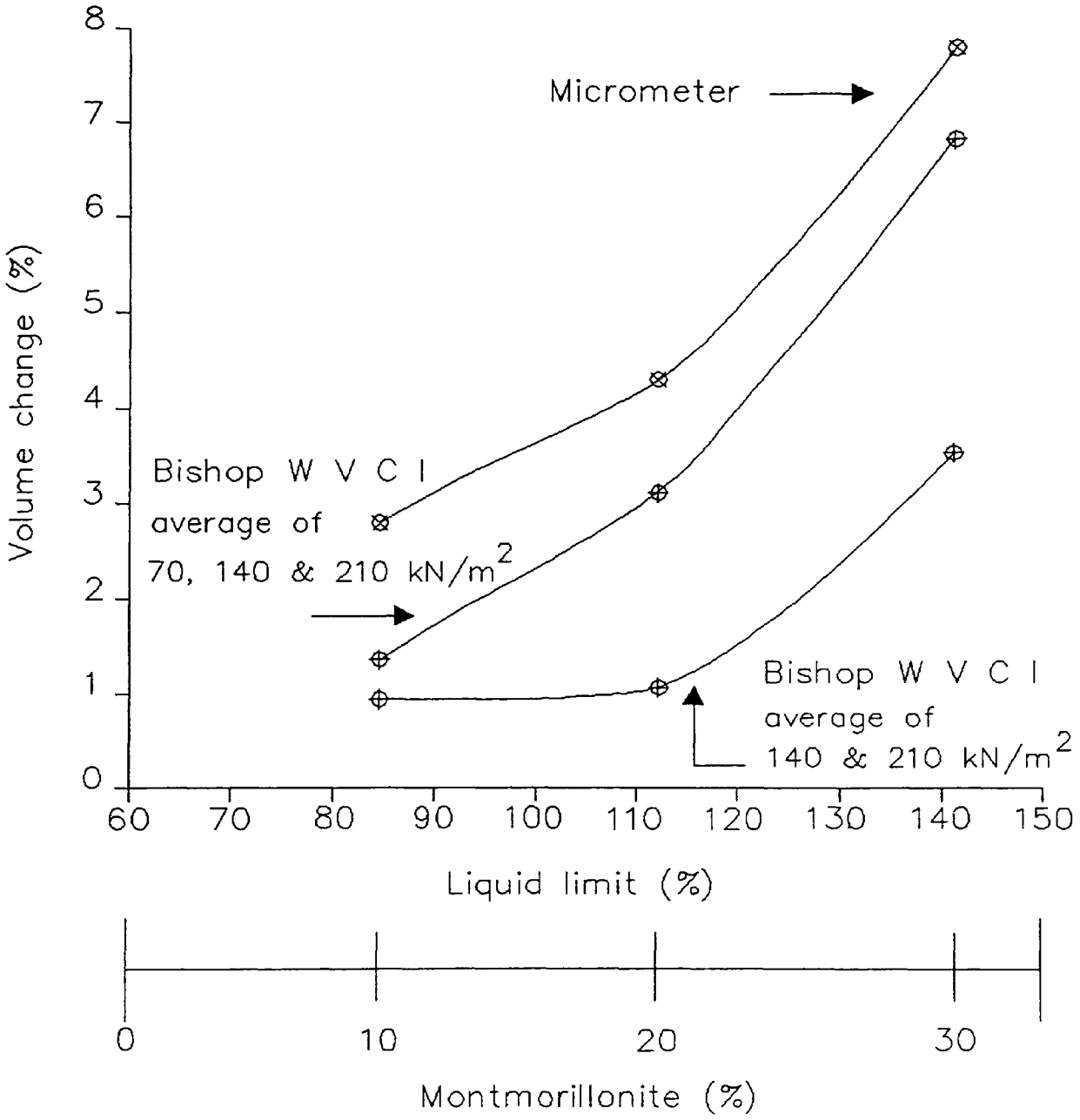

Figure 7.52 Volume changes measured by micrometer and the Bishop water volume change indicator, by samples in the second phase, versus montmorillonite contents and their corresponding liquid limits.

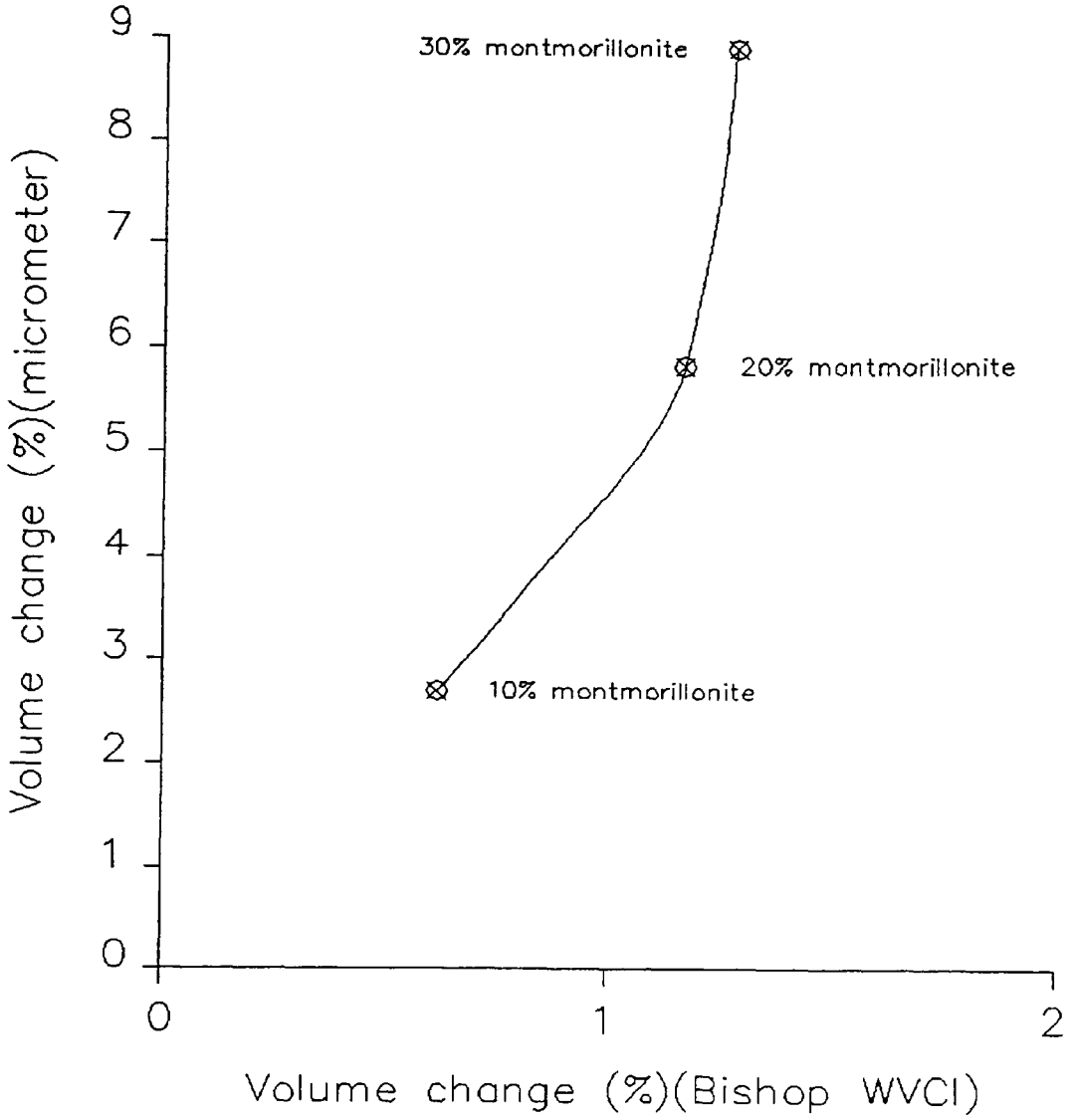

Figure 7.53 Volume changes measured by micrometer versus those by the Bishop water volume change indicator in the first phase.

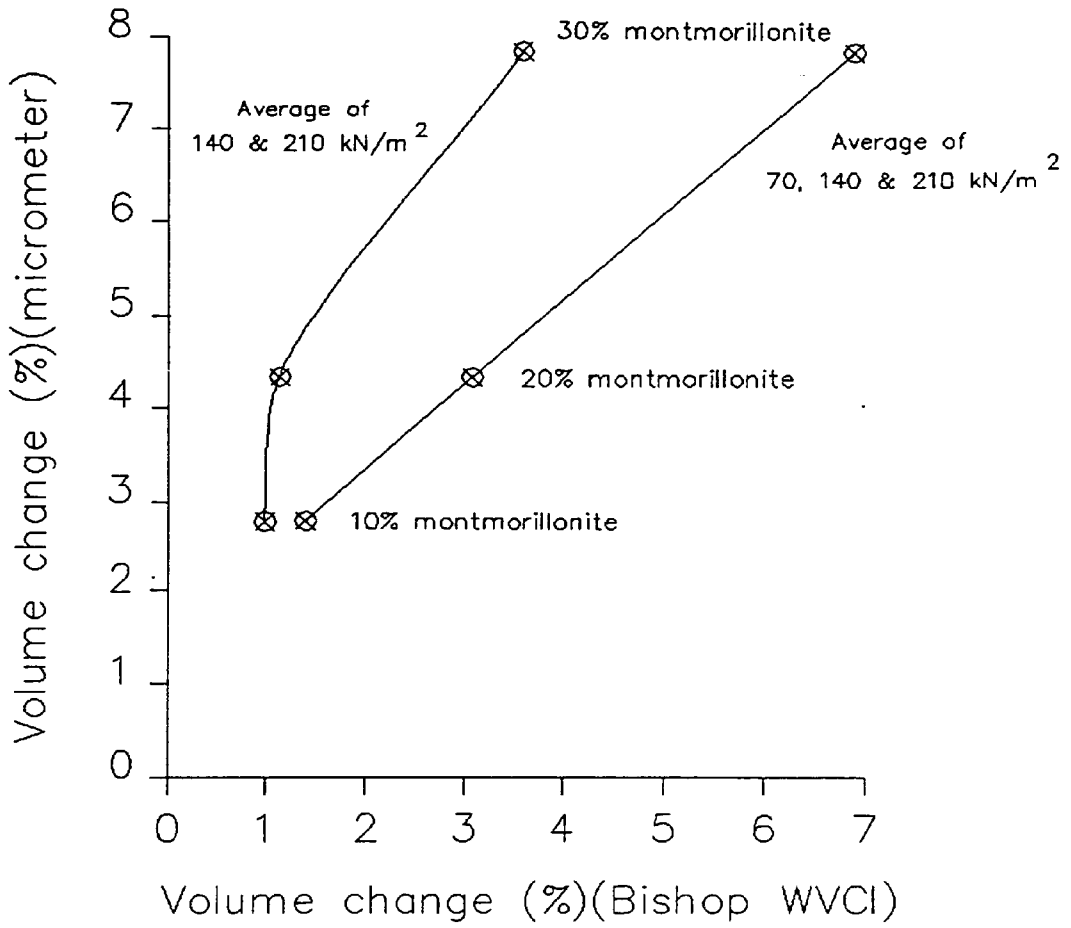

Figure 7.54 Volume changes measured by micrometer versus those by the Bishop water volume change indicator in the second phase.

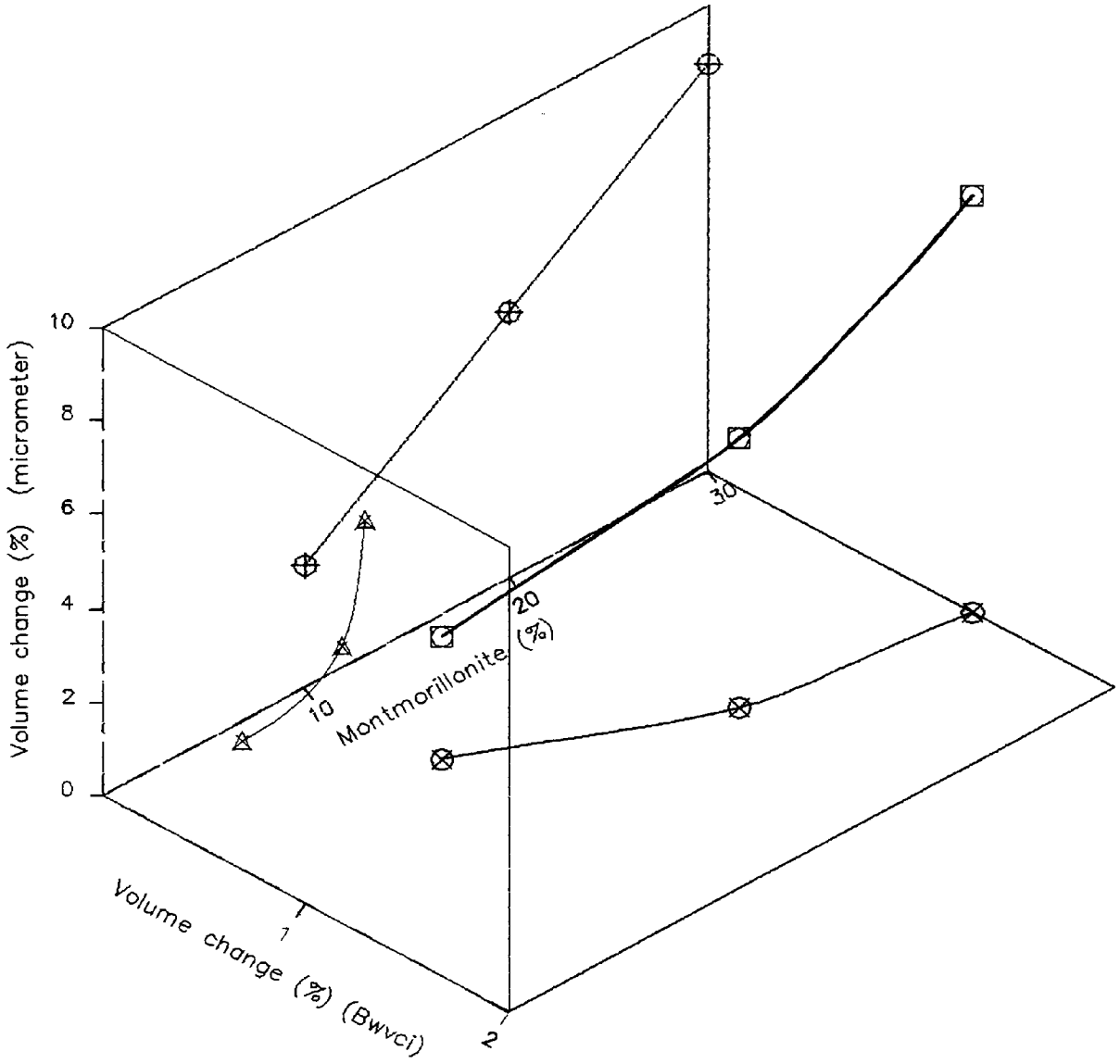

Figure 7.55 Three dimensional relationship of percentage volume changes, measured by micrometer and the Bishop water volume change indicator (Bwvci), and the montmorillonite content of samples in the first phase under 207 kN/m^2 confining cell pressures.

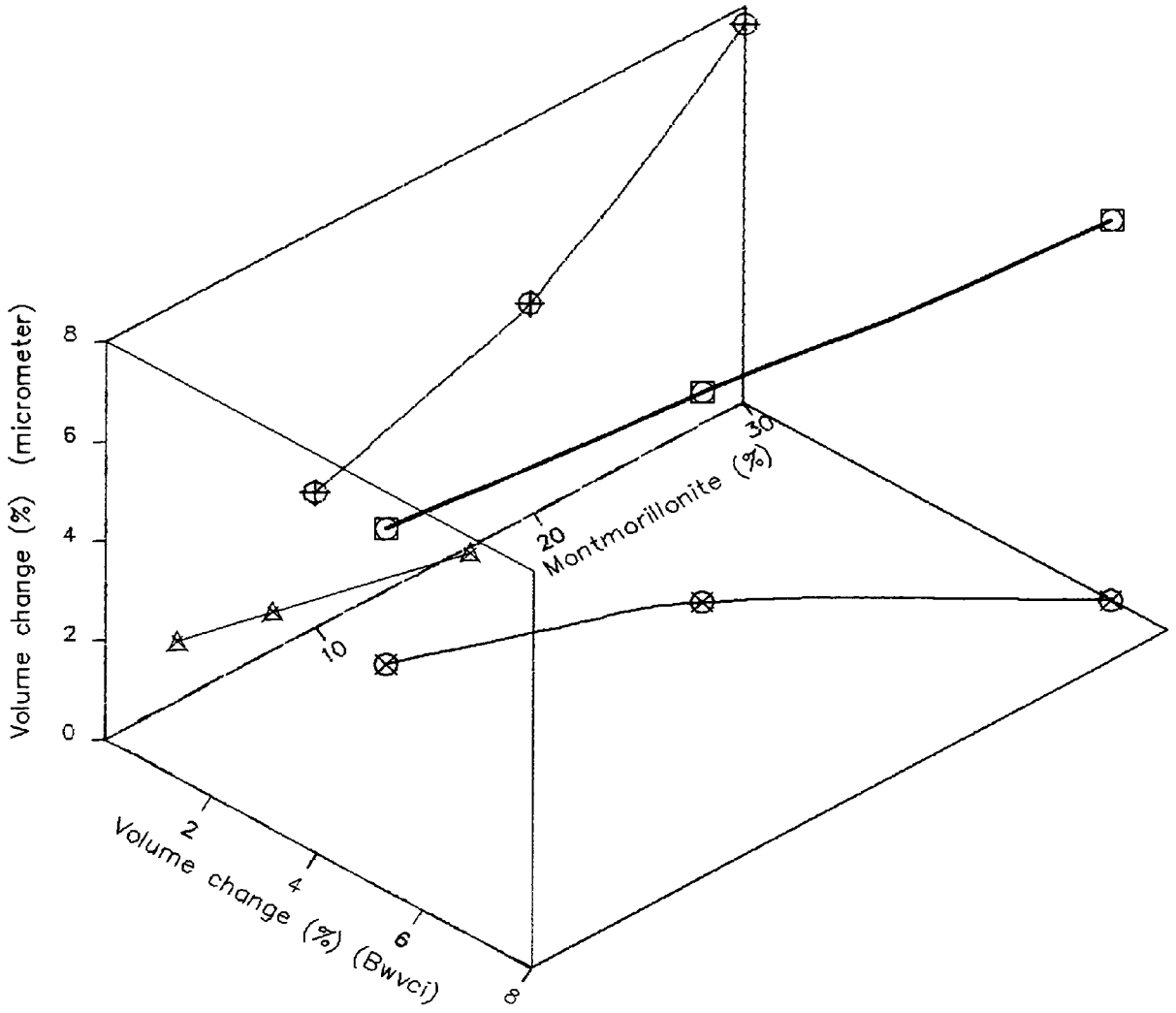

Figure 7.56 Three dimensional relationship of percentage volume changes, measured by micrometer and the Bishop water volume change indicator (Bwvci), and the montmorillonite content of samples in the second phase. The values represent averages of 70, 140 & 210 kN/m^2 cell pressures.

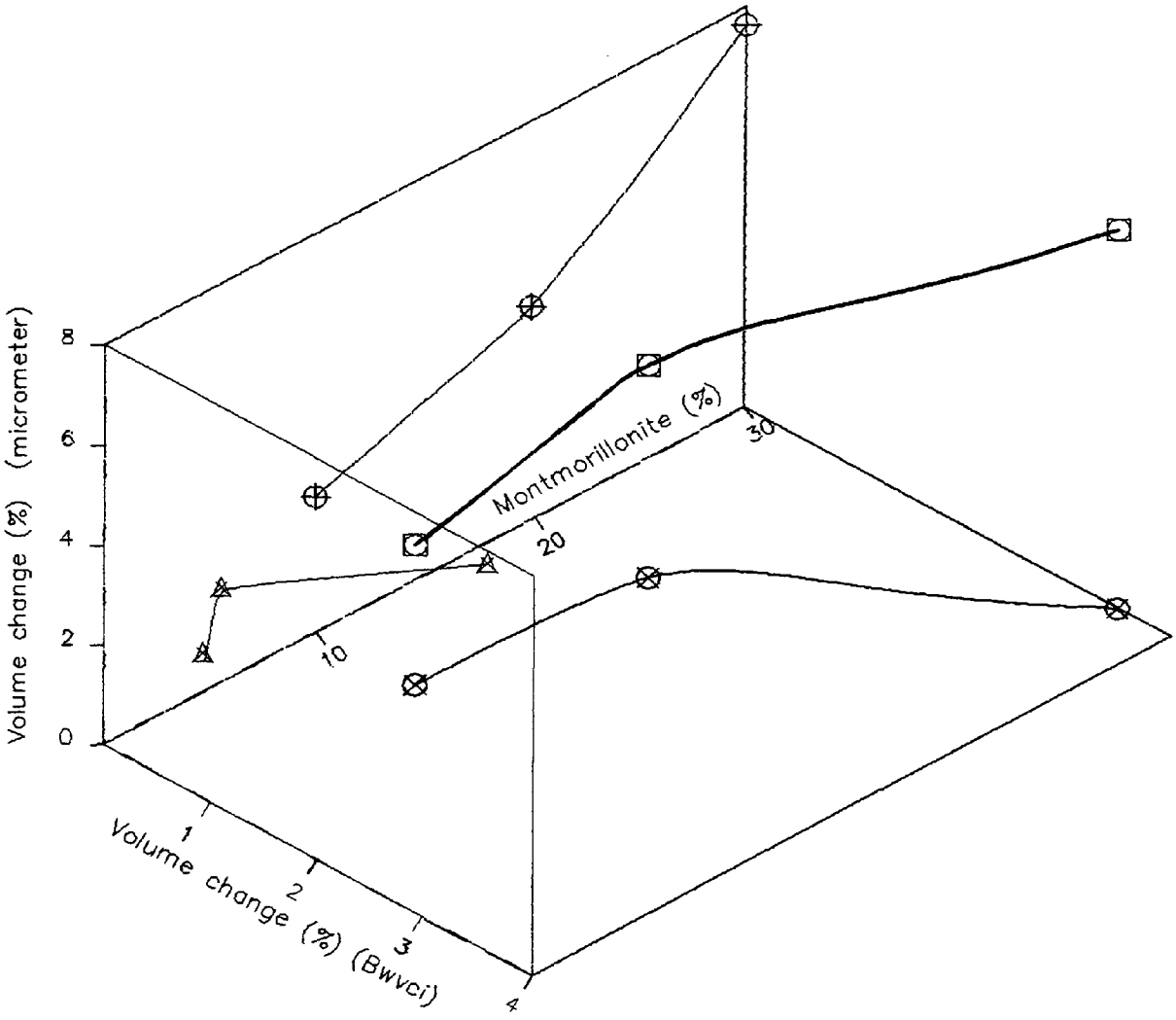

Figure 7.57 Three dimensional relationship of percentage volume changes, measured by micrometer and the Bishop water volume change indicator (Bwvci), and the montmorillonite content of samples in the second phase. The values represent averages of 140 and 210 kN/m^2 cell pressures.

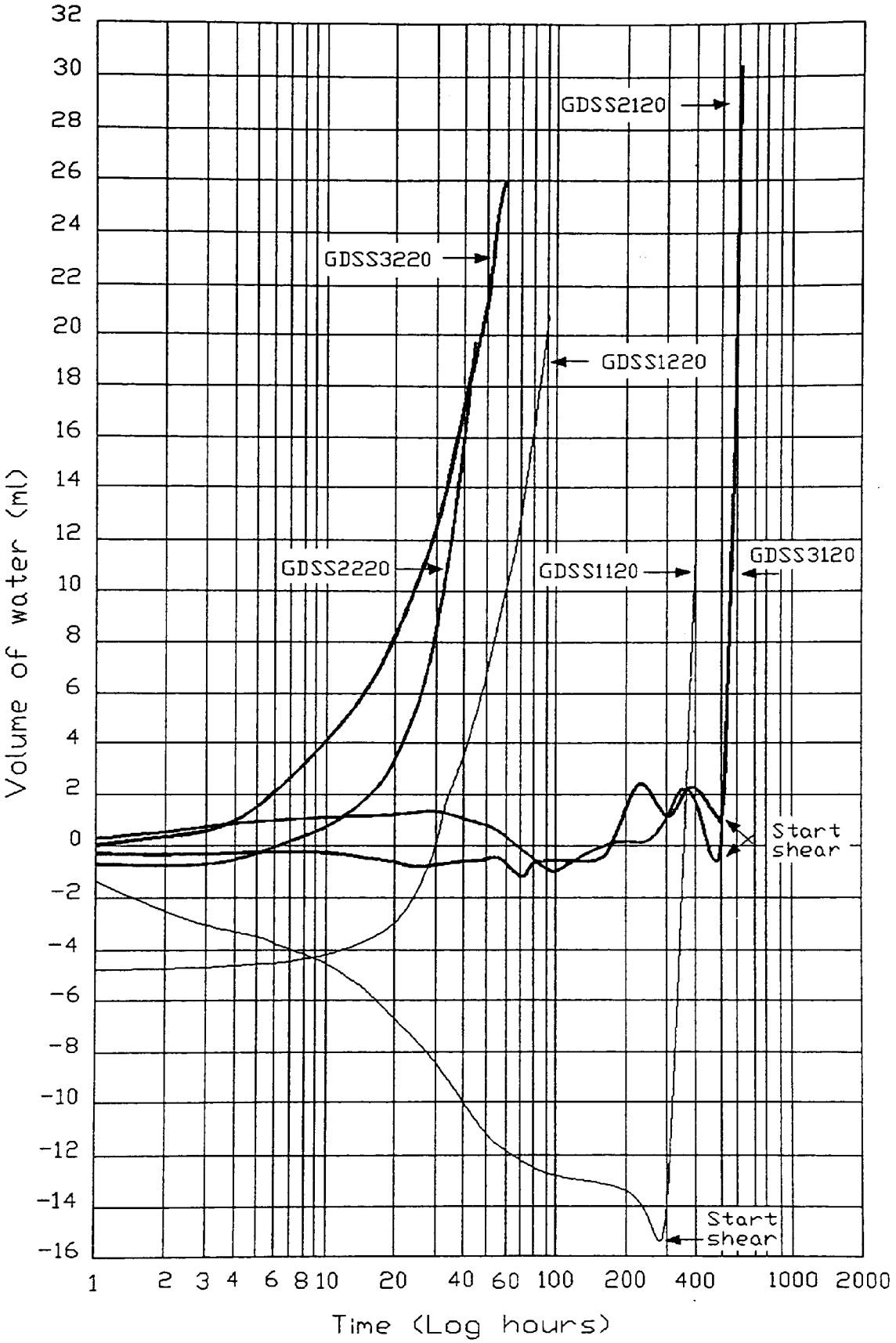

Figure 7.58 Volume of water, entering or leaving the Bishop Wesley cell, versus time.

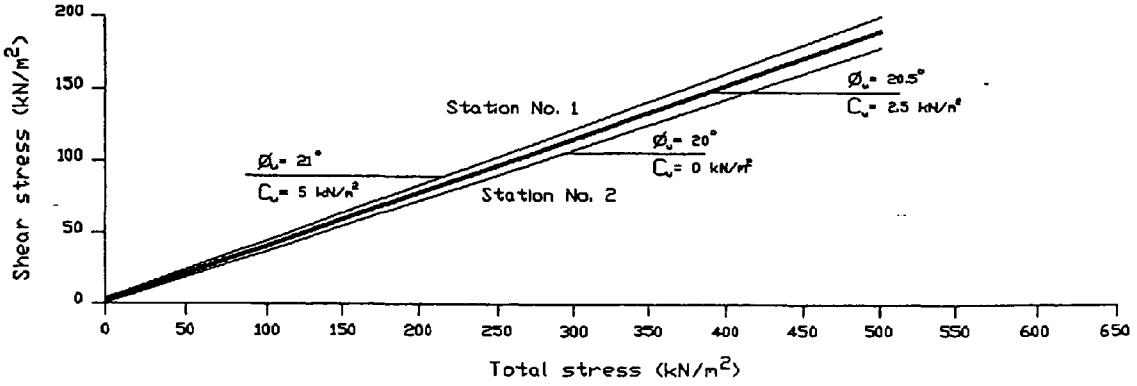

Figure 7.59 The total failure envelopes of samples containing 10% montmorillonite tested in stations No. 1 and 2 after expansion has taken place.

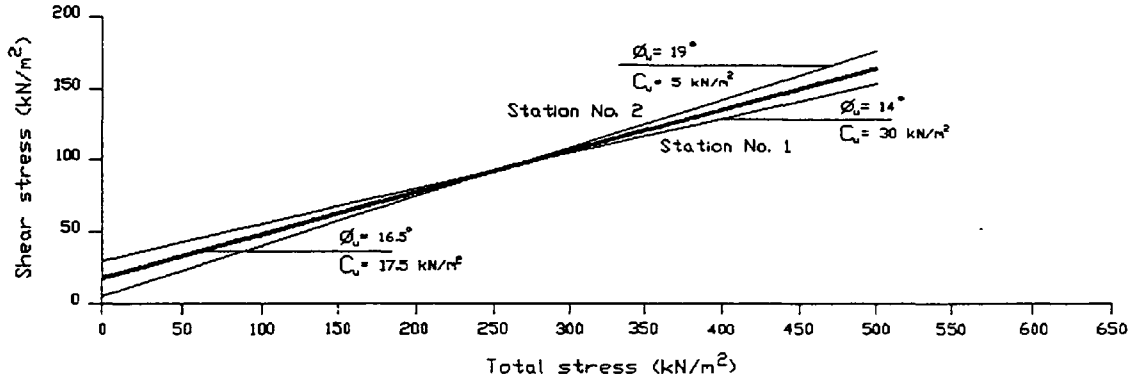

Figure 7.60 The total failure envelopes of samples containing 10% montmorillonite tested in stations No. 1 and 2 where no expansion has taken place.

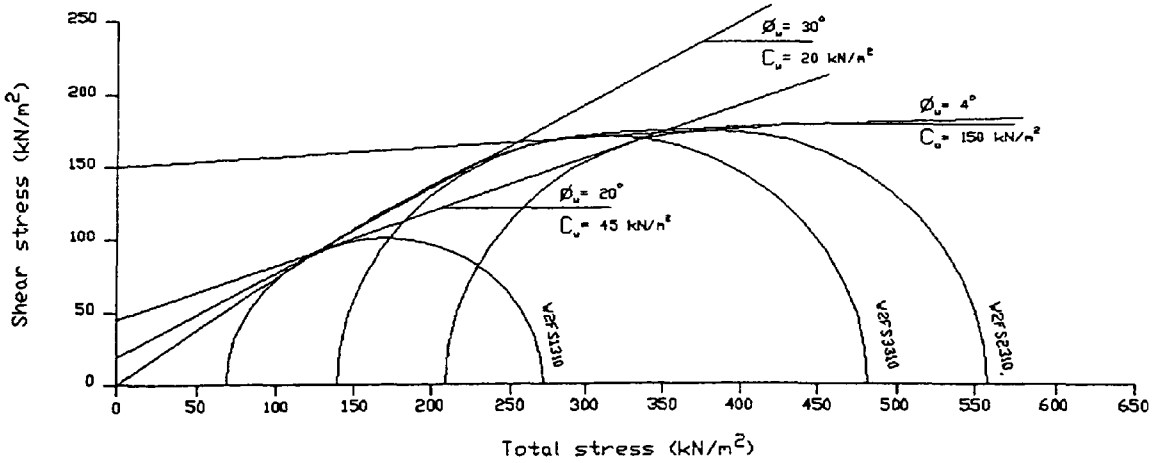

Figure 7.61 The total failure envelope of samples containing 10% montmorillonite tested in station No. 4 where no expansion has taken place and there were no pore air or pore water back pressures.

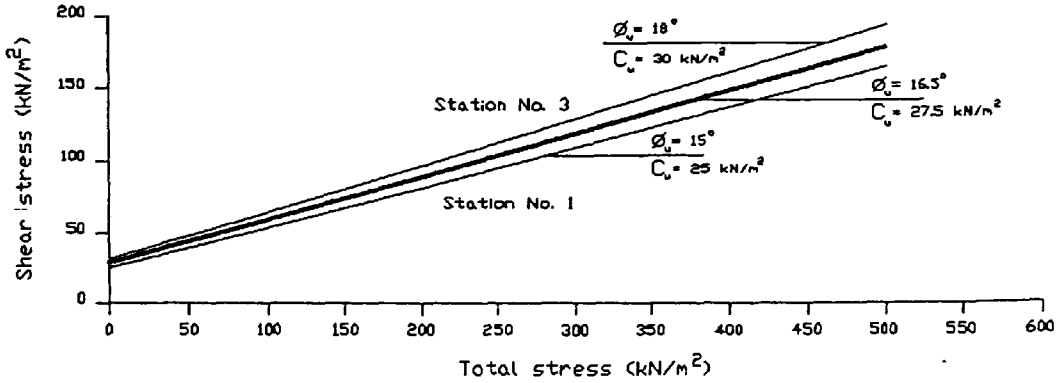

Figure 7.62 The total failure envelopes of samples containing 20% montmorillonite tested in stations No. 1 and 3 after expansion has taken place.

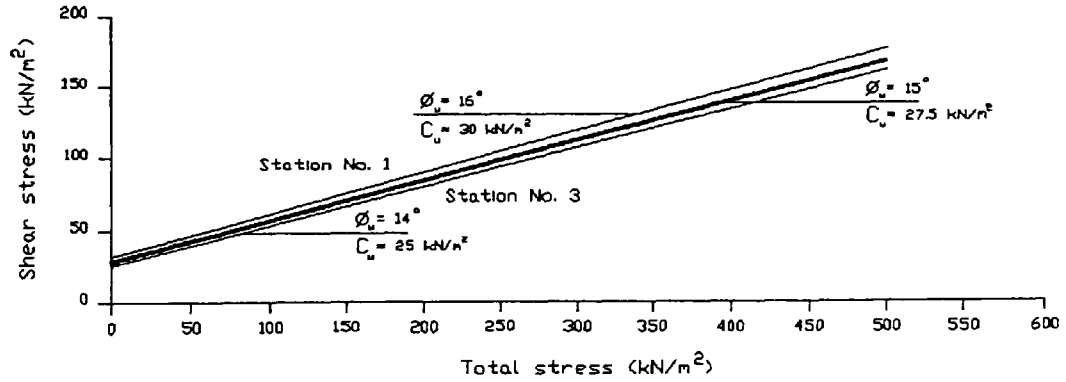

Figure 7.63 The total failure envelopes of samples containing 20% montmorillonite tested in stations No. 1 and 3 where no expansion has taken place.

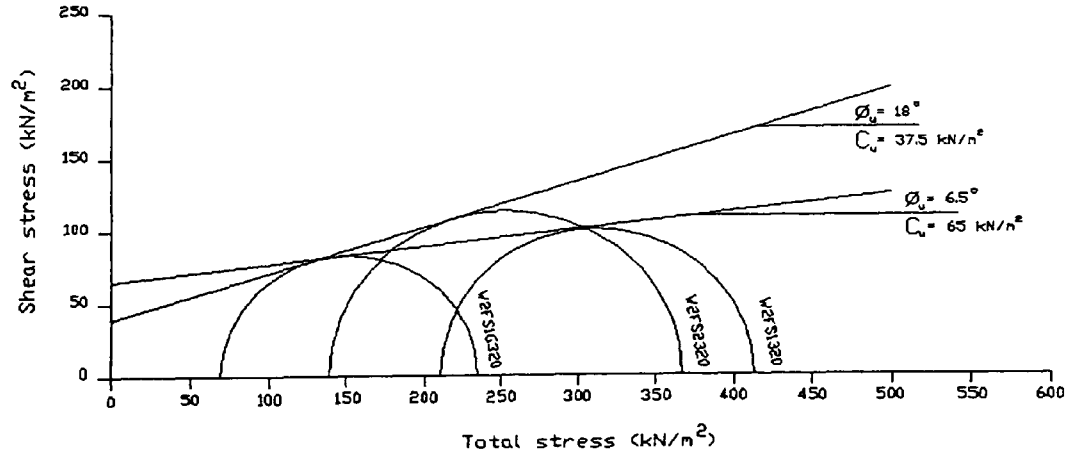

Figure 7.64 The total failure envelope of samples containing 20% montmorillonite tested in station No. 4 where no expansion has taken place and there were no pore air or pore water back pressures.

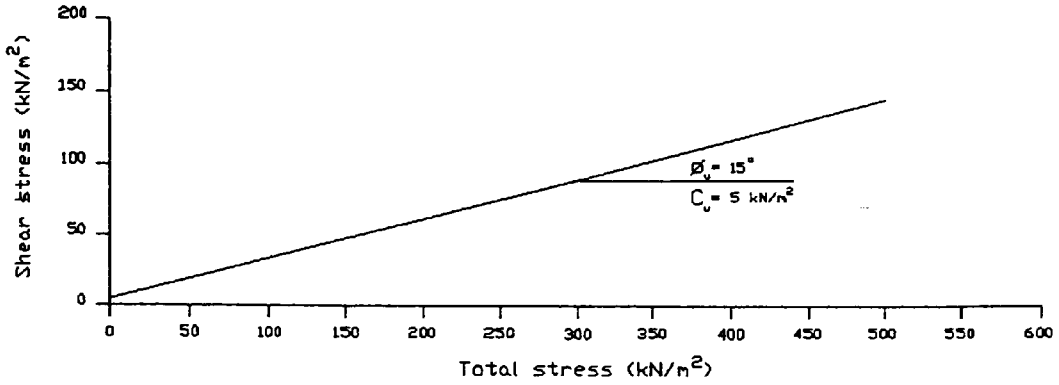

Figure 7.65 The total failure envelope of samples containing 30% montmorillonite tested in station No. 1 after expansion has taken place.

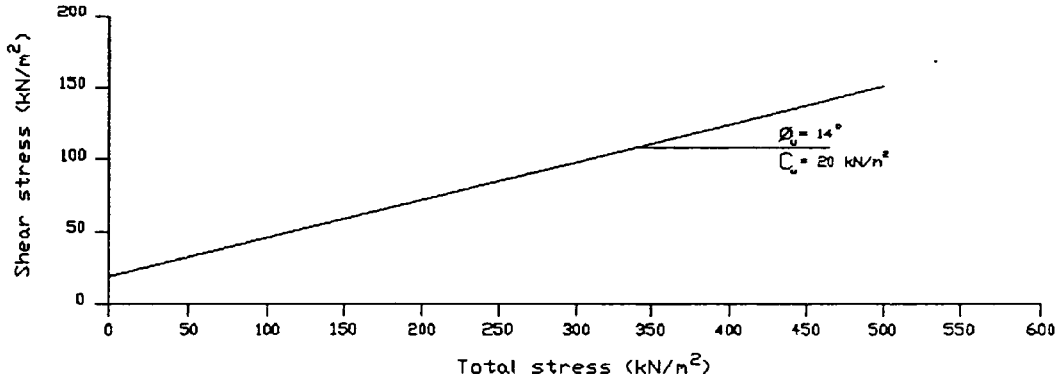

Figure 7.66 The total failure envelope of samples containing 30% montmorillonite tested in station No. 1 where no expansion has taken place.

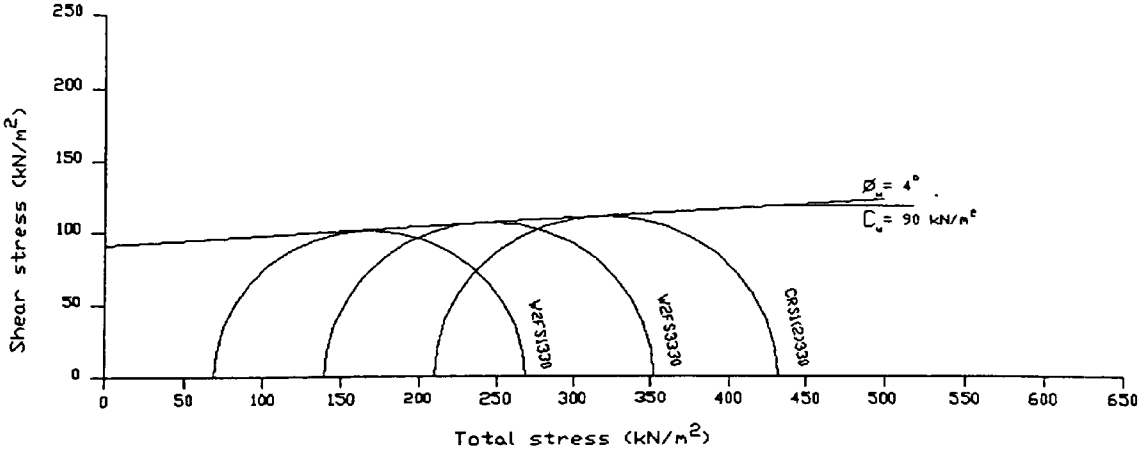

Figure 7.67 The total failure envelope of samples containing 30% montmorillonite tested in stations No. 1 and 4 where no expansion has taken place and there were no pore air or pore water back pressures.

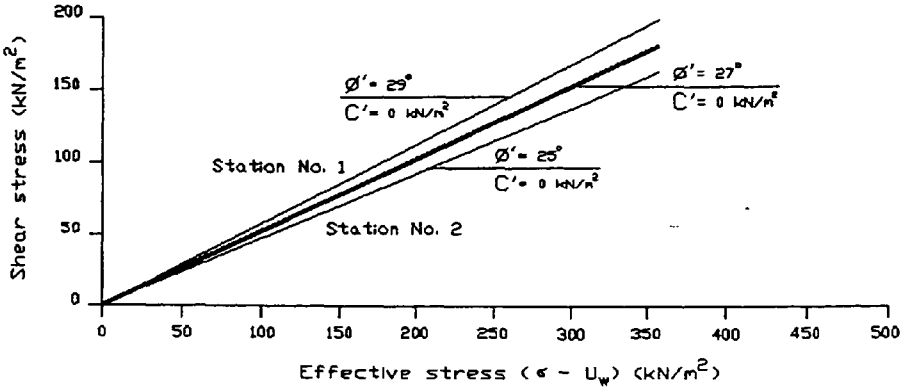

Figure 7.68 The effective stress failure envelopes of samples containing 10% montmorillonite tested in stations No. 1 and 2 after expansion has taken place.

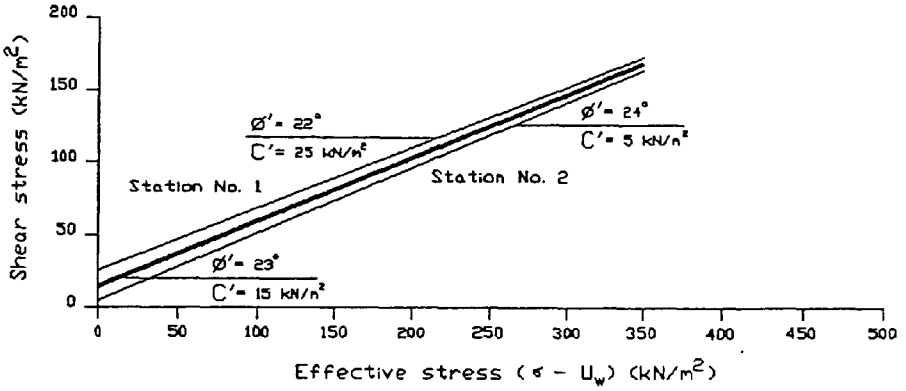

Figure 7.69 The effective stress failure envelopes of samples containing 10% montmorillonite tested in stations No. 1 and 2 where no expansion has taken place.

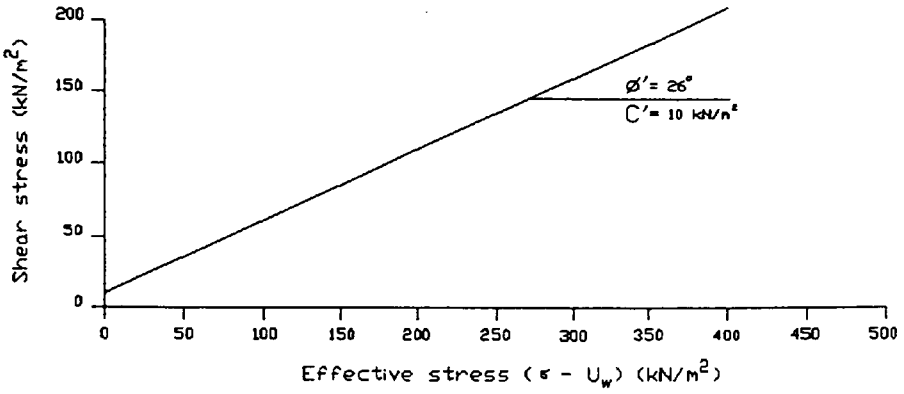

Figure 7.70 The effective stress failure envelope of samples containing 20% montmorillonite tested in stations No. 1 and 3 after expansion has taken place.

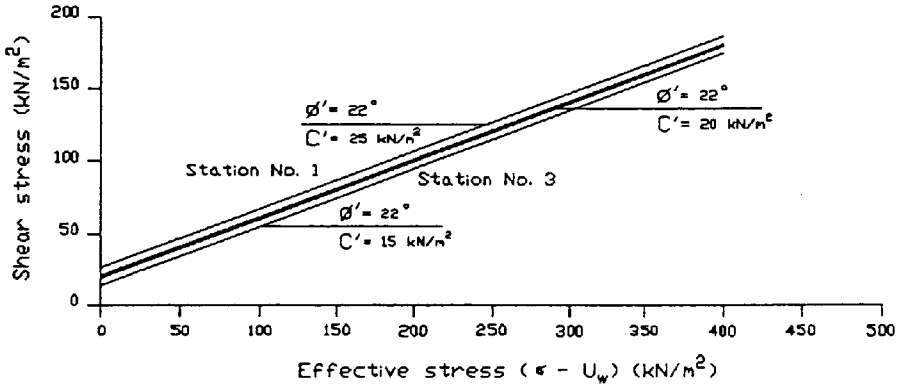

Figure 7.71 The effective stress failure envelopes of samples containing 20% montmorillonite tested in stations No. 1 and 3 where no expansion has taken place.

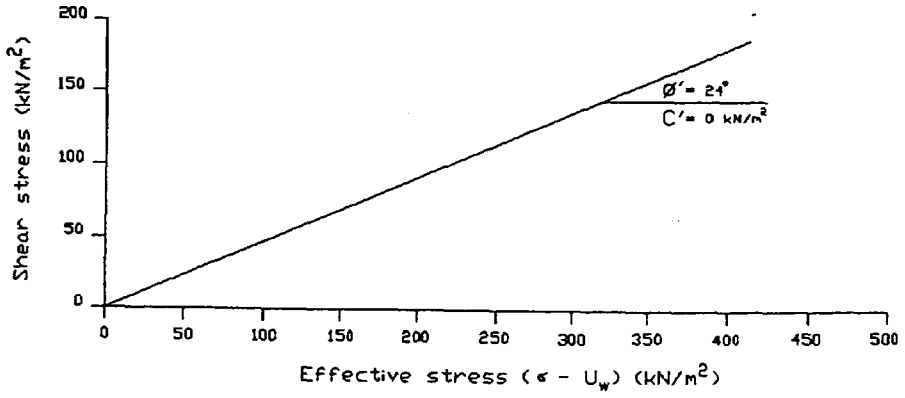

Figure 7.72 The effective stress failure envelope of samples containing 30% montmorillonite tested in station No. 1 after expansion has taken place.

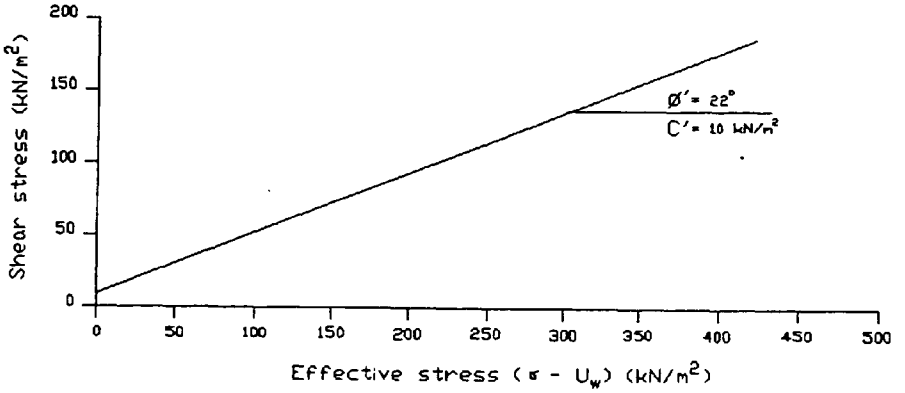

Figure 7.73 The effective stress failure envelope of samples containing 30% montmorillonite tested in station No. 1 where no expansion has taken place.

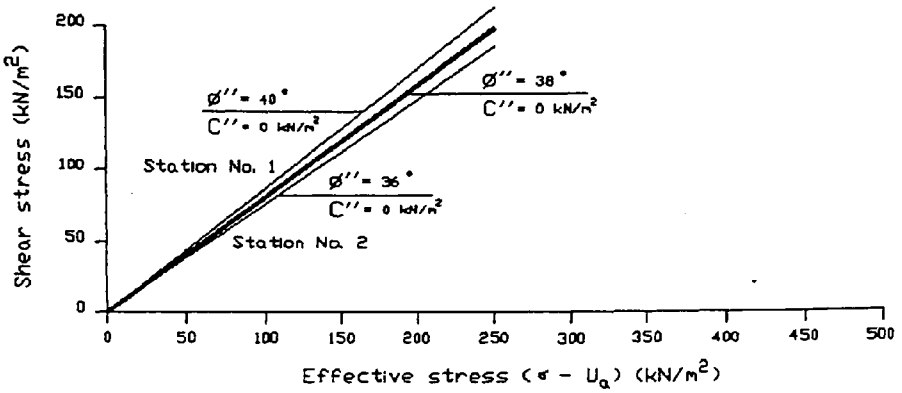

Figure 7.74 The effective stress failure envelopes of samples containing 10% montmorillonite tested in stations No. 1 and 2 after expansion has taken place.

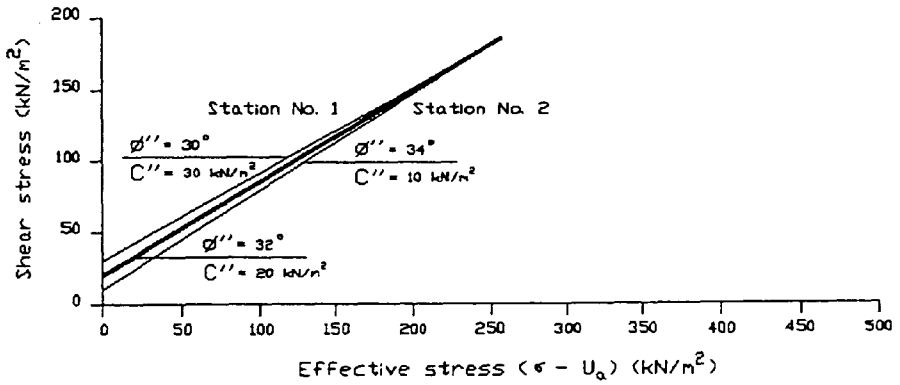

Figure 7.75 The effective stress failure envelopes of samples containing 10% montmorillonite tested in stations No. 1 and 2 where no expansion has taken place.

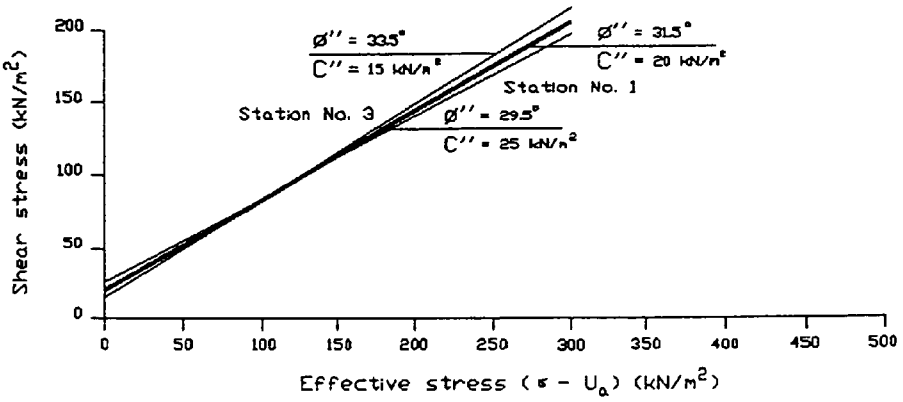

Figure 7.76 The effective stress failure envelopes of samples containing 20% montmorillonite tested in stations No. 1 and 3 after expansion has taken place.

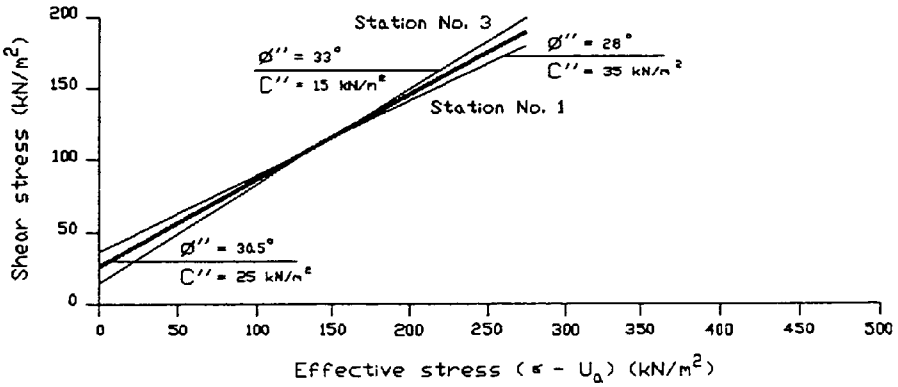

Figure 7.77 The effective stress failure envelopes of samples containing 20% montmorillonite tested in stations No. 1 and 3 where no expansion has taken place.

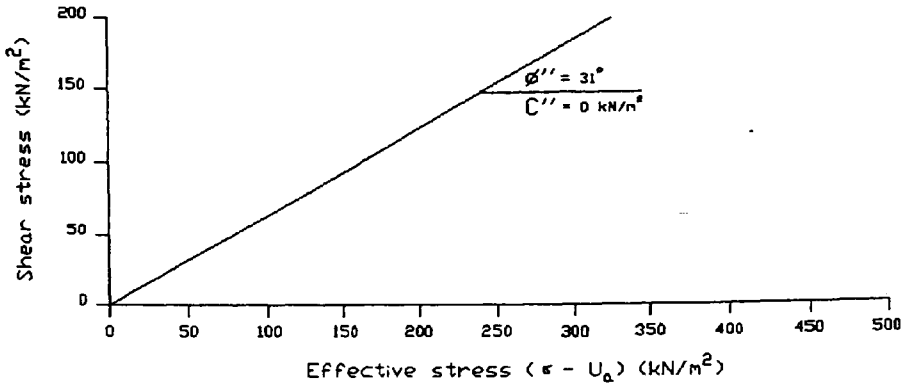

Figure 7.78 The effective stress failure envelope of samples containing 30% montmorillonite tested in station No. 1 after expansion has taken place.

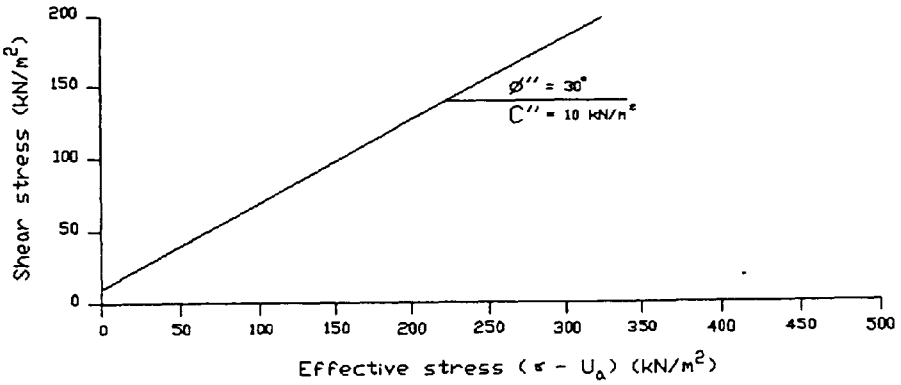

Figure 7.79 The effective stress failure envelope of samples containing 30% montmorillonite tested in station No. 1 where no expansion has taken place.

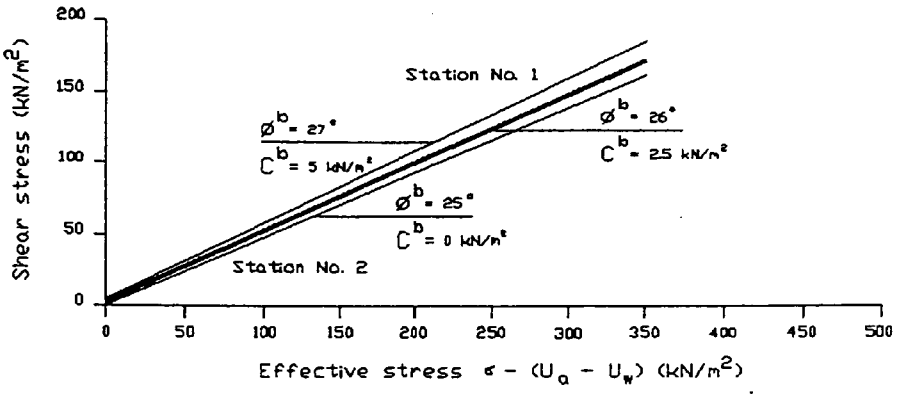

Figure 7.80 The effective stress failure envelope of samples containing 10% montmorillonite tested in stations No. 1 and 2 after expansion has taken place.

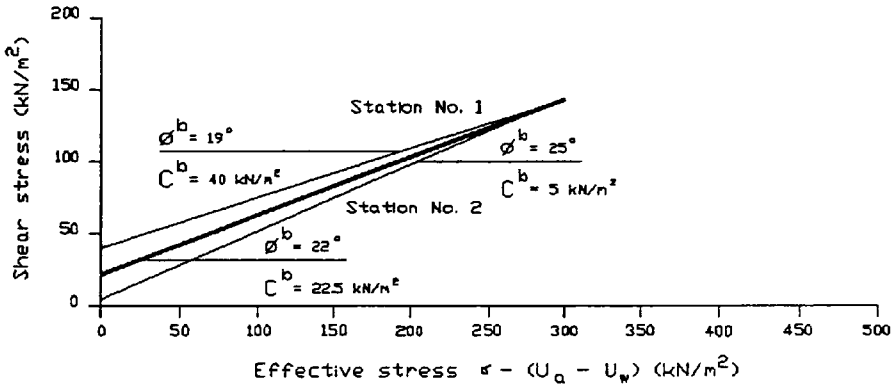

Figure 7.81 The effective stress failure envelopes of samples containing 10% montmorillonite tested in stations No. 1 and 2 where no expansion has taken place.

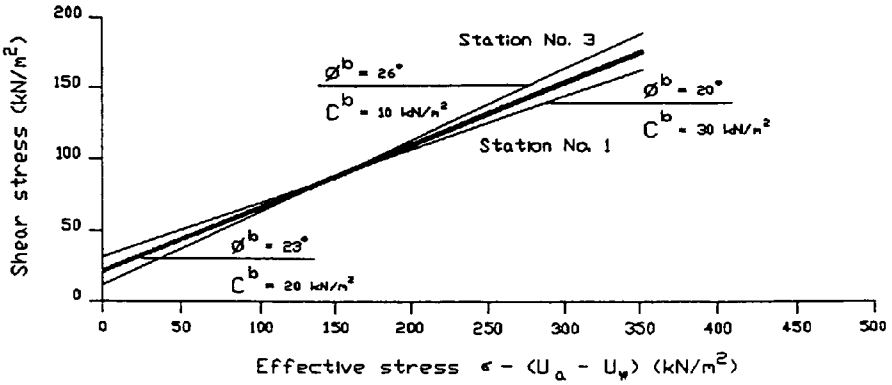

Figure 7.82 The effective stress failure envelopes of samples containing 20% montmorillonite tested in stations No. 1 and 3 after expansion has taken place.

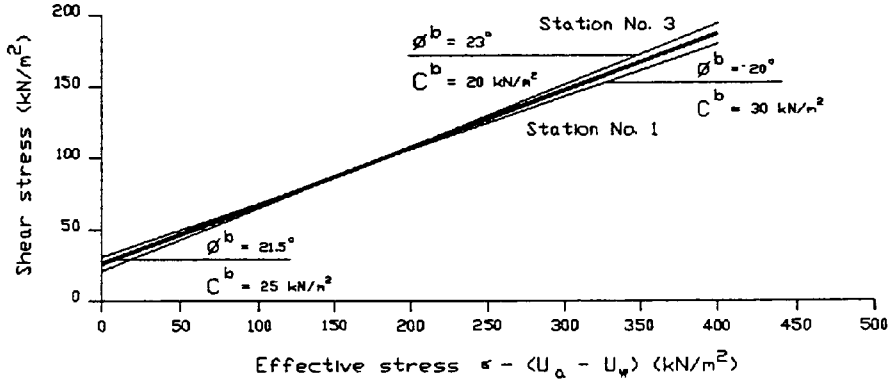

Figure 7.83 The effective stress failure envelopes of samples containing 20% montmorillonite tested in stations No. 1 and 3 where no expansion has taken place.

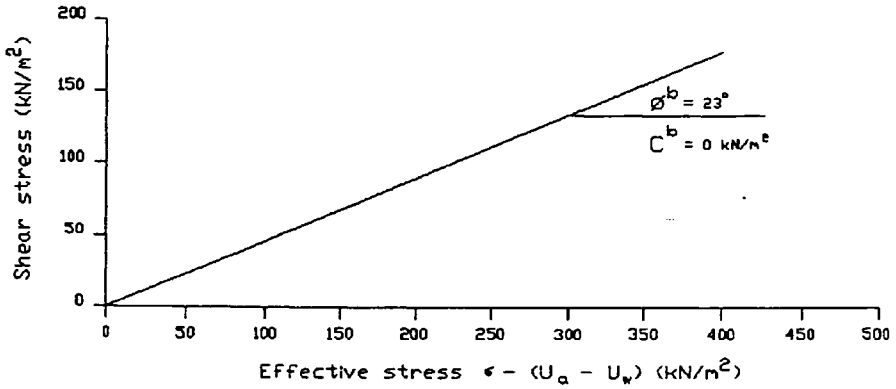

Figure 7.84 The effective stress failure envelope of samples containing 30% montmorillonite tested in station No. 1 after expansion has taken place.

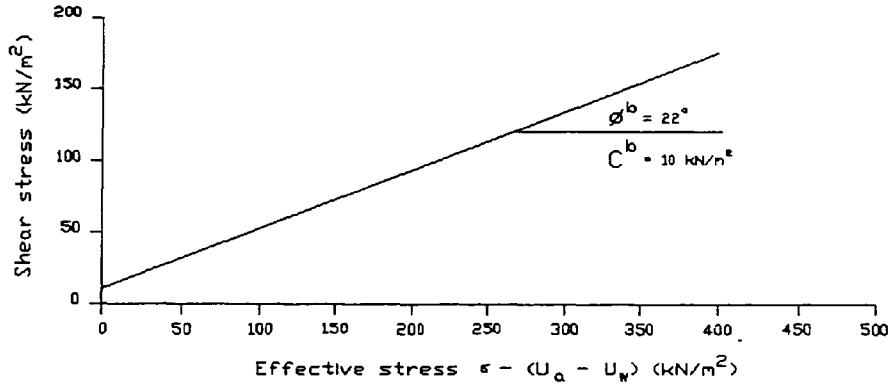

Figure 7.85 The effective stress failure envelope of samples containing 30% montmorillonite tested in station No. 1 where no expansion has taken place.

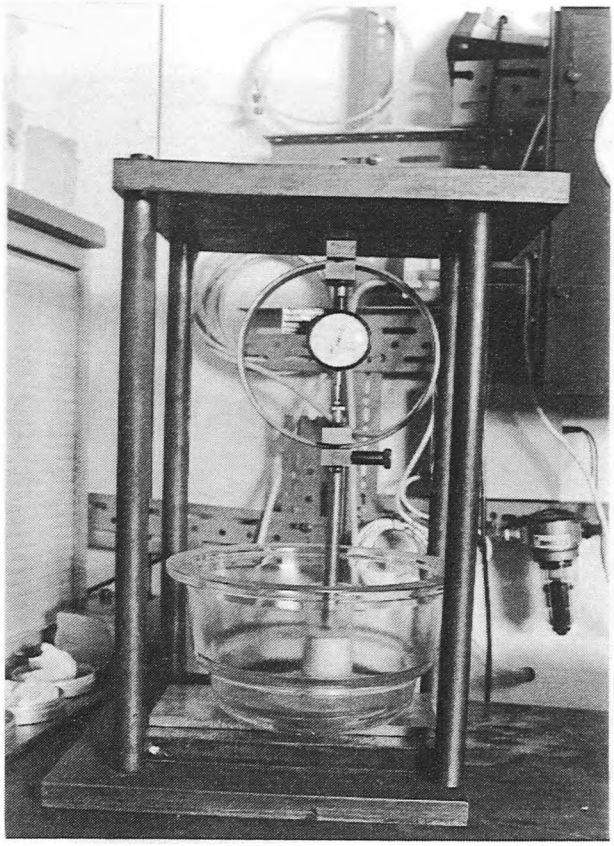

Plate 7.1 Apparatus for the measurement of swell pressure under no confining pressure (After Abdi (1992)).

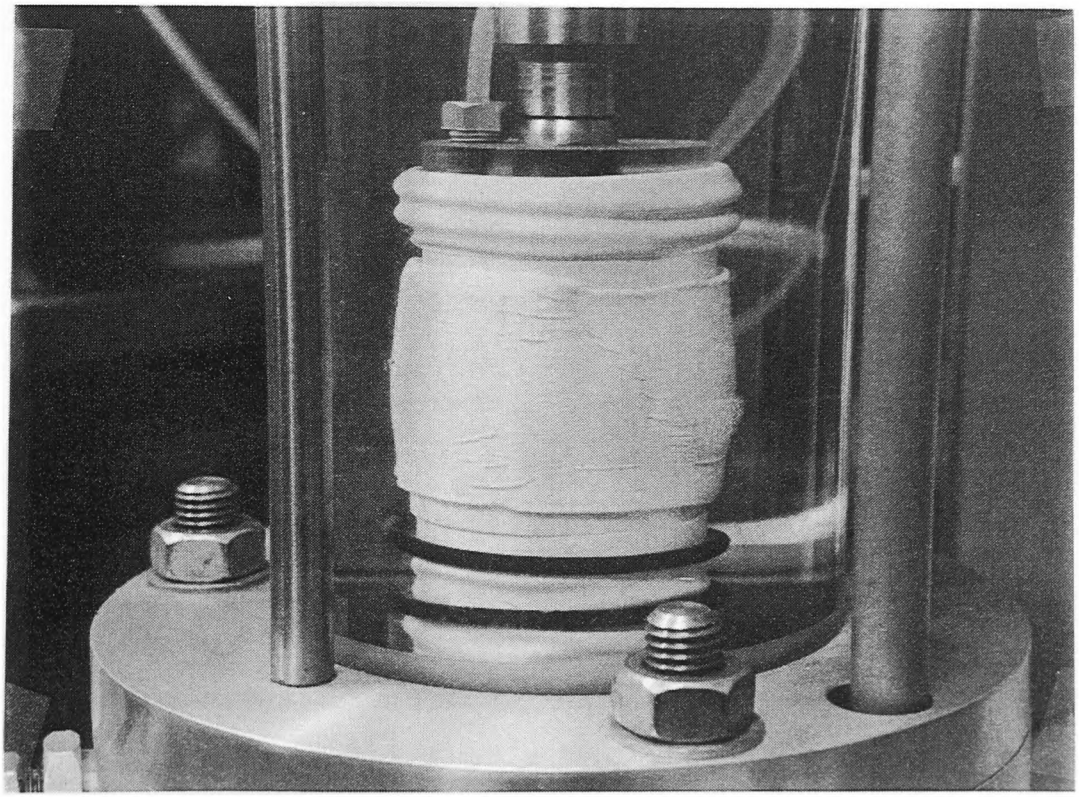

Plate 7.2 Sample showing shear plane in rubber membrane.

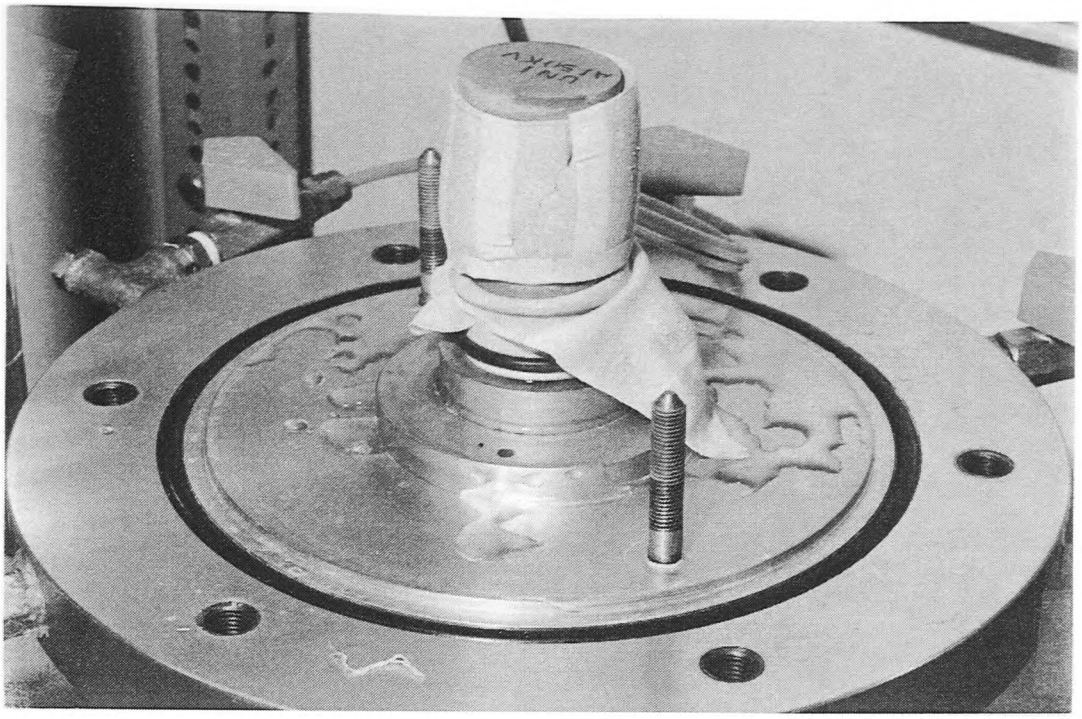

Plate 7.3 Sample showing shear plane.

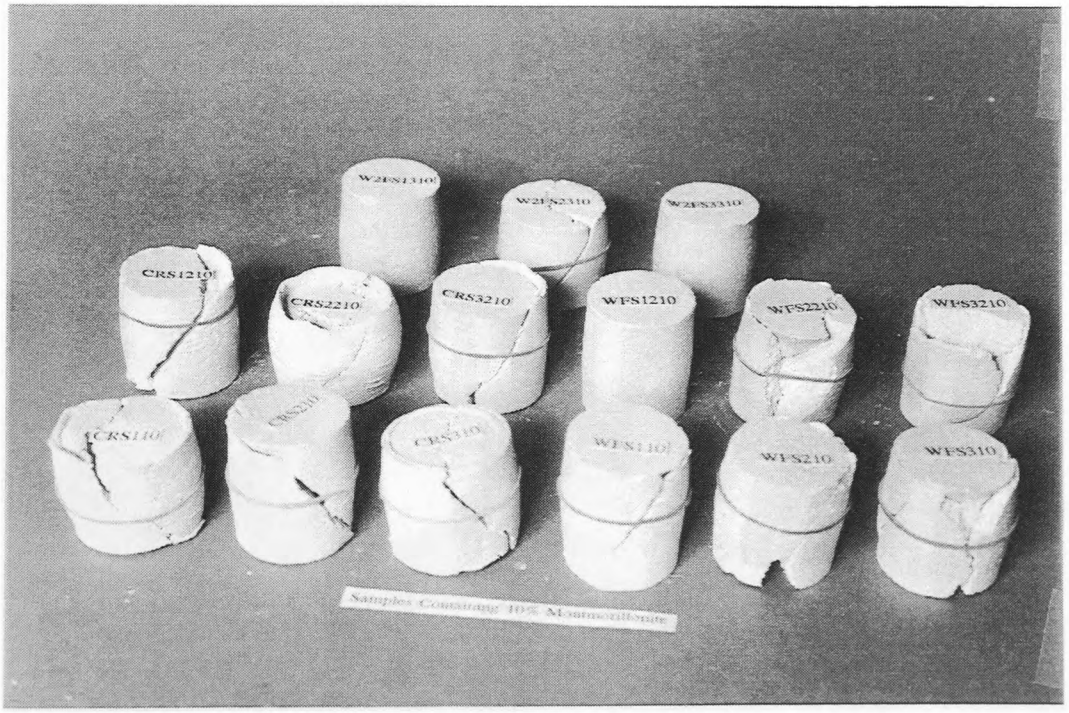

Plate 7.4 Samples containing 10% montmorillonite.

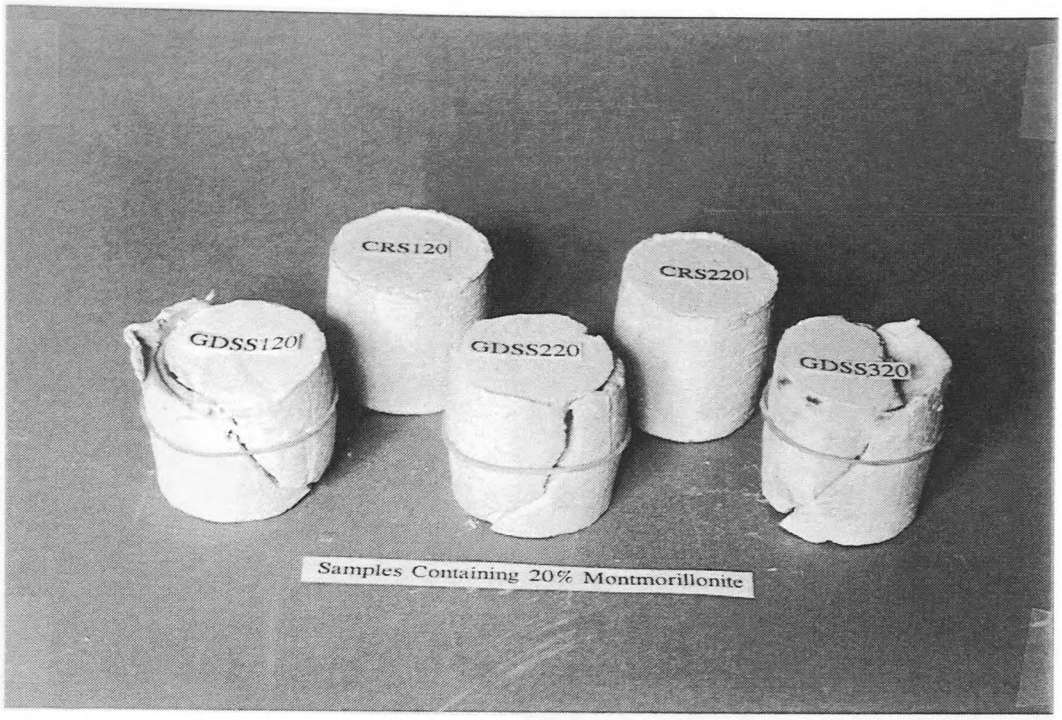

Plate 7.5 Samples containing 20% montmorillonite sheared after expansion had taken place.

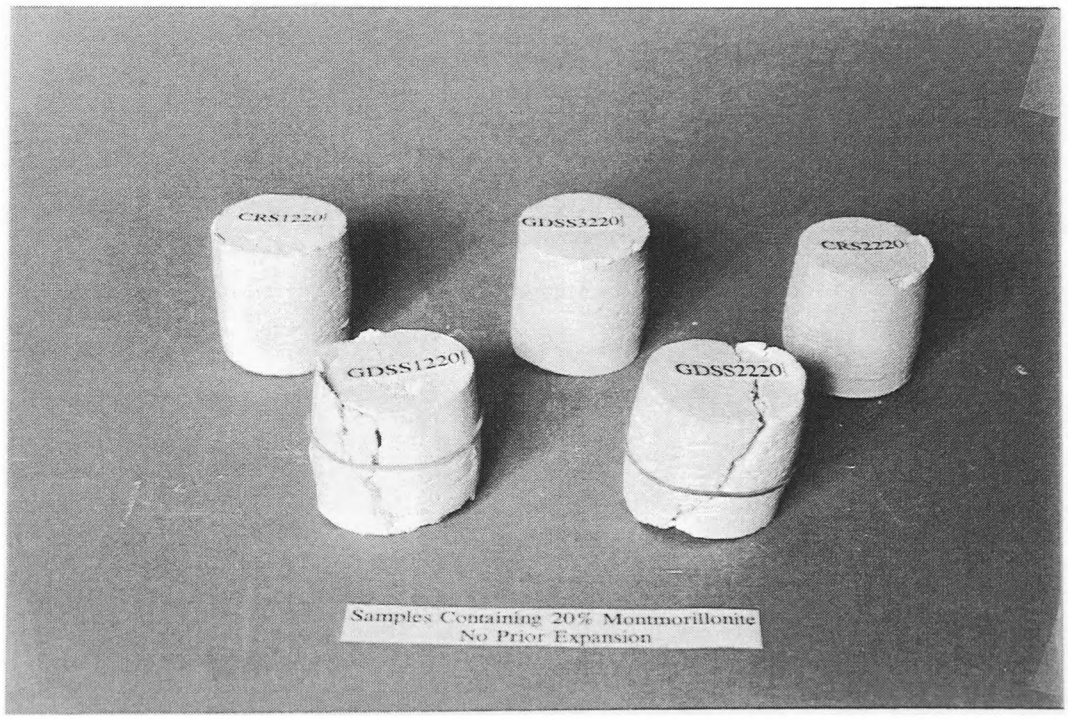

Plate 7.6 Samples containing 20% montmorillonite sheared without prior expansion.

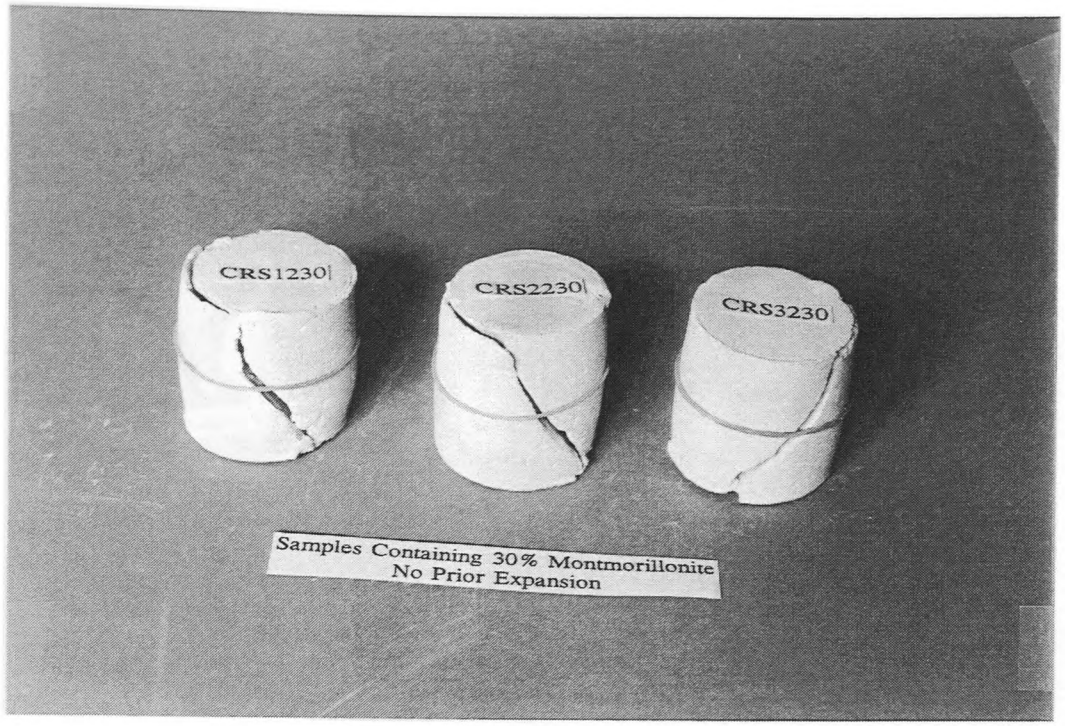

Plate 7.7 Samples containing 30% montmorillonite sheared without prior expansion.

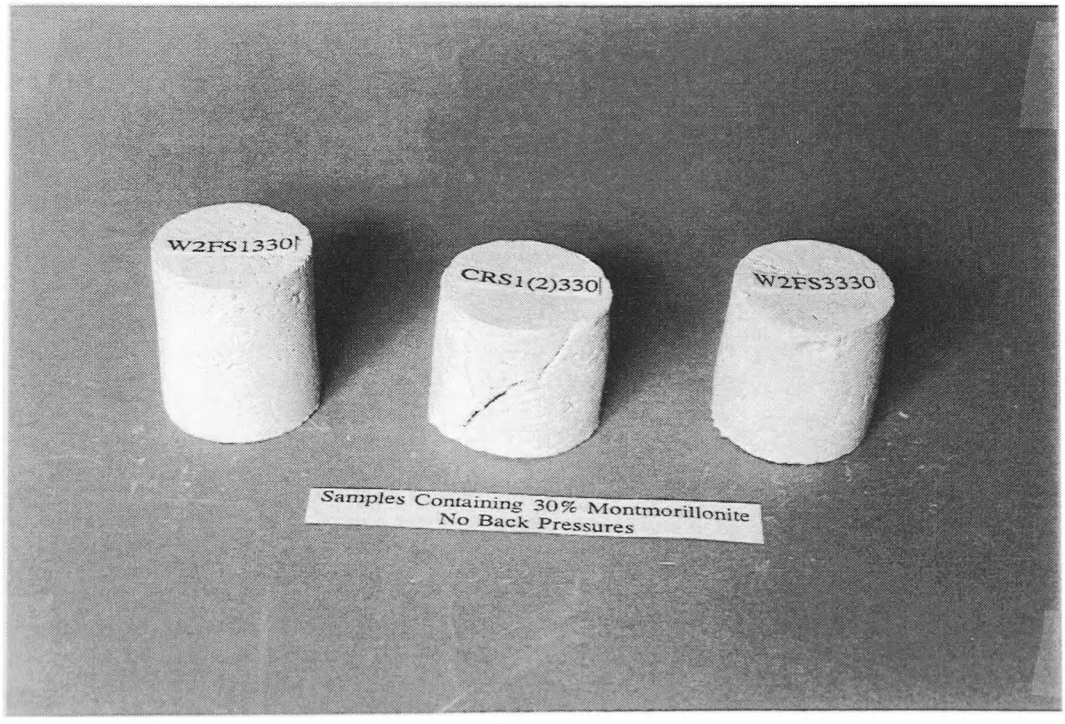

Plate 7.8 Samples containing 30% montmorillonite with no back pressures.

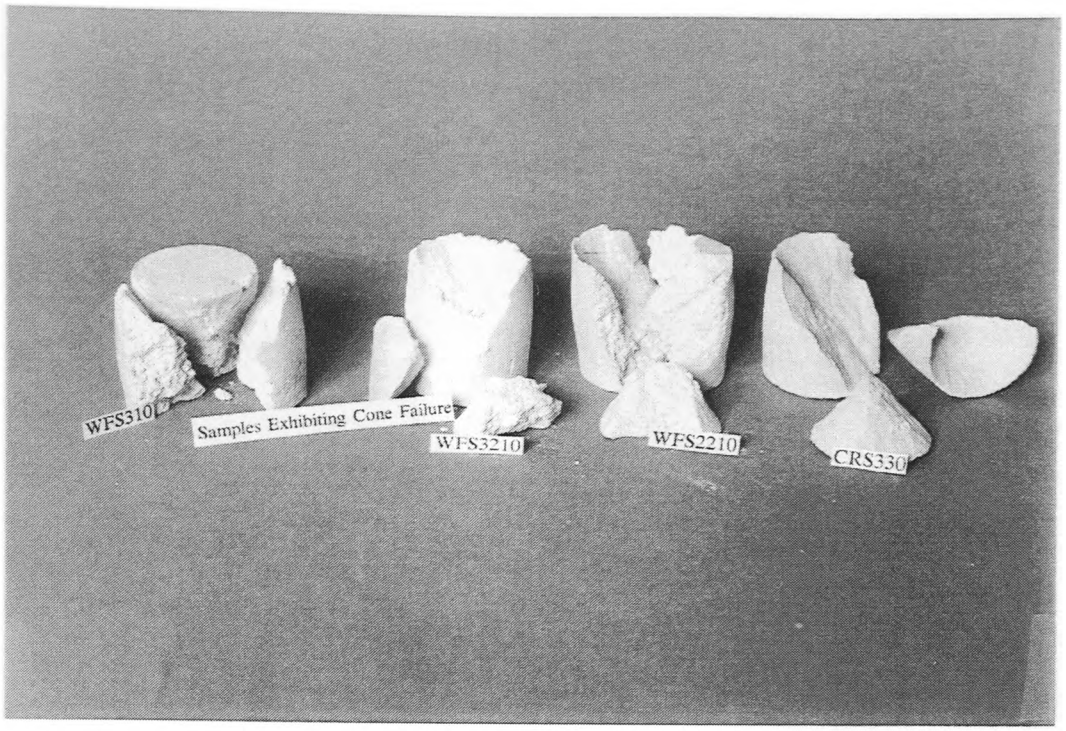

Plate 7.9 Samples with conical failure.

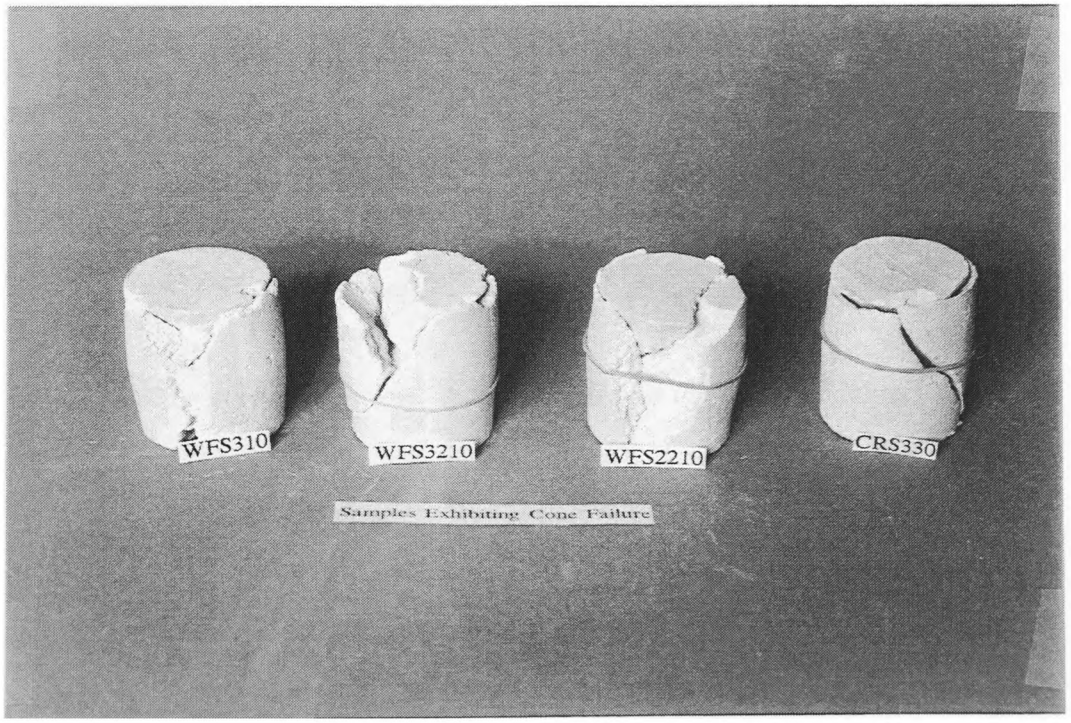

Plate 7.10 Samples with conical failure.

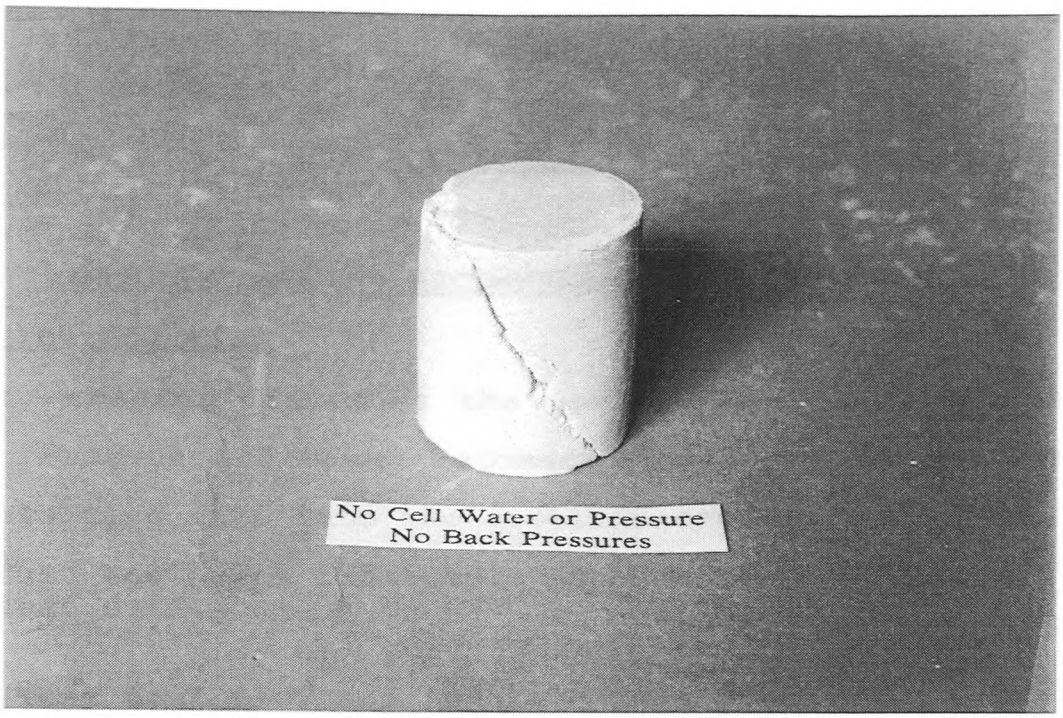

Plate 7.11 Sheared sample without confining or back pressures.

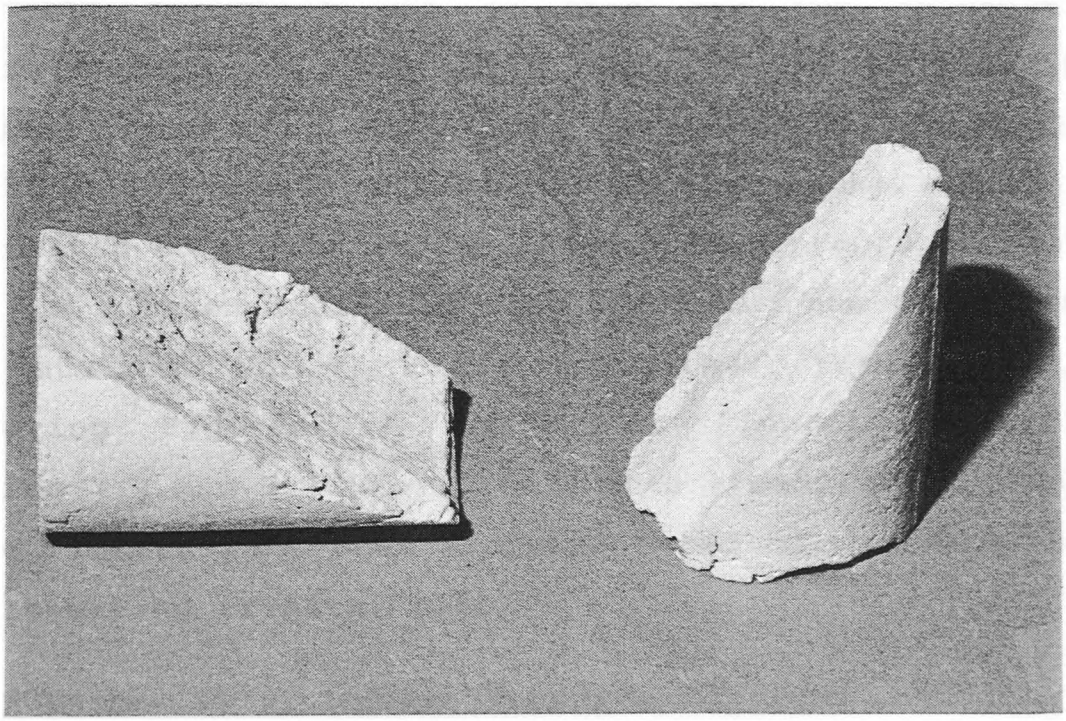

Plate 7.12 Sheared sample without confining or back pressures.

CHAPTER EIGHT

CONCLUSIONS AND RECOMMENDATIONS FOR FUTURE WORK

8.0 Introduction

This chapter discusses the main conclusions derived from the research and makes recommendations for future work. The conclusions fall into two distinct categories:

1) test equipment and sample preparation,
2) test data.

8.1 Test Equipment and Sample Preparation

8.1.1 Double-Walled Triaxial Cell

The double-walled triaxial cell, developed for the research, performed satisfactorily. It has certain advantages over the other two cells referred to in Chapter Six, Section 6.1.1. The most important one is that the two chambers have separate entry and exit ports. This allows the apparatus to be used both as a single or double-walled triaxial cell enabling the monitoring of the sample volume change to be maintained t0 a high degree of accuracy throughout testing. This is further indicated when comparing the performance of test stations No. 1, 2 and 3 together. For example, when comparing Figures 7.7 and 7.8 or Figures 7.10 and 7.11, Figures 7.7 and 7.10 indicate a more steady state condition. These Figures have been produced based on the data from the double-walled triaxial cell.

8.1.2 Bishop Water Volume Change Indicators

The changes in the total and water volumes were measured using two Bishop (twin burette) double tube, double acting

water volume change indicators. The Bishop water volume change indicator (1) (Figure 6.5) in station No. 1 is connected to the underside of the porous ceramic disc and measures the volume of water taken in by the soil samples. Similarly for station No. 2, the twin burette water volume change No. (2) is provided to perform the same task (Figure 6.6). These indicators have worked satisfactorily because they confirmed the anticipated soil behaviour. However, more sensitive equipment would have been advantageous.

The data obtained from the indicators are presented in Tables 7.14 to 7.17 for samples tested in the first and second phases and containing 10%, 20% and 30% montmorillonite respectively. The same data representing the volume of water intake by the soil samples are presented pictorially in Figures 7.2 to 7.13. They show that, as the montmorillonite content of the soil samples increases, so does the affinity for water and hence greater volumes of water are absorbed. The same trend is followed when considering the total volume change by the soil samples containing 10% to 30% montmorillonite.

The Bishop water volume change indicator (2) was connected to the inner chamber of station No. 1 to monitor the water movement due to expansion (or shrinkage) of the soil sample. Its performance, however, has raised two questions when considering the results of samples tested in the first phase. Considering the amount of montmorillonite (10%, 20% and 30%) and the water intake by the samples, greater expansion by each series of soil samples, especially those containing 30% montmorillonite, was expected. However, the

volume increases from the soil samples containing 10% montmorillonite to those containing 30% do not present the anticipated linear relationship.

Digital pressure controllers were used in station No. 3 to monitor the water intake by the samples and maintain the cell fluid and pressure. The pore water back pressure (2) (Figure 6.7) was used to supply and monitor the volume of water taken in by the soil samples. Cell pressure was produced and maintained by the digital pressure controller (1). However, the change in the volume of the soil samples was not measured by this controller. This is evident from Figure 7.58 where highly fluctuating relationships were obtained. This is due to a lack of control over the change in the volume of the cell. A Hall Effect Local Displacement Transducer (see Chapter Six - Section 6.9.1, Chapter Seven - Section 7.15 and Section 8.1.6) was therefore employed. The changes in the volume of the soil samples using the transducer are illustrated in Figure 7.23 and follow the same trend as those of the other test stations.

Total Volume Change

The total volume of the soil samples increased at first, then came to equilibrium in virtually every case. Since the equilibration time varied according to the type of soil, the maximum volume changes were reached over different periods of time. The final volumes therefore provide consistent criteria by which the soil samples can be compared.

Water Volume Change

The intake water volumes generally exhibited an initially large and rapid increase and then reached virtual

equilibrium. They were around 2 to 4 ccs for samples confined under 210 kN/m^2 and 12 ccs for those under 70 kN/m^2. Typical values are illustrated in Figures 7.2 to 7.13 where the water intake by the soil samples against time are presented. After this initial rapid increase only a small (about 0.5 cc) but constant inflow of water was recorded and persisted for the remainder of the test.

Water phase

The water volume changes generally increased with increasing plasticity. This relationship is well manifested in Figures 7.2 to 7.13. The volume changes comprised of immediate and secondary phases, although it is the immediate phase which consistently demonstrated an increase with increasing plasticity. The Figures indicate average water intakes of 2 to 4 ccs, increasing with plasticity for samples containing 10% to 30% montmorillonite respectively.

Air phase

The air phase volume changes were calculated as the difference between the soil solids and the water phase volume changes. These changes are presented in Tables 7.25 to 7.32. It can be seen that the volumes of air generally decreased between 10% and 16% from the initial to the final conditions.

8.1.3 Diffused Air Volume Indicator

During the early stages of the testing programme a persistent problem was encountered with sealing the chamber of the diffused air volume indicator. However, this problem was eventually solved by the use of flexible silicone rubber sealant. Thereafter the indicator performed satisfactorily.

A diffused air volume indicator was connected to station No. 1 only. Tables 7.29 to 7.32 show the quantities of diffused air measured by the indicator and in some soil samples significant volumes were recorded. Although de-aired water was used, it was inevitable that air would diffuse due to the way in which the de-aired water was incorporated into the system using a back pressure of air. This is not uncommon and has been stated by others such as Fredlund (1973) and Williams (1988).

8.1.4 Preparation of Test Specimens

The reasons for using artificially constituted clay samples were reviewed in Chapter Six, Section 6.10. The presentation in Section 6.10.3 shows that there is only a small proportion of impurities present in the kaolinite and sodium montmorillonite used. This is not usually the case in the field. However, using artificially constituted soils, like any other experimental programme, some variables are eliminated to produce a basis for a reasonable experimental model.

In order to ensure specimen consistency it was necessary to carefully control the clay mineral storage (dry), mineral blending (dry), addition of water, conditioning of prepared mixes and finally specimen forming (compaction). Nevertheless, slight departures of the final moisture content and density from the target values did occur and were attributed to evaporation effects and the specimen forming process respectively. The variations in the soil sample density and moisture content throughout each specimen were minimal and this was corroborated by the careful

examination of selected specimens. The initial moisture contents were found to be 30% ± 1% and the average initial densities were 1770 ± 10 kg/m^3. The homogeneity, along the lengths of the soil samples, was further verified by the number of conical failures resulting from shear strength testing (see Chapter Seven, Section 7.17.4). Small variations of initial moisture content and void ratio between specimens were reduced as far as possible. This was considered important to achieve a consistent trend in the test results.

8.1.5 Hall Effect Local Displacement Transducer

The Hall Effect Local Displacement Transducer used to measure the volume change of the soil samples in station No. 3 worked satisfactorily. This can be seen when Figures 7.23 and 7.58 are compared. This is in contrast to the results of the volume changes had they been measured using the displacement of water in the cell (see Chapter Seven, Section 7.15). However, the transducer has a limited range, which renders it unsuitable for use on samples with a high percentage of expanding lattices, such as those being tested, under low confining cell pressures. It is suggested that similar calipers with a larger monitoring range should be developed and employed. In the meantime, higher confining cell pressures are recommended to ensure completion of the test and a reduction in the risk of exhausting the range of the caliper.

8.2 Test Data

The underlying motivation for this investigation was the need to provide the engineer with improved techniques for predicting the swelling behaviour encountered in many unsaturated soils.

The initial phase of the research involved a survey of existing swell prediction methods. After developing suitable equipment (see Chapter Six, Section 6.9.1), an experimental programme of three test series was undertaken. Liquid limit, plastic limit, plasticity index, initial dry density, initial moisture content and initial degree of saturation of the soil samples were studied prior to testing.

Soil matrix suction $(U_a - U_w)$ represents the difference between pore air and pore water pressures due to surface tension and is consistent with the simple capillary model. It is from this term, however, that the special difficulties in applying the principle of effective stress to unsaturated soils arise.

A change in the value of the term $(U_a - U_w)$ does not correspond directly to a change in the confining cell pressure. The term signifying matrix suction represents a pressure difference due to surface tension which directly acts over only a part of the surface area of the soil particles but can have a significant influence on the soil; matrix suction is a function of the air content. In an unsaturated soil there is no continuity of the air which appears in an occluded state.

When measuring volume change properties of expansive clays, the stress changes are designed to cause a volume increase.

These are therefore generally designed to ensure constantly decreasing matrix suction ($U_a - U_w$) and net normal stress ($\sigma - U_a$) (see Chapter Seven, Tables 7.1 to 7.5). This constant decrease in the stress state variables can be achieved by conducting the following cycle of stress component changes:

i) increase in pore water pressure (U_w),
ii) decrease in pore air pressure (U_a), and
iii) decrease in total stress (σ).

In this series of testing, however, only i) and iii) were implemented.

The measured volume changes were consistently smaller than anticipated. The overall magnitude of water volume change increased with increasing plasticity whereas no such relationship was observed with the total volume change behaviour.

The soil specimen is initially at $(\sigma - U_a)_i$ and $(U_a - U_w)_i$ and is then allowed continuous access to water. Swelling takes place until equilibrium is attained.

8.2.1 Sample Moisture Content

The data presented in Tables 7.6 to 7.9 and discussed in Section 7.2 indicate that in most cases the final moisture content was greatest at the bottom of the sample and decreased towards the top. This is a function of the introduction of pore water back pressure at soil sample base level. However, in some cases moisture content was highest at the middle, which is attributed to a combination of the side filter paper drains and the rubber membrane enclosing the soil sample. The initial moisture content of the samples was 30% and increased to between 30.2% and 58.2% at the end

of testing. These final values of moisture content increased with increasing montmorillonite content and were also a function of the test conditions.

The duration of each test (see Section 7.2.1) had an effect on the final moisture content of the soil samples tested in the first phase. These samples were under test conditions for a minimum period of thirty days. In the second phase, however, no direct relationship between the duration of each test and the final moisture contents could be established. It is thought that the shear planes developed, in this phase, have influenced the water intake differently and hence affected the moisture content. The soil samples with side filter paper drains showed greatest moisture content at the middle. It was found that half the samples with side filter paper drains reached the highest moisture content and hence degree of saturation at the middle section.

8.2.2 Free Expansion of the Soil Samples

No axial expansion was experienced by the soil samples during the first phase of testing. This was because the soil samples were restrained at the bottom by the porous ceramic disc and at the top by the load cell (see Section 7.3). However, Table 7.10 shows that samples tested in the first phase expanded axially as soon as the equipment was dismantled and the soil samples were removed. Free expansion, therefore, refers to a combination of expansions obtained under stress conditions and after the soil samples have been removed from the cell. This is due to the suppression of the inherent expansiveness while the samples were in the cell and under applied stresses. The increase in

the height of the soil samples takes place without further access to water. This rapid expansion is believed to be due to stress relief rather than a gradual process resulting from a progressive increase in the intake of water. The free axial expansion recorded for these samples was as much as 4.6% of the original height. The soil samples tested in the second phase, presented in Tables 7.11 to 7.13, show decreases in heights even after the removal of stresses and allowing for free expansion to take place. This reduction in height is due to the shearing process and further consolidation of the soil samples.

Most of the soil samples, in the first phase, tended to more radial expansion at the bottom than the top (see Table 7.10) where they had greater access to water. However, the greatest degree of radial expansion, experienced by 50% of the soil samples, was at the middle hence producing the barrelling effect.

In the second phase, most of the soil samples containing 10% montmorillonite expanded more at the top than at the bottom. This pattern reverses as the montmorillonite content increases. That is, the samples with 30% montmorillonite expanded more at the bottom than at the top. The soil samples, in the second phase, also expanded most at the middle compared to the top and bottom; this being a function of the shear process as well as the provision of side filter paper drains and the rubber membrane.

The pattern in the two phases cannot be realistically compared as in the second phase shear was also involved

which resulted in shortening of the heights of soil samples due to axial deformation.

Even though the initial diameter to height ratio was 0.76, the ratio of percentage expansion radially to axially was greater than 1 and as high as 8.13 for samples tested in the first phase (see Section 7.3.3). This is a reflection of high and low confining cell pressures, respectively, as well as the influence of montmorillonite content and changes in stress conditions. In the second phase, the ratio of radial to axial dimensions (see Tables 7.11 to 7.13) at the end of testing remained generally below one. This behaviour is expected as the soil samples have undergone axial deformation and cannot be directly compared to the results of the first phase.

Other than the effect of side filter paper drains, there was no apparent trend in the relationship between the duration of each experiment and the final free expansion of the test samples in the first phase. This is further explained in Section 7.3.5. The soil samples, containing 30% montmorillonite, tested under higher confining cell pressures experienced bigger axial increase during free expansion than those tested under lower pressures. This is due to suppression of potential expansiveness while under bigger confining cell pressures. As soon as this higher pressure is removed the soil samples expand with a bigger magnitude. Similarly, bigger free radial expansions were recorded by samples tested under higher confining cell pressures.

In the second phase, a better pattern emerged. Tables 7.11 to 7.13 show that generally samples left to expand and then sheared exhibited more expansion than those sheared immediately after assembly.

8.2.3 Water Intake Versus Time

Comparing the graphs in Figures 7.2 to 7.13 for samples with 10%, 20% and 30% montmorillonite, it can be seen that in every case the gradient is shallowest for samples with least montmorillonite. The gradient increased with an increase in the amount of montmorillonite present in the samples and reached the steepest level with maximum montmorillonite i.e. 30%.

Samples tested under low confining cell pressures, in the first phase, absorbed water at a faster rate and greater quantity than those under high confining cell pressures. The graphs in Figure 7.6, relating to such samples tested under lower confining cell pressure, show a very steep gradient. It follows that greater stresses imposed by larger and heavier structures on a site will restrict the flow of water in a clay soil. Therefore the more stable the moisture movement or variation, the less likelihood there is of unpredictable heave or shrinkage taking place. A detailed analysis of this is provided in Section 7.5 and the magnitudes of water intake are summarised and presented in Tables 7.14 to 7.17.

8.2.4 Expansion Versus Time

There was a delay, even for a short period of one hour, from the moment that the soil samples had access to water up to

the time when expansion was observed (see Section 7.6). This was due to three reasons namely: adsorption of water by minerals, absorption of water by minerals, and void spaces. Figures 7.14 to 7.25 show a pictorial representation of expansion versus time, the magnitudes of which are summarised in Tables 7.14 to 7.17. One general observation is that as the confining cell pressures increase there is a corresponding decrease in the expansion observed.

The provision of side filter paper drains was also found to affect the behaviour of the soil samples. The reaction time between the water and the expanding lattices of the soil samples was reduced.

8.2.5 Axial Swell Pressure Versus Time

During the first phase of testing approximately 90% of the total swell pressures developed in the first hour (see Figures 7.26 to 7.29). This increased to around 95% in the first two to four days (see Section 7.7). Thereafter, the swell pressures developed at a slower rate and tended to a near constant value towards the end of the tests.

There is an interesting contrasting point with that mentioned in the previous Section. It was mentioned, in Section 8.2.4, that there was a delay of at least one hour from the start of the sample having access to water up to the time when a change in volume was observed. However, here it is stated that most of the swell pressure developed in the first hour. This may be due to the fact that as soon as an unsaturated soil has access to water, swell pressures develop instantaneously whereas, as explained in Section

8.2.4, it takes longer for the soil particles to absorb water and show expansion.

The swell pressures are plotted against the montmorillonite content in Figure 7.30 from which a direct relationship can be obtained. As the montmorillonite content increases so does the rate of increase in axial swell pressure although the relationship is not linear. The swell pressure developed by samples, containing 30% montmorillonite, tested under different confining cell pressures are separated. Figure 7.30 clearly shows the effect of confinement on the magnitude of swell pressure.

8.2.6 Swell Pressures Without Confining Pressures

Soil samples containing 10%, 20% and 30% montmorillonite were made and tested, without confining pressures, in a separate piece of apparatus devised by Abdi (1992) (see Section 7.8). It was found that at least 75% and up to 98% of the total swell pressures developed in the first few days of testing and the remaining fraction over a much longer period (see Figures 7.32 to 7.34). The higher value relates to the sample with the side filter paper drain.

A pair of samples with similar compositions was made and tested with and without side filter paper drains. A bigger magnitude of swell pressure was observed from the sample tested with the side filter paper drain. As evident from Figure 7.32, both samples took almost equal lengths of time for completion.

The swell pressures developed by two samples, containing 30% montmorillonite, one tested in Abdi's apparatus and the other in the double-walled triaxial cell were compared. The

maximum swell pressure obtained from Abdi's apparatus, after 2772 hours, was 163 kN/m^2 whereas the soil sample in the double-walled triaxial cell developed 262 kN/m^2 after only fifty hours. This is attributed to the fact that the sample in Abdi's apparatus is not confined laterally. The other reason is the flexibility of the proving ring and the stiffness of the load cell.

8.2.7 Volume Change (micrometer) and Time Versus Montmorillonite Content

The relationships between volume change (%) and duration of testing (days) against montmorillonite content, for samples tested in the first phase, are presented in Figure 7.35. They show that as the montmorillonite content increases so do the volume changes and the time taken for the pore water pressures to stabilise. Table 7.21 shows that samples containing 10% and 20% montmorillonite experienced average free expansions of 2.7% and 5.8% respectively. Samples containing 30% montmorillonite, tested under low and high confining cell pressures, show average free expansions of 18.4% and 8.9% respectively. This illustrates an obvious trend in the increase in montmorillonite content resulting in greater free expansion. The samples tested under lower confining cell pressures expanded by a much bigger magnitude which further demonstrates the effect of confining cell pressures on the performance of expanding lattices (see Section 7.9).

A linear relationship between percentage volume change and percentage montmorillonite content, for samples tested in the first phase, can be established. The relationship

between duration of testing and the percentage of montmorillonite is slightly curved.

In the second phase, both volume change and duration of testing increased curvi-linearly with the montmorillonite content (see Figure 7.36). This illustrates the extremely sensitive nature of the concept of monitoring the variable components of the unsaturated clays. The average percentages of free expansion, for all test conditions, of the soil samples containing 10%, 20% and 30% montmorillonite were 2.8%, 4.4% and 7.9% respectively. This compares favourably with the results previously mentioned during the first phase of testing. The graphs corresponding to volume changes, based on their respective confining cell pressures, are plotted in Figure 7.36 to illustrate their effect.

8.2.8 Water Intake and Expansion Versus Montmorillonite Content

Water intake and expansion as percentages of initial volume against montmorillonite content, obtained under all the various test conditions using Bishop water volume change indicators, are discussed in Section 7.10. Figures 7.39 to 7.42 show that the water intake and expansion increase with increasing montmorillonite content of the soil samples.

The change in water intake and expansion, for samples tested in the first phase, with montmorillonite content follow the same trend (see Figure 7.39). The water intake by samples containing 20% montmorillonite increased 110% compared to those containing 10% montmorillonite and the samples containing 30% increased by 150%. Similarly, the soil samples containing 20% montmorillonite expanded 98% more

than those containing 10% whereas the soil samples containing 30% montmorillonite expanded by 115%. However, if a linear relationship between the water intake and expansion with montmorillonite content is assumed, then 220% and 196%, respectively, for samples containing 30%, should have been achieved.

In the second phase, however, the trend is different. The rates of increase in both water intake and expansion, in samples containing between 20% and 30% montmorillonite, are greater than those in soil samples containing between 10% and 20%. They have obviously been affected by changes in test conditions (confining cell pressures) and the duration of the tests.

The water intake, presented in Figure 7.40, increased by 25% in samples containing 20% montmorillonite whereas it increased by 328% in those containing 30%. This high percentage increase in water intake is influenced by the effect of samples tested under a low confining cell pressure of 70 kN/m^2. For samples tested under 140 and 210 kN/m^2 confining cell pressures, a better trend results. In this case, the values for 20% and 30% montmorillonite change to 82% and 275% respectively.

Similarly, samples containing 20% expanded by 130% whereas those with 30% montmorillonite experienced 427% expansion (see Figure 7.41) compared to those containing 10% montmorillonite. These represent values where the effect of low confining cell pressure is included. If the higher confining cell pressures only are considered then the values

for 20% and 30% montmorillonite modify to 16% and 274% respectively.

8.2.9 Initial and Final Properties of Soil Samples

The volumes of different constituent materials were calculated after the termination of each test. Two samples containing 30% montmorillonite and tested under low confining cell pressures, in the first phase, produced negative volumes of air. Several hypotheses have been considered and discounted.

It is thought that it may be a physical phenomenon. The other hypothesis is whether there are air voids within the lattices which can take up water without affecting the overall volume of the soil samples. It has been found that there are minute amounts of air voids present within the lattices but they are of such small volumes they will not satisfy the present query.

The initial and final void ratios and degrees of saturation, of all the soil samples tested, fall in a narrow band. The initial void ratios (e) and degrees of saturation (Sr), for samples tested in the first phase, are: e = 0.946 ± 0.006 and Sr = 85.2% ± 0.5% (see Table 7.25 and Figures 7.47 and 7.49). The initial void ratios for samples containing 10%, 20% and 30% montmorillonite, tested in the second phase, are 0.941 ± 0.005, 0.941 ± 0.007 and 0.943 ± 0.01 respectively (see Tables 7.26 to 7.28 and Figure 7.48). The initial degrees of saturation for samples containing 10%, 20% and 30% montmorillonite, tested in the second phase, are 85.71% ± 0.5%, 85.54% ± 0.3% and 85.3% ± 0.5% respectively (see Tables 7.26 to 7.28 and Figure 7.50).

The final void ratios of the samples, tested in the first phase, increased by an average of 1.85% from the initial to the final conditions. Similarly, the final degrees of saturation, of the samples tested in the first phase, increased by an average of 21.76% but when the effect of those samples tested under low confining cell pressure is eliminated, the average percentage increase reduces to 6.33% (see Table 7.33 and Figures 7.47 and 7.49).

8.2.10 Shear Strength of Unsaturated Soils

The shear strength of an unsaturated soil consists of an effective cohesion, C', and independent contributions from the net normal stress, $(\sigma - U_a)$, and a further contribution from the matrix suction, $(U_a - U_w)$.

Three different series of testing were undertaken in this phase. The first series comprised samples which were made and put into a saturation phase with the appropriate confining cell pressures and pore water and pore air back pressures. Once the samples had reached equilibrium, that is, when saturation had ceased and no further expansion was observed, the rate of deformation was calculated and the soil sample was then sheared. The rates of deformation used in this experimentation ranged between 0.0008 and 0.0067 mm/min. The second series comprised soil samples made with the same composition and sheared immediately after equipment assembly. The same values of confining cell pressure and pore air and pore water back pressures as in the previous series were used. In the third series, samples similar to the first two series were made and sheared as

soon as the equipment was assembled but there were no pore air or pore water back pressures.

The shear failure envelopes for this study are presented, in four formats, in Figures 7.59 to 7.85. They are: total stress, effective stress considering the pore water back pressure, effective stress considering the pore air back pressure and effective stress considering matrix suction.

The Mohr circles for an unsaturated soil are plotted in accordance with Fredlund's terminology. That is, the net normal stress axis, $(\sigma - U_a)$, is comparable to the effective stress axis, $(\sigma - U_w)$, for saturated soils.

When considering total stresses a clear pattern emerges. In all three compositions (10%, 20% and 30% montmorillonite) the angle of internal friction, ϕ_u, decreases as the test series change from saturation and expansion prior to shear to no saturation or expansion and no back pressure prior to shear.

The effect of water (and/or air) on the cohesive intercepts is the reverse of that on the angle of internal friction for all stress conditions. In other words, as the access to water is restricted the value of cohesion increases.

The effective stresses with respect to pore water back pressure $(\sigma - U_w)$, illustrate the same trend. The effective stress angle of internal friction, ϕ', decreases as the access to water is restricted. Conversely, the effective stress cohesive intercepts increase as access to water is restricted.

Similarly, the same trend occurs when evaluating the effective stresses based on the pore air back pressure

$(\sigma - U_a)$. It is evident, from Figures 7.74 to 7.79, that the effective stress cohesions increase as the soil samples have less access to water.

The effective stresses with respect to matrix suction generally show a similar pattern to those with respect to pore water and pore air back pressures. The effective stress cohesive intercepts increase as access to water is restricted.

The values of ϕ^b are found to be consistently less than ϕ'' with respect to pore air back pressures. This further emphasises the role that matrix suction plays in the behaviour of unsaturated soils. Therefore, it is not sufficient to determine values of ϕ'' alone in the case of unsaturated soils.

The values of ϕ^b are found to be higher than ϕ_u, with respect to total stresses, and ϕ' with respect to pore water back pressures. The following relationships were found to be generally applicable:

$$\phi'' > \phi' > \phi^b > \phi_u \qquad \text{and} \qquad C' < C'' \approx C^b < C_u$$

The values of effective stress angles of internal friction, with respect to pore air back pressure, are found to be higher than those with respect to pore water back pressure, matrix suction or the total stress. This is due to the fact that the magnitude of pore air back pressure is bigger than the pore water back pressure hence producing this great difference. As explained above it is not sufficient to evaluate the value of ϕ'' alone but ϕ^b should also be considered.

A significant point established from the tests is that the values of the angle of internal friction, whether total or effective, decreased as the amount of montmorillonite in the soil samples increased. This, of course, further indicates the affinity to water of montmorillonite. The bigger intake of water weakens the shearing resistance of soil samples. In addition, it is evident that the effective stress angles of internal friction obtained from the samples undergoing saturation and expansion prior to shear were generally greater than those sheared immediately after assembly. This is further indication that the soil samples after saturation and expansion are in a normally consolidated state, whereas those in the second series, where they were sheared immediately after assembly, appear to act as an overconsolidated clay due to the stress state. There is also experimental evidence (Satija (1978)) of probable curved failure envelopes.

8.3 Recommendations For Future Work

1) There is limited published information on the strengths of unsaturated expansive soils. From this and the results of the present study the following recommendations are made:
   a) Measure shear, compressive and tensile strengths of unsaturated soils before and after expansion.
   b) Vary stress state variables and compare the effects.
   c) Vary the initial soil properties and study the behaviour.

d) Compare results of direct shear testing unsaturated soils with triaxial tests which would form a basis for parametric studies of shear strength.

e) Compare consolidated undrained and consolidated drained test results and establish possible differences in shear strength parameters.

f) Take the specimens to failure in compression by reducing the radial stress and conduct a controlled stress path analysis.

g) Using stress path analysis, study the effect of dilatancy on the value of effective stress angle of internal friction.

2) Shear strength has been studied in this investigation at a constant soil suction. To study further the influence of soil suction the following recommendations are made:

a) The influence of variation in soil suction on the behaviour of unsaturated soil is studied.

b) The influence of soil suction on the swelling potential of expansive clays is studied.

c) Various techniques for measuring soil moisture suction in the laboratory are further investigated.

3) Examination of the swell / suction relationship for as many soils as possible would prove of great value to the engineer, particularly with the advent of reliable field suction measurement equipment.

4) The reliability of available instruments for measuring field suction should be assessed with a view to relating suction to in situ swell for a variety of soil types and environments.

5) Devices to measure the radial and axial expansions independently should be regularly incorporated into triaxial testing especially when single-walled cells are used.

6) Results for natural soils should be compared with those for artificially constituted soils.

7) Recurrent wetting and drying cycles need to be simulated in the modified double-walled triaxial cell.

REFERENCES

Abdi, M.R. (1992). Effects of gypsum on lime-stabilised kaolinite. Ph.D. Thesis, Polytechnic of Wales, U.K.

Abeyesekera, R.A. and Lovell, C.W. (1981). Volume changes in compacted clays and shales on saturation. Transp. Res. Rec. No. 790, Washigton, 67-73.

Agarwal, K.P. and Sharma, S.C. (1973). A method for measuring swelling pressure of an expansive soil. Proc. 3rd Int. Conf. on Expansive Soils, Haifa, Vol. 1, 155-159.

Aitchison, G.D. (1956). The circumstances of unsaturation in soils with particular reference to the Australian environment. Proc. 2nd Australian - New Zealand Conf. on SM & FE, 173-191.

Aitchison, G.D. (1961). Relationships of moisture stress and effective stress functions in unsaturated soils. Proc. Pore Pressure and Suction in Soils, Butterworths, London, 47-52.

Aitchison, G.D. (1965). Engineering concepts of moisture equilibria and moisture changes in soils. Proc. Symp. Moisture Equilibria and Moisture Changes in Soils Beneath Covered Areas, Butterworth, Australia, 7-21.

Aitchison, G.D. (1967). The separate roles of site investigation, quantification of soil properties, and selection of operational environment in the determination of foundation design on expansive soils. Proc. 3rd Asian Reg. Conf. on SM & FE, Haifa, Vol. 2, 72-77.

Aitchison, G.D. (1973). The quantitative description of the stress deformation behaviour of expansive soils. Proc. 3rd Int. Conf. on Expansive Soils, Haifa, Vol. 2, 79-82.

Aitchison, G.D. and Martin, R. (1973). A membrane oedometer for complex stress-path studies in expansive clays. Proc. 3rd Int. Conf. on Expansive Soils, Haifa, Vol. 1, 161-167 and Vol. 2, 83-88.

Aitchison, G.D. and Peter, P. (1973). The measurement of matrix suctions in expansive clays using the membrane oedometer. Proc. 3rd Int. Conf. on Expansive Soils, Haifa, Vol. 1, 79-81 and Vol. 2, 97-99.

Aitchison, G.D. and Richards, B.G. (1965). A broad-scale study of moisture conditions in pavement subgrades throughout Australia. 2. Techniques adopted for the measurement of moisture variables. Proc. Symp. Moisture Equilibria and Moisture Changes in Soils Beneath Covered Areas, Butterworths, Australia, 191-204.

Aitchison, G.D. and Woodburn, J.A. (1969). Soil suction in foundation design. Proc. 7th ICSMFE, Mexico, Vol. 2, 1-8.

Ali, E.F.M. and Elturabi, M.A.D. (1984). Comparison of two methods for the measurement of swelling pressure. Proc. 5th Int. Conf. on Expansive Soils, Adelaide, 72-74.

Alpan, I. (1957). An apparatus for measuring the swelling pressure in expansive soils. Proc. 4th ICSMFE, London, Vol. 1, 3-5.

Altmeyer, W.T. (1956). Discussion on the paper "Engineering properties of expansive clays" by W.G. Holtz and H.J. Gibbs, Trans. ASCE, Vol. 121, 666-669.

Arthur, J.R.F., Chua, K.S., Dunstan, T. and Rodriguez del C, J.I. (1980). Principal stress rotation: A missing parameter. J. Geotech. Eng. Div., Proc. ASCE, Vol. 106, No. GT4, Paper 15375, 419-433.

Atkinson, J.H. and Bransby, P.L. (1978). The mechanics of soils, An introduction to critical state soil mechanics. McGraw-Hill Book Co. (UK) Ltd.

Attinger, R.O. and Köppel, J. (1983). A new method to measure lateral strain in uniaxial and triaxial compression tests. Rock Mechanics and Rock Engineering, Vol. 16, 73-78.

Bailey, S.W. (1980). Summary of recommendations of AIPEA nomenclature committee on clay minerals. American Mineralogist, Vol. 65, 1-7.

Baker, R., Kassiff, G. and Levy, A. (1973). Experience with a psychrometric technique. Proc. 3rd Int. Conf. on Expansive Soils, Haifa, Vol. 1, 83-95.

Bandyopadhyay, S.S. (1981). Prediction of swelling potential for natural soils. J. Geotech. Eng. Div., Proc. ASCE, Vol. 107, No. GT5, Technical Note, 658-661.

Barden, L., Madedor, A.O. and Sides, G.R. (1969). Volume change characteristics of unsaturated clay. J. SM & FDiv., Proc. ASCE, Vol. 95, No. SM1, Paper 6338, 33-51.

Beal, N.S. (1984). Direct determination of linear dimension versus moisture content relationship in expansive clays. Proc. 5th Int. Conf. on Expansive Soils, Adelaide, 62-66.

Bell, F.G. (1983). Engineering properties of soils and rocks. 2nd Ed., Butterworths, U.K.

Bishop, A.W. (1959). The principle of effective stress. Tecknisk Ukeflad, No. 39.

Bishop, A.W. (1969). Pore pressure measurements in the field and in the laboratory. Proc. 7th ICSMFE, Mexico, Specialty Sessions, Vol. 3, 427-444.

Bishop, A.W., Alpan, I., Blight, G.E. and Donald, I.B. (1960). Factors controlling the strength of partly saturated cohesive soils. Proc. Res. Conf. on Shear Strength of Cohesive Soils, Boulder, 503-532.

Bishop, A.W. and Blight, G.E. (1963). Some aspects of effective stress in saturated and partly saturated soils. Gèotechnique, Vol. 13, No. 3, 177-197.

Bishop, A.W. and Donald, I.B. (1961). The experimental study of partly saturated soil in the triaxial apparatus. Proc. 5th ICSMFE, Paris, Vol. 1, 13-21.

Bishop, A.W. and Gibson, R.E. (1963). The influence of the provisions for boundary drainage on strength and consolidation characteristics of soils measured in the triaxial apparatus. Laboratory Shear Testing of Soils, ASTM Special Technical Publication No. 361, 435-458.

Bishop, A.W. and Henkel, D.J. (1962). The measurement of soil properties in the triaxial test. 2nd Ed., Edward Arnold (Publishers) Ltd., London.

Bishop, A.W. and Wesley, L.D. (1975). A hydraulic triaxial apparatus for controlled stress path testing. Gèotechnique, Vol. 25, No. 4, 657-670.

Blight, G.E. (1961). Strength and consolidation characteristics of compacted soils. Ph.D. Thesis, University of London, U.K.

Blight, G.E. (1965a). The time-rate of heave of structures on expansive clays. Proc. Symp. Moisture Equilibria and Moisture Changes in Soils Beneath Covered Areas, Butterworths, Australia, 78-88.

Blight, G.E. (1965b). A study of effective stresses for volume change. Proc. Symp. on Moisture Equilibria and Moisture Changes in Soils Beneath Covered Areas, Butterworths, Australia, 259-269.

Blight, G.E. (1967). Effective stress evaluation for unsaturated soils. J. SM & FDiv., Proc. ASCE, Vol. 93, No. SM2, Paper 5146, 125-148.

Blight, G.E. and De Wet, J.A. (1965). The acceleration of heave by flooding. Proc. Symp. Moisture Equilibria and Moisture Changes in Soils Beneath Covered Areas, Butterworths, Australia, 89-92.

Bocking, K.A. and Fredlund, D.G. (1980). Limitations of the axis translation technique. Proc. 4th Int. Conf. on Expansive Soils, Denver, Vol. 1, 117-135.

Bolt, G.H. (1956). Physico-chemical analysis of the compressibility of pure clays. Gèotechnique, Vol. 6, No. 2, 86-93.

Brackley, I.J.A. (1971). Partial collapse in unsaturated expansive clay. Proc. 5th Reg. Conf. for Africa on SM & FE, Luanda, 1-23 to 1-30.

Brackley, I.J.A. (1975a). Swell under load. Proc. 6th Reg. Conf. for Africa on SM & FE, Durban, Vol. 1, 65-70.

Brackley, I.J.A. (1975b). A model of unsaturated clay structure and its application to swell behaviour. Proc. 6th Reg. Conf. for Africa on SM & FE, Durban, Vol. 1, 71-79.

Brackley, I.J.A. (1983). An empirical equation for the prediction of clay heave. Proc. 7th Asian Reg. Conf. on SM & FE, Haifa, Vol. 1, 8-14.

Bradley, W.F. (1945). Molecular association between montmorillonite and some polyfunctional organic liquids. J. of American Chemical Society, Vol. 67, 975-981.

Brown, G. (1984). Crystal structures of clay minerals and related phyllosilicates. Phil. Trans. of the Royal Soc., London, A311, 221-240.

BS 1377 (1975). Methods of test for soils for civil engineering purposes. British Standard Institution, U.K.

BS 1377 (1990a). Methods of test for soils for civil engineering purposes. Part 7, Shear Strength Tests (Total Stress) and/or Part 8, Shear Strength Tests (Effective Stress). British Standard Institution, U.K.

BS 1377 (1990b). Methods of test for soils for civil engineering purposes. Part 2, Classification Tests, British Standard Institution, U.K.

Burland, J.B. (1962). The estimation of field effective stresses and the prediction of total heave using a revised method of analysing the double oedometer test. Civil Engineering in South Africa, SAICE, 133-137.

Burland, J.B. (1965). Some aspects of mechanical behaviour of partly saturated soils. Proc. Symp. Moisture Equilibria and Moisture Changes in Soils Beneath Covered Areas, Butterworths, Australia, 270-278.

Burland, J.B. (1984). Building on expansive soils. Proc. 1st Nat. Conf. on Science and Technology of Buildings, Khartoum, 59-82.

Chang, R.K. (1969). Pressure plate apparatus for volumetric measurement of suction, swelling pressure, and consolidation in clay soils. Canadian Geotech. J., Vol. 6, No. 2, 209-212.

Chen, F.H. (1973). The basic physical property of expansive soils. Proc. 3rd Int. Conf. on Expansive Soils, Haifa, Vol.1, 17-25.

Chen, F.H. (1975). Foundations on Expansive Soil. Elsevier, New York.

Clayton, C.R.I., Khatrush, S.A., Bica, A.V.D. and Siddique, A. (1989). The use of Hall Effect semiconductors in geotechnical instrumentation. Geotech. Testing J., ASTM, Philadelphia, Vol. 12, No, 1, 69-76.

Cole, D.M. (1978). A technique for measuring radial deformation during repeated load triaxial testing. Canadian Geotech. J., Vol. 15, No. 3, 426-429.

Coleman, J.D. (1962). Stress/strain relations for partly saturated soil. Correspondence, Gèotechnique, Vol. 12, No. 4, 348-350.

Cooling, L.F. (1961). Pore pressure and suction in soils. Discussion, Proc. Pore Pressure and Suction in Soils, Butterworths, London, 63-74.

Coulomb, C.A. (1776). Essai sur une application des regeles des maximus et minimus a quelque problemes de statique relatif a l'architecture. Memoirs Divers Savants Academie Science, Paris.

Cox, D.W. (1979). Volume change of compacted clay fill. Proc. Conf. on Clay Fills, London, 79-86.

Croney, D. and Coleman, J.D. (1960). Pore pressure and suction in soil. Proc. Pore Pressure and Suction in Soils, Butterworths, London, 31-37.

Croney, D., Coleman, J.D. and Black, W.P.M. (1958). Movement and distribution of water in soil in relation to highway design and performance. Highway Res. Board, Special Report No. 40, Washington, 226-252.

Croney, D., Coleman, J.D. and Bridge, P.M. (1952). The suction of moisture held in soil and other porous materials. Road Res. Technical Paper No. 24, Road Res. Lab., HMSO.

Dagg, M. and Russam, K. (1966). The relation between soil shrinkage and the development of surface cracks in an experimental road in Kenya. RRL Report No. 12, Road Research Laboratory, Ministry of Transport, UK.

Dakshanamurthy, V. and Raman, V. (1973). A simple method of identifying an expansive soil. Soils and Foundations, Japanese Soc. of SM & FE, Vol. 13, No. 1, 97-104.

Das, B.M. (1985). Advanced soil mechanics. McGraw-Hill Book Co., Singapore.

Davidson, D.T. (1949). Exploratory evaluation of some organic cations as soil stabilizing agents. Proc. of Highway Res. Board, Vol. 29, 531-537.

Davidson, D.T. and Glab, J.E. (1949). An organic compound as a stabilizing agent for two soils-aggregate mixtures. Proc. of Highway Res. Board, Vol. 29, 537-543.

Davies, J.T. and Rideal, E.K. (1963). Interfacial phenomena. 2nd Ed., Academic Press Inc., New York.

Davies, M.C.R. (1993). Private communication. University of Wales College of Cardiff, U.K.

De Bruijn, C.M.A. (1961). Swelling characteristics of a transported soil profile at Leeuhof Vereeniging (Transvaal). Proc. 5th ICSMFE, Paris, Vol. 1, 43-49.

De Bruijn, C.M.A. (1965). Annual redistribution of soil moisture suction and soil moisture density beneath two different surface covers and the associated heaves at the Onderstepoort test site near Pretoria. Proc. Symp. Moisture Equilibria and Moisture Changes in Soils Beneath Covered Areas, Butterworths, Australia, 122-134.

De Bruijn, C.M.A. (1973a). Moisture redistribution in Southern African soils. Proc. 8th ICSMFE, Moscow, Vol. 2, Part 2, 37-44.

De Bruijn, C.M.A. (1973b). Moisture redistribution and soil movements at Vereeniging (Transvaal). Proc. 3rd Int. Conf. on Expansive Soils, Haifa, Vol. 1, 279-288.

Dennen, W.H. and Moore, B.R. (1986). Geology and Engineering. W.C. Brown Publishers, Iowa, U.S.A.

Didier, G. (1973). Swelling pressures of soils - experimental device - field of utilization. Proc. 3rd Int. Conf. on Expansive Soils, Haifa, Vol. 1, 187-193.

Didier, G., Kastner, R. and Bourdeau, Y. (1980). New Cell for study of swelling soils. Proc. 4th Int. Conf. on Expansive Soils, Denver, Vol. 1, 18-33.

Donald, I.B. (1956). Shear strength measurements in unsaturated non-cohesive soils with negative pore pressures. Proc. 2nd Australia-New Zealand Conf. on SM & FE, 200-205.

Donald, I.B. (1961). The mechanical properties of saturated and partly saturated soils with special reference to the influence of negative pore water pressure. Ph.D. Thesis, University of London, U.K.

Donaldson, G.W. (1965). A study of level observations on buildings as indications of moisture movements in the underlying soil. Proc. Symp. Moisture Equilibria and Moisture Changes in Soils Beneath Covered Areas, Butterworths, Australia, 156-164.

Donaldson, G.W. (1969). The occurrence of problems of heave and the factors affecting its nature. Proc. 2nd Int. Res. and Eng. Conf. on Expansive Clay Soils. Texas A & M Univ., 25-36.

Driscoll, R. (1984). A review of British experience of expansive clay problems. Proc. 5th Int. Conf. on Expansive Soils, Adelaide, 192-196.

Dudley, J.H. (1971). Remote measurement of radial deformations. J. SM & FDiv., Proc. ASCE, Vol. 97, No. SM6, Technical Note, 965-968.

Eberl, D.D. (1984). Clay mineral formation and transformation in rocks and soils. Phil. Trans. of the Royal Soc., London, A311, 241-257.

Edil, T.B. and Alanazy, A.S. (1992). Lateral swelling pressures. Proc. 7th Int. Conf. on Expansive Soils, Dallas, Vol. 1, 227-232.

El-Ruwayih, A.A. (1976). Design manufacture and performance of a lateral strain device. Gèotechnique, Vol. 26, No. 1, 215-216.

El-Sohby, M.A. and Rabbaa, S.A. (1984). Deformational behaviour of unsaturated soils upon wetting. Proc. 8th Reg. Conf. for Africa on SM & FE, Harare, Vol. 1, 129-137.

Escario, V. (1969). Swelling of soils in contact with water at a negative pressure. Proc. 2nd Int. Res. and Eng. Conf. on Expansive Clay Soils, Texas A & M University, 207-217.

Escario, V. (1980). Suction controlled penetration and shear tests. Proc. 4th Int. Conf. on Expansive Soils, Denver, Vol. 2, 781-797.

Escario, V. and Sáez, J. (1973). Measurement of the properties of swelling and collapsing soils under controlled suction. Proc. 3rd Int. Conf. on Expansive Soils, Haifa, Vol. 1, 195-200.

Escario, V. and Sáez, J. (1986). The shear strength of partly saturated soils. Gèotechnique, Vol. 36, No. 3, 453-456.

Esquevin, J. (1958). Les silicates de Zinc. Etude de Produits de Synthese et des Mineraux Naturels, Hese Sci., Paris.

Farmer, V.C. and Palmieri, F. (1975). The characterization of soil minerals by infrared spectroscopy. "Soil Components, Vol. 2, Inorganic Compounds", Ed: E. Gieseking, Springer-Verlag, New York, Chapter 17, 573-670.

Fourie, A.B. (1989). Laboratory evaluation of lateral swelling pressure. J. of Geotech. Eng., Proc. ASCE, Vol. 115, No. 10, Technical Note, 1481-1486.

Fredlund, D.G. (1969). Consolidometer test procedural factors affecting swell properties. Proc. 2nd Int. Res. and Eng. Conf. on Expansive Clay Soils, Texas A & M University, 435-456.

Fredlund, D.G. (1973). Volume change behaviour of unsaturated soils. Ph.D. Thesis, University of Alberta, Edmonton, Alta, Canada.

Fredlund, D.G. (1974). Engineering approach to soil continua. Proc. 2nd Symp. on the Application of Solid Mechanics, Hamilton, Vol. 1, 46-59.

Fredlund, D.G. (1975). A diffused air volume indicator for unsaturated soils. Canadian Geotech. J., Vol. 12, No. 4, 533-539.

Fredlund, D.G. (1979). Appropriate concepts and technology for unsaturated soils. 2nd Canadian Geotechnical Colloquium, Canadian Geotech. J, Vol. 16, No. 1, 121-139.

Fredlund, D.G. and Morgenstern, N.R. (1976). Constitutive relations for volume change in unsaturated soils. Canadian Geotech. J., Vol. 13, No. 3, 261-276.

Fredlund, D.G. and Morgenstern, N.R. (1977). Stress state variables for unsaturated soils. J. of the Geotech. Eng. Div., Proc. ASCE, Vol. 103, No. GT5, Paper 12919, 447-466.

Fredlund, D.G., Morgenstern, N.R. and Widger, R.A. (1978). The shear strength of unsaturated soils. Canadian Geotech. J., Vol. 15, No. 3, 313-321.

Fredlund, D.G. and Rahardjo, H. (1985). Theoretical context for understanding unsaturated residual soil behavior. Proc. 1st Int. Conf. on Geomechanics in Tropical Lateritic and Saprolitic Soils, Brazil, 295-306.

Fredlund, D.G., Rahardjo, H. and Gan, J.K.M. (1987). Non-linearity of strength envelope for unsaturated soils. Proc. 6th Int. Conf. on Expansive Soils, New Delhi, Vol. 1, 49-54.

Freundlich, H. (1935). Thixotropy. Hermann and Co., Paris.

Gan, J.K.M. and Fredlund, D.G. (1988). Multistage direct shear testing of unsaturated soils. Geotech. Testing J., ASTM, Vol. 11, No. 2, 132-138.

Gibbs, H.J. and Coffey, C.T. (1969). Techniques for pore pressure measurements and shear testing of soil. Proc. 7th ICSMFE, Mexico, Vol. 1, 151-157.

Gibson, R.E. and Henkel, D.J. (1954). Influence of duration of tests at constant rate of strain on measured drained strength. Gèotechnique, Vol. 4, 6-15.

Gillot, J.E. (1987). Clay in engineering geology. Developments in Geotechnical Engineering, Vol. 41, Elsevier Science Publishers, Amsterdam.

Green, H. and Weltmann, R.N. (1946). Thixotropy. Colloid Chemistry, Vol. 6, 328-347.

Grim, R.E. (1942). Modern concepts of clay minerals. J. of Geology, Vol. 50, 225-275.

Grim, R.E. (1959). Physico-chemical properties of soils: clay minerals. J. SM & FDiv., Proc. ASCE, Vol. 85, No, SM2, Paper 1998, 1-17.

Gulhati, S.K. (1972). Shear behaviour of compacted soils in the saturated and partially saturated states. Ph.D. Thesis, Indian Institute of Technology, Delhi, India.

Gulhati, S.K. (1975). Shear behaviour of partially saturated soil. Proc. 5th Asian Reg. Conf. on SM & FE, Bangalore, 87-90.

Gulhati, S.K. and Satija, B.S. (1981). Shear strength of partially saturated soils. Proc. 10th ICSMFE, Stockholm, Vol. 1, 609-612.

Gupta, S.P., Bhadrari, R.K. and Dinesh, M. (1983). Insitu engineering behaviour of an Indian black cotton soil deposit. Proc. 7th Asian Reg. Conf. on SM & FE, Haifa, 19-24.

Hamilton, J.J. (1980). Behavior of expansive soils in Western Canada. Proc. 4th Int. Conf. on Expansive Soils, Denver, Vol. 2, 815-833.

Harman, C.G. and Fraulini, F. (1940). Properties of Kaolinite as a function of its particle size. Am. Ceramic Soc. J., Vol. 23, 253-259.

Harvey, J.C. (1982). Geology for geotechnical engineers. Cambridge University Press, U.K., 13.

Head, K.H. (1982). Manual of soil laboratory testing. Pentech Press Ltd., Vol. 2, U.K.

Hendricks, S.B. (1941). Base exchange of the clay mineral montmorillonite for organic cations and its dependence upon adsorption due to Van der Waals' forces. J. of Physics and Chemistry, Vol. 45, 65-81.

Hendricks, S.B., Nelson, R.A. and Alexander, L.T. (1940). Hydration mechanism for the clay mineral montmorillonite saturated with various cations. J. Am. Chemical Soc., Vol. 62, Part. 1, 1457-1464.

Henkel, D.J. and Gilbert, G.D. (1952). The effect of the rubber membrane on the measured triaxial compression strength of clay samples. Géotechnique, Vol. 3, No. 1, 20-29.

Hight, D.W., Gens, A. and Symes, M.J. (1983). The development of a new hollow cylinder apparatus for investigating the effects of principal stress rotation in soils. Gèotechnique, Vol. 33, No. 4, 355-383.

Hilf, J.W. (1956). An investigation of pore water pressure in compacted cohesive soil. Ph.D. Thesis, Univ. Colorado, U.S.A.

Ho, D.Y.F. and Fredlund, D.G. (1982a). Increase in strength due to suction for two Hong Kong soils. Proc. ASCE Geotech. Eng. Div., Specialty Conf. on Engineering and Construction in Tropical and Residual Soils, Honolulu, 263-295.

Ho, D.Y.F. and Fredlund, D.G. (1982b). Strain rates for unsaturated soil shear strength testing. Proc. of the 7th Southeast Asian Geotech. Conf., Hong Kong, Vol. 1, 787-803.

Holtz, W.G. and Gibbs, H.J. (1956). Engineering properties of expansive clays. Trans. ASCE, Vol. 121, 641-663.

Hoskings, J.S. (1940). The soil clay mineralogy of some Australian soils developed on granitic and basaltic parent material. Australian Council of Sci. and Indus. Res., Vol. 13, 206-216.

Houwink, R. and Burgers, W.G. (1939). Elasticity, Plasticity and structure of matter. Cambridge University Press, U.K., 376pp.

Hvorslev, M.J. (1939). über die Festigheitseigenschaften gestorter bindiger Boden: Ingeniorvidenskabelige Skrifter, A. 45, Copenhagen.

Iversen, K. and Moum, J. (1974). The paraffin method - triaxial testing without a rubber membrane. Gèotechnique, Vol. 24, No. 4, Technical Note, 665-670.

Jennings, J.E.B. (1961). A revised effective stress law for use in the prediction of the behaviour of unsaturated soils. Proc. Pore Pressure and Suction in Soils, Butterworths, London, 26-30.

Jennings, J.E.B. (1969). The engineering problems of expansive soils. Proc. 2nd Int. Res. and Eng. Conf. on Expansive Clay Soils, Texas A & M Univ., 11-17.

Jennings, J.E.B. (1973). The engineering significance of constructions on dry subsoils. Proc. 3rd Int. Conf. on Expansive Soils, Haifa, Vol. 2, 27-32.

Jennings, J.E.B. and Burland, J.B. (1962). Limitations to the use of effective stresses in partly saturated soils. Gèotechnique, Vol. 12, No. 2, 125-144.

Jennings, J.E.B. and Evans, G.A. (1962). Practical procedures for building in expansive soil areas. The South African Builder, Vol. 50, No. 4, 15-23.

Jennings, J.E.B. and Kerrich, J.E. (1962). The heaving of buildings and the associated economic consequences, with particular reference to the Orange Free State Goldfields. The Civil Engineer in South Africa, Trans. of the SAICE, Vol. 4, Part 11, 221-248.

Jennings, J.E.B. and Knight, K. (1957). The prediction of total heave from the double oedometer test. Proc. Symp. on Expansive Clays, SAICE, Vol. 7, No. 9, 285-291.

Johnson, A.L. and Davidson, D.T. (1947). Clay technology and its application to soil stabilization. Proc. of Highway Res. Board, Vol. 27, 418-430.

Johnson, L.D. (1974). An evaluation of the thermocouple psychrometric technique for the measurement of suction in clay soils. U.S. Army Engineer Waterways Experiment Station, Technical Report S-74-1.

Johnson, L.D. (1979). Overview of design of foundations on expansive soils. U.S. Army Engineer Waterways Experiment Station, Miscellaneous Paper. GL-79-21, Vicksburg, U.S.A.

Johnson, L.D. (1987). Measurement of horizontal and vertical swell pressures from a triaxial laboratory test: Feasibility study. U.S. Army Engineer Waterways Experiment Station, Miscellaneous Paper. GL-87-23, Vicksburg, U.S.A.

Johnson, L.D. (1989). Horizontal and vertical swell pressures from a triaxial test: Feasibility study. Geotech. Testing J., ASTM, Vol. 12, Part. 1, Technical Note, 87-92.

Johnson, L.D. and Desai, C.S. (1975). A numerical procedure for predicting heave. Proc. 2nd Australian - New Zealand Conf. on Geomechanics, Inst. of Engineers, Brisbane, Nat. Conf. Publication No. 75/4, 269-273.

Jones, D.E. (1979). The expansive soil problem. Underground Space, Vol. 3, No. 5, 221-226.

Jones, D.E. and Holtz, W.G. (1973). Expansive soils - the hidden disaster. Civil Engineering, ASCE, Vol. 43, No. 8, 49-51.

Justo, J.L., Delgado, A. and Ruiz, J. (1984). The influence of stress-path in the collapse-swelling of soils at the laboratory. Proc. 5th Int. Conf. on Expansive Soils, Adelaide, 67-71.

Justo, J.L. and Saetersdal, R. (1981). Design parameters for special soil conditions. Design Parameters in Geotechnical Engineering, BGS, London, (7th ECSMFE, Brighton, 1979), Vol. 5, 127-158.

Kassiff, G., Baker, R. and Ovadia, Y. (1973). Swell-pressure relationships at constant suction changes. Proc. 3rd Int. Conf. on Expansive Soils, Haifa, Vol. 1, 201-208.

Kassiff, G. and Ben-Shalom, A. (1971). Apparatus for measuring swell potential under controlled moisture intake. J. of Materials, ASTM, Vol. 6, Part 1/2, 3-15.

Kassiff, G., Etkin, A. and Zeitlen, J.G. (1967). Failure mechanism of canal lining in expansive clay. J. SM & FDiv., Proc. ASCE, Vol. 93, No. SM1, Paper 5068, 95-118.

Katz, J.R. (1933). The laws of swelling. Trans. of the Faraday Soc., Vol. 29, 279-300.

Kawakami, H. and Abe, H. (1975). Volume change characteristics and collapse in unsaturated soils during triaxial test. Proc. 5th Asian Reg. Conf. on SM & FE, Bangalore, Vol. 1, 111-116.

Keen, B.A. and Raczkowski, H.J. (1921). The relation between the clay content and certain physical properties of a soil. J. of Agricultural Sci., Vol. 11, 441-449.

Kenney, T.C., Moum, J. and Berre, T. (1967). An experimental study of Bonds in a natural clay. Proc. 1st Geotechnical Conf. of Oslo, 65-69.

Kenney, T.C. and Watson, G.H. (1961). Multi-stage triaxial test for determining C' and ϕ' of saturated soils. Proc. 5th ICSMFE, Paris, Vol. 1, 191-195.

Klementev, I. (1974). Lever-type apparatus for electrically measuring volume change. Gèotechnique, Vol. 24, No. 4, Technical Note, 670-671.

Komornik, A. and David, D. (1969). Prediction of swelling pressure of clays. J. SM & FDiv., Proc. ASCE, Vol. 95, No. SM1, Paper 6358, 209-225.

Komornik, A., Livneh, M. and Smucha, S. (1980). Shear strength and swelling of clays under suction. Proc. 4th Int. Conf. on Expansive Soils, Denver, Vol. 1, 206-226.

Komornik, A. and Zeitlen, J.G. (1965). An apparatus for measuring lateral soil swelling pressure in the laboratory. Proc. 6th ICSMFE, Montreal, Vol. 1, 278-281.

Komornik, A. and Zeitlen, J.G. (1970). Laboratory determination of lateral and vertical stresses in compacted swelling clay. J. of Materials, ASTM, Vol. 5, Part. 1, 108-128.

Krohn, J.P. and Slosson, J.E. (1980). Assessment of expansive soils in the United States. Proc. 4th Int. Conf. on Expansive Soils, Denver, Vol. 1, 596-608.

Ladd, C.C. and Lambe, T.W. (1961). The identification and behavior of compacted expansive clays. Proc. 5th ICSMFE, Paris, Vol. 1, 201-205.

Lade, P.V. (1982). Localization effects in triaxial tests on sand. Proc. IUTAM Conf. on Deformation and Failure of Granular Materials, Delft, 461-471.

Lade, P.V. and Tsai, J. (1985). Effects of localization in triaxial tests on clay. Proc. 11th ICSMFE, San Francisco, Vol. 2, 549-552.

Lambe, T.W. (1954). The permeability of fine-grained soils. ASTM Proc., Vol. 59.

Lambe, T.W. (1960). A mechanistic picture of shear strength in clay. Proc. of the ASCE Res. Conf. on Shear Strength of Cohesive Soils, Univ. of Colorado, 555-580.

Lambe, T.W. (1967). Stress path method. J. SM & FDiv., Proc. ASCE, Vol. 93, No. SM6, Paper 5613, 309-331.

Lambe, T.W. and Marr, W.A. (1979). Stress path method: second edition. J. Geotech. Eng. Div., Proc. ASCE, Vol. 105, No. GT6, Paper 14655, 727-738.

Lambe, T.W. and Whitman, R.V. (1969). Soil mechanics. John Wiley & Sons, New York, 29.

Lee, R.K.C. and Fredlund, D.G. (1984). Measurement of soil suction using the MCS 6000 sensor. Proc. 5th Int. Conf. on Expansive Soils, Adelaide, 50-54.

Leonards, G.A. and Altschaeffl, A.G. (1964). Compressibility of clay. J. SM & FDiv., Proc. ASCE, Vol. 90, No. SM5, Paper 4049, 133-155.

Lewin, P.I. (1971). Use of servo mechanisms for volume change measurement and Ko consolidation. Gèotechnique, Vol. 21, No. 3, Technical Note, 259-262.

Lewis, W.A. and Ross, N.F. (1955). An investigation of the relationship between the shear strength of remoulded cohesive soil and the soil moisture suction. Road Res. Lab., Res. Note RN/2389/WAL.NFR.

Livneh, M., Shklarsky, E. and Uzan, J. (1973). Cracking of flexible pavements based on swelling clay. Preliminary theoretical analysis. Proc. 3rd Int. Conf. on Expansive Soils, Haifa, Vol. 1, 257-265.

Loiselle, A., Massiera, M. and Usha, S.R. (1971). A study of the cementation bonds of the Outardes River Region. Canadian Geotech. J., Vol. 8, No. 3, 479-498.

Lytton, R.L. and Woodburn, J.A. (1973). Design and performance of mat foundations on expansive clay. Proc. 3rd Int. Conf. on Expansive Soils, Haifa, Vol. 1, 301-307.

MacEwan, D.M.C. (1948). Complexes of clays with organic compounds I. Trans. of the Faraday Soc., Vol. 44, 349-367.

MacEwan, D.M.C. (1955). Interlamellar sorption by clay minerals. Proc. 1st Nat. Conf. on Clays and Clay Technology, California Div. of Mines, San Francisco, Bull. No. 169, 78-85.

MacEwan, D.M.C. and Wilson, M.J. (1980). Interlayer and intercalation complexes of clay minerals. "Crystal Structures of Clay Minerals and Their X-ray Identification." Mineralogical Soc., Monograph No. 5, Chapter 3, 197-248.

MacIver, B.N. and Hale, G.P. (1970). Engineer manual on laboratory soil testing: engineering and design. HQs: Dept. of the Army, Office of the Chief of Engineers, Washington.

McDowell, C. (1956). Interrelationship of load, volume change, and layer thicknesses of soils to the behavior of engineering structures. Proc. Highway Res. Board, Washington, Vol. 35, 754-772.

McKeen, R.G. (1981). Design of airport pavements for expansive soils. U.S. Dept. of Transportation, Federal Aviation Authority, Report FAA/RD-81/25.

McKeen, R.G. and Hamberg, D.J. (1981). Characterization of expansive soils. Transp. Res. Rec. No. 790, Washington, 73-78.

McQueen, I.S. and Miller, R.F. (1968). Calibration and evaluation of a wide-range gravimetric method for measuring moisture stress. Soil Science, Vol. 106, No. 3, 225-231.

Marchant, J.A. and Schofield, C.P. (1978). A combined constant pressure and volume change apparatus for triaxial tests at low pressures. Gèotechnique, Vol. 28, No. 3, Technical Note, 351-353.

Marsal, R.J. and Resines, J.S. (1960). Pore pressure and volumetric measurements in triaxial compression tests. Proc. of the ASCE Res. Conf. on Shear Strength of Cohesive Soils, Univ. of Colorado, 965-983.

Marshall, C.E. (1949). The colloidal chemistry of silicate minerals. Academic Press Inc., New York, 195pp.

Matyas, E.L. and Radhakrishna, H.S. (1968). Volume change characteristics of partially saturated soils. Gèotechnique, Vol. 18, No. 4, 432-448.

Menzies, B.K. (1975). A device for measuring volume change. Gèotechnique, Vol. 25, No. 1, Technical Note, 133-134.

Menzies, B.K. (1976). Design, manufacture and performance of a lateral strain device. Gèotechnique, Vol. 26, No. 3, Technical Note, 542-544.

Mielenz, R.C. and King, M.E. (1955). Physical-chemical properties and engineering performance of clays. Proc. 1st Nat. Conf. on Clays and Clay Technology, California Div. of Mines, San Francisco, Bull. No. 169, , 196-254.

Millot, G. (1970). Geology of clays (translators: W.R. Farrand and H. Paquet). Springer-Verlag, New York.

Mitchell, P.W. and Avalle, D.L. (1984). A technique to predict expansive soil movements. Proc. 5th Int. Conf. on Expansive Soils, Adelaide, 124-130.

Mitchell, R.L. and MacKechnie, W.R. (1972). Construction on (volumetrically active) soils. Rhodesian Engineer, Vol. 10, Part 5, 43-50.

M.I.T. (1963). Engineering behaviour of partially saturated soils. phase Report No. 1, Soil Stabilization.

Morgenstern, N.R. and Balasubramonian, B.I. (1980). Effects of pore fluid on the swelling of clay-shale. Proc. 4th Int. Conf. on Expansive Soils, Denver, Vol. 1, 190-205.

Mou, C.H. and Chu, T.Y. (1981). Soil-suction approach for evaluation of swelling potential. Transp. Res. Rec. No. 790, 54-60.

Murthy, M.K., Sridharan, A. and Nagaraj, T.S. (1987). Shear behaviour of partially saturated soils. Indian Geotechnical Journal, Vol. 17, No. 2, 142-158.

Nagaraj, T.S. and Srinivasa Murthy, B.R. (1983). An approach for prediction of swelling soil behaviour. Proc. 7th Asian Reg. Conf. on SM & FE, Haifa, Vol. 1, 52-55.

Nambiar, M.R.M., Venkatappa Rao, G. and Gulhati, S.K. (1985). Multistage triaxial testing: A rational procedure. Proc. Symp. Strength Testing of Marine Sediments: Laboratory and In-situ Investigation, ASTM, STP883, 274-293.

Nayak, N.V. and Christensen, R.W. (1971). Swelling characteristics of compacted, expansive soils. Clays and Clay Minerals, Vol. 19, Part. 4, 251-261.

Newland, P.L. (1965). The behaviour of soils in terms of two kinds of effective stress. Proc. Int. Res. and Eng. Conf. on Expansive Clays, Texas A & M University, 78-92.

Newman, A.C.D. (1987). The interaction of water with clay mineral surfaces. "Chemistry of Clays and Clay Minerals", Ed: A.C.D. Newman, Mineralogical Soc., Monograph No. 6, London, Chapter 5, 237-274.

Noble, C.A. (1966). Swelling measurements and prediction of heave for a lacustrine clay. Canadian Geotech. J., Vol. 3, No. 1, 32-41.

Odom, I.E. (1984). Smectite clay minerals: properties and use. Phil. Trans. of the Royal Soc., London, A311, 391-409.

Ofer, Z. (1980). Instruments for laboratory and in situ measurement of the lateral swelling pressure of expansive clays. Proc. 4th Int. Conf. on Expansive Soils, Denver, Vol. 1, 45-53.

Ofer, Z., Blight, G.E. and Komornik, A. (1983). An insitu swelling pressure test. Proc. 7th Asian Reg. Conf. on SM & FE, Haifa, Vol. 1, 64-70.

Ofer, Z., Blight, G.E. and Komornik, A. (1984). Simultaneous determination of in situ swelling pressure and shear strength. Proc. 5th Int. Conf. on Expansive Soils, Adelaide, 80-84.

Olson, R.E. and Mesri, G. (1970). Mechanisms controlling compressibility of clays. J. SM & FDiv., Proc. ASCE, Vol. 96, No. SM6, Paper 7649, 1863-1878.

Osman, M.A. and Charlie, W.A. (1984). Engineering properties of expansive soils in Sudan. Proc. 5th Int. Conf. on Expansive Soils, Adelaide, 311-315.

Parry, R.H.G. and Nadarajah, V. (1973). Multistage triaxial testing of highly overconsolidated clays. J. of Testing and Evaluation, Vol. 1, No. 5, 374-381.

Pennington, R.P. and Jackson, M.L. (1947). Segregation of the clay minerals of polycomponent soil clays. Proc. of Soil Soc. of America, Vol. 12, 452-457.

Peter, P. and Martin, R. (1973). A simple psychrometer for routine determinations of total suction in expansive soils. Proc. 3rd Int. Conf. on Expansive Soils, Haifa, Vol. 2, 89-96.

Peterson, R.W. (1992). Shear strength of unsaturated soil. Proc. 7th Int. Conf. on Expansive Soils, Dallas, Vol. 2, 89-94.

Pidgeon, J.T. (1980). A comparison of existing methods for the design of stiffened raft foundations on expansive soils. Proc. 7th Reg. Conf. for Africa on SM & FE, Accra, Vol. 1, 277-290.

Pile, K.C. (1980). The relationship between matrix and solute suction, swelling pressure, and magnitude of swelling in reactive clays. Proc. 3rd Australian - New Zealand Conf. on Geomechanics, Wellington, Vol. 1, 197-201.

Pile, K.C. and McInnes, D.B. (1984). Laboratory technology for measuring properties of expansive clays. Proc. 5th Int. Conf. on Expansive Soils, Adelaide, 85-93.

Preece, E.F. (1947). Geotechnics and geotechnical research. Proc. of Highway Res. Board, Vol. 27, 384-416.

Radhakrishna, H.S. (1967). Compressibility of partially saturated soils. Ph.D. Thesis, Univ. of Waterloo, U.S.A.

Raman, V. (1967). Identification of expansive soils from the plasticity index and the shrinkage index data. The Indian Engineer, Indian ICE, Calcutta, Vol. 11, No. 1, 17-22.

Ranganatham, B.V. and Satyanarayana, B. (1965). A rational method of predicting swelling potential for compacted expansive clays. Proc. 6th ICSMFE, Montreal, Vol. 1, 92-96.

Rengmark, F. and Eriksson, R. (1953). Apparatus for investigation of swelling, compression and elastic properties of soils. Proc. 3rd ICSMFE, Zurich, Vol. 1, 180-183.

Richards, B.G. (1965). Measurement of the free energy of soil moisture by the psychrometric technique using thermistors. Proc. Symp. Moisture Equilibria and Moisture Changes in Soils Beneath Covered Areas, Butterworths, Australia, 39-46.

Richards, B.G. (1967). Moisture flow and equilibria in unsaturated soils for shallow foundations. Proc. Symp. on Permeability and Capillarity, ASTM, STP 417, 4-33.

Richards, B.G. (1980). Measurement of soil suction in expansive clays. Instn. of Engineers, Civ. Eng. Trans., Australia, Vol. CE22, Part 3, 252-261.

Richards, B.G., Peter, P. and Martin, R. (1984). The determination of volume change properties in expansive soils. Proc. 5th Int. Conf. on Expansive Soils, Adelaide, 179-186.

Ross, C.S. and Hendricks, S.B. (1945). Minerals of montmorillonite group. U.S. Geology Survey Professional Paper 205-B, 79pp.

Rowlands, G.O. (1972). Apparatus for measuring volume change suitable for automatic logging. Gèotechnique, Vol. 22, No. 3, Technical Note, 525-526.

Salas, J.A.J. and Serratosa, J.M. (1957). Foundations on swelling clays. Proc. 4th ICSMFE, London, Vol. 1, 424-428.

Samuels, S.G. (1950). The effect of base exchange on the engineering properties of soils. Dept. of Sci. and Indus. Res., Bldg. Res. Stn., Report C176, 16pp.

Satija, B.S. (1978). Shear behaviour of partially saturated soils. Ph.D. Thesis, Indian Institute of Technology, Delhi, India.

Satija, B.S. and Gulhati, S.K. (1979). Strain rate for shear testing of unsaturated soil. Proc. 6th Asian Reg. Conf. on SM & FE, Singapore, 83-86.

Schmertmann, J.H. (1969). Swell sensitivity. Gèotechnique, Vol. 19, No. 4, Technical Note, 530-533.

Schreiner, H.D. (1988). Volume change of compacted highly plastic African clays. Ph.D. Thesis, Imperial College of Science and Technology, UK.

Seed, H.B. and Chan, C.K. (1961). Structure and strength characteristics. Proc. Symp. on Compacted Clays, Trans. of the ASCE, Vol. 126, Part. 1, 1344-1385.

Seed, H.B., Woodward, R.J. and Lundgren, R. (1962). Prediction of swelling potential for compacted clays. J. SM & FDiv., Proc. ASCE, Vol. 88, No. SM3, Paper 3169, 53-87.

Seed, H.B., Woodward, R.J. and Lundgren, R. (1963). Prediction of swelling potential for compacted clays. Trans. ASCE, Vol. 128, Part. 1, Paper 3501, 1443-1477.

Sharpe, P. (1978). A device for automatic measurement of volume change. Gèotechnique, Vol. 28, No. 3, Tecnical Note, 348-350.

Skempton, A.W. (1961). Effective stress in soils, concrete and rocks. Proc. Pore Pressure and Suction in Soils, Butterworths, London, 4-16.

Snethen, D.R. (1972). Lateral swelling pressure relationships for two Oklahoma clays. Ph.D. Thesis, Oklahoma State University, U.S.A.

Snethen, D.R. (1979). An evaluation of methodology for prediction and minimization of detrimental volume change of expansive soils in highway subgrades. Waterways Experiment Station, Vicksburg, U.S.A., Report No. FHWA-RD-79-49.

Snethen, D.R. (1980). Characterization of expansive soils using soil suction data. Proc. 4th Int. Conf. on expansive Soils, Denver, Vol. 1, 54-75.

Snethen, D.R. (1984). Evaluation of expedient methods for identification and classification of potentially expansive soils. Proc. 5th Int. Conf. on Expansive Soils, Adelaide, 22-26.

Snethen, D.R. and Haliburton, T.A. (1973). Lateral swelling pressures in compacted Oklahoma cohesive soils. Highway Res. Rec. No. 429, Nat. Res. Council, U.S.A., 26-28.

Spiel, S. (1940). Effect of adsorbed electrolytes on properties of monodispersed clay-water systems. Am. Ceramic Soc. J., Vol. 23, 33-38.

Sposito, G. (1989). Exchangeable ions. "The chemistry of soils." Open University Press, U.K., Chapter 9, 170-187.

Sridharan, A. (1968). Some studies on the strength of partly saturated clays. Ph.D. Thesis, Purdue Univ., U.S.A.

Sridharan, A. and Allam, M.M. (1982). Volume change behavior of desiccated soils. J. Geotech. Eng. Div., Proc. ASCE, Vol. 108, No. GT8, Paper 17264, 1057-1071.

Sridharan, A. and Venkatappa Rao, G. (1971). Effective stress theory of shrinkage phenomena, Canadian Geotech. J., Vol. 8, No. 4, 503-513.

Sridharan, A. and Venkatappa Rao, G. (1972). Physico-chemical mechanisms controlling the strength, consolidation and swelling behaviour of clays. Proc. Symp. Strength and Deformation Behaviour of Soils, Indian Geotech. Soc., Bangalore, Vol. 1, 11-17.

Sridharan, A. and Venkatappa Rao, G. (1973). Mechanisms controlling volume change of saturated clays and the role of the effective stress concept. Gèotechnique, Vol. 23, No. 3, 359-382.

Stevens, J.B. and Matlock, H. (1976). Measurements beneath the surface of expansive clay. Transp. Res. Rec. No. 568, Washington, 35-47.

Sullivan, R.A. and McClelland, B. (1969). Predicting heave of buildings on unsaturated clay. Proc. 2nd Int. Res. and Eng. Conf. on Expansive Clay Soils, Texas A & M Univ., 404-420.

Tadanier, R. and Nguyen, V.U. (1984). Index properties of expansive soils in New South Wales. Proc. 5th Int. Conf. on Expansive Soils, Adelaide, 321-326.

Terzaghi, K.V. (1936). The shearing resistance of saturated soils and the angle between the planes of shear. Proc. 1st ICSMFE, Vol. 1, 54-56.

Tomlinson, M.J., Driscoll, R. and Burland, J.B. (1978). Foundations for low-rise buildings. The Structural Engineer, Vol. 56A, Part A, No. 6, 161-173.

Towner, G.D. (1961). Influence of soil-water suction on some mechanical properties of soils. J. of Soil Science, Vol. 12, No. 1, 180-187.

Van der Merwe, D.H. (1964). The prediction of heave from the plasticity index and percentage clay fraction of soils. Trans. SAICE, Vol. 6, No. 5, 103-107.

Vijayvergiya, V.N. and Ghazzaly, O.I. (1973). Prediction of swelling potential for natural clays. Proc. 3rd Int. Conf. on Expansive Soils, Haifa, Vol. 1, 227-236.

Vijayvergiya, V.N. and Sullivan, R.A. (1972). Simple technique for identifying heave potential. Proc. of the Workshop on Expansive Clays and Shales in Highway Design and Construction, Denver, Vol. 1, 275-294.

Warlam, A.A. (1942). Improvements in triaxial compression apparatus. 5th Progress Report on Cooperative Research on Stress deformation and Strength Characteristics of Soils, Harvard Univ., IV, 2, 3, 5 and 6.

Warlam, A.A. (1944). Recent developments in triaxial compression apparatus. 7th Progress Report on Cooperative Research on Stress deformation and Strength Characteristics of Soils, Harvard Univ., II, 33-36 and 42-50.

Warlam, A.A. (1946). Stress-strain and strength properties of soils. Sc.D. Thesis, Harvard Univ., 22-25, 41, 211-233.

Warlam, A.A. (1960). Recent progress in triaxial apparatus design. Proc. of the ASCE Res. Conf. on Shear Strength of Cohesive Soils, Univ. of Colorado, 859-876.

Weaver, C.E. and Pollard, L.D. (1973). The chemistry of clay minerals. Elsevier Publishing Co., New York.

Wheeler, S.J. (1988). The undrained shear strength of soils containing large gas bubbles. Gèotechnique, Vol. 38, No. 3, 399-413.

Williams, A.A.B. (1958). Discussion of paper "The prediction of total heave from the double oedometer test" by J.E.B. Jennings, and K. Knight, Trans. SAICE, Vol. 8, No. 6, 121-128.

Williams, A.A.B. and Donaldson, G.W. (1980). Building on expansive soils in South Africa: 1973-1980. Proc. 4th Int. Conf. on Expansive Soils, Denver, Vol. 2, 834-844.

Williams, A.A.B., Pidgeon, J.T. and Day, P.W. (1985). Expansive soils. Civ. Eng. in South Africa, Trans. SAICE, Vol. 27, Part 7, 367-377 & 407.

Williams, S. (1988). Swelling behaviour of unsaturated expansive clays. Ph.D. Thesis, Polytechnic of Wales, U.K.

Winkler, H.G.F. (1949). Clays and their properties - An interpretation. Research, Vol. 2, 175-183.

Winterkorn, H.F. (1953). Job experience with exchange phenomena involving inorganic ions. ASTM, STP 142, 29-43.

Winterkorn, H.F. and Baver, L.D. (1934). Sorption of liquids by soil colloids. I: Liquid intake and swelling by soil colloidal material. Soil Science, Vol. 38, 291-298.

Winterkorn, H.F. and Moorman, R.B. (1941). A study of changes in physical properties of Putnam soil induced by ionic substitution. Proc. of Highway Res. Board, Vol. 21, 415-434.

Wiseman, G. and Zeitlen, J.G. (1960). Swelling studies on a laboratory compacted clay. Proc. 1st Asian Reg. Conf. on SM & FE, New Delhi, Div. I, Communication vii, 1-16.

Xin, J.Z. and Ling, Q.X. (1992). A new method for calculating lateral swelling pressure in expansive soil. Proc. 7th Int. Conf. on Expansive Soils, Dallas, Vol. 1, 233-238.

Yong, R.N., Japp, R.D. and How, G. (1971). Shear strength of partially saturated clays. Proc. 4th Asian Reg. Conf. on SM & FE, Bangkok, Vol. 1, 183-187.

Yong, R.N. and Warkentin, B.P. (1975). Soil properties and behaviour. Developments in Geotechnical Engineering, Vol. 5, Elsevier Scientific Publishing Co., Amsterdam.

Zein, A.K.M. (1985). Swelling characteristics and microfabric of compacted black cotton soil. Ph.D. Thesis, Univ. of Strathclyde, Glasgow, U.k.